

DEVELOPMENT OF A STIRLING ENGINE

BATTERY CHARGER BASED ON A

LOW COST

WOBBLE MECHANISM

A thesis submitted for the
Degree of Doctor of Philosophy
in Mechanical Engineering at the
University of Canterbury,
Christchurch, New Zealand.

Donald Murray Clucas

1993

ENGINEERING
LIBRARY
THESIS
TK
2943
.C649
1993



Stirling Engine Battery Charger or Generator

To my dear wife.

Abstract

The benefits of the Stirling Cycle have been known for well over a century but several specific problems have prevented its common use in modern society.

During 1989 this PhD project was undertaken to investigate various applications for the Stirling Engine and develop the one most likely to succeed commercially and be manufactured within New Zealand. The Stirling Engine Battery Charger For Yachts was selected and this thesis outlines the design development up to and including testing a pre-production prototype.

Although the system is specifically designed to allow scaling to accommodate future designs of total energy system for yachts and for use in other applications, this thesis is restricted to the development of an air charged, 200 Watt (electric), LPG heated, hermetically sealed and pressurised unit suitable for charging 12 volt batteries. The chosen design utilised the four cylinder double acting configuration and incorporated a modified alternator to also act as a starter motor.

Several of the key problems with the Stirling Engine which have prevented its commercialisation are identified early in the thesis and the succeeding Chapters present investigations and possible solutions to each. These investigations resulted in the development of a new kinematic mechanism design, further piston seal research, a combined starter alternator, alternative heat exchanger designs and another general system layout.

To aid Stirling Engine design and optimisation a computer modelling package was developed. This system was based on a commercial Spreadsheet program and a customised published Quasi Steady Flow simulation routine. To verify the simulation an Alpha configuration engine was manufactured and tested prior to designing the prototype unit.

The prototype engine/alternator successfully met its design power of 200 Watts. This thesis concludes with the detailed design of the prototype, its performance characteristics, a review of the system viability and recommendations for further development and other applications.

Table of Contents

1	INTRODUCTION	1
1.1	Project Background	1
1.2	Why Investigate the Stirling Cycle	2
1.3	Possible Applications	4
1.3.1	Recharging Wheelchair Batteries	5
1.3.2	Ocean Going Racing and Cruising Yachts	5
1.3.3	Military Applications	5
1.3.4	Waste Heat Recovery	5
1.3.5	Telecommunications	6
1.3.6	Waste Burner Generator	6
1.4	Application Selection	6
1.5	Introduction to the Yacht Application	7
1.5.1	Total Energy System	8
1.5.2	Battery Charger for Yachts	8
1.6	Objectives Of The Project	9
1.6.1	Primary Objective	9
1.6.2	Secondary Objectives	9
1.6.3	Chapter Contents	10
2	The Stirling Engine	12
2.1	Introduction	12
2.2	The Ideal Stirling Cycle	12
2.3	Practical Stirling Engine	14
2.4	Engine Configuration	14
2.5	Literature	16
2.6	Brief History	17

2.7 Comparison With Internal Combustion Engines	19
2.7.1 Energy source	19
2.7.2 Energy Sink	20
2.7.3 Long Engine Life	21
2.7.4 Balance	21
2.7.5 Starting	21
2.7.6 Exhaust emissions	21
2.7.7 Quiet operation	22
2.8 Marine applications	22
2.8.1 Philips Marine Applications	23
2.8.2 Marine Applications Outside Philips.	23
2.9 Conclusions	27
3 Battery Charging on Yachts	28
3.1 Introduction	28
3.2 Energy Requirements	28
3.3 Batteries	30
3.3.1 The Lead Acid Battery, General.	30
3.3.2 Starting-Lighting-Ignition (SLI) Battery	33
3.3.3 House Battery (Deep Cycle)	34
3.3.4 Charging and Discharging Deep Cycle Batteries	34
3.4 Battery Charging Methods	35
3.4.1 Standard Automotive Type Alternator	35
3.4.2 Photovoltaic	39
3.4.3 Wind Generators	40
3.4.4 Tow Generators	41
3.4.5 Portable Generators	42
3.5 Voltage Regulation	42

3.5.1 Standard Alternator Voltage Regulation	43
3.5.2 Marine Regulator	45
3.5.3 Shunt Regulators.	45
3.6 Summary of Conclusions of Chapter 3	45
4 Preliminary Engine Generator Design	47
4.1 General Design Procedure	47
4.2 Initial Design Requirements.	47
4.3 Nominal Engine Power	49
4.4 Generator Selection	51
4.5 Working Fluid and Pressurisation.	52
4.5.1 Choice of Working Fluid	52
4.5.2 Pressurisation	54
4.6 Cycle Temperature	55
4.6.1 Cold Heat Sink	56
4.6.2 Hot Heat Source Temperature	59
4.6.3 Estimated SEBCY Efficiency	59
4.7 Engine Speed	59
4.8 Heater Combustion System	60
4.8.1 LPG	60
4.8.2 Burner Design	61
4.8.3 Enhancement of the Burner Heat Transfer.	61
4.8.4 Heater Head	63
4.9 Engine Arrangement	63
4.9.1 Possible Scaling	64
4.9.2 Lubrication	64
4.9.3 Starting	64
4.9.4 Stirling Engine Performance Prediction	66

	vi
4.9.5 Comparison of Engine Configurations	66
4.9.6 Beale and West First Order Equations	67
4.9.7 Optimum Configuration by Kirkley	71
4.9.8 Geometric and Parasitic Loss Considerations.	72
4.9.9 Shuttle Loss	78
4.9.10 Appendix Loss	78
4.9.11 Comparison of the Configurations	78
4.9.12 Decision Matrix	84
4.10 Mechanisms	87
4.11 Summary of Conclusions of Chapter 4	88
5 Wobble Yoke	90
5.1 Introduction	90
5.2 Mechanism requirements	90
5.3 Review of existing designs	92
5.3.1 Wobble Plate	92
5.3.2 Swash Plate	93
5.3.3 Slider Crank	94
5.3.4 Twin Ross Yoke	95
5.4 Wobble Yoke	97
5.4.1 Type 1	98
5.4.2 Type 2	101
5.4.3 Patents, Prior Art	101
5.4.4 Wobble Yoke Kinematics	103
5.4.5 Comparison with simple harmonic and slider crank	107
5.4.6 Connecting Rod Bearing Load.	109
5.4.7 Beam Moments	109
5.4.8 Eccentric Bearing Load	110

5.4.9 Engine torque	110
5.4.10 Engine Balance	110
5.5 Case Study	111
5.6 Design variations	116
5.6.1 Twin Alpha Configuration	116
5.6.2 Rigid Piston-Connecting Rod Joint	116
5.6.3 Flexure Joints	118
5.6.4 Totally Rigid Beam-Connecting Rod-Piston	118
5.6.5 Inverted Yoke	118
5.6.6 Strengthened Wobble Yoke	120
5.6.7 Variable Stroke	120
5.7 Other Applications	120
5.7.1 Compressors and Hydraulics	120
5.7.2 Internal Combustion Engines	121
5.7.3 Two Ram Positioning Device	121
5.8 Summary of Conclusions for Chapter 5	121
6 Test Engines and Experimental Apparatus	123
6.1 Summary of Engines	123
6.2 DMC 1	125
6.3 DMC 2	125
6.4 DMC 3	129
6.4.1 Mechanism Housing	129
6.4.2 Motoring	131
6.4.3 Dynamometer	131
6.4.4 Engine Starter	131
6.4.5 Data Acquisition and Engine Control	134
6.4.6 Speed Control	135

6.5 DMC 4	137
7 Seals	140
7.1 Introduction	140
7.2 Brief Stirling Engine Seal History	141
7.3 Piston Seal Design Requirements	143
7.4 Initial Seal Experience	144
7.5 Seal Ring Material Testing and Selection	145
7.5.1 Materials	147
7.5.2 Measurement of Material Characteristics	147
7.5.3 Friction Power Loss Measurement	148
7.5.4 Seal Heating	149
7.5.5 Results of Seal Material Testing	149
7.6 Cylinder Mounted Seals For Engine Use	152
7.7 Seal Simulation.	154
7.7.1 Seal Preferential Pumping	155
7.7.2 Seal Leak Paths	156
7.7.3 Seal Simulation Results	157
7.8 Cylinder Mounted Seals in Operation	163
7.9 Seal Design for the SEBCY	165
7.9.1 Single Lip Cylinder Mounted Piston Seal for Double Acting Engines	166
7.9.2 Simulation of the Seal Pressure Loading	167
7.10 Conclusions From Chapter 7	168
8 Heat Transfer System	172
8.1 Introduction	172
8.2 Quasi Steady Flow Model, QSFM	173

8.2.1 Non-steady flow	173
8.2.2 The Model	173
8.2.3 Designer - Computer Interface	176
8.3 Heat Exchanger Optimisation	176
8.3.1 Steepest Ascent Techniques	181
8.3.2 Grid Search	181
8.3.3 Optimisation Verification	185
8.4 Heat Exchanger Design, Testing and Simulation Verification	186
8.4.1 Description of DMC 3's Heat Exchangers	186
8.4.2 Engine Data Measurement and Recording	191
8.4.3 Results From DMC 3 Tests	194
8.5 Conclusions from Chapter 8	200
9 SEBCY Prototype Design, DMC 5.	202
9.1 Component Design	203
9.1.1 Wobble Yoke And Alternator Housing	203
9.1.2 Manual Starter	206
9.1.3 Alternator	207
9.1.4 Alternator Stator	209
9.1.5 Alternator Rotor	209
9.1.6 Alternator Field Coil	211
9.1.7 Driveshaft	211
9.1.8 Driveshaft Bearings	211
9.1.9 Eccentric Bearing	211
9.1.10 Driveshaft Lock Nut	212
9.1.11 Base Plate	212
9.1.12 Wobble Yoke, General.	212
9.1.13 Wobble Yoke Nutating Pin	214

9.1.14 Wobble Yokes	214
9.1.15 Wobble Yoke Beams	215
9.1.16 Wobble Yoke Pivot Block	215
9.1.17 Cylinder Block	215
9.1.18 Piston Seals	216
9.1.19 Pistons	217
9.1.20 Rod Seal	217
9.1.21 Connecting Rod-Piston Flexure Joint	218
9.1.22 Cold End Heat Exchanger	219
9.1.23 Regenerator	222
9.1.24 Hot End Heat Exchanger and Cylinder Head	222
9.1.25 Initial LPG Burner For Engine Testing	223
9.1.26 LPG Burner For Production Engines	223
9.1.27 Burner Capacity.	225
9.1.28 Air Requirement.	225
9.1.29 Exhaust	227
9.2 SEBCY Electronic Control System	227
9.2.1 Basic Circuit Design	227
9.2.2 Pilot Light	228
9.2.3 Battery Charge Determination, SEBCY Starting and Stopping	228
9.2.4 Electric Starting	228
9.2.5 Engine Speed Control and Voltage Regulation	229
9.2.6 Control Panel	230
9.3 SEBCY Testing	230
9.3.1 Alternator Motoring Tests	231
9.3.2 Engine Motoring Tests	231
9.3.3 Driven Tests	231
9.3.4 Prime Mover Testing	234

9.4 Conclusions for Chapter 9	236
10 Conclusions and Recommendations	239
10.1 Conclusions	239
10.2 Recommendations	242
REFERENCES	244
APPENDIX A	Properties of liquid petroleum gas mixtures.
APPENDIX B	Seal analysis program listing
APPENDIX C	Quasi Steady Flow Model and graphical output from SODA
APPENDIX DMC 5	Production drawings for DMC 5

List of Figures

Figure 2.1 Ideal Stirling Cycle.	13
Figure 2.2 Real Stirling engine.	14
Figure 2.3 Alpha, Beta and Gamma configurations. The four cycle double acting layout is a special case of the Alpha configuration.	15
Figure 2.4 Free piston linear alternator.	16
Figure 2.5 Last commercially produced Stirling engine prior to 1937, after Hargreaves, (1991).	17
Figure 2.6 Energy transfer.	20
Figure 2.7 Ericssons huge marine engine.	22
Figure 2.8 Four cylinder double acting wobble plate engine, after Hargreaves, (1991)	23
Figure 2.9. Marine applications of the Stirling engine	24
Figure 2.10 Similar developments.	26
Figure 3.1 Yacht with diesel propulsion engine.	28
Figure 3.2 Lead-acid battery construction.	31
Figure 3.3 Charge-discharge curves for a single lead-acid cell.	32
Figure 3.4 Automotive DC generator, after (Bosch)	36
Figure 3.5 Automotive claw pole alternator, (Bosch)	37
Figure 3.6 Basic alternator and regulator circuit diagram.	38
Figure 3.7 Stationary field coil alternator.	39
Figure 3.8 Characteristics of a marine alternator.	40
Figure 3.9 Yacht with tow and wind generators.	41
Figure 3.10 (a) Comparison of a high charge rate marine regulator and an automotive regulator. (b) & (c) Marine regulator performance.	44
Figure 4.1 Flow of steps followed in the design process, after Pahl and Beitz (1988)	48
Figure 4.2 SEBCY overall function and its effects on the surroundings.	49
Figure 4.3 Alternator test equipment.	51

Figure 4.4 Test results of a commercial automotive. Power and efficiency versus shaft speed for various battery terminal voltages.	53
Figure 4.5 Philips 1002C generator set, after Hargreaves (1991).	55
Figure 4.6 Stirling cycle ideal efficiency verse hot and cold end temperature.	56
Figure 4.7 Possible methods for cooling the engine.	58
Figure 4.8 Finned and tubular hot end heat exchangers.	63
Figure 4.9 Effects of operating and geometric factors on the Schmidt power, (Reader and Hooper, 1983).	72
Figure 4.12 Finned heater head dimensions.	73
Figure 4.11 Configuration comparison for 200 and 10 000 W engines. (a) Overall engine dimensions. (b) Component size. (c) Heat flux for finned and unfinned head. (d) Parasitic losses.	83
Figure 4.14 Popular Stirling engine mechanism designs, also refer to figure 5.1. The swash and wobble plate engines are both Z form engines.	88
Figure 5.1 Various engine designs.	96
Figure 5.2 Spherical crank rocker, after Chiang (1988)	98
Figure 5.3 (a) Wobble yoke notation. (b) Offset of bearing centre d from the cylinder pitch radius. (c) Piston positions at top dead centre. (d) Cylinder order viewed from the burner end.	99
Figure 5.4(a) Type 1 and (b) Type 2 wobble yoke layout.	100
Figure 5.5 Relevant patents (a). Axial piston machine by J. Ziegler (1985). (b). Axial internal combustion engine by R Wehr (1932).	102
Figure 5.6 Comparison of kinematic piston motion for wobble yoke, simple harmonic and slider crank mechanism.	108
Figure 5.7 Piston acceleration for various maximum beam angle and similar stroke.	109
Figure 5.8 Radial loads on bearing d. (a) inertia, (b) pressure, (c) combined.	112
Figure 5.9 (a) Beam angular acceleration. (b) Total beam moment. (c) Load on bearing a.	113

Figure 5.10 (a) Radial load on bearing b for beam on the x axis. (b) Combined radial and axial load on bearing c. (c) Ideal shaft torque calculated from the beam moments.	114
Figure 5.11 Out of balance moment.	115
Figure 5.12 Schematic diagrams of wobble yoke used in alternative configurations. (a) rigid piston connecting-rod. (b). Flexure joint. (c). Using rigid beam-piston and toroidal cylinders. Toroidal cylinder machining method.	117
5.13 Alternative wobble yoke configurations. (a). Inverted yoke. (b) Strengthened drive shaft.	119
Figure 5.14 Satellite or solar collector dish utilising the wobble yoke.	121
Figure 6.1 Basic engine design for the DMC 1 gamma configuration engine.	124
Figure 6.2 Sketch of DMC 2, a converted motorcycle engine.	126
Figure 6.3 Photo of DMC 2 showing the added buffer space.	129
Figure 6.4 DMC 3 mechanism housing.	130
Figure 6.5 DMC 3 motoring apparatus.	132
Figure 6.6 Hermetically sealed dynamometer for DMC 3 and the control equipment used.	133
Figure 6.7 Representative data sampled by the data acquisition. Results show axial seal friction force for various interface pressure at 1250 RPM, refer to Chapter 7.	135
Figure 6.8 (a) Portion of a raw data signal read into the computer. (b) The resulting pressure curve after the raw signal had been processed. Note the angular consistency of the results.	136
Figure 7.1 Piston seal system used by United Stirling in a double acting engine, (West, 1986).	143
Figure 7.2 Test apparatus used for assessing seal materials. This apparatus was used in conjunction with the DMC 3 engine shown in Figures 6.4 and 6.5.	146
Figure 7.3. Example of seal material test data. (a). Instantaneous friction force. (b). average coefficient of friction.	150

Figure 7.4 Example of seal material test data. (a) Instantaneous power consumption. (b). Average cycle power consumption.	151
Figure 7.5 Cylinder mounted seal arrangement.	153
Figure 7.6. The effect of reversing the pressure differential across a lip type seal.	155
Figure 7.7 Seal types modelled. Ranging from the simplest Type 1 to the most realistic, Type 4.	158
Figure 7.8. Type 1 seal analysis. (a). Cycle pressure and seal activation pressure over one shaft revolution. (b). Resulting seal ring friction power.	160
Figure 7.9 Type 4 seal analysis. (a). Cycle pressure and the seal hydraulic closing pressure for one shaft revolution. (b). Resulting seal leakage.	161
Figure 7.10 Type 4 seal analysis. (a) Variation of the mean cycle pressure for various seal activation pressure over 10 000 cycles. (b). Resulting engine indicated power due to the mean pressure variation (thermodynamic and friction losses not included).	162
Figure 7.11 Variation of indicated power and shaft power for seal activation pressure. Engine shaft speed was 1500 RPM and the mechanism housing pressure was 10 Bar.	164
Figure 7.12 Possible variations of the seal design which could enhance the performance by optimising the seal pressure loading to suit the application. Seal (a) was initially used in DMC 5.	166
Figure 7.13 Cylinder mounted lip seal characteristics. (a). Cycle pressures and pressure differential across the seal. (b). Seal closing pressure with and without seal back venting.	169
Figure 7.14 Seal closing pressure when $L_l = 2, 1.5$ and 1 for $L_o = 2$	170
Figure 8.1 Minimum cell division for the QSFM.	174
Figure 8.2 Typical optimisation technique used to design the prototype engine.	177
Figure 8.3 Optimisation techniques. Heat exchanger optimisation for a Stirling engine requires a numerical, multi-dimensional and constrained technique, after (??).	180

Figure 8.4 A simple optimisation technique initially developed but not used for the final optimisation.	182
Figure 8.5 Steepest ascent optimisation. Normalised power and efficiency vs. optimisation set.	183
Figure 8.6 Example of desirable and undesirable optimums for a single dimension optimisation.	184
Figure 8.7 Examples of the optimisation verification curves.	187
Figure 8.8 Examples of the optimisation verification curves	188
Figure 8.9 Cross section of DMC 3 heat exchangers, pistons and seal cavities.	189
Figure 8.10 Stacked plate cold end heat exchanger for DMC 3.	192
Figure 8.11 Test results from DMC 3. (a). Measured indicated and shaft power compared with the power calculated by the Beale equation. (b). Compression and expansion space cycle pressure.	196
Figure 8.12 Measured expansion and compression space temperature.	197
Figure 8.13 Measured and simulated indicated power for various stroke lengths.	199
Figure 8.14 Shaft power for various hot end annular gaps compared with the finned insert.	200
Figure 9.1 Pattern used to create a photographic image, hatched areas were blackened.	220
Figure 9.2 Cross section of the cast refractory burner/insulator.	225
Figure 9.3 Schematic diagram of the burner.	226
Figure 9.4 Stationary field coil alternator characteristics. (a) Excitation set to maintain 14.2 volts. (b) Speed constant at 1500 RPM.	233
Figure 9.5 Temperature-time plot for DMC 5's heater head when driven forward and reverse. (At 1500 RPM, 10 Bar mechanism housing pressure and 0.0625 l/s water flow at 13.6 °C)	235
Figure 9.6 Wobble yoke beam side plate broken after 15 hours operation.	236

List of Photos

Photo 6.1 (a) DMC with heat exchangers fitted and dynamometer fitted. (b) Low delta T engine used for demonstrations.	139
Photo 9.1 DMC 5 (a) Assembled. (b) Disassembled	204
Photo 9.2 (a) Manufacturing steps of the mechanism housing. Left to right, wooden pattern, aluminium pattern, finished housing. (b). Recoil manual starter components.	208
Photo 9.3 Alternator components. Top assembled, bottom disassembled.	210
Photo 9.4 Wobble Yoke. (a) Assembled. (b) Disassembled	213
Photo 9.5 Heat Exchangers. Top: etched copper plat for the cold end heat exchanger. Bottom: Heat exchanger partly assembled.	221
Photo 9.6 (a) First burner used on DMC 5 with ceramic caps and steel burner rings. (b). Remote control panel. Left, preliminary circuit showing the starting solenoid and voltage regulator.	224
Photo 9.7 (a) DMC 5 set up in a variable speed lathe for driving tests. (b) Ice formed on the heater heads after driving the engine for 10 minutes.	232

List of Tables

Table 1.1 Decision chart for selecting the most suitable application in New Zealand.	7
Table 3.1 Common 12 Volt yacht appliances.	29
Table 3.2 Daily 12 Volt power requirement for a hypothetical yacht	30
Table 4.1 Preliminary engine specifications and required V_o determined by the various equations.	70
Table 4.2 Required expansion space bore for the required V_o specification in Table 4.1. . . .	70
Table 4.3 Approximate dimensions for engines using various drive mechanisms.	77
Table 4.4 Engine parameters for 200 watt electric output.	79
Table 4.5 Calculated engine data for 200 watt electrical output engine.	80
Table 4.6 Engine parameters for 10 kW shaft output	81
Table 4.7 Calculated engine data 10 kW output engine.	82
Table 4.8 Objectives tree for the SEBCY.	85
Table 4.9 Evaluation table for the five configurations.	86
Table 8.1 Variables passed to the QSFM. Values shown are for DMC 5	179
Table 8.2 Example set of results from a grid search.	185
Table 8.3 Typical sample of recorded and calculated data from one set of results.	195

Nomenclature

A	Area (m^2)
Ah	Amp hour
AC	Alternating Current
B_e	Beale number
BP	Brake power (W)
CD ROM	Compact Disk Read Only Memory
C_n	Configuration number
DAC	IBM computer data acquisition system for a personal computer
DC	Direct Current
DMC	Authors initials used to specify an engine type
d_b	piston diameter
d_r	piston rod diameter
EGR	Exhaust Gas Recirculation
EMF	Electro motive force
FET	Field effect transistor
$F(\theta)_{dn}$	Instantaneous force on bearing d of the n^{th} cylinder
f	Frequency of shaft rotation
I	Wobble yoke mass moment of inertia about the main pivot b ($kg\ m^2$)
IC	Internal combustion engine
k	Coefficient of thermal conduction (W/mK)
L	Length
LCV	Lower calorific value
LPG	Liquified petroleum gas
$M(\theta)_{xx}$	Moment about the x axis
m_n	Piston assembly mass including the connecting rod
m_{bal}	Balance mass
m	Mass flow rate

N	Engine frequency (cycles/s)
n	Cylinder number (n=1 on positive x axis, n=3 on the positive z axis)
P	Pressure (Bar)
$P(\theta)_n$	Instantaneous pressure in the compression space of the n th cylinder (Bar)
$P(\theta)_{n-1}$	Instantaneous pressure in the expansion space of the n th cylinder (Bar)
P_b	Buffer space pressure (Bar)
P_{mean}	Mean cycle pressure (Bar)
P_{max}	Maximum cycle pressure (Bar)
P_{shaft}	Engine Power at the engine output shaft (W)
P_{Sc}	Engine power determined by the Schmidt analysis (W)
PTFE	Polytetrafluoroethylene
PV	Pressure * Velocity
Q	Heat flow (W)
R	Rotational degree of freedom
r	Radius or distance, (m)
r_{bal}	Radius of balance mass, (m)
S	Stroke, (m)
SEBCY	Stirling Engine Battery Charger for Yachts
SEDA	Stirling Engine Design Aid
SF	Safety factor
SLI	Starting Lighting Ignition battery
SOS	Slotted Optical Switch
STM	Stirling Thermal Motors
T	Temperature
TOP FET	Temperature overload protected field effect transistor
$T(\theta)$	Instantaneous torque (Nm)
t	Heat exchanger wall thickness (m)
X	Dead volume ratio, V_d/V_{exp} .

u	Piston/seal interface velocity (m/s)
V	Volume (cm ³)
V_d	Dead volume (cm ³)
W_n	West number
x	Axis passing through the centre of cylinders 3 and 1
y_{bal}	Distance between the balance masses parallel to the engine axis (m)
y	Axis of engine
z	Axis passing through the centre of cylinders 2 and 4

Greek Letters

l	Number of Stirling Cycle in an engine
η	Efficiency
τ	Temperature ratio. T_c/T_H
κ	Swept volume ratio. V_{com}/V_{exp}
α	Phase angle.
Γ	Temperature ratio, $(T_H - T_c)/(T_H + T_c)$
T	Torque (Nm)
γ	Material stress (N/m ²).
θ	Instantaneous crank angle, rad
ω	Crankshaft angular velocity, rad/s
γ	Maximum beam displacement angle, $\gamma = \sin^{-1}(\text{stroke}/2r_{bd})$, rad
κ	$\tan(\gamma)$
$\phi(\theta)$	Instantaneous beam angle, rad

Acknowledgements

In a broad design oriented research project such as this there were few mechanical engineering disciplines that were not utilised. Consequently there were also few members of my Department that have not helped in some manner during the course of this project. The author greatly appreciates the help given and thanks those concerned. Several people involved in the project deserve my deepest gratitude, they are:

Dr John Raine for his excellent help, reassurance, support and guidance throughout the project. I find it difficult to imagine a better supervisor for such a project.

Dr Alan Tucker, Dr Jeremy Astley and Professor Harry McCallion for their assistance and trust in me during the initiation of this project.

Mr Ron Tinker and Mr Eric Cox for their assistance in the laboratory.

Mr Peter Lynn, for the initial inspiration and help at the beginning of the project.

Mr Ken Brown for his professional expertise and diligence in manufacturing the DMC 5 engine components.

Mr Philip Smith for his assistance with the computational work.

Mr Hank Anink, Mr Julian Murphy and Dr R. Dunlop for their assistance with the electronic development.

Mr Geoffrey Leathwick for his patience and expertise with obtaining the materials.

cont.

Mr Bruce Sparks for his assistance with photography.

Mr Hamish Trolove for assistance with the editing of this thesis.

The Department of Mechanical Engineering, The University of Canterbury, for funding the project.

My family and friends for their help and support.

Finally I would like to pay a special tribute to my wife, Jane, for her love and support throughout this project.

1 INTRODUCTION

1.1 Project Background

In recent years the New Zealand economy has been in a recession, and the need for new specialist industries has been emphasised as one strategy for recovery. At the same time there has been growing awareness worldwide of the need for sustainable technology and conservation of energy and natural resources if the Earth is to remain a suitable living environment for our descendants and remaining wildlife. The Earth's eco-system can sustain only a limited amount of abuse from the exploitation of its natural resources, unchecked population growth, and the ever increasing volumes of harmful wastes which are pumped into the environment. Professional engineers with an understanding of energy flows in society, the impact of technology and resource depletion, have a responsibility to lead in caring for the environment and providing a viable long term habitat for human, plant and animal life.

It was against this background that in 1989 the author was motivated to add Stirling engine research to other current energy and environmental research programmes at the University of Canterbury. The design-oriented project undertaken was also considered to have future commercial potential in evolving a product which would contribute, in a modest fashion, to the redevelopment of secondary industry in New Zealand following the de-regulation of the economy in the mid-1980's.

The externally heated closed cycle Stirling Engine which expands and contracts one mass of working fluid has been admired for its favourable environmental qualities for many decades. However, despite the considerable effort in research and development since the renaissance of the Stirling Engine in 1938 at Philips Eindhoven, model engines are the only mass produced Stirling Engine prime movers available worldwide. High production costs and several technical difficulties have prevented market acceptance and substantial commercialisation.

1.2 Why Investigate the Stirling Cycle

The Stirling Cycle principle originated prior to the development of the modern internal combustion engine, and during the nineteenth century was successfully applied to many applications, often as a safe alternative to the steam engine. However, due to lack of suitable materials, appropriate technology, and the rapid development of the higher specific output internal combustion engines and electric motors, production of commercial Stirling engines nearly ended around the turn of the century.

Prior to the Second World War, Philips began researching a small portable and quiet generator to power valve radios in remote areas. They subsequently developed, among many other engines, the Philips 1002C Stirling Engine of which several hundred were produced. Around the same time transistors were beginning to replace the power hungry valves used in radio equipment and it was decided that further production of the 1002C engine was not warranted and modern batteries were more suitable, (Hargreaves, 1991). Most of the 1002C engines which were manufactured were subsequently distributed internationally in universities and other research institutions, including the University of Canterbury. Philips went on to develop propulsion engines, cryogenic refrigeration plant and stationary engines all based on the Stirling Cycle. Inspired by Philips, the Stirling Cycle Machine has had a major revival throughout the world particularly within the last twenty years. It's many qualities include:

- **Low noise level** - no atmospheric cylinder ports and no explosive combustion.
- **High efficiency** - theoretically equivalent to the Carnot efficiency, $1 - T_K/T_H$.
- **Low vibration** - dynamically balanced mechanisms can be produced.
- **Multi-fuel capability** - the engine is externally heated so virtually any heat source with sufficient temperature can be used.
- **Reliability** - due to external combustion no combustion products are in contact with the working components, allowing long component life and in some cases maintenance free operation.
- **Low pollutant emission** - external combustion allows more control over the combustion products and choice of fuel than with internal combustion engines.
- **CFC-Free Refrigeration** - driving the cycle causes a heat pump effect and considerable research is devoted to cryogenics and heat pumps.

Limited commercial success has been mainly due to engine complexity, and high manufacturing and material costs. For example, a Stirling engine for an automobile is about twice the price of a comparable diesel engine (Machine Design, 1989). Reasons for this are often attributed to:

- Extreme material requirements of the heat exchangers.
- Harsh sealing environment requiring dry running dynamic seals in some designs.
- Complex power control systems to give suitable accelerator response times.
- Considerably higher cooling load in comparison to diesel engines of similar power.

Consequently, despite the positive qualities, there are few commercially produced engines available today. Technically these obstacles are solvable but manufacturing costs and market acceptance will remain a major barrier.

1.3 Possible Applications

An early task in this project was the selection of a suitable application to base the project on. It was decided that research of a specialised component, for example a seal system, may aid future Stirling Engine research but would do little to promote the use and understanding of the Stirling Engine, particularly in New Zealand. It could be argued that an important reason for limited commercialisation of the Stirling Engine is the lack of public awareness and acceptance of the engine as a clean alternative. Hence an application was sought which would:

- Help to promote the Stirling Engine as a realistic design option.
- Be manufacturable in New Zealand after the development of suitable technology.

Many applications were investigated and the following paragraphs give brief descriptions of some of the main contenders.

1.3.1 Recharging Wheelchair Batteries

A problem associated with electric wheelchairs is running out of power in locations and at times when it is inconvenient to stop and recharge. An on board Stirling Engine battery charger could be used to recharge the batteries quietly and efficiently. An added bonus is "on board" heating from the Stirling Engine waste heat, paraplegics suffer from cold due to poor circulation, particularly in the legs.

1.3.2 Ocean Going Racing and Cruising Yachts

The primary auxiliary power supply for yachts is generally a marine diesel engine. This is often used for generating electricity, refrigeration, desalination, heat pumping and propulsion. Often this engine is run for many hours of the day and is the scourge of many sailors due to noise, vibration, odours and inefficiency. It is possible to produce a total energy package based on the Stirling Engine which would be less disturbing to the boat occupants. A similar concept was developed for the Winnebago motor home, (Bragg, 1978).

1.3.3 Military Applications

For military applications the Stirling Engine has many advantages such as its multi-fuel capability and quiet operation, (Flynn et al, 1960).

1.3.4 Waste Heat Recovery

Many companies and local bodies use incinerators which waste the heat generated from the combustion process, Stirling Engines could be used to convert this energy.

1.3.5 Telecommunications

Repeater stations require an efficient and reliable electrical supply often in places where mains electricity is not available or economic to supply. A Stirling Engine system could be an alternative.

1.3.6 Waste Burner Generator

Many remote villages in underdeveloped and developing countries require contemporary fuels for prime movers which are often hard to obtain. However biomass or other wastes such as rice hulls are often available. These wastes could be used to heat a Stirling Engine energy conversion system, (West, 1986) .

1.4 Application Selection

An indication of the reasoning used in the selection process is presented in Table 1.1 showing the considered merits of each application. A score of 1-10 is given, 1 being less desirable than 10. (This type of presentation is very subjective and serves only as an indication).

Final success of the project will require that a market exists which can afford to pay the additional cost of the Stirling Engine system and this is taken into account in Table 1.1.

Application ^a	1.3.1	1.3.2	1.3.3	1.3.4	1.3.5	1.3.6
Suits Stirling Engines qualities ^b	8	9	8	8	6	6
Suitable for N.Z. ^c	8	10	5	7	6	2
Manufact. in N.Z. ^d	10	10	8	8	10	10
Public Awareness ^e	6	8	4	6	6	7
Viable Market ^f	6	8	4	6	5	6
Known Previous Research ^g	10	8	2	7	2	1
Major Competitor ^h	4	6	1	3	3	3
Total	52	59	32	45	38	35

- a. Refers to previous paragraph numbers
- b. eg. Environmentally and/or user friendly
- c. Does the application suit N.Z markets
- d. Are there local manufacturing facilities and materials available
- e. Will the application generate public awareness and appreciation of the Stirling Engine
- f. Are there enough possible purchasers with sufficient disposable income.
- g. Has there been considerable previous research of this application and is there scope for further research.
- h. For example the internal combustion engine, solar, wind etc.

Table 1.1 Decision chart for selecting the most suitable application in New Zealand.

From a possible score of 70 the marine engine ranked highest and was chosen the most suitable application.

1.5 Introduction to the Yacht Application

Off-shore and coastal yachts (sail boats) place an increasingly high demand on both prime mover and electric power while both in motion and when moored, (Calder, 1990). The typically powered devices are navigational aids, refrigeration, microwaves, desalinises, stereo, radio, computers, winches, compressors and air conditioners. In most cases these loads are directly (belt, gear) or

indirectly (electric, hydraulic) powered by the main propulsion diesel engine which is typically greater than 10 kW. Occasionally most of the energy these devices require can be supplied during motoring out of a harbour or while motor sailing. However, more often than not the main propulsion engine is run a little above idle more than 1 hour per day to charge batteries and in some cases provide refrigeration regardless of weather, sea conditions and if the craft is moored or mobile. Unfortunately the load on the engine is very low compared to propulsion requirements and hence low efficiencies and fouling of the engine occur. In addition diesel engines are noisy, polluting and transmit a vibration through the craft often making living conditions uncomfortable detracting from the pleasures of sailing.

It was decided that the Stirling Engine is an ideal candidate for an auxiliary power supply due to its quiet characteristics, high part load efficiency and is unaffected by environmental conditions, unlike solar, wind and tow generators, Section 3.4.

1.5.1 Total Energy System

The ideal Stirling Engine system for a yacht would supply the total auxiliary energy requirements including electricity generation and propulsion. From the Winnebago motor home project, (Bragg, 1978), it seems likely that such a system is indeed feasible and interest in this application is growing internationally.

1.5.2 Battery Charger for Yachts

For a new field of research and development it was decided that a total energy system would be outside the feasible limits of the Department's resources and it was decided to concentrate on the main concern of the yacht owners, that is, charging the batteries. However in developing this system the design should be suitable for scaling up for higher power requirements. This was a major influencing and sometimes compromising factor on the overall engine design.

1.6 Objectives Of The Project

1.6.1 Primary Objective

To produce and test a commercially viable prototype Stirling Engine 12 volt 200 watt battery charging system suitable for yachting applications. The design, however, was also to be suitable for being used in similar applications other than yachts, for example remote holiday homes and villages. In addition the design was required to allow parametric scaling for multi kilowatt engines, which may have better commercial prospects.

1.6.2 Secondary Objectives

In achieving the primary objective, 1.6.1, many design difficulties with the Stirling Engine were solved or eliminated in a cost effective manner while meeting the overall design requirements. Addressing some of these design difficulties led to several key topics of novel research which are presented in the appropriate Chapters of this thesis. Novel research and development presented in this thesis includes:

- **The overall Stirling Engine battery charger system:** The system design requirements are developed and by using a methodical design approach the system was successfully developed.
- **Wobble Yoke kinematic mechanism:** This novel mechanism, invented by the author, avoids the use of spherical bearings allowing single degree of freedom bearings to be used in parallel axis multiple cylinder machines. The mechanism kinematic and load Equations are derived. The use of this mechanism is not limited to Stirling engines and other applications are presented.
- **Piston seals:** Investigations of piston sealing techniques led to the development a novel cylinder mounted seal system offering some advantage over conventional piston ring

designs. Computer code was developed to simulate the seal behaviour over several thousand engine cycles, this allowed seal design optimisation.

- **Heat transfer systems:** Previously there have been many extensive projects concerned with the heat exchanger modelling and design. The objectives of this project did not include adding to this theory. Several alternative heat exchanger systems were developed, however, and optimisation of these heat exchangers was aided by use of a customised published simulation program.
- **Control and battery charging:** For commercial success the SEBCY must be self regulating, easy to install and use. This posed many system design problems which are presented and overcome.
- **Alternator and starter:** To enable a self starting and compact engine/alternator system, a modified automotive alternator was developed. Using modern electronic components it was found possible to alternately switch the star wound alternator windings to work as a starting motor powered from the system battery.

1.6.3 Chapter Contents

- Chapter 2: Introduction to the Stirling Cycle and relevant literature.
- Chapter 3: Review of battery design and battery charging technology currently used on yachts.
- Chapter 4: Preliminary engine design. Comparison of various engine designs and selection of the most appropriate.
- Chapter 5: Development of the wobble yoke mechanism and its kinematic Equations. Use of these Equations in a case study of the SEBCY application. Presentation of other applications for the wobble yoke.
- Chapter 6: Five Stirling engines were made and tested over the duration of this project. The construction, test equipment and results of testing these engines are discussed.

The second engine was based on a converted two stroke motorcycle engine. The third engine, originally used for seal testing, made use of the wobble yoke and had an internal hermetically sealed dynamometer to remove uncertainties with atmospheric seal losses.

Chapter 7: Seal technology used with Stirling engines and development and testing of the cylinder mounted seals.

Chapter 8: Design and optimisation of the SEBCY heat exchangers. Various optimisation techniques are evaluated. The simple grid search technique was chosen, this is the most reliable but also the most computer time consuming. A flat plate compact cold end heat exchanger is developed and techniques for manufacture are evaluated.

Chapter 9: Detailed design of the SEBCY preproduction prototype. Manufacturing and assembly problems are discussed. The prototype test results are reported and evaluated.

Chapter 10: Project conclusions and recommendations.

2 The Stirling Engine

2.1 Introduction

This Chapter discusses the ideal Stirling Cycle, the practical engine, its various configurations, and applications. The Stirling Cycle principles are discussed first as it gives the reader a better insight of the historical developments discussed later in the Chapter. Stirling Cycle technology is now a vast subject ranging from cryogenic coolers to domestic heat pumps with an equally large amount of supporting literature. For the sake of brevity the following is restricted to prime movers.

2.2 The Ideal Stirling Cycle

The Stirling engine is a device that operates on a closed regenerative thermodynamic cycle. Cyclic compression and expansion of the working fluid occurs at different temperature levels while flow is controlled by volume changes rather than valves (Walker, 1980). The ideal Stirling Cycle is represented in Figure 2.1. The main thermodynamic components required for the Stirling cycle are:

- (i) variable volume expansion space where the working fluid absorbs heat from the surroundings,
- (ii) regenerator which absorbs and releases heat respectively from and to the working fluid and
- (iii) variable volume compression space where the working fluid rejects heat to the surroundings.

The work done on the pistons by the gas is determined by integrating the area of the pressure-volume diagram. To increase the area while keeping the swept volume constant the mean cycle pressure can be increased by engine pressurisation. This has a similar effect to turbocharging an internal combustion engine but does not require a continuous supply of pressurised working fluid due to being a closed cycle. Engine pressurisation is essential if high power densities are required. Increasing the temperature difference $T_{\max} - T_{\min}$

is another method for increasing the work done. The ideal thermal efficiency of the Stirling cycle is equivalent to the Carnot

efficiency, $1 - T_{\min}/T_{\max}$ (Walker, 1980). Therefore increasing the temperature difference also has the effect of increasing the ideal cycle efficiency. For an ideal cycle the amount of heat rejected in the process 4-1 is equal to the heat received in process 2-3. Rather than waste this energy, a regenerator, which is usually made from fine wire mesh, is used to absorb the heat in process 4-1 and give it back to the working fluid in process 2-3. Increasing the dead volume, V_d , (internal volume not swept by the pistons) decreases the pressure amplitude and hence the work done per cycle. The phasing of the pistons is also critical and generally for a prime mover the expansion space variation leads the compression space variation by 90 to 120 degrees.

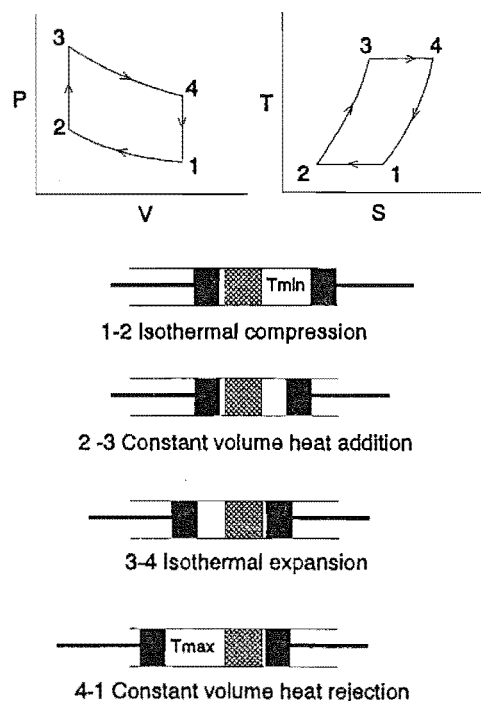


Figure 2.1 Ideal Stirling Cycle.

2.3 Practical Stirling Engine

The real Stirling engine does not, however, behave as described in Section 2.2. In most real engines the pistons are linked by some form of mechanism or gas spring which causes continuous piston motion. Also isothermal processes are not possible at useful engine speeds as the cylinder walls have finite conductivity. Consequently a continuous cycle of near adiabatic compression, near constant volume heat addition, near adiabatic expansion and near constant volume heat rejection results. For an engine of practical power delivery the rate of heat transfer through the cylinder wall is insufficient and heat exchangers are required between the expansion space and regenerator and the compression space and regenerator Figure 2.2. The void volume of these heat exchangers decreases the work done per cycle by adding dead volume, V_d . Pressure drop due to flow loss from restricting flow paths in the heat exchangers also reduces the engine power and efficiency. This creates a very complex simulation and optimisation problem which is dealt with in Chapter 8.

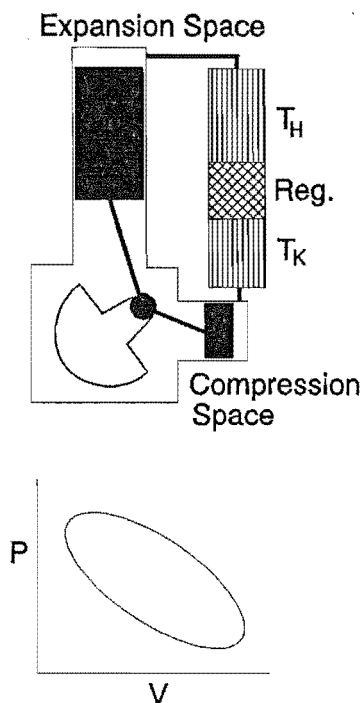
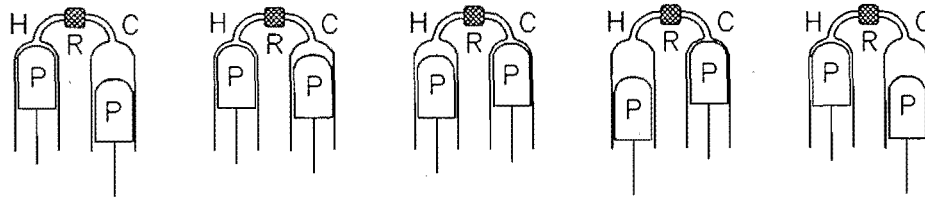


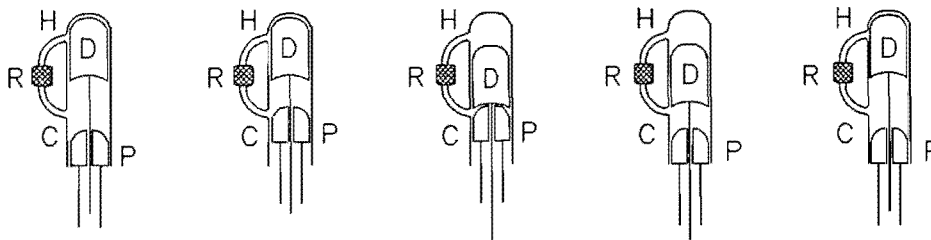
Figure 2.2 Real Stirling engine.

2.4 Engine Configuration

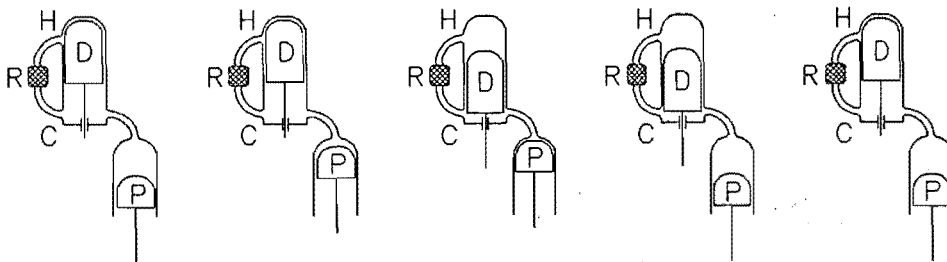
The Stirling engine can be realised in a number of configurations which were categorised by (Kirkley, 1962) as shown in Figure 2.3. The four cycle double acting configuration shown is a special case of the alpha configuration and was chosen for the prototype SEBCY, Chapter 4.



Alpha

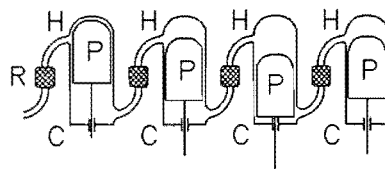


Beta



Gamma

H=Hot
R=Regenerator
C=Cold



P=Piston
D=Displacer

Four Cycle Double Acting, FCDA

Figure 2.3 Alpha, Beta and Gamma configurations. The four cycle double acting layout is a special case of the Alpha configuration.

The pistons or displacers do not have to be connected via a rigid mechanism and Beale developed the first free piston engine, (Reader and Hooper, 1983). The free piston engine has great potential and recently has been the subject of considerable research for both prime mover and cooling devices, Figure 2.4. The requirement for an output drive shaft for larger engines eliminated the free piston engine from this project and the following is restricted to kinematic (rigid link) engines.

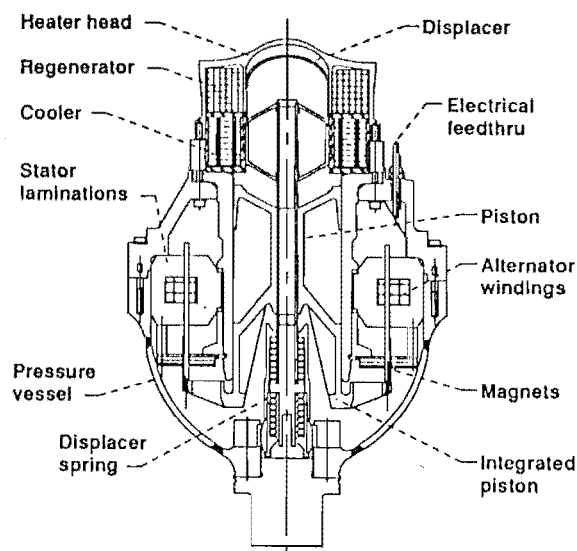


Figure 2.4 Free piston linear alternator.

2.5 Literature

The number of publications on Stirling Cycle related topics has grown considerably over the last 20 years. For historical developments publications such as Finkelstein (1959), Walker (1980), Sier (1973), Ross (1977) and Hargreaves (1991), Percival (1974) should be consulted. For general background and theory there are several excellent texts such as Walker (1970 and 1980), Reader and Hooper (1983), Hargreaves (1991), Martini (1983), West (1986) and Urieli and Berchowitz (1984). Research and development publications began during the 19th century in *The Engineer* and *Engineering* periodicals. The first quarter of the 20th century saw the renaissance of the Stirling engine and later excellent reviews were published in the *Philips Technical Review* series. The 1966 IECEC saw the first Stirling engine publication and year by year the number has increased until the present time when a complete volume of the IECEC proceedings is devoted to the Stirling cycle. Unfortunately few of these proceedings are held in New Zealand. From this and several other recent projects the University of Canterbury Engineering Library now subscribes

and the 1992 proceedings onwards are available. All abstracts for previous years are published in the Martini Memorial volume (Walker 1986) up to 1986 and the rest are easily obtained from the Engineering Library Engineering Index CD ROM. During 1982 the first international conference devoted solely to the Stirling cycle was held. The International Stirling Engine Conference is now held regularly and all the proceedings, (1982, 1984, 1986, 1988, 1991, 1993) are now held at the University of Canterbury.

2.6 Brief History

The first design for a practical closed cycle regenerative engine was published by Robert Stirling in his 1816 patent titled "Improvements for diminishing the consumption of fuel, and in particular an engine capable of being applied to the moving of machinery on a principle entirely new". The patent could have been divided into two patents as it deals with heat exchangers and the Stirling engine as an application of the heat exchangers. Robert Stirling was an ordained minister of the

Church of Scotland and with the assistance of his younger brother James produced serviceable engines well before the correct theory was available to analyze and design them. There is considerable debate over which brother provided the intellect, (Reader 1991, Sier 1991). It would appear that Robert Stirling provided at least the initial concepts as his patent was applied for while James was still very young. The Stirling brothers had moderate success and utilised the regenerator and engine pressurisation which was not adopted by other engine manufactures for almost a century. The major failing of their engines was the lack of suitable materials for the hot

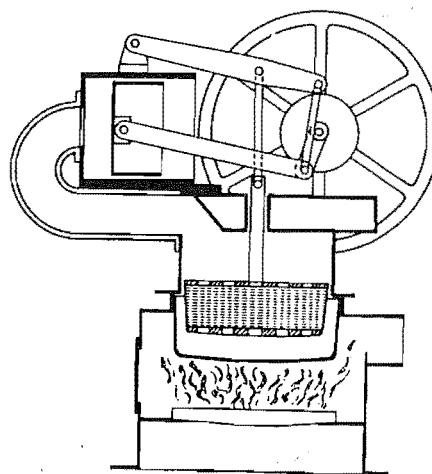


Figure 2.5 Last commercially produced Stirling engine prior to 1937, after Hargreaves, (1991).

end heat exchanger. The hot air engine, as they were then known, used air as the working fluid, and was popular due to its relative safety compared to the steam engine. Later in the century when better materials were available, many thousands of hot air engines were produced generally to drive water pumps or fans. Most of these were of low power and heavy due to operating at atmospheric pressure, but did not require an operator with a steam ticket. Commercial competition from internal combustion engines and electric motors meant that only a small number of engines were being manufactured after the turn of the century.

In 1937, Philips of Eindhoven, the Netherlands, required an engine to generate electricity for remote radios. H. de Brey made a systematic comparison of past prime movers and concluded the hot air engine offered the best prospects (Hargreaves 1991). Use of modern heat resistant materials, engine pressurisation, higher engine speed, and the regenerator enabled the Philips engineers to dramatically increase the engines power per kilogram by a factor of 50, reduce its physical size per unit power by a factor of 125, and improve its efficiency by a factor of 15 (Reader and Hooper, 1983). Problems with seals, heating, lubrication and power control frustrated the engineers. Batteries were sufficient when transistors replaced the power hungry valves used in radio equipment thereby eliminating this market for Stirling engines. Philips realised the potential of their engine and continued work on prime movers and later cooling engines.

In 1949 a Philips air charged engine exploded. This occurred when lubricating oil leaked into the working space and then ignited in the pressurised air due to the high temperature (Hargreaves 1991). After an investigation it was decided that future engines should use an inert gas. Later engines used nitrogen, hydrogen or helium. The latter two gases are now preferred for high performance engines due to better heat transfer and viscous properties. It was then decided to rename the engine to Stirling engine. The engine developments at Philips went through several stages brought about by successive engineering developments including: pressurisation, rhombic drive, roll sock seal, swash plate, variable angle wobble plate, variable angle swash plate. Engines

from several Watts to hundreds of kilowatts were produced and tested but the major Stirling Cycle commercialisation was from refrigerating machines. Many licensees were contracted, drawn by the prospect of producing better propulsion engines but it was found that the extra cost of the Stirling engine, approximately twice a comparable diesel, made the automobiles prohibitively expensive. Some other applications which the licensees investigated were space and under water power plants.

In 1976 Ford, a licensee, moved its resources to more pressing problems in its company marking the end of major automotive developments. Philips decided in 1979 that its future products would not include the Stirling engine. The head engineer Dr. R. Meijer set up a licensee company in the USA to further develop and market Stirling engines under the company name Stirling Thermal Motors (STM). The work at STM is based on the STM4-120 engine which is a four cycle double acting variable stroke engine with very promising performance.

Many other research teams and individuals have worked on or are working on the Stirling engine but there are still few commercially produced prime movers, other than models, available.

2.7 Comparison With Internal Combustion Engines

The invention of the internal combustion, (IC), engine undoubtedly brought about the early commercial demise of the Stirling engine due to its fast development to a higher power to weight ratio engine. Today the Stirling engine can match power performance and better many other attributes of the IC engine, but the considerable investment in IC engine manufacturing technology is very difficult to compete with.

2.7.1 Energy source

The Stirling engine only requires a sufficient temperature difference $T_{\max} - T_{\min}$ to operate. Senft produced a demonstration engine which has run with a temperature difference of only 0.4°C , (Senft, 1991). The maximum temperature difference is limited by the heat sink temperature, usually atmospheric and hot end material temperature limit. The heat source can be chemical, solar, nuclear or thermal storage. By use of heat pipe technology the heat source does not have to act directly on the hot end heat exchanger, (Hargreaves 1991, Meijer 1970). This can allow a more convenient heat exchanger design and much higher rates of heat transfer.

2.7.2 Energy Sink

As stated by the Second Law of Thermodynamics heat must be dissipated from an engine, Figure 2.6, (Rogers and Mayhew, 1983). Considerable heat is discharged from an internal combustion engine by the exhaust direct to the atmosphere. In a diesel engine about $1/3$ of the heat supplied by combustion is dissipated by the exhaust and $1/3$ by the radiator. With the Stirling engine, heat rejected by the exhaust has not gone through the

engine cycle and is therefore wasted. Consequently, to maintain a high engine efficiency, more heat must be dissipated by the radiator. This puts about twice the thermal load on the radiator than a comparable diesel engine, (Walker et al, 1993). This is less of a concern with marine engines but can add considerable expense and bulk when the heat is dissipated to the atmosphere via a radiator.

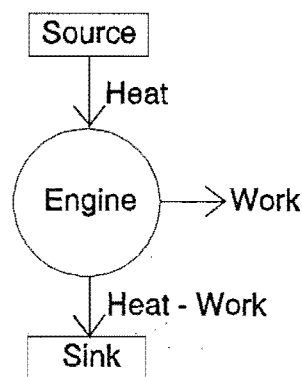


Figure 2.6 Energy transfer.

2.7.3 Long Engine Life

Because the engine is closed cycle the heat must be transferred through a pressure wall unlike the internal combustion engine. Consequently no combustion products are in contact with the engine working components allowing long engine life and fewer lubricant changes.

2.7.4 Balance

Single cylinder Stirling engines can be completely dynamically balanced using the rhombic drive and likewise multiple cylinder engines when the swash plate is used.

2.7.5 Starting

Once sufficient temperature difference is achieved Stirling engines are very easy to start. Four cycle double acting engines are theoretically self starting (Rice, 1991) but in practice require a small shaft rotation due to friction and seal leakage. The STM4-120 can be started by suddenly changing the angle of the variable angle swash plate (STM, 1990). Free piston engines are also theoretically self starting but a small nudge is sometimes required (Walker, 1980). Achieving the high temperatures before the engines starts is a problem for combustion heat sources. In high performance engines the combustor requires a blower which can be driven by the engine shaft once rotating but requires an auxiliary drive when preheating.

2.7.6 Exhaust emissions

During the 1970's low toxic exhaust emission was a popular advantage of the Stirling engine over internal combustion engines. Recent developments in reducing internal combustion engine emissions have decreased this benefit. Oxides of nitrogen are the worst emission and these can be reduced by exhaust gas recirculation, EGR (Reader and Hooper, 1983)

2.7.7 Quiet operation

Quiet operation is a consequence of being a closed cycle, unlike the internal combustion engine which has intermittent cylinder intake, combustion, and exhaust. The heater blower and continuous fuel combustion often emit the most noise from the Stirling engine. If gears are used, as used with the rhombic drive, careful design is required to ensure gear noise is not excessive.

2.8 Marine applications

Marine applications for the Stirling engine are certainly not novel. There have been many research projects on this subject, some of which are briefly noted in the following.

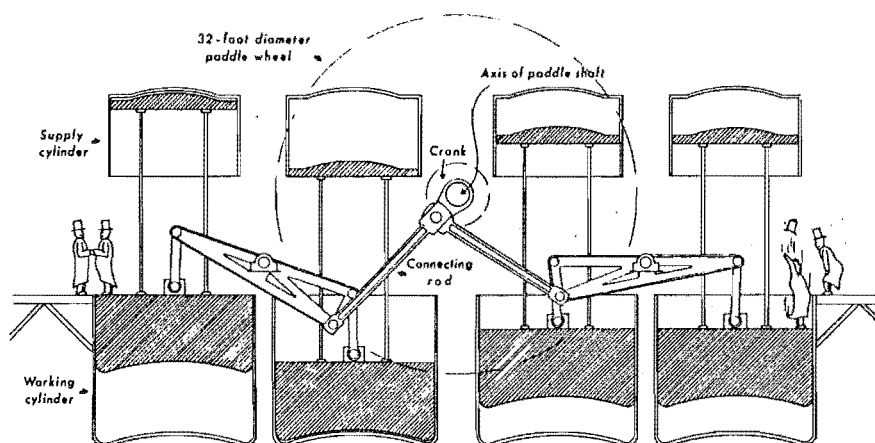


Figure 2.7 Ericsson's huge marine engine.

Possibly the most notable marine application of a hot air engine was a huge engine designed by John Ericsson in 1853 and fitted in a 2200 ton ship Figure 2.7. The cylinders were fourteen feet diameter and the pistons had a stroke of six feet. The ship never met its expectations developing only a fraction its design power. After sinking on a sea trial the hot air engine was replaced by a steam engine (Ross, 1977).

2.8.1 Philips Marine Applications

Philips saw a great potential for their engine in marine applications. In 1946 they signed a contract with the US navy to develop three engines of 200, 750, and 1500 W over a 10 year period. The most relevant of these was a small 200 W four cycle double acting electric generator, Figure 2.8, (Hargreaves, 1991).

Until the publication of this text the author was not aware of research on small, <1 kW, four cycle double acting engines other than for models. The initial designs for the prototype SEBCY engine had already been developed by this stage (Clucas and Raine, 1992). The development of this Philips engine ended in 1948 when engine testing was disrupted by seal and lubrication difficulties. In 1957 a two cylinder beta configuration engine was fitted

as an auxiliary engine to a boat which produced 2 HP and gave a boat speed of about 6 km/hr. In 1950 a small beta configuration engine was also fitted to a small skiff which was propelled silently around the waters of Dordrecht. In 1959 a 40 HP rhombic drive engine charged with hydrogen at a mean pressure of 105 a m was fitted to a small motor yacht to get practical marine experience. A flat four boxer engine was also built in 1966 but tests were not entirely satisfactory and before modifications could be performed more urgent projects had to be addressed, Figure 2.9(a).

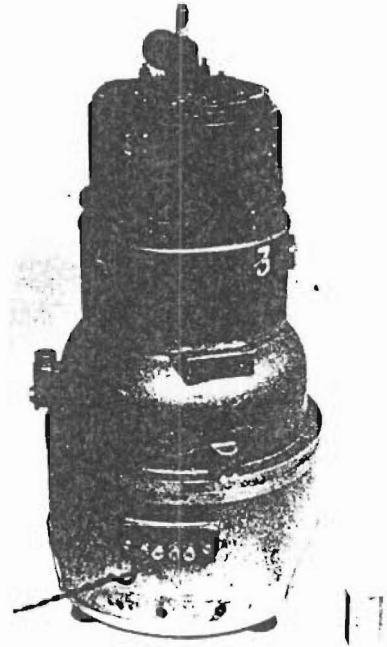


Figure 2.8 Four cylinder double acting wobble plate engine, after Hargreaves, (1991)

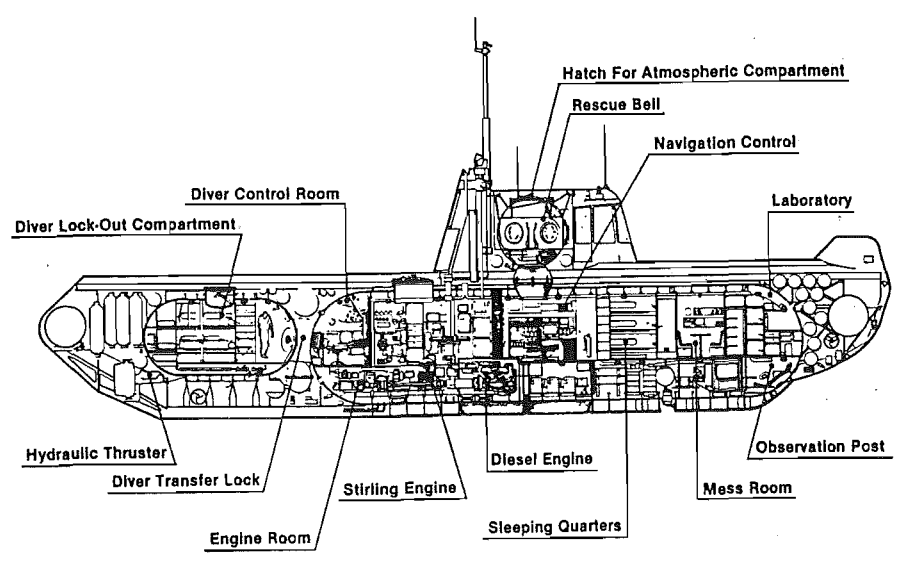
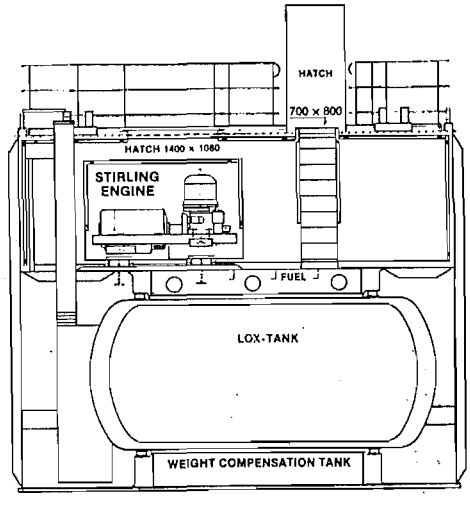
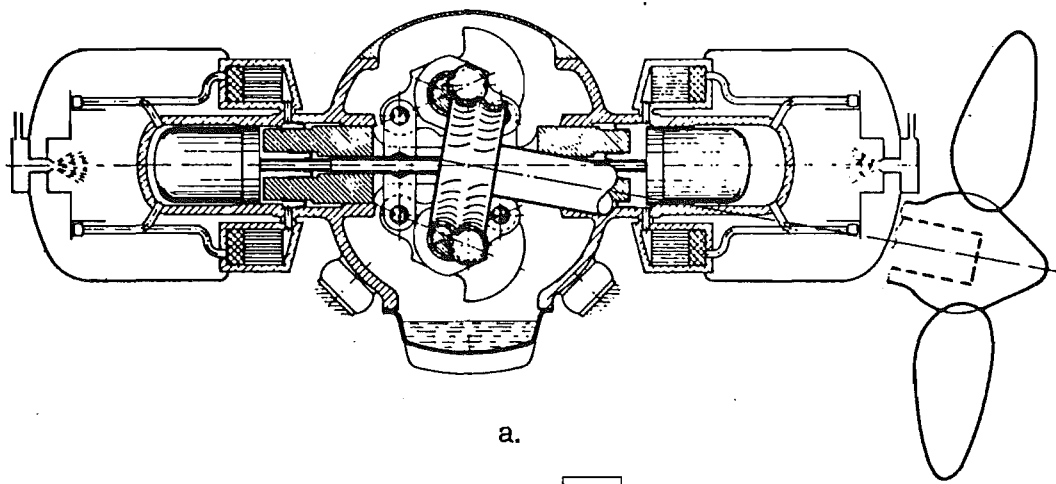


Figure 2.9. Marine applications of the Stirling engine

2.8.2 Marine Applications Outside Philips.

Other marine applications include:

- (i) **Submersibles:** (Nilsson, 1988), Figure 2.9(b) and (c).
- (ii) **Torpedoes:** (Walker, 1980)
- (iii) **Auxiliary power:** (Walker 1980, Bartolini 1991, Walker 1991)
- (iv) **Propulsion:** (Walker et al, 1988), (Reader and Hooper, 1983), (Benvenuto, 1991)
- (v) **Trickle battery chargers,** (Walker, 1986).

The most applicable of these to this project are:

- (i) **Ross silent boat engine:** Walker et. al. (1991) presented a conceptual design for a 10 kW 20 bar air charged twin opposed engine suited to sailing boats Figure 2.10(a). It appears, however, the mechanism would not be able to rotate. The yoke must rotate about an axis normal to the page, however the rigid connecting rods are fixed to the yoke extremity. Despite this oversight the concept seems viable but no hardware had been developed up to 1991 (Walker, 1991).
- (ii) **Winnebago motor home:** Stirling Power Systems produced a compact 10 HP V-2 engine system designed to provide all auxiliary power requirements for a Winnebago motor home including air conditioning and electricity Figure 2.10(b). It has been suggested that this system would be suitable for yacht applications but no references have yet been found of this having been accomplished.
- (iii) **Yacht Battery Charger:** Bartolini (1991) published details of a 500 W battery charging Stirling engine based on a single cylinder beta configuration Figure 2.10(c). At the time

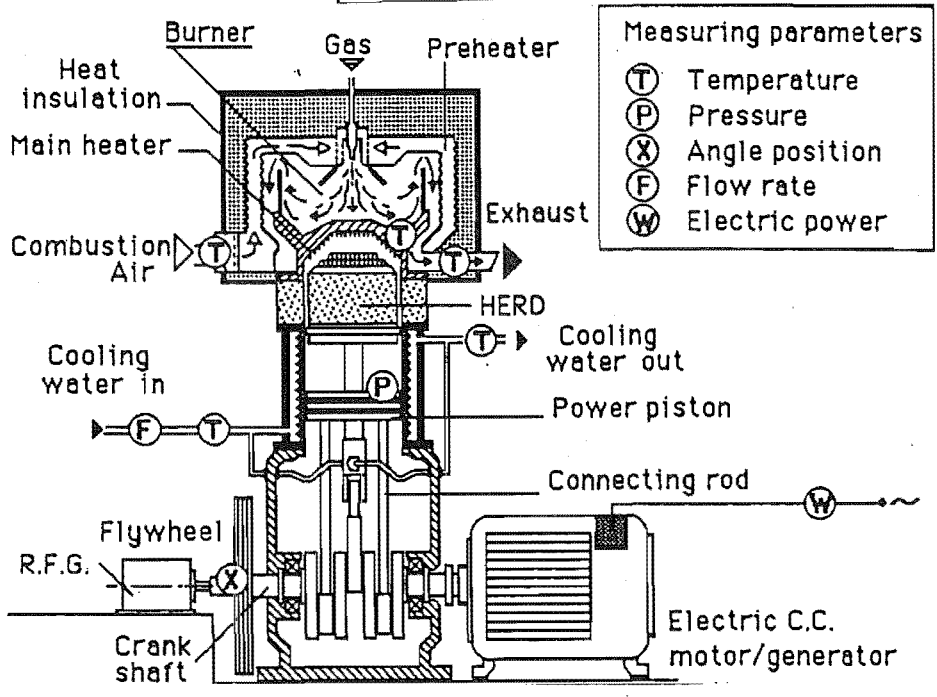
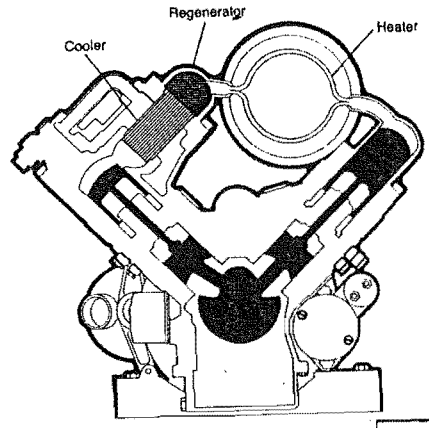
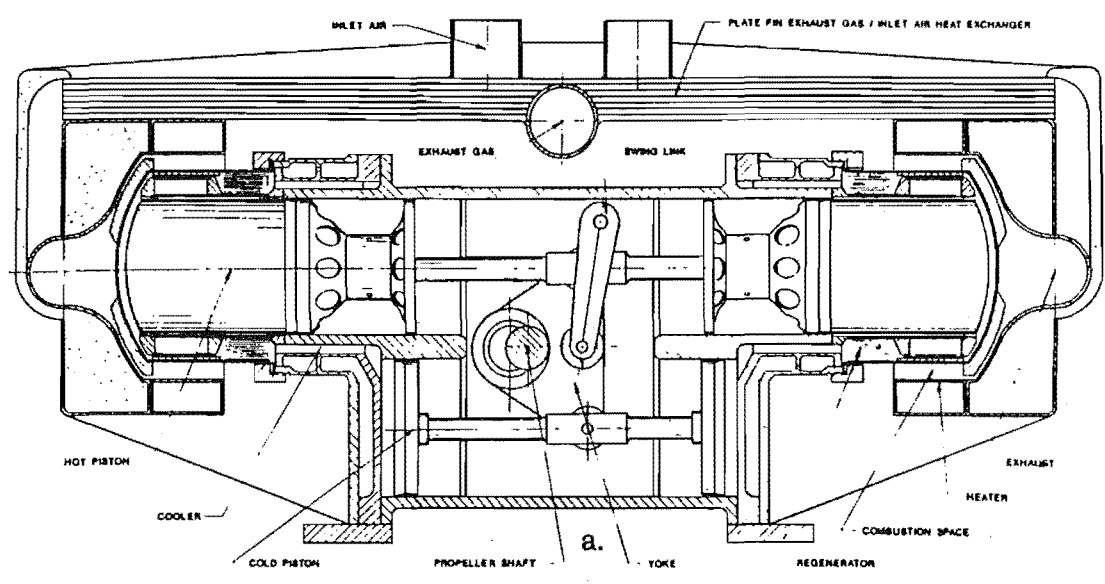


Figure 2.10 Similar developments.

c.

of publication this engine had developed a fraction of its design power. Scaling from Figure 2.10(c) where the bore is 100mm diameter the system appears quite bulky for its power.

- (iv) **Ross Yoke:** reports of a small generator based on the Ross yoke engine have been published, but no reports of hardware being available on the market have yet been found.

2.9 Conclusions

- Modern Stirling Cycle research includes: Free piston engines, refrigeration, cryogenics, space power generation, solar energy conversion, auxiliary power units, heat pumps, prime movers, cogeneration plants. The scope for Stirling Cycle research is vast and this project investigates one application that is auxiliary power generation.
- There is a vast amount of literature on the Stirling engine and emphasis in this review has been on prime movers suited to marine applications.
- The Stirling engine does not operate as an ideal Stirling Cycle, and simulation-optimisation of the engine is very complex, refer Chapter 8.
- The Stirling Engine is ideally suited to marine applications and there has been considerable research and development on this subject.
- There have been several recent developments with a similar theme to this project and some commercial competition may exist from other Stirling Engine manufacturers.

3 Battery Charging on Yachts

3.1 Introduction

A boat's electrical system is stand alone, on board the electricity is generated, stored and dissipated. Electricity generation and storage is of prime concern to the yacht owner and this Chapter discusses the requirements for a small battery charging unit, battery technology, and existing battery charging methods.

3.2 Energy Requirements

Every yacht's electrical needs are different according to the owner's requirement, area in the world it frequents, and size of the vessel. Large yachts, longer than 15 m, have sufficient space and capital invested to have a separate engine generator system dedicated to single or three phase power generation. This allows continuous operation of standard household appliances. The owner of smaller yachts, however, does not enjoy these luxuries and

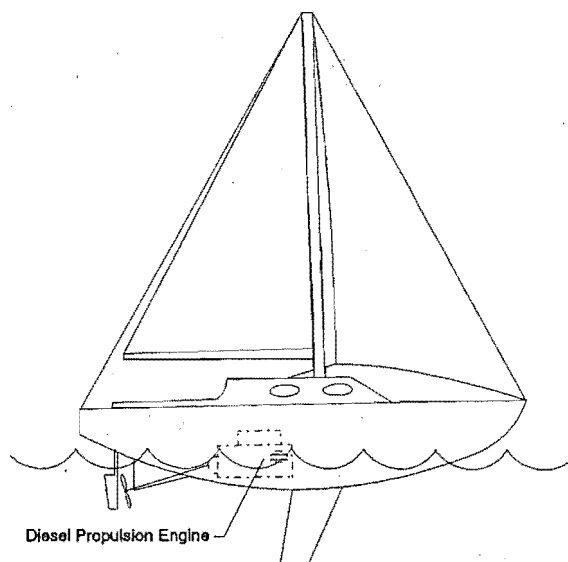


Figure 3.1 Yacht with diesel propulsion engine.

most have to rely on DC appliances powered by electricity stored in batteries. Generally the batteries are charged by an alternator which is driven by the main propulsion engine, Figure 3.1.

In some instances DC to AC inverters or AC generators driven by the propulsion engine enable AC powered devices to be used.

There are four steps in evaluating a boats DC electrical system, (Calder, 1990):

1. determine the power requirements of the boat,
2. provide necessary electrical storage capacity,
3. provide adequate charging capabilities; and
4. establish correct voltage regulation levels to maintain system harmony.

This project deals with steps 3 and 4. Table 3.1 gives a list of commonly used appliances on a yacht and the current they draw from a 12 Volt battery.

Anchor light	1.0 Amp
Anchor windlass	80-300 Amp
Autopilot	1-30 Amp
Bilge blower	2.5 Amp
Cabin fan	1.0 Amp
Cabin light	1.5-3.5 Amp
Depth sounder	0.1-0.5 Amp
Fluorescent light	0.7-1.8 Amp
Freshwater pump	5.0 Amp
Spot light	10.0 Amp
Knotmeter	0.1 Amp
Loran	1.0-1.5 Amp
Masthead light	1.0-1.7 Amp
Radar	4.0-8.0 Amp
Refrigeration	5.0-7.0 Amp
Running lights	3.0 Amp
SatNav	0.2-0.8 Amp
Spreader lights	8.0 Amp
SSB (max)	35 Amp
Strobe light	0.7 Amp
Audio stereo	1.0 Amp
VHF (max)	5.0-6.0 Amp
Wind speed ind.	0.1 Amp

Table 3.1 Common 12 Volt yacht appliances.

Not all these loads greatly contribute to the daily power consumption, for example, occasional use of electric motors, such as used on windlasses, can be neglected as they generally draw a high current for a short period of time and overall have negligible effect on battery charge.

To enable calculations of the required power from the SEBCY, Table 3.2 gives the daily 12 Volt power requirement for a hypothetical yacht, (Calder, 1990).

Appliance	Rating (Amps)	Daily hours of use (hours)	Total daily load (amp hours)
6 lights	1.5 each	2 each = 12	18
1 refrigeration compressor	5	10	50
Masthead navigation lights	1.5	8	12
2 fans	1 each	5 each = 10	10
VHF radio, tape deck	2 total	5 total	10
		Total	100

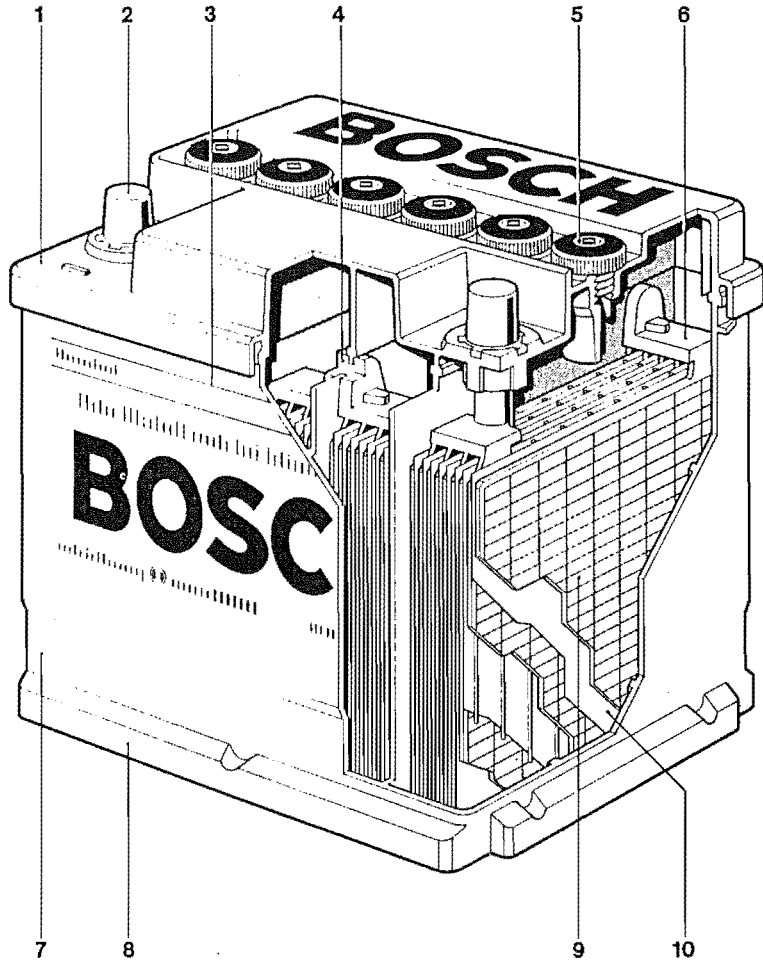
Table 3.2 Daily 12 Volt power requirement for a hypothetical yacht.

3.3 Batteries

Currently lead-acid batteries are most commonly used in yachting applications. Although there has been considerable development on batteries the lead acid is still the most cost effective electricity storage device, (Calder, 1990). On many yachts there are at least two lead acid batteries, one for starting and the other for general appliances.

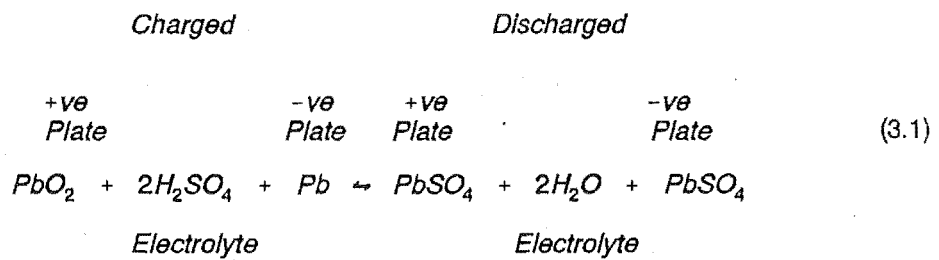
3.3.1 The Lead Acid Battery, General.

Lead positive and negative electrodes are immersed in dilute sulphuric acid, Figure 3.2. When the battery is fully charged lead peroxide covers the positive plate (anode) and spongy lead covers the negative plate (cathode). During discharge electrolysis converts the active materials of both plates to lead sulphate while liberating water, Equation 3.1 left to right. While charging this reaction is reversed, Equation 3.1 right to left.



- | | | |
|-----------------------|---------------|--------------------------------|
| 1 Cover | 5 Vent plug | 9 Positive and negative plates |
| 2 Post | 6 Plate strap | 10 Plastic separators |
| 3 Electrolyte level | 7 Bottom case | |
| 4 Intercell connector | 8 Bottom rail | |

Figure 3.2 Lead-acid battery construction.



Full discharge of a lead-acid battery must be avoided due to the formation of excessive lead sulphate which can lead to irreparable battery damage by two modes. First the lead sulphate

occupies a greater volume than the lead peroxide and severe battery sulphation can cause large mechanical stresses in the plates causing them to crack and shed the active material. Second if the sulphation is severe the sulphate becomes very difficult to re-convert during subsequent charging.

During charging the absorption of negative and positive charges by the anode and cathode respectively causes an increasing back EMF, (electro motive force), also referred to as charging resistance. Therefore as the battery becomes charged at a constant charging voltage the charging current will gradually diminish. Conversely if an electrical load is applied to the battery (discharge) the emf will cause the current to flow in the opposite direction and the emf will gradually diminish. Figure 3.3 shows the charge and discharge voltage curves of a single lead-acid cell.

On open circuit after charging the voltage drops almost immediately to 2.2 Volts. When an electrical load is applied the voltage drops rapidly to slightly above 2 Volts and remains nearly constant until the cell is almost discharged. The battery voltage then begins to diminish more rapidly. The battery should then be recharged before the sudden Voltage decline or excessive

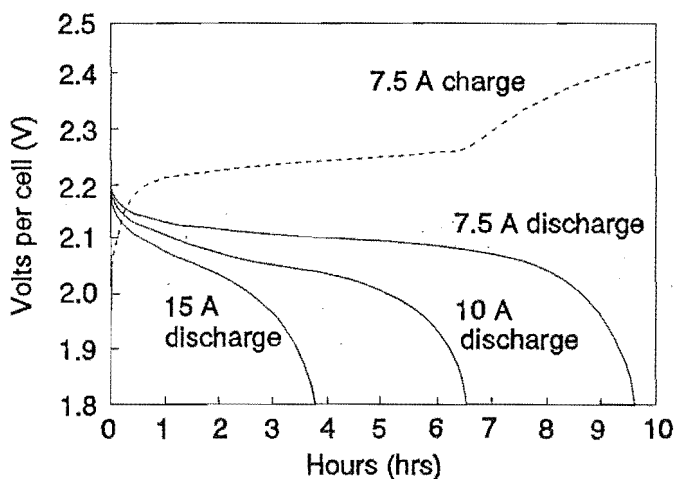


Figure 3.3 Charge-discharge curves for a single lead-acid cell, after Young and Griffiths (1980).

sulphation of the plates will occur. For a standard 12 volt battery 6 cells in series are required. A lead acid battery will over time self discharge at a rate of around 1% per day at 27° C. Consequently, for yachts that are left unattended for long periods, (several months), it is very important to keep the batteries charged or eventual sulphation and destruction of the battery will

occur. This can be achieved on a yacht by using a solar cell, Section 3.4.2, rated at 0.2-0.4% of the battery Ah rating, (Calder, 1990).

The recommended charging routine for lead acid batteries is:

1. **Bulk charging.** High current charging at a constant amperage of up to 25% of the battery Ah rating. During this period the battery terminal voltage is below 13.6 Volts.
2. **Float charging.** The battery is held at a constant voltage of between 13.6 and 14.4 Volts. As the back emf increases the acceptance current diminishes.

On charging, while the plates are being de-sulphated, hydrogen and oxygen are absorbed by the chemical reaction. When the battery is nearly fully charged, (85-90% of its Ah rating), most of the lead sulphate has been converted and further bulk charging will cause dissociation of the electrolyte, dangerously giving off hydrogen and oxygen and is a process often termed 'gassing'. This liberates water from the battery and is the reason why regular topping with distilled water is required. At this point float charging should commence, Figure 3.10(b).

3.3.2 Starting-Lighting-Ignition (SLI) Battery

The SLI battery should be used solely for starting the main propulsion engine and for safety reasons should be kept charged at all times. Typically this is an automotive type battery which will deliver very high current, 1000 A, for short periods and will have a relatively long life provided it is kept charged. Generally this battery would recharge while the main engine is running for propulsion needs.

On engine starting the SLI battery must supply short bursts at very high amperage. To achieve this the battery has many thin plates and low density active material. This maximises the active material

surface area and minimises the electrolyte diffusion time. Thin plates and low density active material cannot handle repeated discharges and are normally discharged only a few percent during engine starting. For example a starter motor drawing 400 Amps for 5 seconds uses 0.55 Ah or 0.55% of a 100 Ah capacity battery.

3.3.3 House Battery (Deep Cycle)

The house battery supplies power to the ancillary devices and is often a deep cycle battery of about 85-120 Ah capacity for smaller yachts. The deep cycle battery is used for its ability to withstand continual deep discharges, down to 50% of its Ah rating. The construction is more robust than SLI batteries by having thicker plates, stronger grids, denser active material and heavier plate separators. The consequence is lower peak current due to less plate surface area and slower electrolyte diffusion time. The current demands from most ancillary electrical loads on a yacht are low but for extended periods, Table 3.2. Therefore much longer discharge periods must be endured before charging is required.

3.3.4 Charging and Discharging Deep Cycle Batteries

The recommended routine is discharge the battery to 50% of its Ah rating then bulk charge at a rate equivalent to 25% of its Ah rating up to 80-90% of its Ah rating then float charge at 13.6-13.8 volts. For example a 100 Ah battery would be discharged to 50 Ah then charged at 25 Amps until the battery reaches 85 Ah then has its voltage held at 13.6 Volts until fully charged. In this case only 50% of the battery capacity is used and charging time to reach 85 Ah is approximately 1.5 hours at 25 amps. The time taken to reach full charge could be several more hours. Consequently batteries charged by running the main propulsion engine are rarely fully charged due to the discomfort caused by the diesel engine. For a total power consumption of 100 Ah per day the engine would have to be run at least 4 hours per day at an engine load of only 500 Watts, 5% of a 10 kW engines rated output with an overall efficiency of around 5-10%. To lower the engine running time more battery capacity can be added. It is recommended that the daily consumption

should be 25% of the battery capacity therefore 400 Ah of battery storage is needed. So one charging run at 100 Amps would take little more than one hour allowing for the inefficiencies in charging. But the continuous alternator output should only be 85% of its rated output to prevent overheating and destruction of the alternator. Therefore an alternator rated at 120 Amps is required and the engine load is around 1300 W or 13% of a 10 kW engines rated output. This is a more favourable situation but the yacht owner has to purchase the extra battery capacity, a much more expensive alternator, a voltage regulator which can bulk charge up to 85% of the battery capacity, find the area for extra battery storage and still have to run the diesel engine for 1 hour per day.

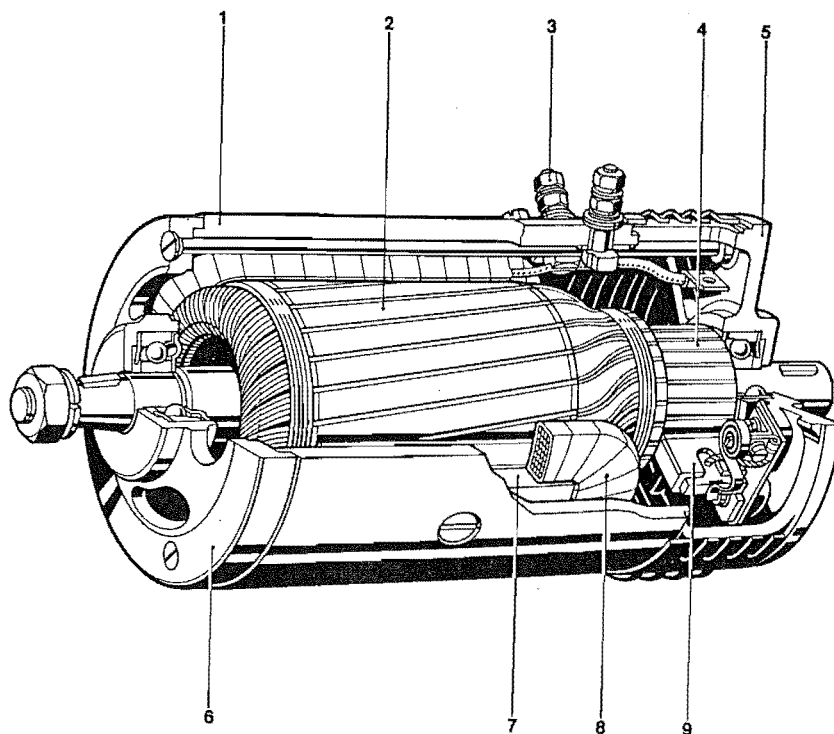
3.4 Battery Charging Methods

In most cases battery charging on small yachts is similar to that used with modern automobiles. The significant difference is that it is preferable to avoid running the engine on board a yacht, whereas, in an automotive application during most times of electrical demand the engine is running. For a correctly designed automotive system the alternator would supply sufficient current to meet the electrical demand while still having sufficient capacity to charge the battery if required.

There are many devices available for charging lead-acid batteries on yachts. They all have advantages and disadvantages and the choice of which to use is entirely dependent on the application and yacht owner's preference. The following describes and compares those methods which are commonly used.

3.4.1 Standard Automotive Type Alternator

Increasing electricity demand in automotive applications led to the development of the three phase alternator which supersedes the DC generator shown in Figure 3.4. The automotive DC generator has deficiencies of zero output at idle and the need for maintenance due to full electrical output



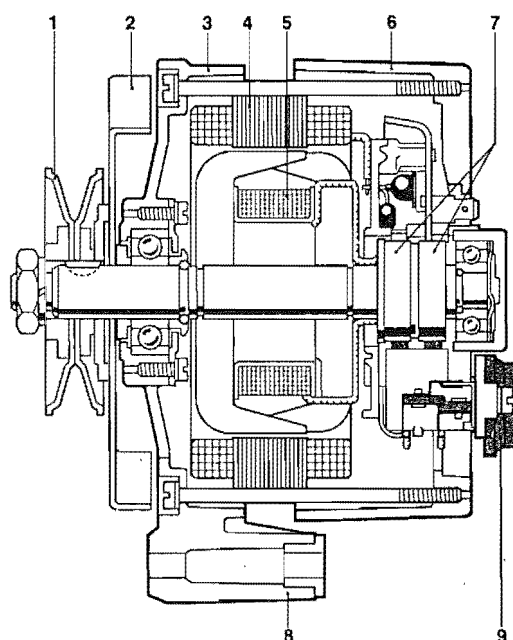
- | | | |
|----------------|---------------------|---------------------------------|
| 1 Stator frame | 4 Commutator | 7 Pole shoe |
| 2 Armature | 5 Commutator shield | 8 Excitation winding |
| 3 Terminal | 6 Drive end shield | 9 Brush holder and carbon brush |

Figure 3.4 Automotive DC generator, after (Bosch)

being passed through a commutator. The development of semiconductor diodes meant the alternating current of AC machines could be reliably rectified in a solid state diode bridge allowing cheap production of compact and reliable three phase alternators. The main features of the alternator are:

- It generates at lower speeds than DC generators (generally above 1000 rpm).
- Rectification is by solid state electronics.
- The diodes will only allow current to flow to the battery, the battery cannot discharge through the alternator.

- It has better power to weight ratio than DC generators.
- It is more reliable giving a longer maintenance free life.
- It is resistant to adverse environmental conditions such as high temperature, damp, dirt and vibration.
- It can operate in either direction of rotation.
- It requires a relatively simple and efficient voltage regulator.



- | | | |
|--------------------|----------------------|----------------|
| 1 Pulley | 4 Stator core | 7 Slip rings |
| 2 Fan | 5 Excitation winding | 8 Mounting arm |
| 3 Drive end shield | 6 Slip ring shield | 9 Regulator |

Figure 3.5 Automotive claw pole alternator, (Bosch)

The standard compact claw-pole alternator, Figure 3.5 has a rotating field created by exciting the rotor field winding and rotating the shaft. When the alternator is excited a small current, < 4 Amps, flows through the excitation winding via a set of brushes and slip rings. This current induces a magnetic field in the rotor causing the left and right hand ends (claws) to become magnetic poles. The magnetic circuit follows the path of least resistance through the laminated stator core which

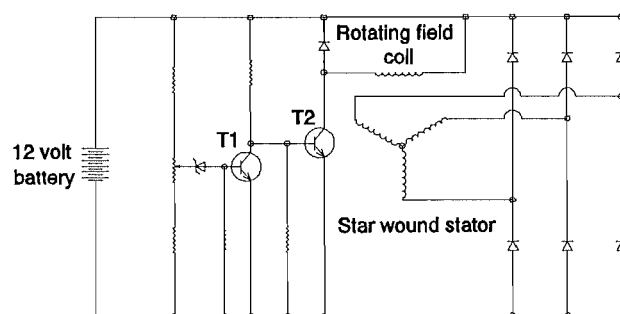
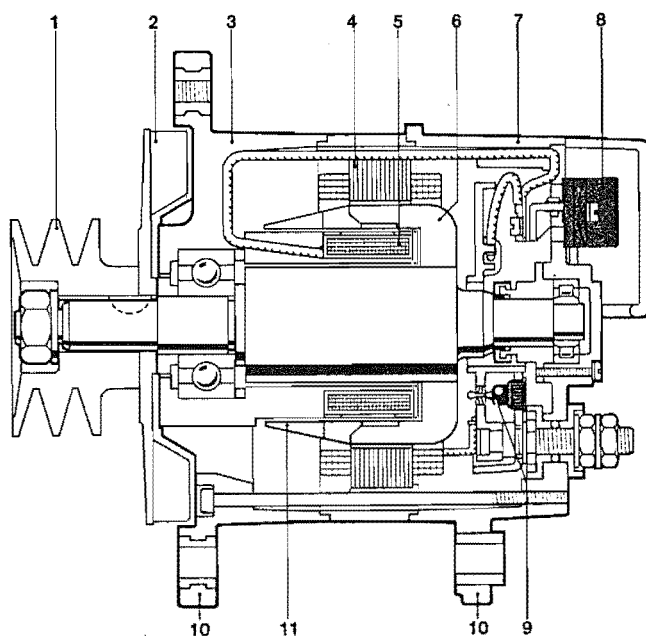


Figure 3.6 Basic alternator and regulator circuit diagram.

induces a voltage in the stator windings. Most alternator stators are wound three phase star with alternator current equal to the phase current and alternator voltage equal to 1.73 times the phase voltage, Figure 3.6. The slip rings can be removed if a stationary field coil is used this gives longer life without maintenance, slightly less friction loss and no arcing due to the absence of sliding contacts, Figure 3.7. The consequence is higher manufacturing costs and added air gaps for the field magnetic flux to pass through.

Generally an alternator is belt driven by the propulsion engine to recharge the batteries. The alternator to engine speed ratio is geared to ensure the alternator will provide sufficient current at slightly above the engine idle speed and will not destruct at maximum engine speed. For most alternators shaft speeds between 1500 and 2000 rpm give the best efficiency but power output increases with speed for a given field strength, Figure 3.8.

There are many alternators available suited to yacht applications. Generally when the propulsion engine is supplied it will have a standard automotive alternator fitted and this is acceptable in many instances. It is recommended, however, that it should be replaced by an approved marine alternator which is explosion protected.



- | | | |
|--------------------|----------------------|-----------------------|
| 1 Pulley | 5 Excitation winding | 9 Power diode |
| 2 Fan | 6 Windingless rotor | 10 Mounting arm |
| 3 Drive end shield | 7 Rear end shield | 11 Conductive element |
| 4 Stator core | 8 Regulator | |

Figure 3.7 Stationary field coil alternator.

3.4.2 Photovoltaic

Solar to electric energy conversion is very popular on yachts. Whilst the initial capital cost is expensive running costs and maintenance is negligible. Their efficiency ranges from 4% to around 14% for cells typically used on yachts. The one obvious drawback is that when there is no sun, there is no power output. For the hypothetical yacht with 100 Ah per day electrical load the required generating capacity is 115 Ah allowing for inefficiency in storage and retrieval from the battery. This requires about 2.5 m² exposed cell area at an overall efficiency of 10% assuming 500 w/m² insolation for 5 hours per day. This level of insolation is marginal with continual boat motion

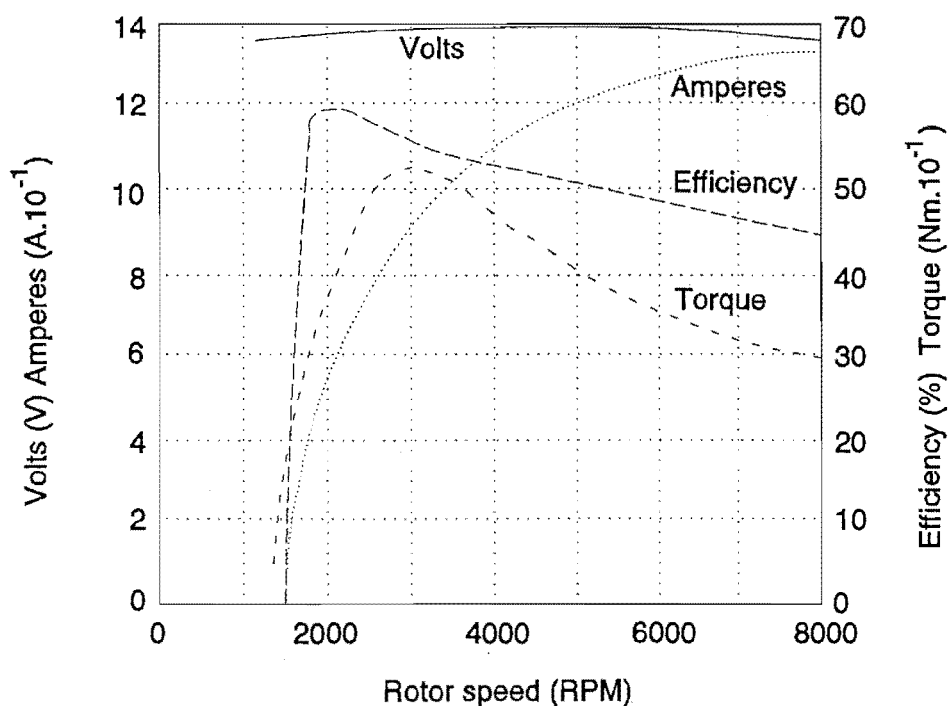


Figure 3.8 Characteristics of a marine alternator.

and shading by the sail. On a yacht less than 15 m in length it is difficult to find enough space that would not be shaded by the sails. Also to obtain the high efficiency the cell should be perpendicular to the sun's rays this may be possible to maintain on a land based unit but a boat is in continual motion. Some yacht owners mount them on the deck, on the dodger, in the rigging, or off the safety rails. Over charging is possible with solar cells and voltage regulators are essential. The solar cell is ideal, however, for keeping the battery charged when the yacht is not in use, Section 3.3.1.

3.4.3 Wind Generators

These are also very popular as the running cost is very low and the idea lends itself to the concept of yachts, Figure 3.9. Analogous to solar cells they generate no power when there is no wind. To obtain a reasonable power output, wind of around 10 knots is required. It is general to select a

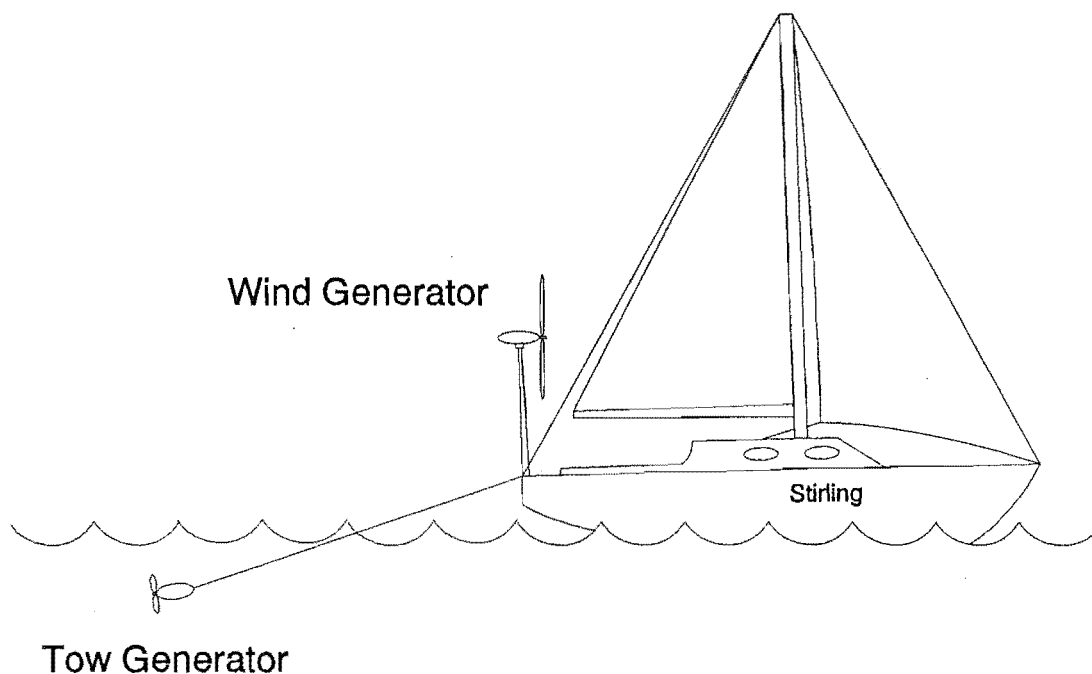


Figure 3.9 Yacht with tow and wind generators.

sheltered harbour to moor and if moored for longer than a day other means of power generation would be required. Again voltage regulation is essential. Some tending may be necessary making them less suitable for charter applications. Wind speed increases with height above the sea, due to boundary layer effect, and the spinning blade is a safety concern so selecting the mounting position is critical. Noise can also be a problem, but this generally depends on the blade design.

3.4.4 Tow Generators

The basic principle is that the yacht tows a propeller in the water, which rotates some form of generator Figure 3.9. These are less popular but quite effective providing the boat is under sail power. They are obviously inefficient to use while motoring, an alternator driven directly from the motor would be preferable. The prime disadvantage is they can only be used when the boat is moving relative to the water at a speed greater than around 3 knots. So again if the yacht is

moored for several days some other power generation system is required. These devices are more popular with ocean cruising yachts where long distances are travelled and the added drag is not important. Racing yachts would not use either wind or tow generators due to added drag, albeit minimal compared to the sail power. Tow generators on a long line make good fish lures and there are reports of them having been eaten.

Both wind and tow generators can use DC generators, excited alternators, or permanent magnet alternators.

3.4.5 Portable Generators

Many types of portable generator are available. Most use petrol which yachtsmen avoid taking on board a yacht for safety reasons. LPG fueled IC engines are possible but no accounts of commercial success of this method have been found, noise and fumes are still a problem. There are small diesel generators available but they have similar noise, vibration and fumes problems to the main propulsion engine. The major advantages are the load is more closely matched to the engine size, AC power can be provided, and wear on the main engine can be reduced.

3.5 Voltage Regulation

A voltage regulator is generally required to ensure long battery life and the system voltage remains within the safe limits for the appliances used. Most alternators are supplied with a built in regulator but these do not give the fastest charging times.

To enable bulk charging at continual high current, a manual voltage regulator override can be used. Generally a manual system allows the user to put full excitation on the alternator during bulk charging. (As the battery becomes charged the standard automotive voltage regulator drops the charging current, Figure 3.10(a)). But the voltage regulator must be reconnected for the last 10-

15% of the charging or excessive heating and gassing of the battery will occur. Requiring skilled manual input, this is unsuitable for charter yacht applications.

Automatic high charge rate regulators are becoming available. These maintain a high constant current charge rate until the terminal voltage reaches 14.4 Volts, at which point they hold a voltage of 14.4 Volts and the charging current tapers off. When the charge acceptance rate falls below 5% of the Ah rating the regulator trips to 13.2 Volts to float charge, Figure 3.10 (b). This sequence is complicated by appliances being used while the battery is charging due to sudden voltage changes.

3.5.1 Standard Alternator Voltage Regulation

The voltage produced in the stator winding is proportional to the rotational speed and strength of the rotating claw-pole magnetic field. Engine speed is always changing so to maintain a constant charging voltage, particularly during the float charging phase, the strength of the rotating field is modified. This is easily accomplished by a transistorised voltage regulator, Figure 3.6. There are many different electronic voltage regulators available but most work by a similar principle.

Referring to Figure 3.6. Transistor T_1 only conducts when the breakdown voltage of the zener diode is reached. This switches off T_2 which cuts the excitation current which in turn reduces the generated voltage. When the battery voltage drops below the set limit the zener diode ceases to conduct and causes T_2 to switch on the excitation current. The excitation current is chopped, rather than dissipated as in a rheostat device, giving high regulator efficiency. Depending on the battery terminal voltage, this sequence of events can occur at rates around 1000 Hz. During bulk charging the frequency is zero and excitation is continuously on and when fully charged the excitation is continuously off. The charging voltage can be set by variation of the potentiometer, a voltage divider, supplying the zener diode. Automotive regulators are preset at 13.6-13.8 Volts which is below the gassing voltage and continuous running will not over charge the battery. It was stated in Section 3.3.4 that the maximum charge rate for bulk charging should be 25% of the

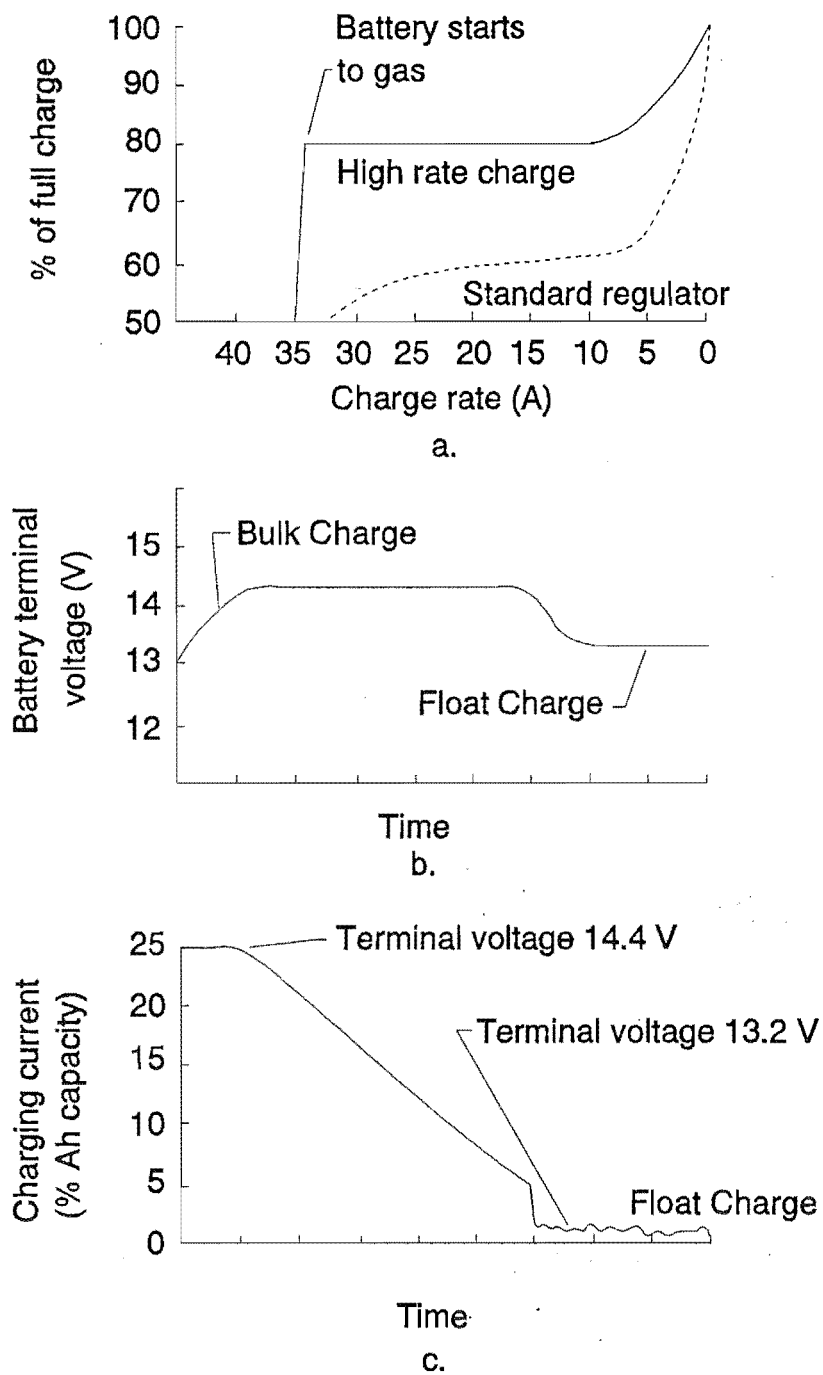


Figure 3.10 (a) Comparison of a high charge rate marine regulator and an automotive regulator. (b) & (c) Marine regulator performance.

battery Ah rating. A standard regulator as described above would charge at a much lower rate, extending the charging time. Figure 3.10(a) shows the current from a standard regulator and a high charge rate regulator.

3.5.2 Marine Regulator

Many special marine regulators are available for providing fast charging. As shown in Figure 3.10, they generally bulk charge at 25% of the battery capacity until the terminal voltage is 14.2 Volts. The voltage is then held at 14.2 Volts while the current tapers off. Once 85% of the battery capacity is reached the current is again reduced for float charging at 13.2-13.6 Volts.

3.5.3 Shunt Regulators.

The shunt regulator is a solid-state device which converts excess power to heat as the battery becomes charged. It does not control the output from the source like the automotive regulator. These are often used with low amperage devices when energy loss is not of concern once the battery is charged, for example solar cells, wind and tow generators often use these.

3.6 Summary of Conclusions of Chapter 3

- Deep cycle battery charging is of prime concern to yacht owners. The SLI battery can be charged by the propulsion engine.
- For the yacht sizes targeted, 100 amp hours per day capacity is required but no two yachts have identical power requirements and this is a typical value.

- None of the current battery charging systems for yachts are ideal and there is a market for another system.
- The SEBCY should be self monitoring, quiet, and suitable for use on charter yachts.
- The automotive claw pole alternator is cheap, easy to control and reliable.
- Stationary field coil alternators are more reliable, less likely to cause an explosion and give less radio interference..
- The automotive voltage regulator is an easy and efficient means of voltage regulation. But requires modification to enable high charging rates.
- A suitable discharge-charge routine is: discharge to 50% of the battery Ah rating, charge at a rate of up to a current equivalent to 25% of the battery Ah rating to 85% of the battery Ah rating. Depending on the charging efficiency and discomfort to the passengers the battery could finally be float charged.

4 Preliminary Engine Generator Design

4.1 General Design Procedure

The design followed a methodical process as shown in Figure 4.1 and described by Pahl and Beitz (1988). The written format for this research thesis did not suit rigorous chronological documentation of each step individually. Broadly, however, task clarification is covered in Chapters 1-4, conceptual design throughout the thesis, embodiment design in Chapters 4 and 10, and detail design in Chapter 10 and Appendix DMC 5.

4.2 Initial Design Requirements.

The overall task is to charge the yacht's house battery with as little discomfort as possible to the people on board the yacht and with minimal adverse effect to the environment, Figure 4.2. From details described in Chapters 1-3 the preliminary SEBCY design requirements are as follows:

- A nominal 12 Volt direct current regulated electric output suited to charging deep cycle lead acid batteries.
- Approximately 115 Ah daily charging capacity, allowing for battery charge and discharge inefficiency, refer Section 3.2 and 3.6.
- It should produce minimal noise, vibration and odorous fumes.
- It should be self regulating, with minimal need for operator input.
- It should require no maintenance.

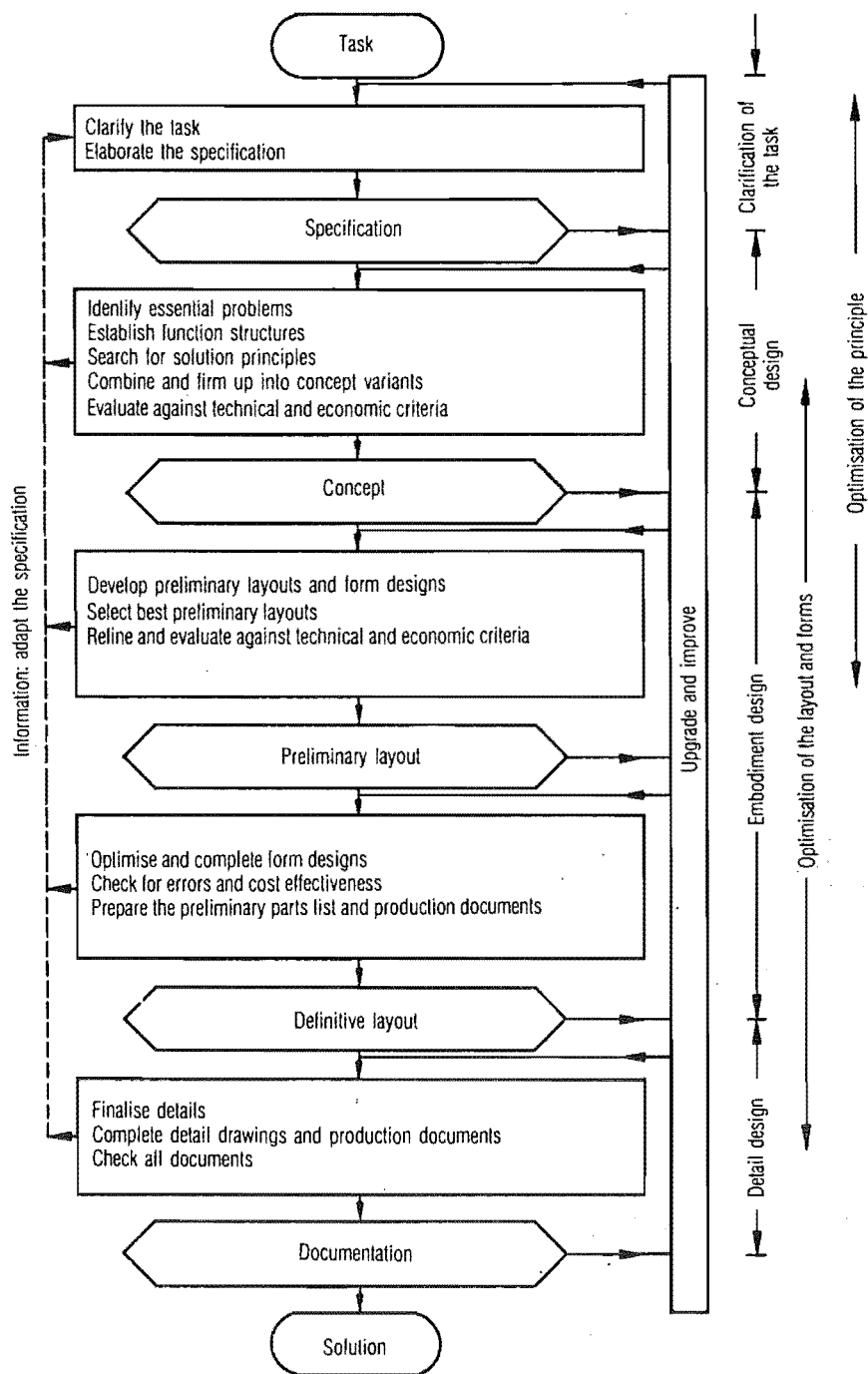


Figure 4.1 Flow of steps followed in the design process, after Pahl and Beitz (1988)

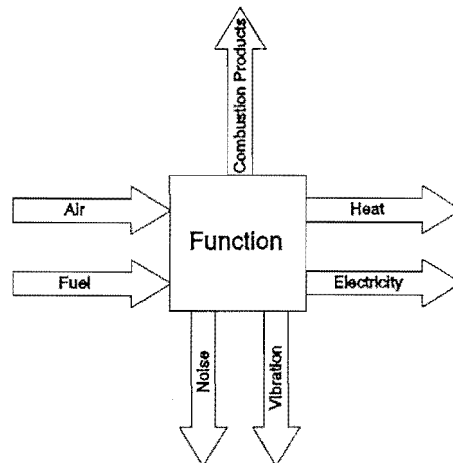
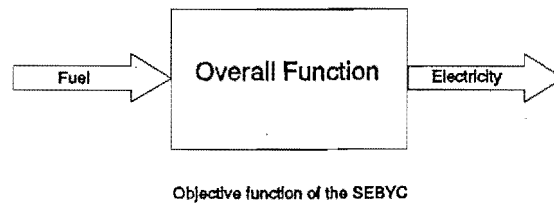


Figure 4.2 SEBCY overall function and its effects on the surroundings.

- For future applications, the general engine design must be able to be scaled to a larger size.

The following Sections build on these design requirements to develop the prototype engine preliminary specifications which enable detailed design and research discussed in Chapters 5-10.

4.3 Nominal Engine Power

If the SEBCY meets the above design requirements then it will not matter how long the engine runs during the day to generate 115 Ah because it would not disturb the occupants and would not require tending. If the engine were to run for 24 hours the required current would be 4.8 Amps or

65 watts at 13.6 volts. The battery electrical load is not continuous, however, and maximum power consumption tends to occur in the early evening, but this is also dependent on time of the year and weather conditions. In hot weather an electric refrigerator is more likely to run during the day and in winter the night time lighting load will be for longer periods than in summer. Consequently, as every yacht has different electricity requirements it is not efficient to have a small engine which runs continuously. For example if the system is designed for 5 amps continuous output and the daily load is only 50 Ah then the extra energy must be wasted or the battery will be overcharged. Conversely if the daily load is 120 Ah the battery will gradually become undercharged and some other charging system would be required. A system with 10 amps output could be developed but this requires automatic start and shut down which applies to any system capable of producing more power than required. For these main reasons a nominal alternator output of 200 watts or 15 amps at 13.6 volts was chosen. This gives ample reserve capacity, a viable kinematic engine design which can be parametrically scaled, reasonable efficiency, and shorter engine run times giving the possibility of longer engine life. If the engine were to run for 24 hrs, 360 Ah could be produced and for 115 Ah, the required output, the engine must run for about 8 hrs.

The number of start-stop sequences depends on the battery capacity. For example a 100 Ah battery with 100 Ah daily load requires 8 hrs charging at 15 amps. But a 100 Ah battery can only be discharged to 50% and recharged at 15 amps to 90% giving only 40 Ah usable battery capacity before recharging. If no electrical loads are applied during charging the engine must run approximately 2.6 hours 3 times per day. The energy used for preheating the engine prior to starting must be considered in the overall system efficiency, and more battery capacity could be added to reduce the number of starts. For example, if a 400 Ah battery is used then 160 Ah capacity is available before charging is required and recharging would take around 11 hours if no electrical load is applied during that time.

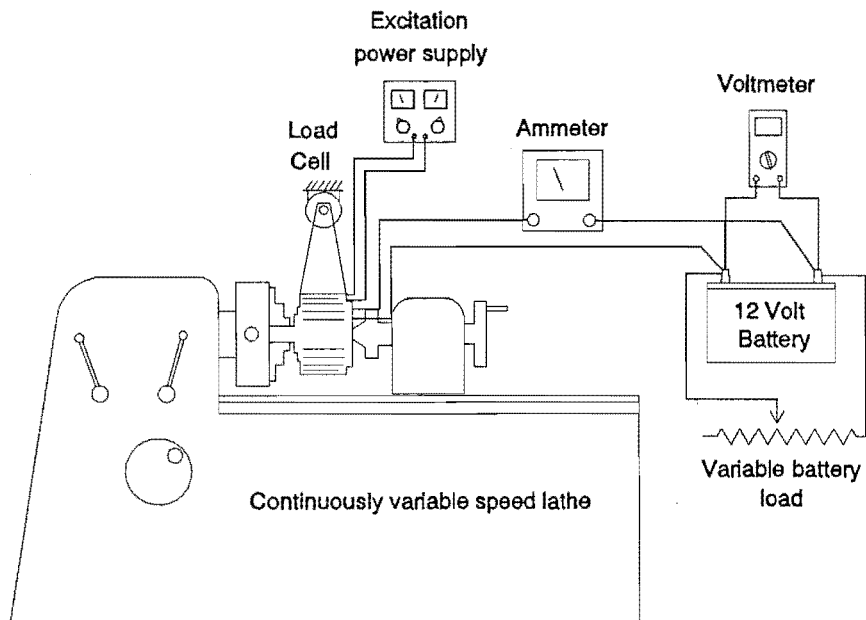


Figure 4.3 Alternator test equipment.

4.4 Generator Selection

Claw pole alternators are cheap, easy to obtain and their control is simple when using an electronic regulator. Figure 3.8 shows that charging would not begin below 1500 rpm for a standard alternator. Bosch manufacture a claw pole alternator suited to low speed generation which was developed for use with large 6 and 8 cylinder cars, which have low engine speed when cruising but still require full alternator output. A Bosch U-KK-14V 30/70 alternator was purchased and tested on a rig shown in Figure 4.3 and Photo 9.7(a). To enable control of the alternator output the regulator was removed and the excitation current was supplied from a variable current

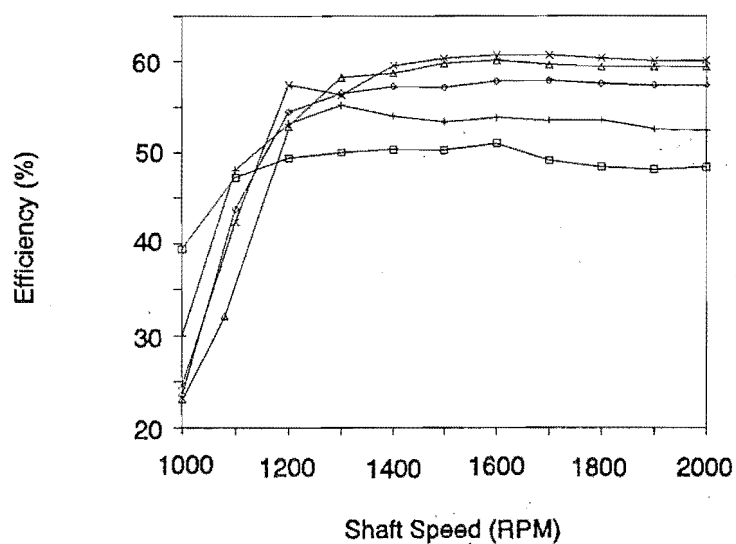
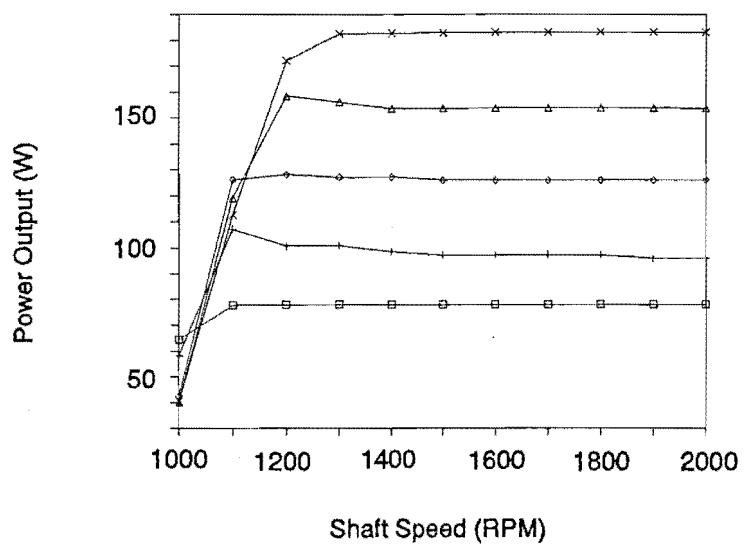
and voltage power supply. Alternator reaction torque, rpm, voltage and current were measured. From these results power output and efficiency were determined for speeds ranging from 1000 to 2000 rpm. The results are shown in Figure 4.4. These Figures show the power and efficiency for various shaft speeds and for various battery terminal voltages. As can be seen the optimum alternator shaft speed is around 1500 rpm. The power increases with increasing terminal voltage due to both current and voltage increasing, (Power = Volts x Amps).

To reduce manufacturing costs and overall volume of the engine it was decided to use the alternator shaft as the main shaft of the engine. This eliminated the need for gears, belts or couplings. Consequently the optimised Stirling engine speed must match the optimum generating speed of the alternator, which is 1500 rpm.

4.5 Working Fluid and Pressurisation.

4.5.1 Choice of Working Fluid

To achieve high power densities suitable for automotive applications, high engine speed is required and hydrogen is a preferred working fluid. Helium is the next best to hydrogen based on physical properties, and, although more expensive, is now used extensively due to its superior practical properties, for example safety, lower rates of diffusion, and because it does not cause hydrogen embrittlement. Engine simulations indicate engine efficiency is virtually independent of the choice of working fluid provided the engine is suitably optimised for that working fluid. Engine power from an air or nitrogen charged engine, however, would generally be 15-20% less than one using hydrogen or helium of the same dimensions. Li (1988) compared the relative performance of the Philips 1002CA engine operating on air and helium and concluded that for an equivalent heat exchanger pressure drop helium can transfer 3.3 times more heat than air.



Battery terminal voltage (V) □ 13 + 13.5 ◇ 14 △ 14.5 × 15

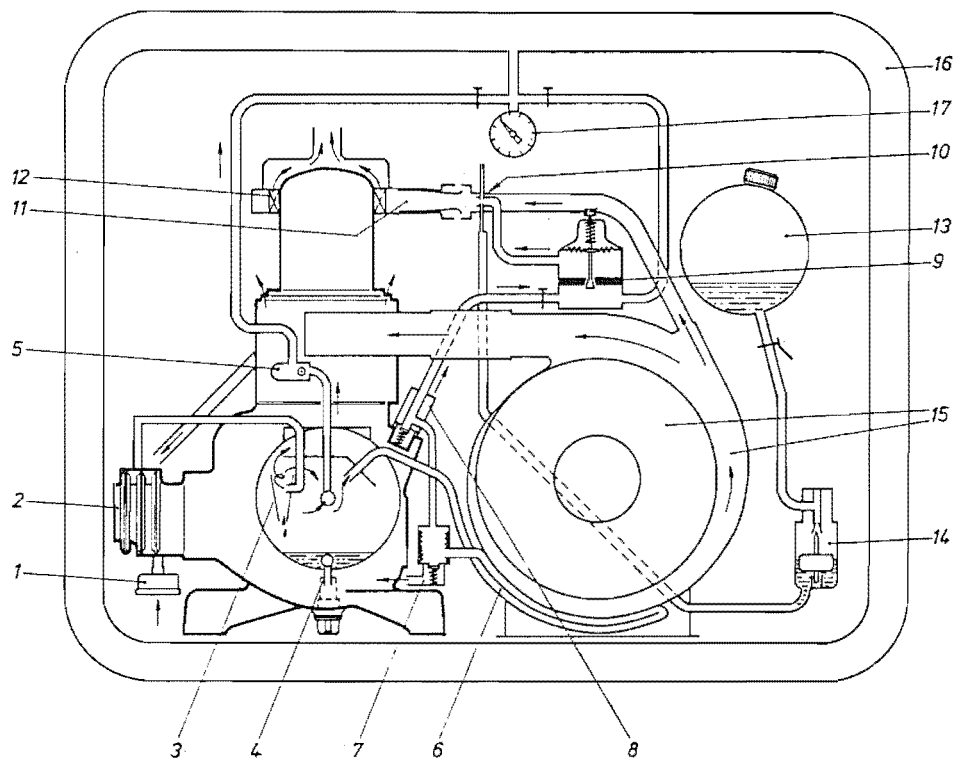
Figure 4.4 Test results of a commercial automotive alternator. Power and efficiency versus shaft speed for various battery terminal voltages.

Hydrogen and helium would be relatively difficult to obtain by the yacht owner should the engine require recharging. This requirement is likely over the life span of the engine, particularly when using the smaller molecule gases which are prone to diffusion through receivers. This is particularly true with heated components where it is possible to lose the complete hydrogen charge within a few hundred hours (Reader and Hooper, 1983). Choosing one of these gases would inhibit sales of the unit, and for this reason readily available air was selected despite its poorer performance.

Safety is of prime concern when air is used due to the possibility of engine lubricants entering the hot space and combusting. This problem can be addressed by minimising free combustible lubricants in the engine which could enter the hot end working space. Providing that the engine mechanism can be designed to operate in this condition. If safety proves to be a continuing problem due to using air, nitrogen or carbon dioxide are relatively easily obtained alternatives. Larger engine designs could be optimised for helium if the application requires this.

4.5.2 Pressurisation

Engine power is almost proportional to the cycle mean pressure, and to achieve an engine of modest size pressurisation is essential. The Philips 1002C engine uses a continuously engine-driven compressor to charge the engine, Figure 4.5. It was found from experience that if this engine was left for several months, some other means of charging the engine was required to enable the engine to be started, the laboratory compressed air supply was often used. Although the SEBCY is hermetically sealed, provision had to be made to allow the owner to charge the engine to the recommended pressure without requiring specialised equipment. Many manual or battery powered pumps are available which are capable of pumping air up to 10 bar. This pressure has proven successful in the Philips 1002C engine and was chosen as a suitable pressure for the



Layout of engine (thick lines) and components of the 102C generator set. The dynamo is situated behind the blower, 15, on the same shaft. 1 = air inlet (filter); 2 = compressor pressurizing engine to about 10 atm; 3 = oil separator; 4 = oil tap; 5 = one-way valve to compression space V_c and to pressurized air reservoir 16 (tubular frame); 6 = air cooler; 7 = safety valve; 8 = feed valve to reducing valve (9) and to crankcase (one-way); 9 = reducing valve; 10 = fuel atomizer; 11 = burner space; 12 = heater; 13 = fuel tank; 14 = carburettor; 15 = blower for combustion air; 16 = tubular frame serving as pressurized air reservoir for starting; 17 = pressure gauge. The generator delivered 200 W at 220 V, 50 Hz.

Figure 4.5 Philips 1002C generator set, after Hargreaves (1991).

preliminary engine design.

4.6 Cycle Temperature

The ideal efficiency of the Stirling Cycle is equivalent to the Carnot efficiency:

$$\eta_{id} = 1 - \frac{T_K}{T_H} \quad (4.1)$$

Where: T_K =Cold heat sink temperature (K)

T_H = Hot heat source temperature (K)

From Figure 4.6 and this Equation it can be seen that for high ideal efficiency a high temperature differential is required. The ideal efficiency is more sensitive to changes of temperature at the cold end and increasing the hot end temperature provides diminishing returns.

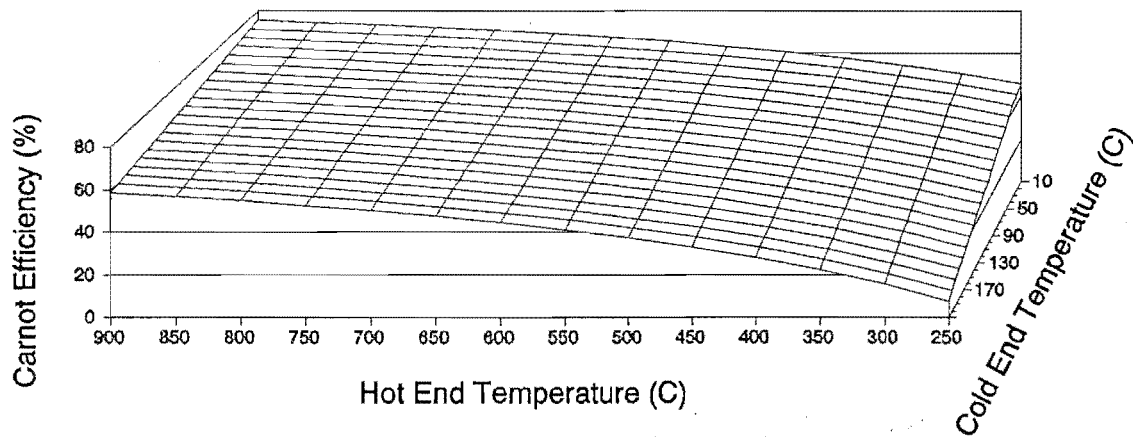


Figure 4.6 Stirling cycle ideal efficiency verse hot and cold end temperature.

4.6.1 Cold Heat Sink

A change of 10° C at the cold end has an equivalent effect on the ideal efficiency of a change of 30° C at the hot end for moderate operating temperatures. Also MTI (Mechanical Technology Inc.) estimate that for each 10° C rise in cooling temperature a 5% power loss can be expected (Reader and Hooper, 1983). Practically, however, the cold end temperature is always higher than the cold sink which is generally the ambient air temperature. For a fluid cooled engine T_K could be taken as the cooling fluid temperature.

Direct air cooling is preferable for a portable unit but requires an external fan to enhance the rate of heat transfer from the cold end fins. If the fan is engine driven, either a magnetic drive or a dynamic atmospheric seal is required. Also air cooling is not suitable for a unit mounted in an enclosed space, for example, an engine compartment or locker of a yacht.

A secondary liquid cooling loop has the advantage of being able to recover the waste heat for onboard cabin and/or water heating which greatly improves the overall system efficiency. Comfortable domestic hot water temperature is 55° C and this was chosen as the final sink temperature. If the engine is used to heat water it is likely the temperature will be lower than this for a considerable time and when 55° C is reached the extra heat would most likely be directed to the sea or a radiator, Figure 4.7. In most cases it is likely that the sea would be the final heat sink as considerable heat needs to be absorbed, probably much more than the occupants of a small yacht would use in a day. As an example assume a 200 Watt electrical output at 10% overall efficiency, for this the fuel heat input is 2 kW. Assuming also that 40% of the heat input is absorbed by the cold end heat exchanger, then the cooling load is 800 Watts. If the engine is run for 8 hours per day then the daily heat removed from the engine is 23 MJ. For heating water from 20° C to 55° C, the required mass of water to absorb this energy is 159 kg or approximately 160 l/day.

Several possible systems to accomplish the heat removal are shown in Figure 4.7. The fluid used in the engine and radiator could be a water-glycol mix and should be kept in a separate cooling loop to the sea water to prevent the engine heat exchanger being fouled. A natural convection radiator could be used for heating the cabin or drying locker. For systems using a combined radiator and water heater, a thermostat could be used to redirect the cooling fluid through the radiator when the water cylinder temperature has reached 55° C. This allows higher engine efficiency, particularly with the sea water cooled type Figure 4.7(d). For maximum system efficiency the engine could be mounted in the base of the hot water cylinder, Figure 4.7(e), and

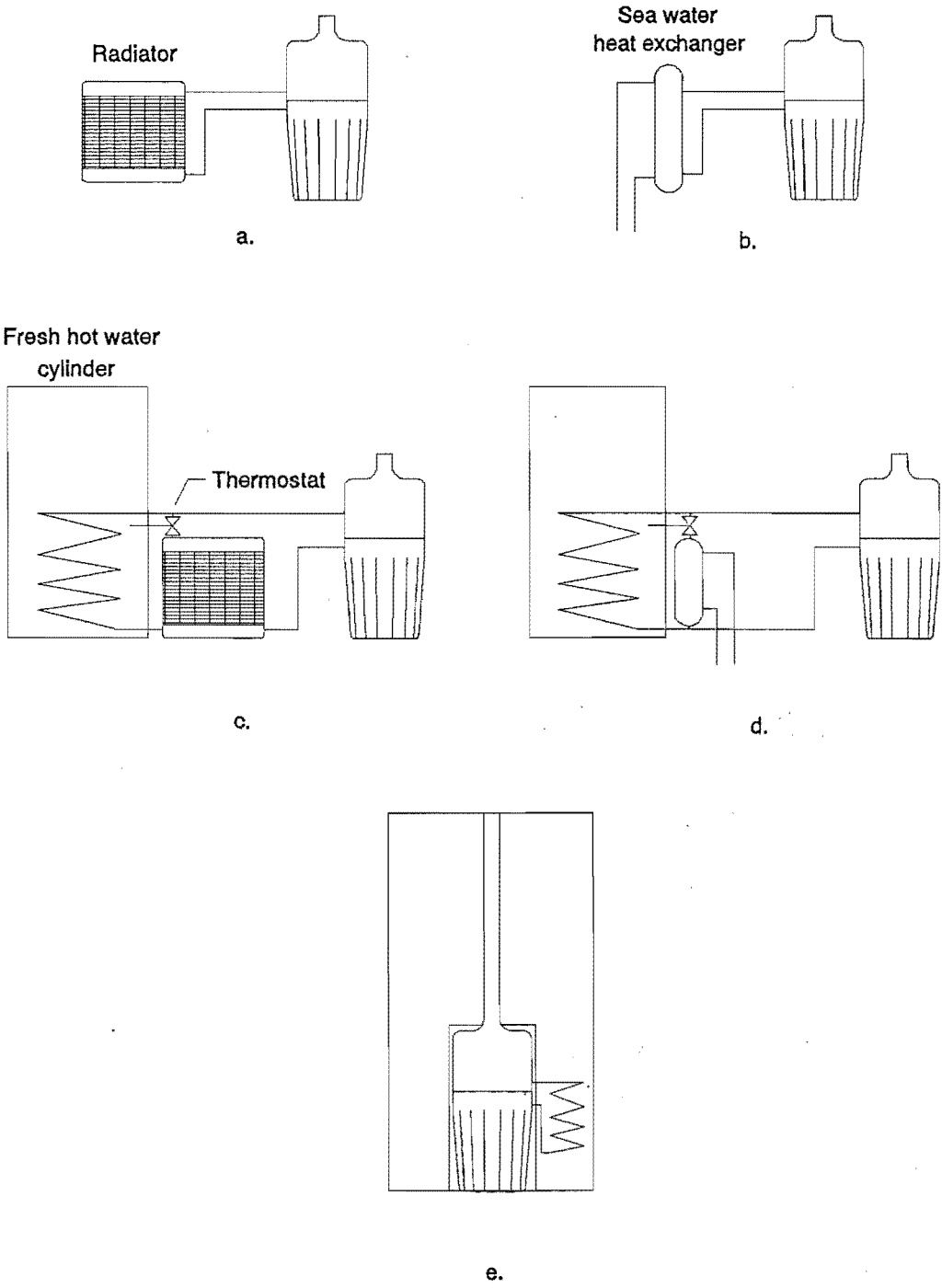


Figure 4.7 Possible methods for cooling the engine.

work in a similar fashion to gas heated hot water cylinders. In this case most of the flue and cooler heat could be absorbed into the water, a very large cylinder or high rate of water usage would of course be required. Providing a high overall efficiency this configuration would be ideal for a larger yacht, holiday home or remote village.

For the yacht application fluid cooling is required and a maximum sink temperature of 60° C was chosen for the preliminary engine design.

4.6.2 Hot Heat Source Temperature

High alloy stainless steel, Avesta 253 MA, was the only readily available heat resistant steel in New Zealand and this was selected for the hot end heat exchanger. This steel has an upper operating temperature of 1100° C, refer (Avesta, 8524). The maximum working stress of the material decreases with temperature. As shown in Figure 4.6 increasing the temperature gives diminishing returns and an operating temperature between 700° C and 750° C was selected.

4.6.3 Estimated SEBCY Efficiency

The resulting Carnot efficiency is 67.4% but real engine efficiency can range between 0.65 and 0.7 of the Carnot efficiency, (Reader and Hooper, 1983). Smaller engines tend to be less efficient than large, as friction and static heat losses are a larger proportion of the engine power. With an alternator efficiency of 60%, the estimated thermal to electrical efficiency is 12% not including heat recovery for cabin or water heating. This is a similar efficiency to a well designed and operated diesel-based system running solely for charging the battery. A simple test was performed on a Ford 10 HP twin cylinder diesel engine similar to that used on a yacht. The overall battery charging efficiency of this system was 3 to 5 %, determined by:

$$\eta_{overall} = \frac{Volts \times Amps}{LCV_{diesel} \times \dot{m}_{diesel}}$$

4.7 Engine Speed

Power output is almost proportional to engine speed within the practical limits to which the heat exchangers have been optimised for. Therefore to keep the engine within a modest size a relatively high engine speed should be used. As described in Section 4.4 the alternator selected has an optimum rotor speed of 1500 rpm so this was selected as the speed for engine optimisation.

4.8 Heater Combustion System

The requirements for the combustion system are:

- Quiet combustion: the combustion system often produces the most noise from Stirling engines.
- Clean combustion with limited odour and toxic exhaust fumes.
- Use of a fuel that can be easily obtained world wide.
- Provision of a high temperature heat source which will give the required rate of heat transfer without using an external blower, (due to there being no external drives).
- Most importantly, that the fuel and combustion system must be safe to use on a yacht.

Diesel is the yacht owner's preferred fuel but there are considerable problems with meeting some of the above requirements. Using conventional combustion techniques, a naturally aspirated premixed LPG, (Liquified petroleum gas), burner meets these requirements. LPG is generally accepted by yacht owners and is often used as a fuel for cooking, refrigeration and heating.

4.8.1 LPG

Liquified petroleum gases are mixtures of hydrocarbons consisting mainly of butane (C_4H_{10} and C_4H_8) and propane (C_3H_8). These gases are sold worldwide under various names and various

percentage mixtures so the combustion system must be able to accommodate the differing gas properties. Appendix A gives the properties of gaseous propane/butane mixtures.

In New Zealand the mixture is around 60% propane and 40% butane by weight and this mixture will be used for the following preliminary calculations.

4.8.2 Burner Design

Most burners used on Stirling engines producing power outputs in excess of a few hundred Watts utilise some form of blower to enhance air fuel mixing and increase the rate of heat transfer to the heated components. For example the Philips 1002C engine is fuelled with kerosene which is drawn into the burner by a pressurised air jet, Figure 4.5. Additional air is forced into the burner by a fan mounted on the generator shaft, consequently energy is consumed in pressurising the air and driving the fan. The fluid cooled SEBCY does not have an auxiliary output to drive a blower and hence a naturally aspirated burner is required. The design of naturally aspirated LPG burners is relatively well developed for gas cooking, home heating and bunsen burners, but the heat transfer coefficient produced by these burners is low and enhancement of the rates of heat transfer is required.

4.8.3 Enhancement of the Burner Heat Transfer.

There are many ways to enhance the rates of heat transfer from the combustion gases to the heater wall. The basic Equation for heat transfer is:

$$Q_{heater} = \frac{(T_H - T)}{\text{Thermal resistance}} \quad (4.2)$$

Where:

T_H = Head temperature

T = Temperature of the source, for example the combustion gas temperature.

To increase Q_{heater} without increasing the fuel flow rate it is possible to:

- Increase the flame temperature by preheating the incoming combustion gases.
- Increase the velocity of the combustion products near the heated wall by inducing turbulence, this however, will increase the pressure drop in the burner.
- Supply around 20% excess air to obtain maximum combustion temperature as was shown by Li (1988) and Philips (Hargreaves, 1990).
- Ensure that initial combustion is occurring close to the heated components and combustion completion occurs over the heated surface. Many researchers have noted that the recombination of various species near the heater wall improves heat transfer, for example Hargreaves (1990) and Li (1988).
- Enhance flame radiation. Flame radiation has a limited effect as was shown by Li (1988).
- Maximise radiation from the surrounding surfaces. By using a refractory type material such as that used in gas radiant heaters the radiant heat transfer can improve the overall heat transfer.
- Increase the surface area of the head. Li (1988) observed that the rate of heat transfer was increased three fold by finning the plain heater head of the Philips 1002C engine.
- Coat the head surface with a catalyst which would enhance exothermic reactions on the heater head surface.

An important point to note is a naturally aspirated combustion system cannot work with high pressure drop so the combustor must be open with wide flow passages shaped to draw in the combustion gas and adequately mix the air and fuel.

These points highlight one of the few thermodynamic advantages of the four cycle double acting configuration for small engines. Li (1988) derived equations relating the power required to cylinder surface area and concluded that an engine up to 5 kW could be produced using a plain heater

head, (internal fins and without tubes). The derivation was, however, restricted to a single heater head. Increasing the number of cylinders increases the possible heater surface area for an engine of similar swept volume.

4.8.4 Heater Head

Tubular heat exchangers are generally used in high power density engines. However, they have the disadvantage of high manufacturing costs due to material and welding requirements. They are also prone to catastrophic failure from tube burn out and uneven heat transfer causing hot spots. Annular finned heat exchangers such as that used on the Philips 1002C engine have a higher thermal mass and consequently longer starting times. The heater head can be cast with external fins and annular internal fins machined or fitted into the head, Figure 4.8.

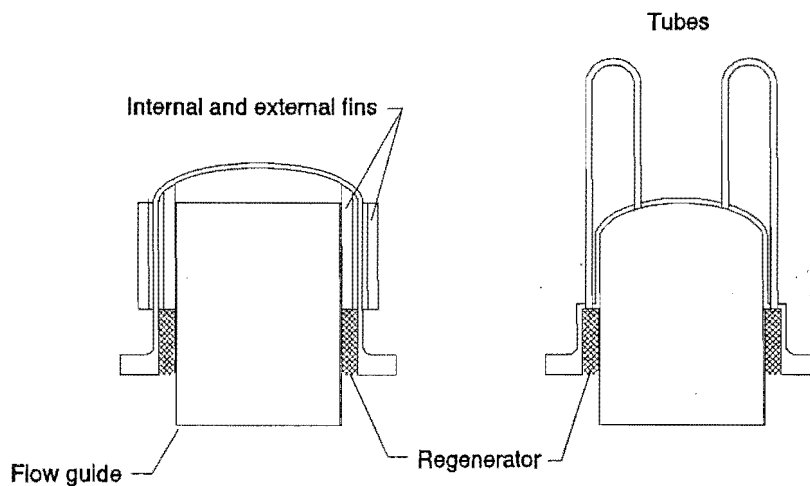


Figure 4.8 Finned and tubular hot end heat exchangers.

4.9 Engine Arrangement

Section 2.4 described the three configurations of Stirling Engines. The following Sections present the series of decisions leading up to the selection of the final prototype arrangement.

4.9.1 Possible Scaling

As suggested in Chapter 1, the battery charging unit by itself may not be commercially secure for an investing company and a range of engines should be designed based on one arrangement which could be parametrically scaled to meet all the yacht's power needs and other possible applications. Therefore an arrangement suitable for powers ranging from tenths of kilowatts to tens of kilowatts would be more versatile.

4.9.2 Lubrication

To prevent fouling of the heat exchangers and possible explosive mixtures, lubricants must be kept from the heat exchangers and working spaces. Hence dry sump technology using sealed prelubricated bearings and dry exposed bearing surfaces is preferable to a wet sump engine. This technique has been used by many manufacturers as it also prevents the need for complex piston rod seals, refer to Section 5.2.

4.9.3 Starting

The SEBCY requires an automatic starter for normal operation, and a manual starting system for emergencies. Free piston Stirling engines are theoretically self starting once sufficient temperature differential is achieved but sometimes they require a small nudge to start (Walker, 1980). Four cycle double acting designs are also theoretically self starting, Rice (1992). (Figure 5.10(c) shows that the engine torque for a four cycle double acting engine is always positive). Practically, however, they are not self starting for the following reason. If an engine with a fixed stroke is left inactive for some time, the pressure in each cycle will equalise and as the volume of each cycle is different the mass of gas in each cycle will also be different. Consequently, to start the engine, compression of the larger mass of gas in the cycle with the largest volume is required. Simply heating the engine would not produce sufficient torque to overcome this compression and friction, hence some means of rotating the engine shaft is required for reliable starting.

A method for converting the three phase alternator to act as a DC starter motor was developed, (refer to Section 9.2.4). This technique eliminates the need for a separate starter motor and ring gear but can only deliver a shaft starting torque of 3 Nm to overcome the initial engine compression.

The Philips 1002C engine is of similar capacity to that required for the SEBCY, it uses a manual rope starter similar to that used on a lawn motor mower. A simple experiment was performed on this engine to determine the torque required to start this engine. A spring balance was fixed to the rope and the engine heated, the tension of the rope to overcome the initial compression was measured and the resulting torque was 8.9 Nm. Once the compression was overcome the engine always started. The last engine designed by Philips of Eindhoven was a single cycle 3 kW gamma configuration engine. To start this engine a fly wheel was spun up to speed by an electric motor. When the starting speed was achieved a clutch engaged the Stirling engine shaft and the inertia of the flywheel would overcome the engine compression. The STM4-120 could utilise the variable stroke to start. (In practice a starter motor is used, possibly due to the lack of hydrodynamic lubrication on the swash plate at low speed). When pre-heating the STM4-120 engine, the swash plate angle could be held at zero degrees, (ensuring the volume of all cycles are equal), to start the engine the swash plate angle could be quickly increased; this would cause pressure differences in the four cycles and the engine would begin to rotate. This system requires a hydraulic accumulator to store pressurised hydraulic fluid to activate the swash plate angle variation.

Engine starting must be considered when choosing the engine arrangement due to costs, complexity, volume and mass associated with additional starting equipment.

4.9.4 Stirling Engine Performance Prediction

Due to the complex nature of the Stirling Cycle performance prediction and engine optimisation, the theory used has been grouped into First, Second and Third order analysis, (Martini, 1983). The First order analysis is often termed "back of the envelope design" as the equations are closed form and can be quickly used to access possible designs or compare engines. The Second order approach utilises some simulation routine, generally solved by cycle iteration, to determine the engine performance based on many assumptions, the results are then modified according to relevant theory. This enables extensive cycle analysis including determination of space temperatures, coefficients of heat transfer and heat exchanger pressure drop. Generally these methods require computer programs and are adequate for detailed engine design. The Third order type analyses are finite element or nodal. For the nodal analysis the engine is divided into discrete volumes and differential equations are simultaneously solved for all volumes. This type of analysis gives a closer representation of the cycle as it is occurring by determining for example mass flow rates, pressure drop, and temperatures for each time step. The accuracy, however, is often similar to the Second order approach and the longer computing time of the Third order analysis makes it less attractive for use with optimisation routines. Ultimately, however, with increased computer speed and better modelling techniques, the Third order method is likely to dominate Stirling engine research in the future.

For preliminary engine design, First order methods require the least information from the designer and has closed form solutions enabling fast comparison of various combinations of engine dimensions. Consequently First order equations are utilised in this Chapter to predict the optimum configuration.

4.9.5 Comparison of Engine Configurations

Any one of the three engine configurations, alpha, beta and gamma, shown in Figure 2.3 could yield the required power for this application. Of the three Stirling engine configurations, there is

no one configuration which excels for all applications. The following investigates the merits of each.

To evaluate each configuration a detailed analytical approach was required. First order equations were combined with basic engineering and Stirling engine theory to enable the calculation of relevant performance, geometric and cost values. A decision matrix technique was then used to evaluate these results and give the optimum configuration for the SEBCY.

4.9.6 Beale and West First Order Equations

William Beale observed that the power of most Stirling engines could be predicted by a simple equation:

$$BP = B_e P_{mean} f V_o \quad (4.3)$$

The Beale number B_e is generally quoted as 0.015 but this relates to hot and cold end temperatures of 650° C and 65° C respectively. Reader and Hooper (1983) found that the Beale number could be modified to accommodate different temperatures by letting:

$$B_e = 0.034 - 0.052 \frac{T_K}{T_H} \quad (4.4)$$

Colin West also noted that the important effect of engine temperature was not taken into account, (West, 1981). By theoretical derivation he determined the form of the West Equation, (4.5), and by examination of published engine data determined the West number:

$$BP = W_n P_{mean} f V_o \frac{T_H - T_K}{T_H + T_K} \quad (4.5)$$

From a small number of engines he estimated the West number W_n should be 0.35 and after examining a larger range of engines modified this to 0.25.

An inconsistency was noted in the Stirling engine literature regarding the use of V_o in the First order Beale and West Equations. The following lists the various authors interpretations of how V_o should be determined:

Walker (1979) **Displacement of the power piston.** In an example of an alpha configuration engine he uses the swept volume of one piston.

Walker (1980) **Displacement of the power piston.** And uses the same example as above.

Walker (1985) **Total volume variation.** This is the piston swept volume in the case of a piston displacer machine and is approximately $\sqrt{2}$ times the swept volume of an alpha configuration machine.

Walker (1991) **Swept volume of the compression space.** An example is given to determine the swept volume of an alpha configuration engine for a particular power of an alpha configuration engine, had the previous nomenclature been used the required swept volume would be 0.707 that determined.

Reader and Hooper (1983) **Power piston swept volume and compression space swept volume.** In an example Pg. 328 of their text, they use V_{sp} or the swept volume for appraisal of a four cycle double acting engine.

Martini (1983) **Displacement of the power piston.**

- Mansoor (1984) **Displacement volume of the engine.**
- Li (1988) **Swept volume of the power piston.**
- Urieli and Berchowitz (1984) **Swept volume.**
- West (1986) **Power piston swept volume and total volume variation.**
- West (1981) **Volume Swept by the power piston.**
- Senft (1982) **Piston swept Volume**

West, (1986), states in his nomenclature that V_o is the swept volume of the power piston, and later states that the power piston for an alpha configuration engine is the expansion piston. Therefore for an alpha configuration engine, the expansion piston swept volume should be used. Later in the text, however, he determines the West number based on the total working space volume variation which for beta and gamma configurations is the piston swept volume and for alpha approximately $\sqrt{2}$ times the expansion piston swept volume. It is also interesting to note that his modification of the West number from 0.35 to 0.25 is a factor of 1.4 which is $\approx \sqrt{2}$.

It must always be remembered, however, that these equations are based on empirical data and only intended to give an approximation of the performance of a well designed engine. Despite this a consistent interpretation of V_o should be used. As an example, the results of the published methods, above, are produced in Tables 4.1 and 4.2.

Engine Parameters		Equation No.	Required Vo (cc)
Required Power (W)=	400		
Pmean (bar)=	10	(4.3) Beale	106.7
TH (K)=	1023	(4.3 & 4.4) Beale	85.3
TK (K)=	300	(4.5) West $W_n=0.35$	83.7
RPM=	1500	(4.5) West $W_n=0.25$	117.1
Swept volume ratio=	0.9		
Bore/stroke=	2		

Table 4.1 Preliminary engine specifications and required V_o determined by the various Equations.

V_o	Equation No.	Required Expansion Bore (mm)	
		Alpha	Beta
$V_o = V_{exp}$	(4.3)	64.8	64.8
	(4.3)	60.1	60.1
	(4.5)	59.7	59.7
	(4.5)	66.8	66.8
$V_o = V_{com}$	(4.3)	67.1	67.1
	(4.3)	62.3	62.3
	(4.5)	61.9	61.9
	(4.5)	69.2	69.2
$V_o = V_{max} - V_{min}$	(4.3)	57.7	67.1
	(4.3)	53.6	62.3
	(4.5)	53.2	61.9
	(4.5)	59.5	69.2

Table 4.2 Required expansion space bore for the required V_o specification in Table 4.1.

From Table 4.2, the West equation gives a considerably smaller bore for the alpha configuration and all other interpretations give an identical bore diameter for both alpha and beta.

The conclusion of this survey it is that the West equation should be used as it has been verified with a large number of engines and gave quite accurate performance predictions. V_o should therefore be taken as the total volume variation in the cycle as this was used to determine W_n .

The West equation alone gives little insight to which is the optimum configuration other than specifying the configuration that would give the smallest bore diameter. This was shown above to be the alpha configuration.

4.9.7 Optimum Configuration by Kirkley

Kirkley (1962) developed closed form equations based on the classic Schmidt analysis for comparison of each of the configurations. Many other authors have also presented similar equations, for example Reader and Hooper (1983), Martini (1983). Kirkley showed that of the piston-displacer configurations, beta and gamma, the gamma configuration gives considerably lower performance due to greater dead volume, (Kirkley, 1962). Consequently the gamma engine is not generally used for engines of high power density and can be eliminated early from the decision process. Hence, the following refers to alpha and beta configurations only.

Based on the Schmidt analysis only the swept volume ratio and phase angle can be optimised to give a minimum bore diameter, as shown in Figure 4.9. Other variables must either be maximum or minimum.

From the West, Beale and Schmidt equations no simple and definitive conclusion could be made as to which is the optimum configuration. Therefore other factors regarding the engine performance and manufacturing costs should also be considered.

Mechanism design, parasitic losses, engine box volume, ability to be scaled and manufacturing costs are now analyzed for the two configurations for both single and multiple cycle engines.

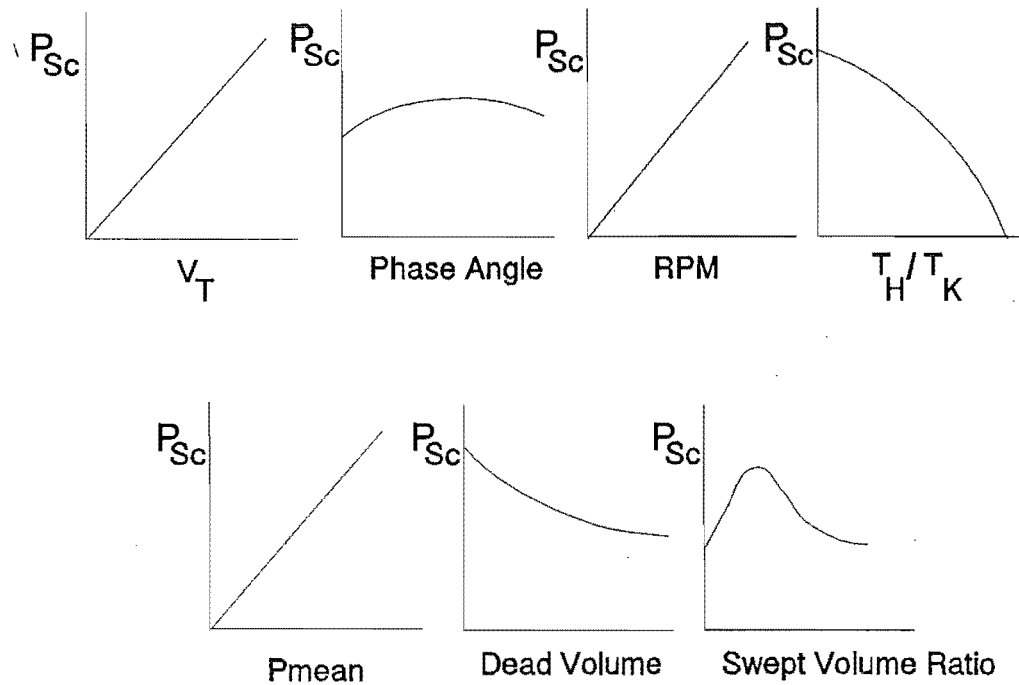


Figure 4.9 Effects of operating and geometric factors on the Schmidt power, (Reader and Hooper, 1983).

For the following Section it appeared appropriate to use the West equation with $W_n = 0.25$ and $V_o = V_{\max} - V_{\min}$ as it is based on the performance of a large number of real engines whereas the Schmidt analysis is purely theoretical, and modified by an estimated factor.

4.9.8 Geometric and Parasitic Loss Considerations.

The following derivation is similar to that published by Li (1988). It was noted that his derivation is restricted to single cylinder designs and power prediction by the Beale number which does not allow changing the heater and cooler temperatures.

Using the West Equation:

$$BP = W_n P_{mean} C_n V f I \Gamma \quad (4.7)$$

where

- BP = Engine shaft power (watts)
- W_n = West number, 0.25
- P_{mean} = Mean cycle pressure (Pa)
- C_n = Configuration number, 1.414, 1 and 1 for alpha, beta and gamma respectively.
- V = swept volume of expansion space for alpha and piston swept volume for beta and gamma configurations respectively (m^3)
- f = cycle frequency (Hz)
- I = Number of Stirling cycles in the engine
- Γ = Temperature ratio $(T_H - T_K)/(T_H + T_K)$

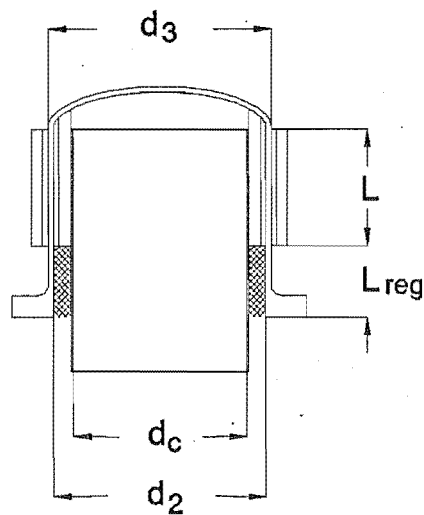


Figure 4.12 Finned heater head dimensions.

Let:

d_c = expansion cylinder diameter

$$a = \frac{\text{stroke}}{d_c} \quad (4.8)$$

$$b = \frac{d_2 - d_c}{2}$$

$$c = \frac{L}{d_c}$$

$$V = \frac{\pi}{4} d_c^3 a \quad (4.9)$$

$$d_c = \sqrt[3]{\frac{4 BP}{W_n C_n \pi a P_{mean} f I \Gamma}} \quad (4.10)$$

The cylinder thickness can be approximated from the maximum cylinder stress by:

$$\sigma = \frac{P_{max} d_2 SF}{2 t_{cyl}} \quad (4.11)$$

where

$P_{max} = (4/3)P_{mean}$ assuming the pressure ratio $P_{max}/P_{min} = 2$ (Walker 1980)

SF = safety factor

t_{cyl} = heater head cylinder wall thickness

therefore:

$$t_{cyl} = \frac{2 P_{mean} SF (d_c + 2 b)}{3 \sigma} \quad (4.12)$$

the external cylinder diameter is:

$$d_3 = d_c + 2b + 2t_{cyl}$$

$$\therefore d_3 = (d_c + 2b) \left(1 + \frac{4 P_{mean} SF}{3 \sigma}\right) \quad (4.13)$$

Assuming that all the heat passes radially through the cylindrical part of the heater head and not the domed top. The temperature drop across the heater wall based on the required heat flow is then given by:

$$Q = \frac{BP}{\eta_{id}} = \frac{2 \pi L k_m \Delta T}{\ln \frac{d_3}{d_2}} \quad (4.14)$$

where

η_{id} = thermal efficiency of the engine (Li 1988, West, 1986)

L = heater length = cd_c (m)

k_m = thermal conductivity of the head material (W/m²K)

ΔT = temperature difference $T_2 - T_3$ (K)

substitute and solve for ΔT :

$$\Delta T = \frac{W_n C_n d_c^2 a P_{mean} f I \Gamma \ln\left(1 + \frac{4 P_{mean} SF}{3 \sigma}\right)}{8 \eta_{id} k_m c} \quad (4.15)$$

External heater head heat transfer area for a plain cylinder is:

$$A_{ext} = \pi b c d_c I (2b + d_c) \left(1 + \frac{4 P_{mean} SF}{3 \sigma}\right) \quad (4.16)$$

The heat loss down the regenerator wall is:

$$Q_{cond} = \frac{k_m \pi (d_3^2 - d_2^2) (T_H - T_K)}{4 L_{reg}} \quad (4.17)$$

The heat flux on the external cylinder wall is given by:

$$q_{cyl} = \frac{\frac{BP}{\eta_{id}} + Q_{cond}}{A_{ext}} \quad (4.18)$$

The losses associated with piston sealing vary considerably with the engine configuration, size, mean cycle pressure and engine speed. The configurations are compared for similar working conditions and hence determining seal velocity and combined seal circumference is sufficient for preliminary design comparison. There are three types of dynamic seal used in Stirling engines:

- (a). Piston Seal. This seals the piston to the cylinder wall and the pressure differential is the working space pressure to buffer space pressure for alpha, beta and gamma and working space to adjacent working space of the double acting design.
- (b). Displacer seal. The pressure difference across the displacer seal in beta and gamma engines has only the heat exchanger pressure drop. Consequently the seal is lightly loaded and slight leakage can be tolerated.
- (c). Rod seal. Beta, gamma and double acting engines require a piston or displacer rod seal. This seal has working space to buffer space pressure across it.

As the displacer seal has comparatively much lower loading than the piston and rod seal, it is neglected in the following.

The total seal circumference for beta, gamma and double acting configurations is given by:

$$L_{sc\beta} = \pi I (d_c + d_{rod}) \quad (4.19)$$

for alpha, assuming the cylinder diameters are equal i.e. $d_{com} = d_{exp} = d_c$

$$L_{sc} = \pi I 2 d_c \quad (4.20)$$

Dynamic seal longevity is related to the seal face PV (pressure x velocity). In this comparison the configurations are compared using same mean cycle pressure, therefore the pressure differential across the seals will be of similar magnitude. Hence a configuration with a lower piston velocity would be preferable. Assuming a sinusoidal piston motion the maximum relative seal velocity is:

$$u_{seal} = \frac{a d_c}{2} \omega \quad (4.21)$$

Space on a small yacht is limited so the engine dimensions should also be considered. The approximate overall engine size can be determined from multiples of stroke length S and the number of cylinders I, Table 4.3, (Reader and Hooper, 1983).

Drive mechanism	Height	Crankcase Width	Crankcase Length	Box Volume
In-line slider-crank	11.5 S	3 S	3 S I	103.5 S ³ I
Rhombic drive	14 S	7 S	3 S I	294 S ³ I
4-cylinder Swashplate	11 S	7.25 S	7.25 S	578 S ³

Table 4.3 Approximate dimensions for engines using various drive mechanisms.

Substituting for S, and using Equation 4.7, a 4 cycle double acting engine with a bore/stroke ratio of 2 the box volume is approximately given by:

$$\text{Box volume} \approx \frac{32.52 BP}{W_n P_{mean} f \Gamma} \quad (4.22)$$

4.9.9 Shuttle Loss

When the piston is at the top of its stroke, the temperature of the top end of the piston cap will be lower than the expansion space gas and wall temperatures due to losses from the thermal gradient down the piston. Therefore, heat will be transferred to the piston. When the piston is at the bottom of its stroke the temperature of the top end of the piston cap will be greater than that of the cylinder wall and heat will be transferred from the piston to the wall. This process occurring at engine speed can transport considerable heat from the hot end to the cold end. The magnitude of the loss can be determined by Equation 4.23, (Reader and Hooper, 1983).

$$Q_{sh} = \frac{0.4 S_l^2 k_g d_b (T_H - T_K)}{x_g L_p} \quad (4.23)$$

4.9.10 Appendix Loss

Due to the variation of pressure during the cycle, gas is pumped into and out of the appendix gap between the piston cap and the cylinder wall. This causes a transfer of enthalpy and pumping loss. The magnitude of this loss can be determined by Equation 4.24, (Reader and Hooper, 1983).

$$Q_{ap} = \left(\frac{\pi d_p}{k_g}\right)^{0.6} \frac{2 L_p (T_H - T_K)}{1.5} \left(\frac{(P_{max} - P_{min}) N C_p^{1.8}}{0.5 R (T_H - T_K)}\right) x_g^{2.6} \quad (4.24)$$

4.9.11 Comparison of the Configurations

To compare the merits of each configuration the above equations were computed by a Spreadsheet program. Required powers of 200 Watt electrical and 10 kW shaft were analyzed for five likely engine configurations. The results are given in Tables 4.4 to 4.7. The configurations analyzed were:

- (i) One cycle alpha, Alpha 1.
- (ii) Two cycle alpha, Alpha 2.
- (iii) Four cycle double acting, FCDA.
- (iv) One cycle Beta, Beta 1.
- (v) Four Cycle Beta, Beta 4.

General engine data			
Elec. Required power (W) =	200		
Alternator Efficiency =	0.6	Engine Shaft Power (W) =	333.3333
TH (K) =	1023		
TK (K) =	333	Γ (temp ratio) =	0.50885
Engine Speed (RPM) =	1500	f frequency (c/s) =	25
Mean cycle pressure (N/m ²) =	1000000	ω (Ang. vel.) (rad/s) =	157.0796
Wn (West number) =	0.25		
a (stroke/bore) =	0.5		
b (int. heater fin depth) =	0.005		
c (heater length/bore) =	1		
d (V_{com}/V_{exp}) =	0.9		
e (displacer length \times a/bore) =	3		
Heater head stress (N/m ²) =	30000000		
Factor of safety =	2		
k (cyl mat cond) (W/mK) =	20		
Lreg (regen length) (m) =	0.03		
Displacer gap (m) =	0.00017		

Table 4.4 Engine parameters for 200 watt electric output

Configuration	Alpha 1	Alpha 2	FCDA	Beta 1	Beta 4
l (number of cycles) =	1	2	4	1	4
Cn (Config. number) =	1.414	1.414	1.414	1	1
dc (cyl. bore) (m) =	0.057	0.046	0.036	0.064	0.041
d2 (m) =	0.067	0.056	0.046	0.074	0.051
d3 (m) =	0.073	0.060	0.050	0.081	0.055
Tcyl (m) =	0.0030	0.0025	0.0021	0.0033	0.0022
Disp. length (m) =	0.086	0.068	0.054	0.097	0.061
Delta T (K) =	0.73	0.46	0.29	0.65	0.26
Ext HX area (m ²) =	0.013	0.017	0.023	0.016	0.028
Conduction loss (W) =	304	414	571	371	686
Shuttle loss (W) =	33	42	52	42	66
Appendix loss (W) =	30.2	41.8	57.7	36.4	69.4
Tot Paras. Loss (W) =	368	497	681	449	821
Heat to cyl. (W) =	494	494	494	494	494
Heat required (W) =	799	908	1065	865	1180
Heat flux (kW/m ²) =	60	52	47	53	42
Fin. flux (kW/m ²) =	20	17	16	18	14
Vol. of HX mat (m ³) =	0.000068	0.00008	0.000096	0.000091	0.000123
Mass of HX mat (kg) =	0.55	0.64	0.77	0.72	0.99
Engine height (m) =	0.330	0.262	0.199	0.451	0.284
Engine width (m) =	0.172	0.137	0.131	0.225	0.142
Engine length (m) =	0.086	0.137	0.131	0.097	0.243
Box Volume (m ³) =	0.0049	0.0049	0.0034	0.0098	0.0098
Power/vol (kW/m ³) =	68	68	98	34	34
Num of pist and disp =	2	4	4	2	8
Piston stroke (m) =	0.029	0.023	0.018	0.032	0.020
Max Pist Vel (m/s) =	2.25	1.79	1.42	2.53	1.59
Rod or comp dia (m) =	0.054	0.043	0.011	0.020	0.013
Seal length (m) =	0.35	0.56	0.60	0.27	0.67

Table 4.5 Calculated engine data for 200 watt electrical output engine.

General engine data			
Elec. Required power (W) =	6000		
Alternator Efficiency =	0.6	Engine Shaft Power (W) =	10000
TH (K) =	1023		
TK (K) =	333	Γ (temp ratio) =	0.50885
Engine Speed (RPM) =	1500	f frequency (c/s) =	25
Mean cycle pressure (N/m ²) =	1000000	w (Ang. vel.) (rad/s) =	157.0796
Wn (West number) =	0.25		
a (stroke/bore) =	0.5		
b (int. heater fin depth) =	0.005		
c (heater length/bore) =	1		
d (Vcom/Vexp) =	0.9		
e (displacer length x a/bore) =	3		
Heater head stress (N/m ²) =	30000000		
Factor of safety =	2		
k (cyl mat cond) (W/mK) =	20		
Lreg (regen length) (m) =	0.03		
Displacer gap (m) =	0.0002		

Table 4.6 Engine parameters for 10 kW shaft output

Configuration	Alpha 1	Alpha 2	FCDA	Beta 1	Beta 4
I (number of cycles) =	1	2	4	1	4
Cn (Config. number) =	1.414	1.414	1.414	1	1
dc (cyl. bore) (m) =	0.178	0.141	0.112	0.200	0.126
d2 (m) =	0.188	0.151	0.122	0.210	0.136
d3 (m) =	0.205	0.165	0.133	0.229	0.148
Tcyl (m) =	0.0084	0.0067	0.0054	0.0093	0.0060
Disp. length (m) =	0.267	0.212	0.168	0.300	0.189
Delta T (K) =	7.08	4.46	2.81	6.31	2.50
Ext HX area (m ²) =	0.115	0.147	0.188	0.144	0.235
Conduction loss (W) =	2377	3078	4012	2960	4965
Shuttle loss (W) =	270	341	429	341	541
Appendix loss (W) =	283.0	391.0	540.3	340.4	650.0
Tot Paras. Loss (W) =	2930	3810	4982	3641	6156
Heat to cyl. (W) =	14826	14826	14826	14826	14826
Heat required (W) =	17203	17904	18839	17786	19791
Heat flux (kW/m ²) =	150	122	100	124	84
Fin. flux (kW/m ²) =	50	41	33	41	28
Vol. of HX mat (m ³) =	0.001309	0.00139	0.001496	0.001804	0.002036
Mass of HX mat (kg) =	10.47	11.12	11.97	14.43	16.28
Engine height (m) =	1.025	0.813	0.618	1.400	0.882
Engine width (m) =	0.535	0.424	0.407	0.700	0.441
Engine length (m) =	0.267	0.424	0.407	0.300	0.756
Box Volume (m ³) =	0.1465	0.1465	0.1023	0.2943	0.2943
Power/vol (kW/m ³) =	68	68	98	34	34
Num of pist and disp =	2	4	4	2	8
Piston stroke (m) =	0.089	0.071	0.056	0.100	0.063
Max Pist Vel (m/s) =	7.00	5.56	4.41	7.86	4.95
Rod or comp dia (m) =	0.169	0.134	0.036	0.063	0.040
Seal length (m) =	1.09	1.73	1.86	0.83	2.08

Table 4.7 Calculated engine data 10 kW output engine.

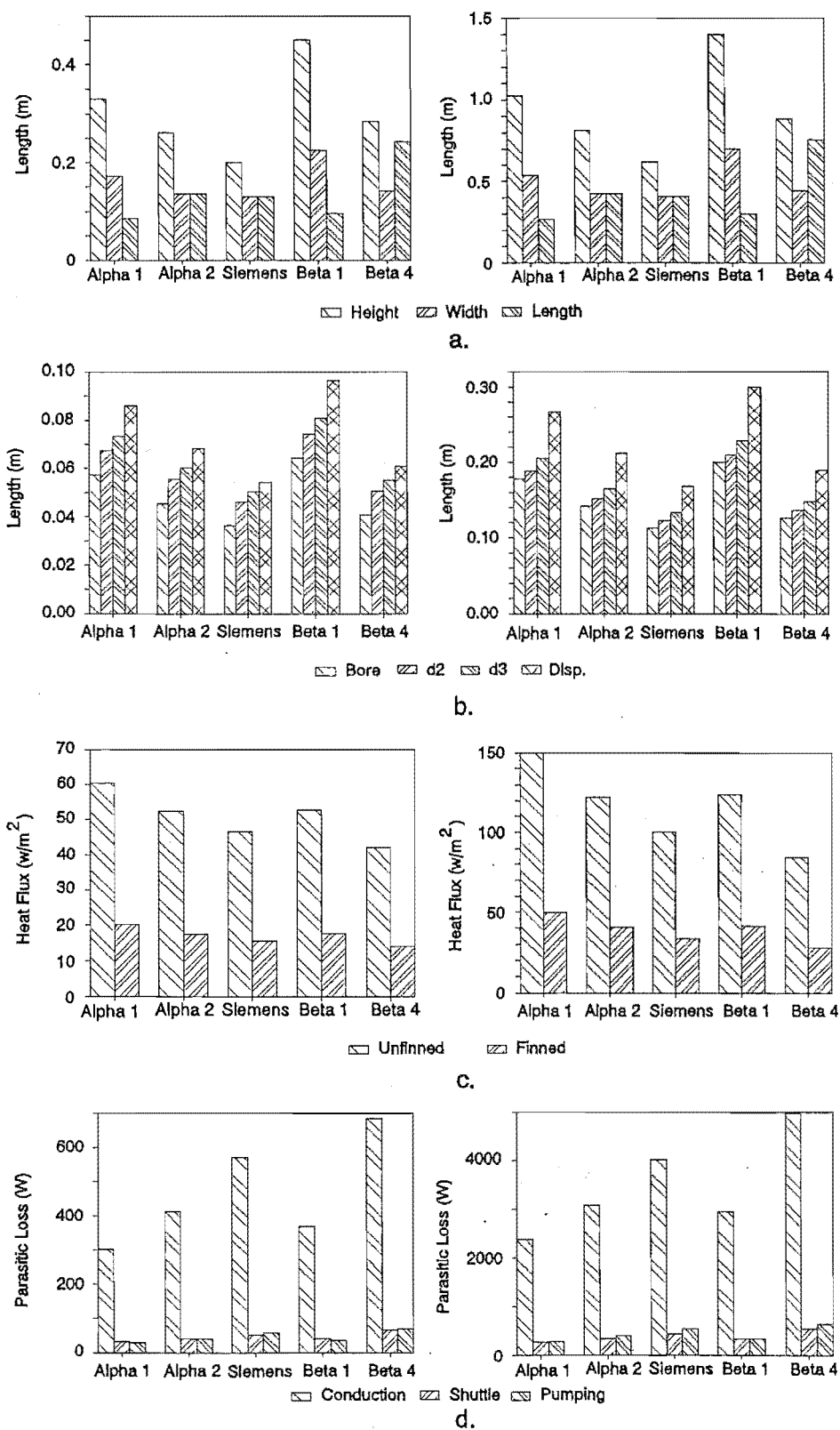


Figure 4.11 Configuration comparison for 200 and 10 000 W engines. (a) Overall engine dimensions. (b) Component size. (c) Heat flux for finned and unfinned head. (d) Parasitic losses.

Some of the results of the calculations are shown graphically in Figure 4.11. It was still too difficult to determine an optimum from these results so a decision aid technique was required.

4.9.12 Decision Matrix

A decision matrix technique was utilised. This is a commonly used technique, for a full description of it refer texts such as Pahl and Beitz (1988).

The objectives tree Table 4.8 and evaluation chart Table 4.9 was developed on a Spreadsheet program which allows easy editing and displaying of the results.

Level 1		Level 2				Level 3		Wt
	L 1		L2	L1*L2			L3	L1*L2*L3
SEBCY	1	Low cost	0.18	0.18	Low Cost	Low Complexity	0.25	0.045
		Reliable	0.25	0.25		Many Similar Components.	0.18	0.032
	1	Efficient	0.12	0.12		Many Bought in Components	0.15	0.027
		Size	0.20	0.20		Low Material Cost	0.25	0.045
		Meets The Objectives	0.25	0.25		Easy to Assembly	0.17	0.031
					Reliable	Low Wear	0.7	0.175
						Low Maintenance	0.3	0.075
					Efficient	Good Heat Exchanger Layout	0.35	0.042
						Low Parasitic Loss	0.2	0.024
						Mechanically Efficient Design	0.25	0.030
						High Burner Efficiency	0.2	0.024
					Compact Design	Height	0.3	0.060
						Width	0.2	0.040
						Length	0.2	0.040
						Volume	0.3	0.060
					Meets the Objectives	Quiet Operation	0.4	0.100
						Low Vibration	0.3	0.075
						Low Starting Torque	0.3	0.075
								$\Sigma Wt = 1.0$

Table 4.8 Objectives tree for the SEBCY.

Level 3	Wt		Alpha 1		Alpha 2		FCDA		Beta 1		Beta 4
	Wt	V1	Wt*V1	V2	Wt*V2	V3	Wt*V3	V4	Wt*V4	V5	Wt*V5
Low Complex.	0.045	8	0.36	6	0.27	3	0.14	4	0.18	1	0.05
Many Similar Components	0.032	3	0.10	6	0.19	8	0.26	3	0.10	8	0.26
Many Bought Components	0.027	5	0.14	5	0.14	7	0.19	4	0.11	4	0.11
Low Mat. Cost	0.045	6	0.27	5	0.23	5	0.23	5	0.23	3	0.14
Easy Assembly	0.031	8	0.24	6	0.18	4	0.12	5	0.15	1	0.03
Low Wear	0.175	3	0.53	3	0.53	7	1.23	3	0.53	2	0.35
Low Maint.	0.075	3	0.23	3	0.23	7	0.53	3	0.23	3	0.23
Heat Exch. Layout	0.042	3	0.13	5	0.21	8	0.34	3	0.13	8	0.34
Low Parasitic Losses.	0.024	8	0.19	6	0.14	3	0.07	6	0.14	2	0.05
Mechanically Efficient	0.030	6	0.18	4	0.12	7	0.21	4	0.12	2	0.06
High Burner Efficiency	0.024	3	0.07	5	0.12	7	0.17	3	0.07	8	0.19
Height	0.060	3	0.18	5	0.30	8	0.48	1	0.06	4	0.24
Width	0.040	3	0.12	6	0.24	8	0.32	2	0.08	4	0.16
Length	0.040	7	0.28	6	0.24	6	0.24	8	0.32	3	0.12
Volume	0.060	5	0.30	5	0.30	9	0.54	3	0.18	3	0.18
Quiet Op.	0.100	4	0.40	4	0.40	8	0.80	4	0.40	3	0.30
Low Vibration	0.075	4	0.30	4	0.30	9	0.68	3	0.23	9	0.68
Low Starting Torque	0.075	1	0.08	4	0.30	8	0.60	3	0.23	8	0.60
$\Sigma Wt*V_i$			4.08		4.43		7.12		3.47		4.06

Table 4.9 Evaluation table for the five configurations.

The technique requires the designer to nominate performance values V_i , these can be determined by judgement or from calculated data. Results calculated in Table 4.5 were utilised where appropriate to specify the value of V_i to remove designer judgement. It can be seen that the four cycle double acting configuration excels for this application, giving the greatest $\Sigma Wt \cdot V_i$. The dominant factors influencing this result were: large heat transfer area for the swept volume, compact design, low vibration, and low starting torque. Based on this analysis the four cylinder double acting engine was selected for the SEBCY.

4.10 Mechanisms

Many mechanisms have been published which give the desired piston motion but few meet the needs of this project. Some of the popular arrangements used by Stirling engine designers are shown in Figure 4.14. United Stirling have had considerable success with the U form, Figure 5.1 (f) which has two crankshafts and an intermediate coupling shaft which gives opposite rotation of the crankshafts and allows complete dynamic balance (West, 1986). Most double acting engines adopted by Philips utilised the Z form either using a wobble or swash type mechanisms which also give good balance. To use the alternator shaft as the main shaft of the engine the Z form was considered compact and allowed easy manufacture of the engine casing. It was also considered that larger versions would fit the engine space of most yachts when lying at an angle parallel to the propeller shaft. The Z form is also more suited to having a cylindrical pressurised crankcase or pressure shell which eliminates the need for atmospheric reciprocating seals on the piston rod, Section 5.2.

A new wobble yoke mechanism was developed for the SEBCY which uses the Z form, similar to the wobble plate, Figure 4.14. A detailed description of the mechanism design is presented in Chapter 5.

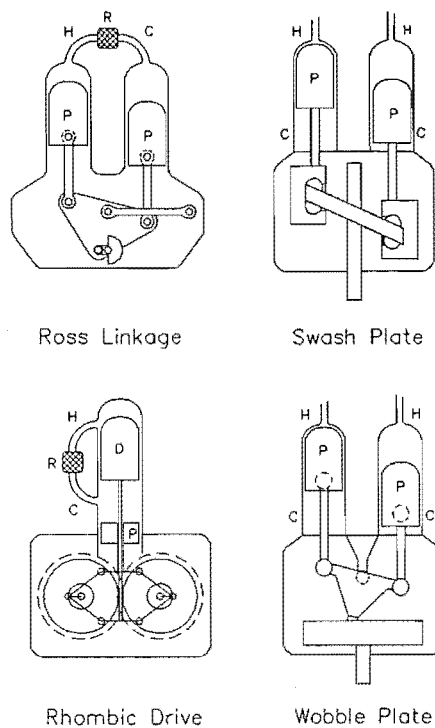


Figure 4.14 Popular Stirling engine mechanism designs, also refer to figure 5.1. The swash and wobble plate engines are both Z form engines.

4.11 Summary of Conclusions of Chapter 4

- The system nominal power output is to be 200 Watts electrical, which gives 15 Amps at 13.6 Volts. This requires a system which has automatic start, regulation and shutdown.
- Use a claw pole alternator which requires an engine shaft speed of 1500 RPM.
- Use air as the working fluid, this requires that there are no free lubricants in the engine mechanism housing.

- Use a crankcase pressure of 10 bar which allows the owner to recharge with readily available equipment if necessary.
- Use secondary fluid cooling to allow the engine to be used in a confined space and waste heat recovery.
- Use a finned head hot end heat exchanger rather than tubular to eliminate welds in the hot zone and reduce the overall engine size.
- Use a naturally aspirated LPG burner. This requires careful burner design to obtain sufficient heat transfer with low burner pressure drop.
- Use a preheater to improve engine efficiency but the preheated air temperature must be below the auto-ignition temperature of the fuel if a premixed flame is used.
- There has been an inconsistency in the literature over the use of the Beale and West First order equations. It is recommended that the West equation is adopted with an added configuration number, C_n .
- Despite higher parasitic losses the four cycle double acting design offers the best attributes for this application.
- Cost effective detail design is of high priority to be competitive with existing engines. It is not expected that the system retail price will be below existing systems but the overall performance will be superior for this application. Highlighting the key improvements over existing technology will be of high priority in marketing the SEBCY.

5 Wobble Yoke

5.1 Introduction

The challenge of developing an engine mechanism with qualities suited to the Stirling Engine has attracted many inventors for more than a century. Consequently an almost bewildering array of possible designs exist for the engineer to select from. Unfortunately few of the existing designs suit this project.

This Chapter evaluates existing mechanisms, describes the development of the wobble yoke design which is based on the classic spherical four bar linkage, investigates its use with the SEBCY and describes some alternative applications which could use the wobble yoke.

5.2 Mechanism requirements

Engines with an output drive shaft generally require a dynamic atmospheric seal¹. In some cases, to reduce the weight of the engine and ensure fast response time for pressure variation power control, this seal is between the housing and the piston connecting rod. Examples of using this technique are the General Motors GPU 3, United Stirling 4-95 Figure 5.1(f), and the Ford swash plate engines. In these cases the mechanism housing is at atmospheric pressure. Hence the dynamic piston rod seal must be capable of sealing the pressure differential between the working space and atmospheric pressure. In some cases the pressure differential may be close to 21 MPa

¹ Magnetic drives are an exception.

of H_2 in high performance engines, (Walker, 1980). This seal has plagued engine designers, often being the life limiting component in these engines. A number of designs reduce the sealing problem to a conventional rotary mechanical seal by designing the mechanism housing as a pressure vessel. The STM4-120 variable angle swash plate engine is an example of this, (Meijer 1986) Figure 5.1(d). In this case the rod seal pressure differential is reduced to the difference between the cycle and mechanism housing pressure. Techniques other than mean pressure variation, however, are required to enable fast response for power control. For example the STM4-120 engine utilises dead volume control by a variable angle swash plate. An added advantage of this method of power control is high part load efficiency (Meijer 1986). Hermetically sealed mechanism housings do not require a dynamic atmospheric seal. In such cases the electric generator is sealed in the pressure vessel and electric conductors are passed through the vessel wall.

Prevention of leakage of mechanism lubricants into the cycle space also requires complex seals often in the form of pumping rings or roll sock seals. This is particularly acute when combustible mixtures can be formed when using air as the working fluid (Hargreaves 1991). For this project the mechanism should:

- Be suitable for engines up to 20 kW to allow parametric engine scaling while maintaining the general engine design.
- Require no free lubricants, as they can enter the working space, eliminating the need for an oil seal on the piston rod and the formation of explosive mixtures.
- Be a compact design that allows the mechanism housing to be pressurised with minimum weight penalty.
- Easy to manufacture and assemble using conventional machine shop equipment, improving the economics of smaller production quantities.
- Be well balanced.

- Be quiet.
- Give the desired piston motion without high piston side loads.
- Have variable stroke for ease of power control with a pressurised mechanism housing.
- Suit double acting engines.
- Be mechanically efficient.

5.3 Review of existing designs

The following paragraphs outline some of the published engine mechanisms which have been or could be used in double acting Stirling Engines.

5.3.1 Wobble Plate

Figure 5.1(a) shows a four cycle double acting engine designed by the well known nineteenth century engineer Sir William Siemens. This engine was based on the wobble plate but there are no reports of the engine ever being manufactured (Walker, 1980). Yu (1986) made an investigation of wobble plates and published an extensive list of relevant patents. At first it seems surprising that with such a large number of patents on the subject that there are no commercial engine^b applications. However a close investigation of many of the patents revealed a lack of understanding of the mechanism kinematics of many designs. Relevant patents are discussed in Section 5.4.3. This impression was confirmed by Colin Campbell (1941) who wrote: "Most of these (..patents..) show a complete ignorance of the kinematics of wobble plates". A common mistake has been to inadequately or over constrain the wobble plate torque reaction (Campbell, 1941). Figure 5.1(b) shows the Bristol wobble plate engine, the torque arm is clearly shown extending from the wobble plate to the housing. The engineers at Philips developed several Stirling Engines based on the wobble plate design (Van Weenan, 1947, Hargreaves, 1991). A variable angle

^b There are successful compressors available based on wobble plate designs.

wobble plate suitable for automotive applications was designed for the ADVENCO engine (Meijer and Ziph, 1979) but was never manufactured Figure 5.1(c). In this design the torque reaction is transmitted through a nutating bevel gear and multi degree of freedom joints are required on both ends of the connecting rod.

The major problems to overcome with the wobble plate design are:

- The loci of the connecting rod bearing follows an arc in one plane, a figure of eight in another and, if designed correctly, a circle in the third, (Campbell, 1941) requiring spherical or universal joints.
- Transferring the torque reaction to the engine casing. This is often achieved with a torque arm (Campbell 1941, Rizzo 1985, Nakesh 1960) or a bevel gear (Meijer and Ziph 1979, Brille 1981).

5.3.2 Swash Plate

Like the wobble plate the swash plate has received extensive design attention but has had more commercial success. Common applications include: automotive air conditioning compressors, hydraulics, pneumatics and Stirling Engines. Swash plate developments at Philips, Ford and STM have successfully led to the STM4-120 engine, Figure 5.1(d). The engine is based on a variable angle swash plate the angle of which is positioned by a hydraulic motor, (Ziph and Meijer, 1981). This is an exceptional engine which is the result of the skill and dedication of the engineers at Philips and later Stirling Thermal Motors.

The envisaged design difficulties with the swash plate for this application are:

- The extreme lubrication requirement of the slipper pads and piston guides. This would require considerable design and development work for each engine size making it less desirable for small production runs of parametrically designed engines.
- Problems have been noted at low speeds, when the torque is high, due to the hydrodynamic lubrication not being fully developed. This sometimes requires power controls to limit the low speed torque.
- Air would be unsuitable as the working fluid due to the lubrication requirements, or the rod seal must prevent lubricants entering the working space over the life of the engine.
- The piston rods have high side load due to the reaction force against the swash plate.
- The design requires many special precision manufactured components which is more suited to high volume production.


5.3.3 Slider Crank

Most internal combustion engines and compressors use this mechanism. Several Stirling Engine designers are using this technology, for example the United Stirling 4-95 (Crouch and Pope 1982). It has the benefit of using existing internal combustion engine technology. There are a number of geometries which give the required piston motion, some of these are shown in Figures 5.1(e) and (f). Figure 5.1(g) shows a compact slider crank which does not require a sliding cross head, this design has the added advantage of good engine balance.

The slider crank mechanism has several disadvantages making it unsuitable for this project, including:

- High piston side loads due to the connecting rod angle which is generally overcome with the use of cross heads which require lubrication. This generally results in additional frictional loss, increased engine size and added rod sealing complexity.
- The mechanism housing is generally not suited to pressurisation for engines of more than a few kilowatts. Consequently complex piston rod seals are required.

5.3.4 Twin Ross Yoke

No references to double acting applications of the Ross Yoke have been located. If the following  Wobble Yoke design was not used this would be a likely candidate due to low piston side loads and ability to be manufactured using conventional machine shop equipment. The mechanism is also suited to using prelubricated bearings, parametric design and low volume production techniques.

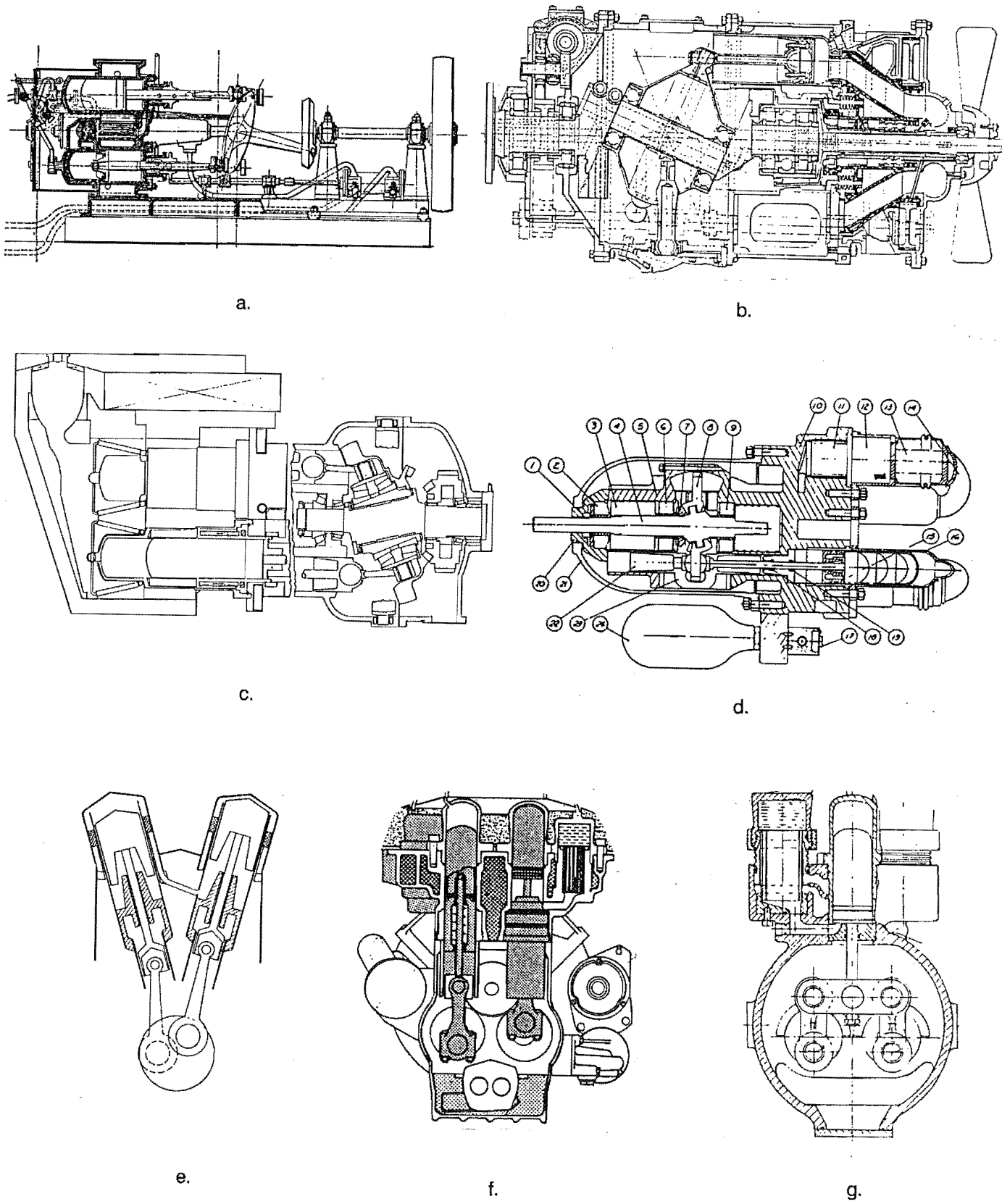


Figure 5.1 (a). Siemens wobble plate after Walker (1980) (b). Bristol axial engine showing the torque arm, after Campbell (1941) (c). Variable angle wobble plate after Meijer and Ziph (1979) (d). Variable angle swash plate, note the long guide on the piston rod, after Hargreaves (1991) (e). Vee form slider crank, note the added engine height due to the cross heads, after Hargreaves (1991) (f). U form slider crank, note the rod seal assembly and the cross heads, after Crouch and Pope (1982) (g). In line twin crank with cross head, note the piston side loads are balanced and do not require a sliding cross head, after Carlqvist and Gothberg (1989)

Important considerations with the Ross yoke are:

- The piston motion is not sinusoidal and phasing would not be consistently 90 degrees for all cycles of a four cycle double acting engine.
- Good engine balance may be difficult to achieve due to the non sinusoidal piston motion (Doige and Walker, 1986).

5.4 Wobble Yoke

The following Sections describe the design of a wobble yoke mechanism developed to meet the requirements of this project. The basis of the design is the spherical crank-rocker, Figure 5.2.

Notation, referring to Figure 5.3:

d_b	piston diameter
d_r	piston rod diameter
$F(\theta)_{dn}$	instantaneous force on bearing d of the n^{th} cylinder
I	wobble yoke mass moment of inertia about the main pivot b (kg m^2)
m_n	piston assembly mass including the connecting rod
n	cylinder number ($n=1$ on positive x axis, $n=3$ on the positive z axis)
$P(\theta)_n$	instantaneous pressure in the compression space of the n^{th} cylinder
$P(\theta)_{n-1}$	instantaneous pressure in the expansion space of the n^{th} cylinder
P_b	Buffer space pressure
R	rotational degree of freedom
r	radius or distance, m
r_{bal}	radius of balance mass
m_{bal}	balance mass
y_{bal}	distance between the balance masses parallel to the engine axis
y	axis of engine
x	axis passing through the centre of cylinders 3 and 1
z	axis passing through the centre of cylinders 2 and 4
θ	instantaneous crank angle, rad
ω	crankshaft angular velocity, rad/s
γ	maximum beam displacement angle, $\gamma = \sin^{-1}(\text{stroke}/2r_{bd})$, rad
κ	$\tan(\gamma)$
$\phi(\theta)$	instantaneous beam angle, rad

Subscripts:

a	nutating bearing centre	b	the main pivot centre
c	wobble yoke-beam bearing centre	d	connecting rod bearing centre
e	crankshaft bearing centre	f	piston-connecting rod bearing centre

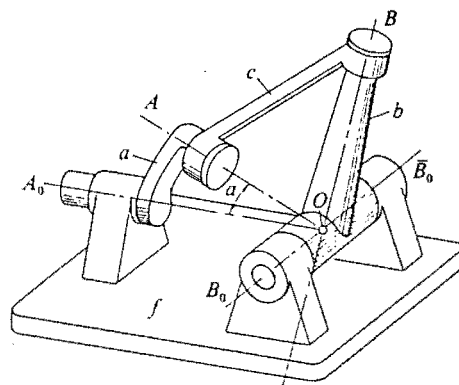


Figure 5.2 Spherical crank rocker, after Chiang (1988)

5.4.1 Type 1

Referring to Figures 5.3 and 5.4(a) this mechanism is based on a beam which pivots about its centre, b , in one plane and is attached to the piston connecting rods at each end via bearings, d , with one degree of freedom R_z . An eccentric bearing, a , is fitted to the driveshaft and is connected to the beam via the wobble yoke and two bearings, c , whose axis pass through the main pivot centre. Bearings c also require one degree of freedom R_x . Providing the maximum beam angle is small < 10 degrees, rotation of the driveshaft causes near sinusoidal motion of the piston when the cylinder is parallel to the axis of the engine. The axis of bearings a, c, e must intersect at the centre of the main bearing, b . This design gives two connecting rods moving on one plane at 180 degrees phasing which can have lower connecting rod bearings, d , with one degree of freedom R_z . The connecting rod ends in the yz plane, 90 degree phase to the beam, move in an arc on the yz plane but on the xy plane in a figure of eight. Therefore a two degree of freedom joint, R_{xz} , is required at both ends of the connecting rod. This is a disadvantage as spherical type joints could introduce added expense and unreliable operation to the system. The type 1 wobble yoke was successfully used for tests on the DMC 3 engine, Section 6.4.

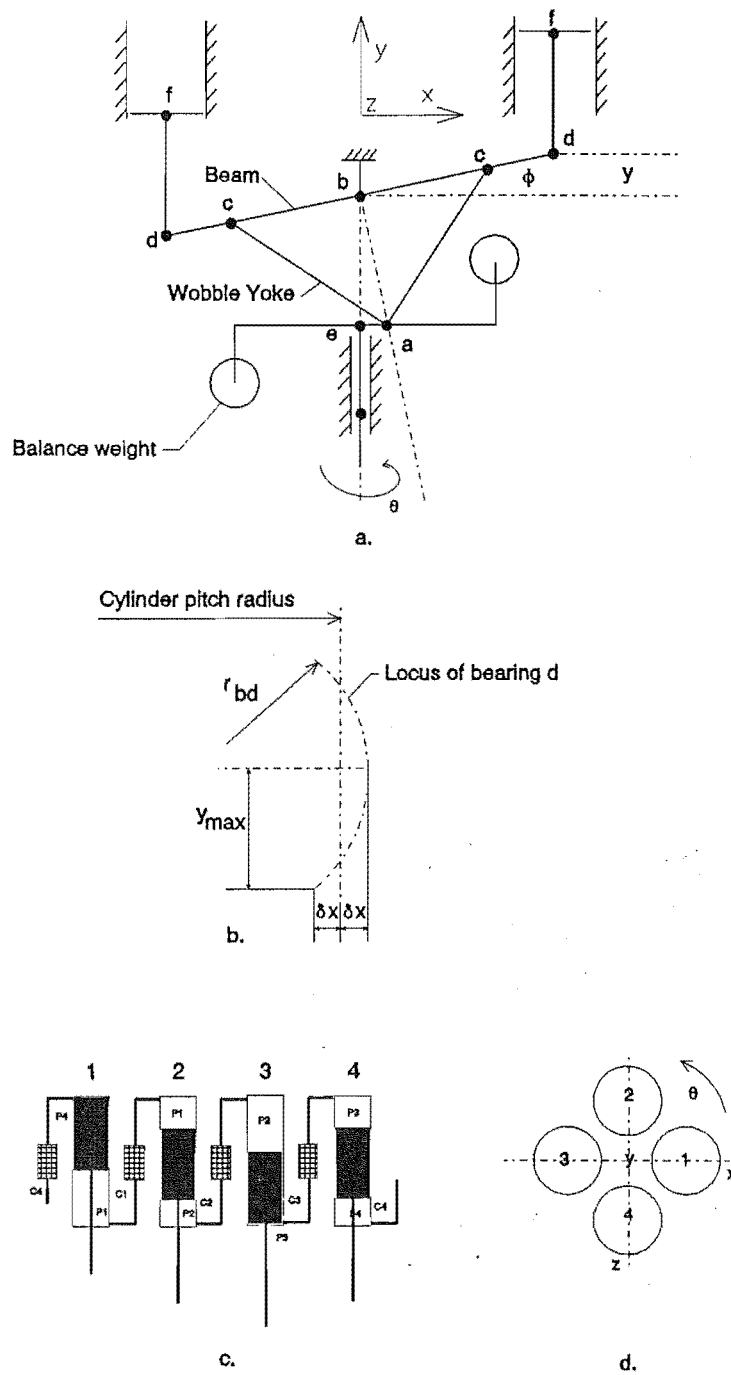


Figure 5.3 (a) Wobble yoke notation. (b) Offset of bearing centre d from the cylinder pitch radius. (c) Piston positions at top dead centre. (d) Cylinder order viewed from the burner end.

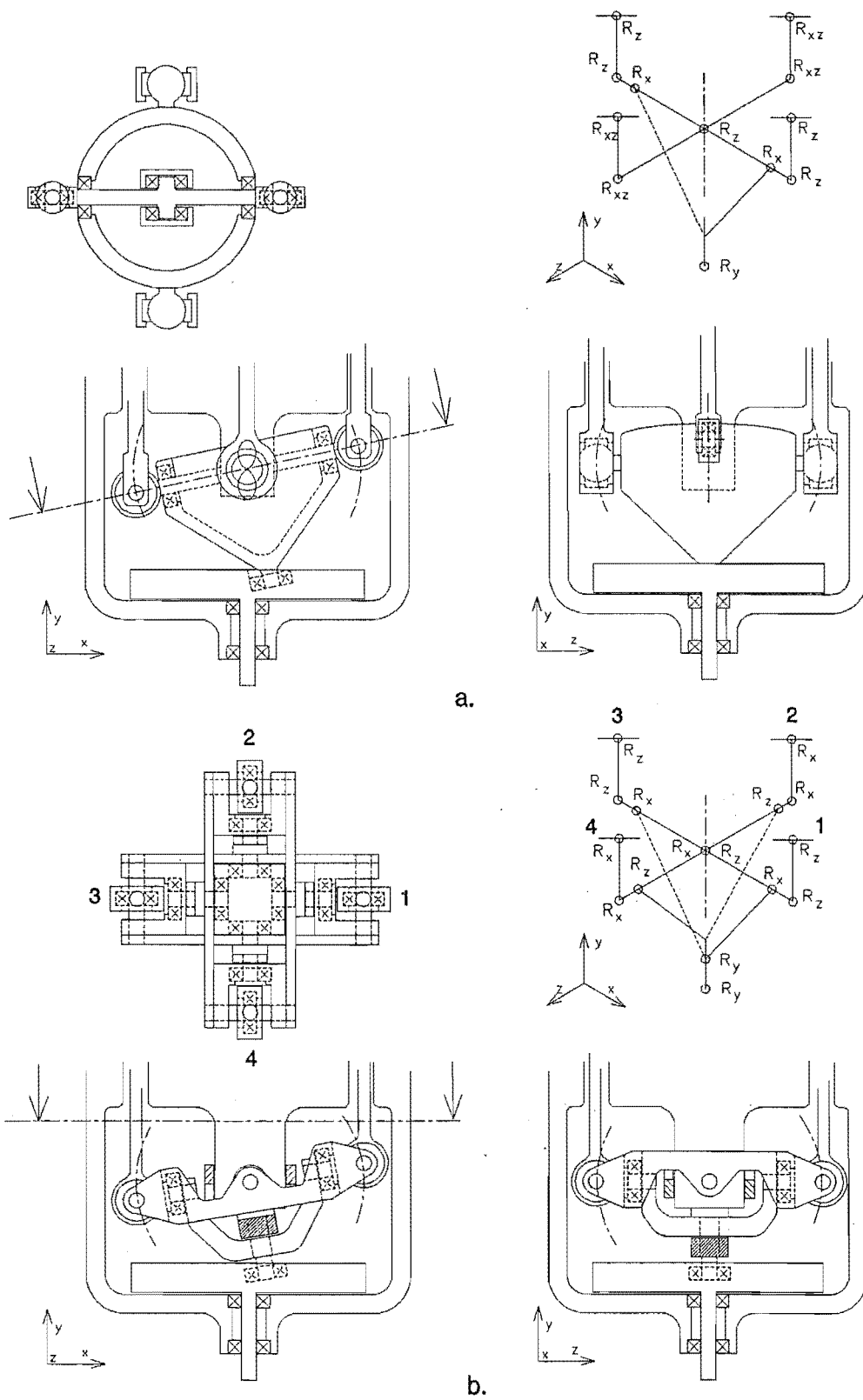


Figure 5.4(a) Type 1 and (b) Type 2 wobble yoke layout.

5.4.2 Type 2

To overcome the requirement for two degree of freedom bearings a second wobble yoke is introduced on the yz plane, Figure 5.4(b). This gives four pistons at 90 degrees phase, all with single degree of freedom bearings.

The advantages this system offers are:

- The torque reaction is taken through the main pivot bearings, b, not slides.
- All bearings can be deep groove ball races or similar.
- Prelubricated sealed bearings can be used.
- Very small horizontal displacement of the connecting rod bearing δx_d , giving low piston side load.

5.4.3 Patents, Prior Art

More than 400 relevant patents and documented mechanisms were examined to determine the novelty of the wobble yoke. Several designs were found which utilise the spherical crank rocker mechanism but none of these reduced all bearings to single degree of freedom which is one advantage of the wobble yoke. The nearest design located was a patent by J. Ziegler (1985) Figure 5.5(a). Like most wobble mechanisms this design requires spherical bearings at the connecting rod ends due to the non planer motion of bearings 34, Figure 5.5(a). The patent by D Wehr (1930) is a classic example of the ignorance of the early wobble mechanism designers regarding loading and kinematics. The elevation view of this mechanism, Figure 5.5(b), appears to be of a similar form to the wobble yoke. The plan view, however, shows that the engine reaction torque is transmitted as a moment about the engine axis through bearing 26, and the visible connecting rod 20 is the only one with planar motion.

5.4.4 Wobble Yoke Kinematics

The following derives the equations of motion for the beams, yoke and pistons using a Cartesian coordinate system. Chiang (1988) develops the kinematics for the spherical four bar linkage, Figure 5.2, by vector analysis.

Referring to Figure 5.3, based on the assumption that r_{ac} remains constant for all θ and the origin is at b, then:

$$r_{ac}^2 = (x_a - x_c)^2 + (y_a - y_c)^2 + (z_a - z_c)^2 \quad (5.1)$$

expand Equation 5.1

$$R_{ac}^2 = x_a^2 - 2x_ax_c + x_c^2 + y_a^2 - 2y_ay_c + y_c^2 + z_a^2 - 2z_az_c + z_c^2 \quad (5.2)$$

where

$$x_a = r_{a\theta} \cos \theta \quad y_a = -\frac{r_{a\theta}}{\kappa} \quad z_a = r_{a\theta} \sin \theta$$

$$x_c = r_{bc} \cos \phi \quad y_c = r_{bc} \sin \phi \quad z_c = 0$$

substitute into 5.2

$$r_{ac}^2 = r_{a\theta}^2 \cos^2 \theta - 2r_{a\theta} \cos \theta r_{bc} \cos \phi + r_{bc}^2 \cos^2 \phi$$

$$+ \left(\frac{r_{a\theta}}{\kappa}\right)^2 + 2\left(\frac{r_{a\theta}}{\kappa}\right) r_{bc} \sin \phi + r_{bc}^2 \sin^2 \phi$$

$$+ r_{a\theta}^2 \sin^2 \theta - 2r_{a\theta} \sin \theta \cdot 0 + 0$$

rearrange and simplify

$$r_{ac}^2 = r_{a\theta}^2 (\cos^2 \theta + \sin^2 \theta) + r_{bc}^2 (\cos^2 \phi + \sin^2 \phi) + \left(\frac{r_{a\theta}}{\kappa}\right)^2$$

$$+ 2r_{a\theta} r_{bc} \left(\frac{\sin \phi}{\kappa} - \cos \phi \cos \theta\right)$$

simplify further

$$r_{ac}^2 - r_{ao}^2 - r_{bc}^2 - \left(\frac{r_{ao}}{\kappa}\right)^2 = 2r_{ao}r_{bc} \left(\frac{\sin\phi}{\kappa} - \cos\phi \cos\theta\right) \quad (5.3)$$

the left side of Equation 5.3 is equal to zero therefore

$$0 = \frac{\sin\phi}{\kappa} - \cos\phi \cos\theta$$

giving the equation for the angular displacement of the beam with respect to θ .

$$\phi = \tan^{-1}(\kappa \cos \omega t) \quad (5.4)$$

Alternatively for each cylinder

$$\phi(\theta) = \tan^{-1}(\kappa \cos(\omega t - (n-1)\pi/2)) \quad (5.5)$$

The above equation gives the angular displacement of the beam for a particular crank angle. The first and second differentials give the angular velocity and acceleration of the beam respectively.

Differentiating Equation 5.5 for beam angular velocity

$$\frac{d \tan\phi}{dt} = -\kappa \omega \sin\omega t$$

$$\frac{1}{\cos^2\phi} \frac{d\phi}{dt} = -\kappa \omega \sin\omega t$$

$$\dot{\phi} = -\kappa \omega \sin\omega t \cos^2\phi \quad (5.6)$$

Differentiating Equation 5.6 to give angular acceleration of the beam.

$$\frac{d^2\phi}{dt^2} = -\kappa\omega^2 \cos\omega t \cos^2\phi + \kappa\omega \sin\omega t 2\cos\phi \sin\phi \frac{d\phi}{dt}$$

$$\frac{d^2\phi}{dt^2} = -\kappa\omega^2 \cos\omega t \cos^2\phi + \kappa\omega \sin\omega t \sin 2\phi \frac{d\phi}{dt}$$

$$\frac{d^2\phi}{dt^2} = -\kappa\omega^2 \cos\omega t \cos^2\phi + \kappa\omega \sin\omega t \sin 2\phi (-\kappa\omega \sin\omega t \cos^2\phi)$$

$$\ddot{\phi} = -\kappa\omega^2 \cos^2\phi (\cos\omega t + \kappa \sin^2\omega t \sin 2\phi) \quad (5.7)$$

Universally for the two wobble yokes at 90 degrees phase

$$\ddot{\phi}(\theta)_x = -\kappa\omega^2 \cos^2(\phi(\omega t)) (\cos(\omega t) + \kappa \sin^2(\omega t) \sin(2\phi(\omega t))) \quad (5.8)$$

$$\ddot{\phi}(\theta)_z = -\kappa\omega^2 \cos^2(\phi(\omega t + \frac{\pi}{2})) (\cos(\omega t + \frac{\pi}{2}) + \kappa \sin^2(\omega t + \frac{\pi}{2}) \sin(2\phi(\omega t + \frac{\pi}{2})))$$

The angular beam displacement is translated to the vertical displacement of bearing, d, for each cylinder as a function of the shaft angle θ by:

$$y(\theta)_{dn} = r_{bd} \sin(\tan^{-1}(\kappa \cos(\omega t - (n-1)\frac{\pi}{2}))) \quad (5.9)$$

The linear velocity, s, tangential to the locus of bearing d (perpendicular to the beam) is given by:

$$\frac{ds}{dt} = \frac{d\phi}{dt} r_{bd}$$

Neglecting the slight x displacement, δx_d , of bearing d the piston velocity is:

$$\frac{dy_f}{dt} \approx \frac{d\phi}{dt} r_{bd} \cos\phi$$

substituting Equation 5.9 and making universal for all cylinders:

$$\dot{y}_f = -\kappa\omega \sin\omega t \cos^2\phi r_{bd} \cos\phi$$

$$\dot{y}(\theta)_m = -r_{bd}\kappa\omega \sin\left(\omega t + (n-1)\frac{\pi}{2}\right) \cos^3\left(\phi\left(\omega t + (n-1)\frac{\pi}{2}\right)\right) \quad (5.10)$$

similarly for acceleration:

$$\frac{d^2y_f}{dt^2} = -r_{bd}\kappa\omega \left(\omega \cos\omega t \cos^3\phi - 3\sin\omega t \cos^2\phi \sin\phi \frac{d\phi}{dt} \right)$$

$$\frac{d^2y_f}{dt^2} = -r_{bd}\kappa\omega \left(\omega \cos\omega t \cos^3\phi - 3\sin\omega t \sin\phi \cos^2\phi (-\kappa\omega \sin\omega t \cos^2\phi) \right)$$

$$\frac{d^2y_f}{dt^2} = -r_{bd}\kappa\omega^2 \cos^3\phi (\cos\omega t + 3\kappa \sin^2\omega t \sin\phi \cos\phi)$$

$$\frac{d^2y_f}{dt^2} = -r_{bd}\kappa\omega^2 \cos^3\phi \left(\cos\omega t + \frac{3}{2}\kappa \sin^2\omega t \sin 2\phi \right)$$

Making universal to all cylinders the piston acceleration is:

$$\begin{aligned} \ddot{y}(\theta)_m = & -r_{bd}\kappa\omega^2 \cos^3\left(\phi\left(\omega t + (n-1)\frac{\pi}{2}\right)\right) \left(\cos\left(\omega t + (n-1)\frac{\pi}{2}\right) \right. \\ & \left. + \frac{3}{2}\kappa \sin^2\left(\omega t + (n-1)\frac{\pi}{2}\right) \sin\left(2\left(\phi\left(\omega t + (n-1)\frac{\pi}{2}\right)\right)\right) \right) \end{aligned} \quad (5.11)$$

5.4.5 Comparison with simple harmonic and slider crank

As a comparison, the above equations for piston displacement, velocity and acceleration are graphed with simple harmonic motion and a slider crank verse crank angle, Figure 5.6. The constants used were:

$$y_{\max} = .010\text{m (stroke/2 for SEBCY)}$$

$$\omega = 157.1 \text{ rad/s (1500 rpm)}$$

$$q = 3.5 \text{ (conrod length/} y_{\max} \text{ generally between 3.5 and 5 (Reader and Hooper, 1983))}$$

$$r_{ab} = 0.050 \text{ m}$$

$$r_{bd} = 0.0604 \text{ m}$$

$$\gamma = 9.53^\circ$$

The kinematic equations are:

Simple harmonic motion

$$y_f = y_{\max} \cos \omega t \quad \dot{y}_f = -y_{\max} \omega \sin \omega t \quad \ddot{y}_f = -y_{\max} \omega^2 \cos \omega t$$

Slider crank (Hannah and Stephens, 1970)

$$y_f = y_{\max} [1 - \cos \omega t + q - \sqrt{(q^2 - \sin^2 \omega t)}] \quad \dot{y}_f = y_{\max} \omega \left[\sin \omega t + \frac{\sin 2\omega t}{2\sqrt{(q^2 - \sin^2 \omega t)}} \right]$$

$$\ddot{y}_f = y_{\max} \omega^2 \left[\cos \omega t + \frac{\sin^4 \omega t + q^2 \cos 2\omega t}{(q^2 - \sin^2 \omega t)^{3/2}} \right]$$

Figure 5.6(a) shows the wobble yoke piston motion is very close to simple harmonic motion and Figure 5.6(c) the maximum acceleration is less than that of a comparable slider crank. This holds true for small maximum beam angles, γ . Figure 5.7 shows the change of piston acceleration for r_{bd} ranging from 60 down to 20 mm for the same stroke and shaft angular velocity. This has the effect of changing the maximum beam angle γ . As γ increases the piston acceleration deviates

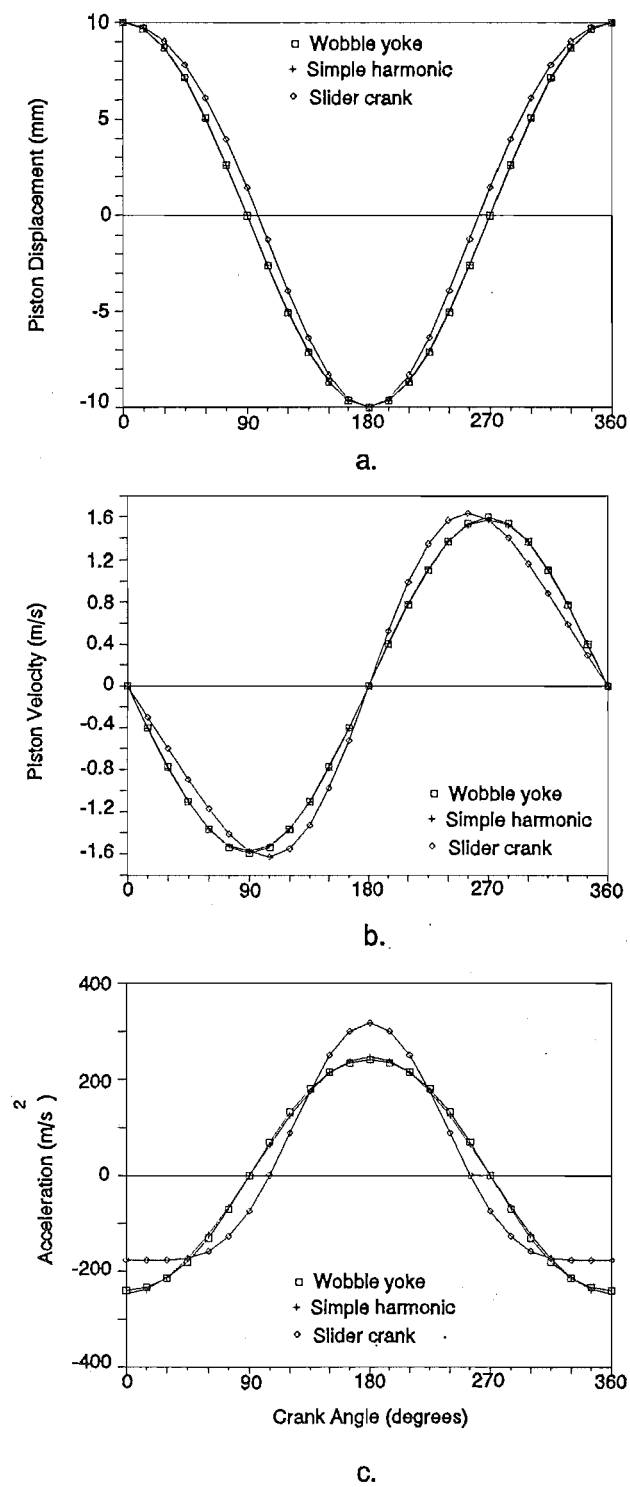


Figure 5.6 Comparison of kinematic piston motion for wobble yoke, simple harmonic and slider crank mechanism.

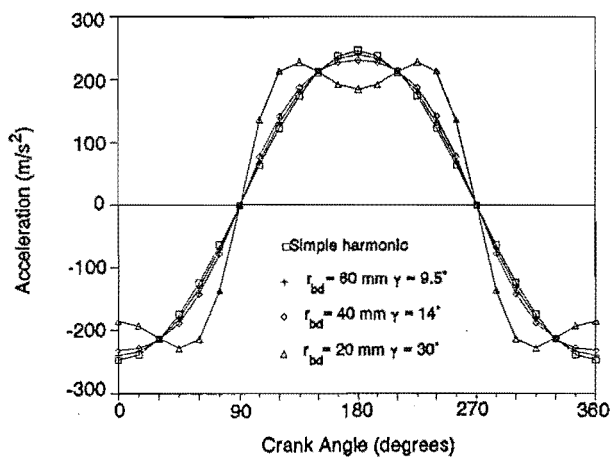


Figure 5.7 Piston acceleration for various maximum beam angle and similar stroke.

increasingly from simple harmonic motion having a detrimental effect on dynamic balance, refer to Section 5.4.10

5.4.6 Connecting Rod Bearing Load.

The connecting rod bearing, d , load is radial and given by:

$$F(\theta)_{d_n} = \frac{\pi}{4} (P(\theta)_n (d_b^2 - d_r^2) - P(\theta)_{n-1} d_b^2 + P_b d_r^2) - \dot{y}(\theta)_n m_n \quad (5.12)$$

5.4.7 Beam Moments

The moments about the main pivot, b , for each beam wobble yoke assembly are:

$$\begin{aligned} M(\theta)_{zz} &= r_{bd} \cos(\phi(\theta)) (F(\theta)_1 - F(\theta)_3) - I \ddot{\phi}(\theta) \\ M(\theta)_{xx} &= r_{bd} \cos(\phi(\theta + \frac{\pi}{2})) (F(\theta)_2 - F(\theta)_4) - I \ddot{\phi}(\theta + \frac{\pi}{2}) \end{aligned} \quad (5.13)$$

5.4.8 Eccentric Bearing Load

The eccentric bearing, a, reacts the beam moments M_{xx} and M_{zz} . The bearing loads perpendicular to axis ab are:

$$F(\theta)_{ax} = \frac{M(\theta)_{zz}}{r_{ab}} \quad F(\theta)_{az} = \frac{M(\theta)_{xx}}{r_{ab}}$$

The resultant bearing load perpendicular to axis ab is:

$$L(\theta)_a = \sqrt{F(\theta)_{ax}^2 + F(\theta)_{za}^2} \quad (5.14)$$

5.4.9 Engine torque

The resultant force on bearing a parallel to the xz plane is:

$$F(\theta)_a = \sqrt{(F(\theta)_{xa} \cos(\phi(\theta)))^2 + (F(\theta)_{za} \cos(\phi(\theta + \pi/2)))^2} \quad (5.15)$$

And the shaft torque is given by:

$$T(\theta) = r_{ae} (F(\theta)_{xa} \cos(\phi(\theta)) \cos(\theta) + F(\theta)_{za} \cos(\phi(\theta + \pi/2)) \sin(\theta)) \quad (5.16)$$

5.4.10 Engine Balance

If the inertia moments M_{xx} and M_{zz} vary with simple harmonic motion, at 90 degrees phase and equal magnitude the engine could be completely balanced by masses rotating at shaft speed, creating an opposing moment (Campbell, 1941). The inertia moments are not simple harmonic, however, and there will be a minor imbalance in the engine. Referring to Figure 5.3(a) two balance masses m_{bal} are positioned at r_{bal} on opposite sides of the shaft with an axial displacement of y_{bal} . A rotating balance moment is created:

$$M(\theta)_{bal} = m_{bal} r_{bal} \omega^2 y_{bal} \quad (5.17)$$

For balance this should equal the inertia moment about the main pivot b:

$$M(\theta)_b = \sqrt{M(\theta)_{zz}^2 + M(\theta)_{xx}^2} \quad (5.18)$$

where $M(\theta)_{zz}$ and $M(\theta)_{xx}$ are calculated using Equations 5.13 without pressure loads.

5.5 Case Study

To graphically show the implications of the previous derivations, the wobble yoke for the SEBCY is used. To determine $P(\theta)_n$ the isothermal analysis given by Urieli and Berchowitz (1984), was used. This method allows fast computation but is conservative in the pressure loads, for example, by the isothermal analysis the engine would ideally produce approximately 900 watts indicated power, from tests on the test engine DMC-3 the real indicated power would be only 400 watts. Indicated power data from the test engine was used for more accurate load determination. It was decided a well known theoretical approach would give a more appropriate demonstration of the equations. The wobble yoke analysis is included in the SEDA^o software package allowing fast editing, computation and graphic visualisation of the results.

The engine parameters used were:

T_H	1023 K	P_{mean}	10 bar
T_K	323 K	V_d	15 cm ³
ω	157.08 rad/s	y_{max}	.010 m (stroke/2)
r_{ab}	.050 m	r_{bd}	0.0604 m
γ	9.53°	I	0.0115 kgm ²
m_n	0.25 kg		

^o Stirling Engine Design Aid, refer Chapters 7 and 8.

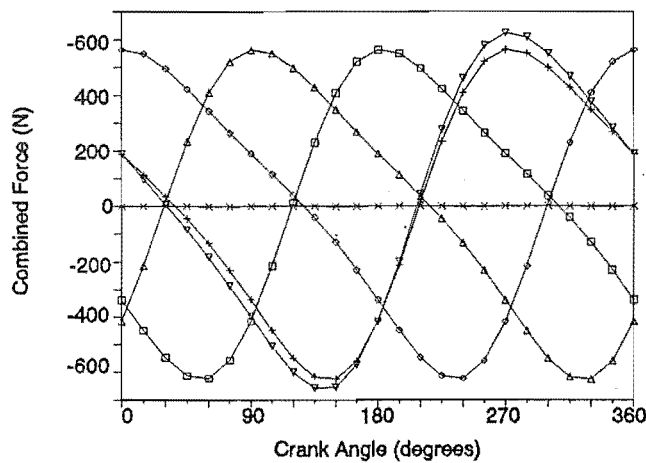
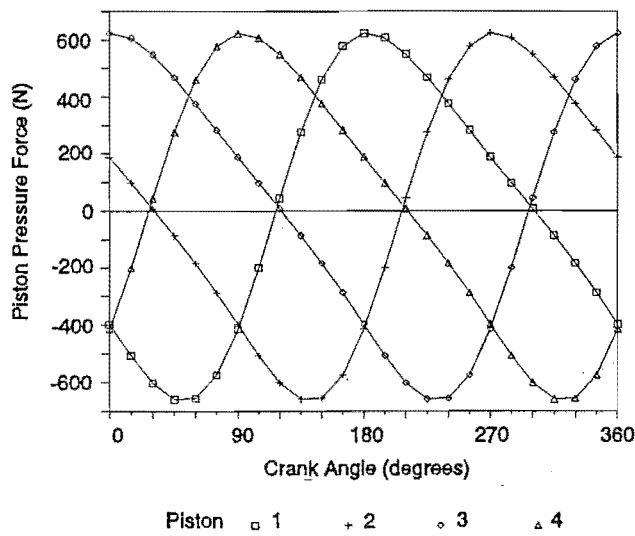
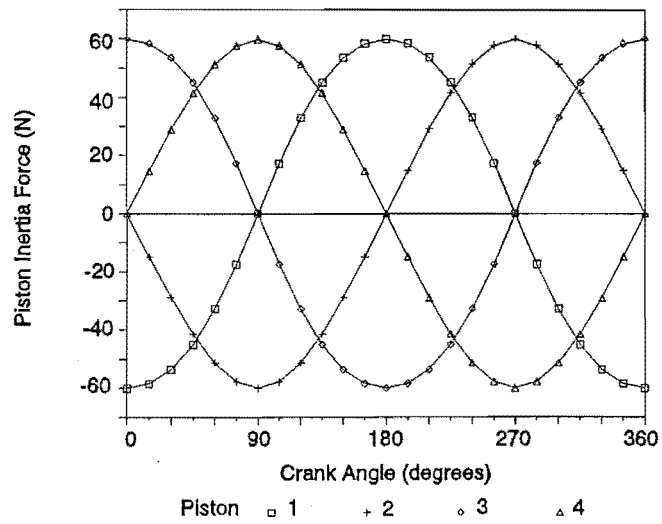
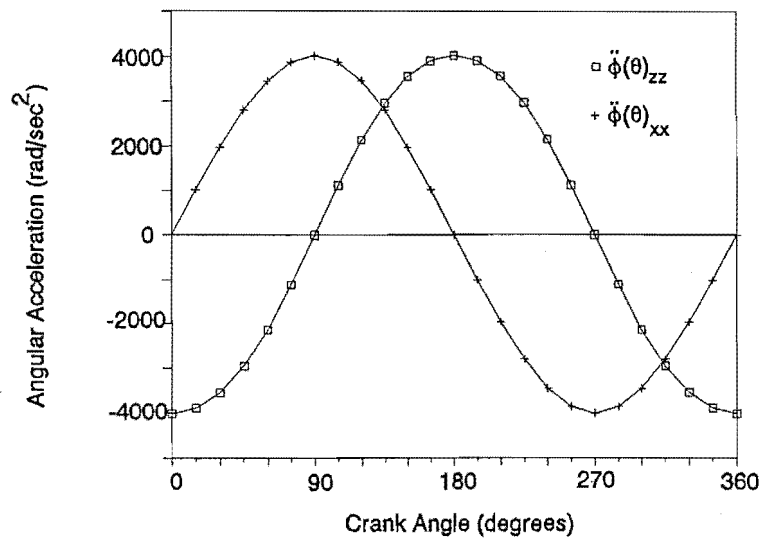
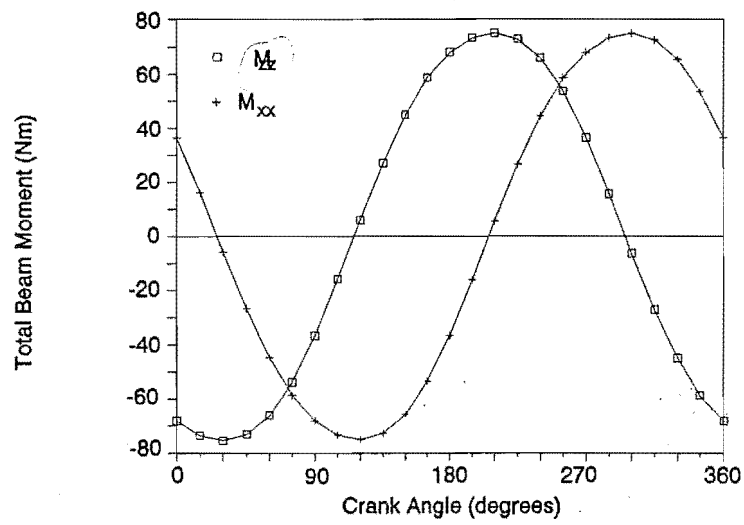


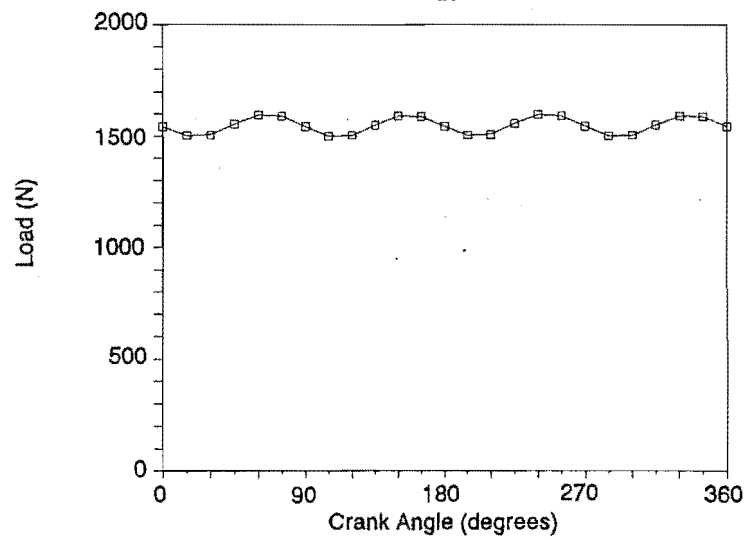
Figure 5.8 Radial loads on bearing d. (a) inertia, (b) pressure, (c) combined.



a.

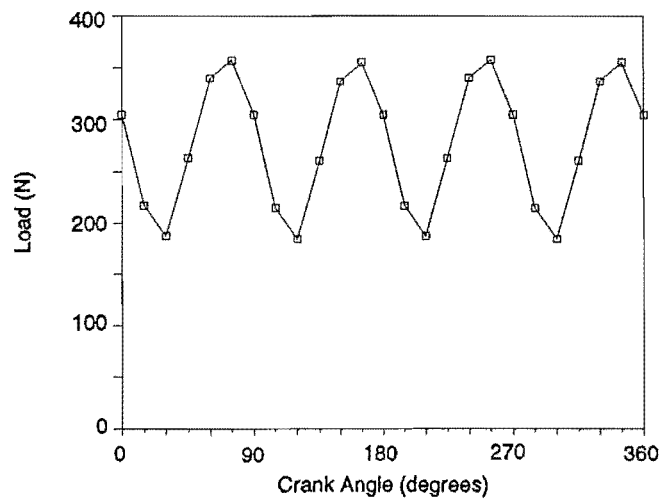


b.

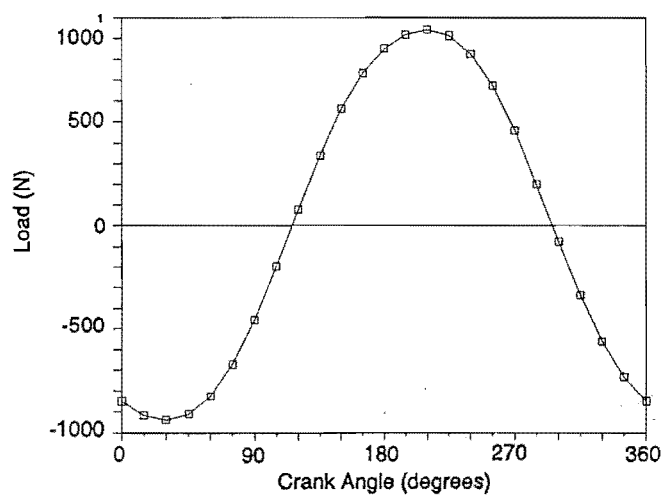


c.

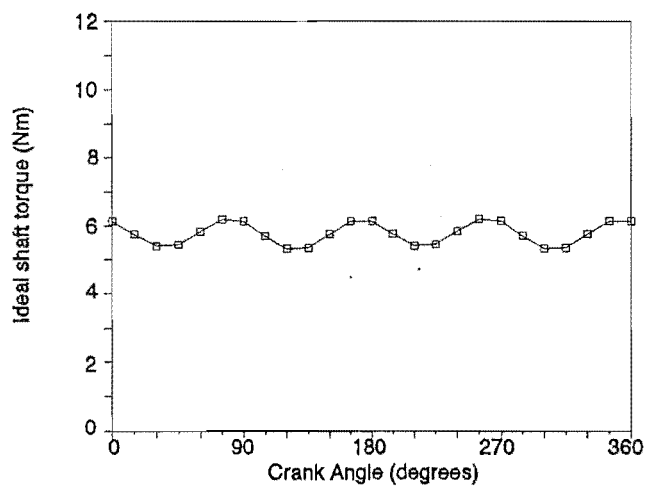
Figure 5.9 (a) Beam angular acceleration. (b) Total beam moment. (c) Load on bearing a.



a.



b.



c.

Figure 5.10 (a) Radial load on bearing b for beam on the x axis. (b) Combined radial and axial load on bearing c. (c) Ideal shaft torque calculated from the beam moments.

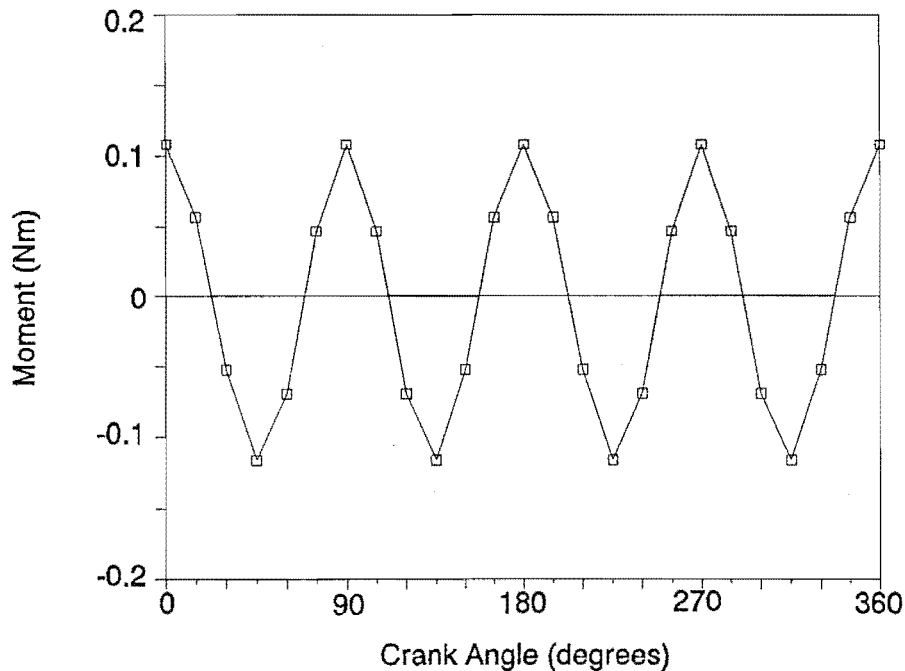


Figure 5.11 Out of balance moment.

Figure 5.8(a) shows the piston inertia for all pistons, as is expected the inertia load follows closely simple harmonic motion and each piston is at 90 degree phasing to the previous. Figure 5.8(b) shows the piston pressure force for all pistons of a four cycle double acting engine with pressure variations calculated according to the ideal Schmidt analysis. Figure 5.8(c) shows the combined piston inertia and pressure load acting on bearing d. It is noted from this figure that the sum of the vertical forces acting on the bearing block b is close to zero. Figure 5.9(a) gives both beam angular acceleration which again is very close to simple harmonic motion. Figure 5.9(b) shows the beam moment due to the piston loads and the inertia due to the wobble yoke. Figure 5.9(c) shows the resolved radial load on bearing a, the small force variation should be noted. The radial load on bearing b for one beam is shown in Figure 5.10(a). Due to high axial and radial loads on bearing c, it's load was used to determine the bearing size required for all bearings in the wobble yoke, Figure 5.10(b) shows the combined load for bearing c. The combined load was calculated

according to the recommendations by FAG (Fag, 1984). The low torque variation, Figure 5.10(c), is also noteworthy as this allows low flywheel mass and ease of engine starting. The out of balance moment shown in Figure 5.11 is very low, but increasing the maximum beam angle is detrimental to engine balance. Consequently for a given swept volume a higher degree of balance dictates a shorter stroke, therefore a larger engine box volume. Also for the same stroke the beam angle could be increased with a corresponding decrease of r_d but a lesser degree of balance. Full engine balance would require an axial shaft with balance weights rotating at 4 times engine speed.

5.6 Design variations

The general mechanism arrangement of two beams and two wobble yokes can be configured in a number of ways. The following Sections outline several alternative arrangements.

5.6.1 Twin Alpha Configuration

The test engine DMC 3 used the wobble yoke driving an alpha configuration piston-heat exchanger set, Section 6.4. The piston masses in this case must be equal to obtain reasonable engine balance. A twin alpha configuration engine is an attractive alternative to the four cycle double acting engine.

5.6.2 Rigid Piston-Connecting Rod Joint

Due to the very small x displacement of bearing d , δx_d , the angular displacement of the piston connecting rod is very small, that is $r_{df} < \delta x_d$. It is possible to rigidly connect the piston to the connecting rod and have a piston seal which will allow the slight piston rocking motion, Figure 5.12(a). This was successfully used on the DMC 3 test engine compression piston, Chapter 8. A similar concept was shown several times for use with a Ross yoke, for example (Fauvel and Walker, 1988).

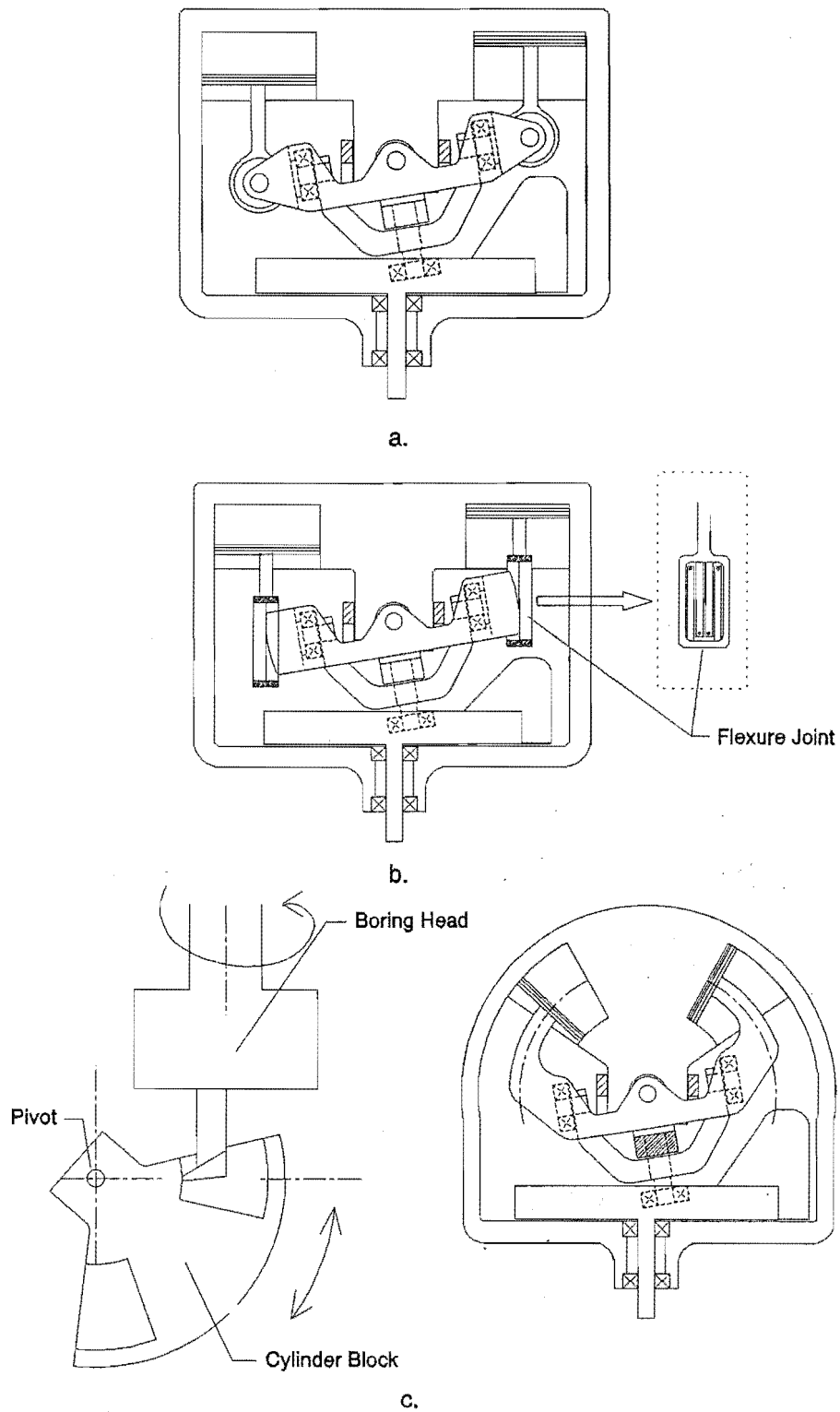


Figure 5.12 Schematic diagrams of wobble yoke used in alternative configurations. (a) rigid piston connecting-rod. (b). Flexure joint. (c). Using rigid beam-piston and toroidal cylinders. Toroidal cylinder machining method.

5.6.3 Flexure Joints

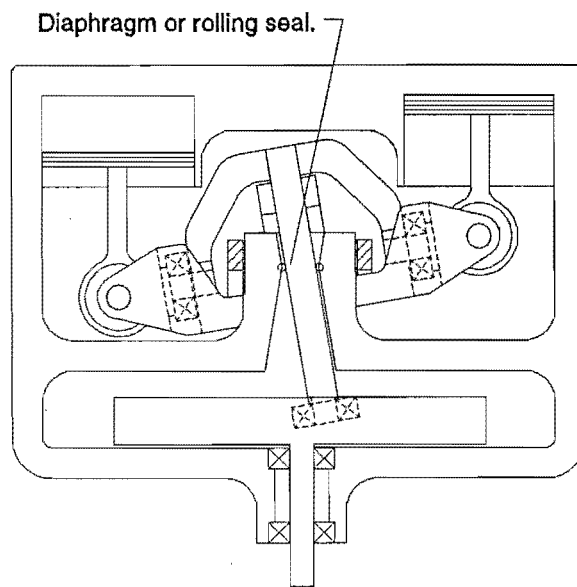
Unlike the Ross yoke the locus of the lower connecting rod bearing, d, follows a true arc. This suits the use of flexure type joints as described by Fauvel and Walker (1988), Figure 5.12(b). The prototype DMC 5 engine uses flexure type joints in place of bearings f due to the small angular displacement of the connecting rod, refer to Chapter 9.

5.6.4 Totally Rigid Beam-Connecting Rod-Piston

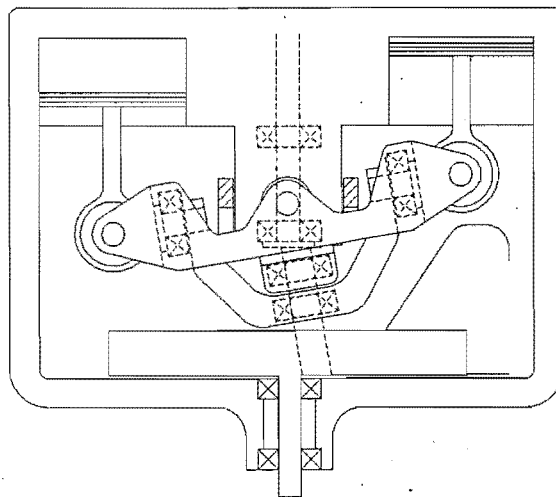
Toroidal cylinders could be used since bearing d follow a true arc. The beam, connecting rod and piston could be manufactured as one rigid item Figure 5.12(c). The only sliding contact would then be the piston seals. Requiring no cross heads and being well balanced and compact this arrangement is an attractive proposition for small clean air compressors. The ability to machine the toroidal cylinders is often questioned. Figure 5.12(c) shows a possible machining technique. To manufacture a machine for this process is simpler than for parallel bores due a single pivot being required rather than precision slides to guide the bore. Prior to beginning this project the author successfully manufactured a toroidal cylinder for a Stirling engine on a lathe. This was accomplished by fitting a fly cutter in the chuck and rotating the bore over it.

5.6.5 Inverted Yoke

Referring to Figure 5.13(a), in this case the nutating drive pin passes through the pressure wall at its centre of nutation, because the shaft is not rotating a diaphragm type seal could be used. The high bending loads in the nutating shaft must be considered. The wobble yoke could be inverted which allows the nutating shaft to pass through the centre of the main pivot block, Figure 5.13(a). This may allow the use of a diaphragm or similar seal as the atmospheric seal for an engine with an external drive, eliminating the sliding atmospheric seal.



a.



b.

5.13 Alternative wobble yoke configurations. (a). Inverted yoke. (b) Strengthened drive shaft.

5.6.6 Strengthened Wobble Yoke

Where the nutating shaft is fitted to the wobble yoke on the DMC 5 engine the shaft is subjected to high bending moments. The design would have to be changed for engines of greater power output. A possible modification is shown in Figure 5.13(b). Each yoke is fitted with a bearing which rotates on a nutating shaft supported by the main driveshaft bearings and a bearing mounted in the central pivot block. This system would also allow a drive for valve gear in alternative applications.

5.6.7 Variable Stroke

Variable stroke power control can be achieved by changing radius r_{ae} , Figure 5.3(a). This could be accomplished by either mechanical, electrical or hydraulic actuators. Like the variable angle swash plate the engine would only be optimally balanced at an angle ϕ of zero degrees and the design balance angle, unless moving balance weights could be used.

5.7 Other Applications

Use of the wobble yoke is not limited to use with the Stirling Engine. The following paragraphs briefly describe other applications.

5.7.1 Compressors and Hydraulics

It would be possible to produce gas compressors, refrigeration compressors, and hydraulic motors/pumps with the wobble yoke. Compact dry air compressors which cannot allow any lubricant in the air supply is an obvious application due to the low piston side loading.

5.7.2 Internal Combustion Engines

Low piston side loads and good engine balance make the wobble yoke an ideal candidate for compact internal combustion or steam engines.

5.7.3 Two Ram Positioning Device

By controlling the distance r_{df} the angle and position of point, a, can be controlled by only two linear actuators. This could be suited to devices for positioning satellite tracking devices or similar. Figure 5.14 shows a satellite tracking system, the actuator perpendicular to the page has been removed for clarity. The linear actuators could be replaced with other methods of rotating each of the two beams, for example a worm drive and stepper motors.

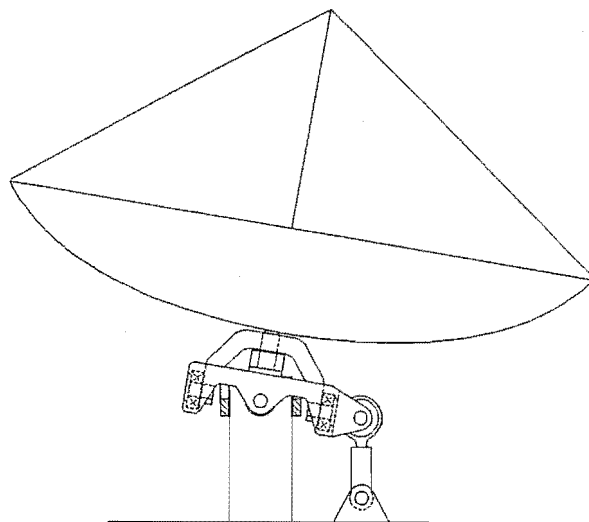


Figure 5.14 Satellite or solar collector dish utilising the wobble yoke.

5.8 Summary of Conclusions for Chapter 5

- There are a large number of mechanism configurations suitable for the Stirling Engine. Few though meet the requirements for this project, reasons include: balance, bearing requirements, reaction torque constraint, overall size.
- The novel wobble yoke mechanism was developed to meet the needs of the SEBCY project. The mechanism advantages over some existing designs include:

- (a) The torque reaction is transmitted through cylindrical bearings which could be rolling element bearings. Previous wobble type designs required a torque arm, slides or a nutating bevel gear.
 - (b) All mechanism bearings for the SEBCY can be prelubricated sealed ball races.
 - (c) Good engine balance, providing small beam angles are used.
 - (d) Possibility for swept volume variation power control.
 - (e) Small angular displacement of the connecting rod giving low piston side loads.
 - (f) Elimination of the need for multi-degree of freedom bearings.
 - (g) Easy manufacture using conventional machine shop equipment.
- Bearing c, Figure 5.3(a) has both radial and axial loads making it the most adversely loaded bearing in the wobble yoke mechanism.
 - The two yokes must have relative freedom about the axis ab to operate, Figure 5.3(a).
 - The basic kinematic equations have been presented and applied to the SEBCY prototype engine.
 - The basic wobble yoke mechanism could be used in many alternative arrangements, some of which have been described.
 - The wobble yoke is also suited to applications other than the Stirling engine.

6 Test Engines and Experimental Apparatus

6.1 Summary of Engines

During the course of this project several Stirling engines were manufactured and tested. They are specified by the authors initials and an engine number according to the chronological order of manufacture. They are:

- DMC 1 A gamma configuration engine working at atmospheric pressure.
- DMC 2 An alpha configuration engine manufactured from a converted twin cylinder motorcycle engine. This engine was used as a proof of principle engine to demonstrate that this project was indeed feasible and to highlight design and manufacturing problems.
- DMC 3 An alpha configuration test engine. This engine was designed for seal, wobble yoke and heat exchanger testing.
- DMC 4 A low temperature demonstration engine. This engine was based on the design by Senft, (1991)
- DMC 5 The prototype SEBCY.

This Chapter discusses the relevant construction techniques, points of interest and performance characteristics of DMC 1,2,3 and 4. DMC 5, the prototype SEBCY, is discussed in detail in Chapter 10.

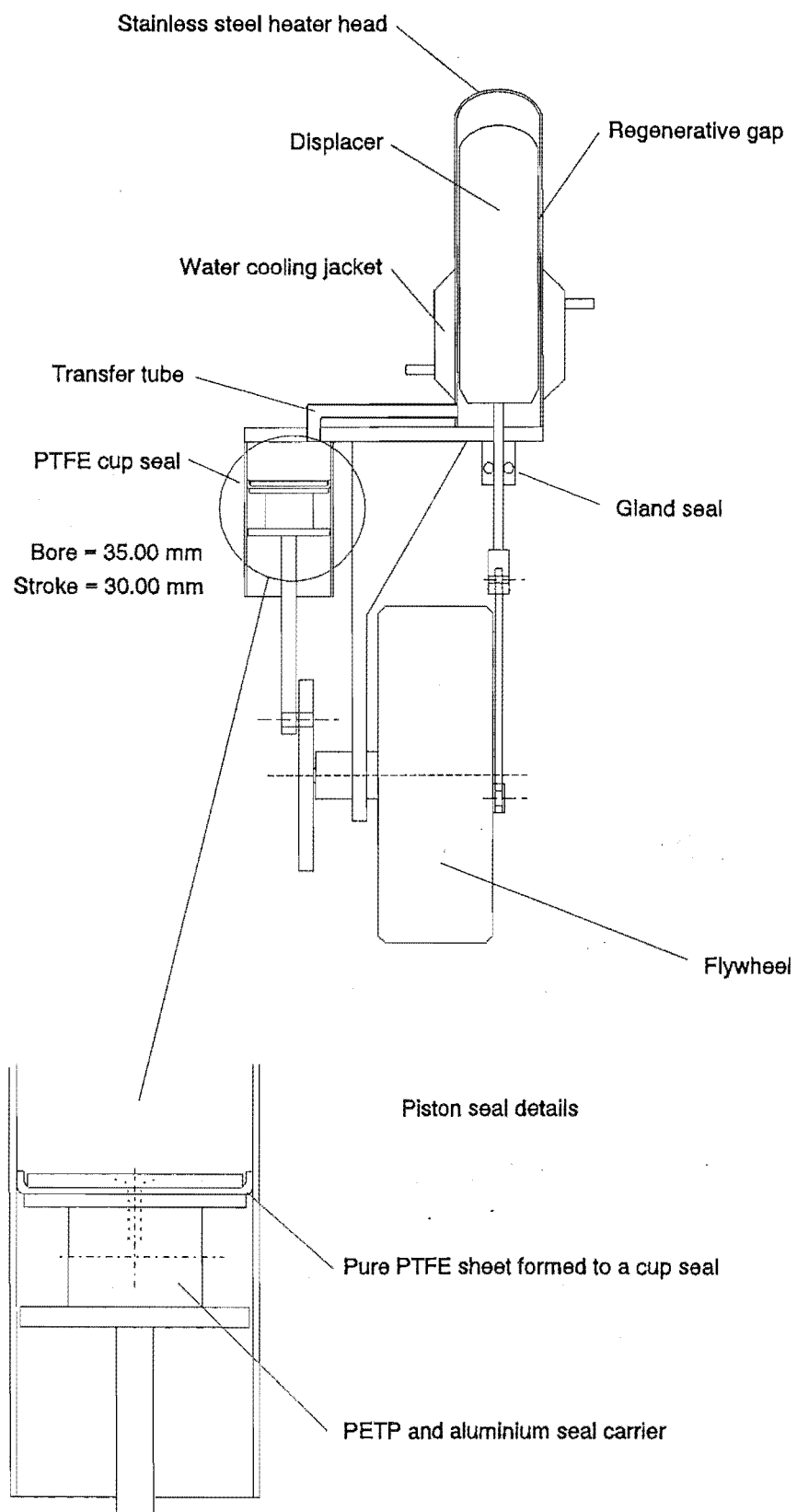


Figure 6.1 Basic engine design for the DMC 1 gamma configuration engine.

6.2 DMC 1

Figure 6.1 shows the construction details of this engine. DMC 1 was a gamma configuration which used air at atmospheric pressure as its working fluid. The significant feature relevant to this project is the piston seal construction. As the engine power was very low a seal design was required that would give low friction loss. Several conventional ring type seals were tried but the most successful was a simple PTFE cup seal. This was simply manufactured with 0.5mm thick pure PTFE sheet. A disk was cut to 2 mm larger diameter than the engine bore and assembled onto a fabricated piston. The piston was then inverted and pressed into the bore. PTFE has low creep resistance and over 12 hours the seal formed to the cylinder, giving a light interference fit and a shape similar to a cup or lip seal. The piston was then removed from the cylinder, and carefully refitted in the cylinder as shown in Figure 6.1. This manufacturing technique worked very well and after 4 years the engine still had excellent compression and was very free to turn over. One of the reasons why this seal was very effective was due to the piston seal running in a cool environment. The higher rate of thermal expansion of the PTFE than the cylinder wall and low creep resistance of PTFE can cause the seal interference to be lost after the first time the engine is run, as noted in Chapter 7, and (Walker, 1980). To overcome this effect some form of seal preloading and/or a split seal is often used.

6.3 DMC 2

Referring to Figures 6.2 and 6.3, this engine was constructed to show that a Stirling engine of modest size can be locally made to meet the power requirements for the SEBCY. In designing and manufacturing this engine considerable practical experience with pressurised air charged engines was gained, much of which could not be taken from the literature. As this was the first research project on the Stirling engine at the University of Canterbury there was little prior practical experience and this proved to be a very valuable engine.

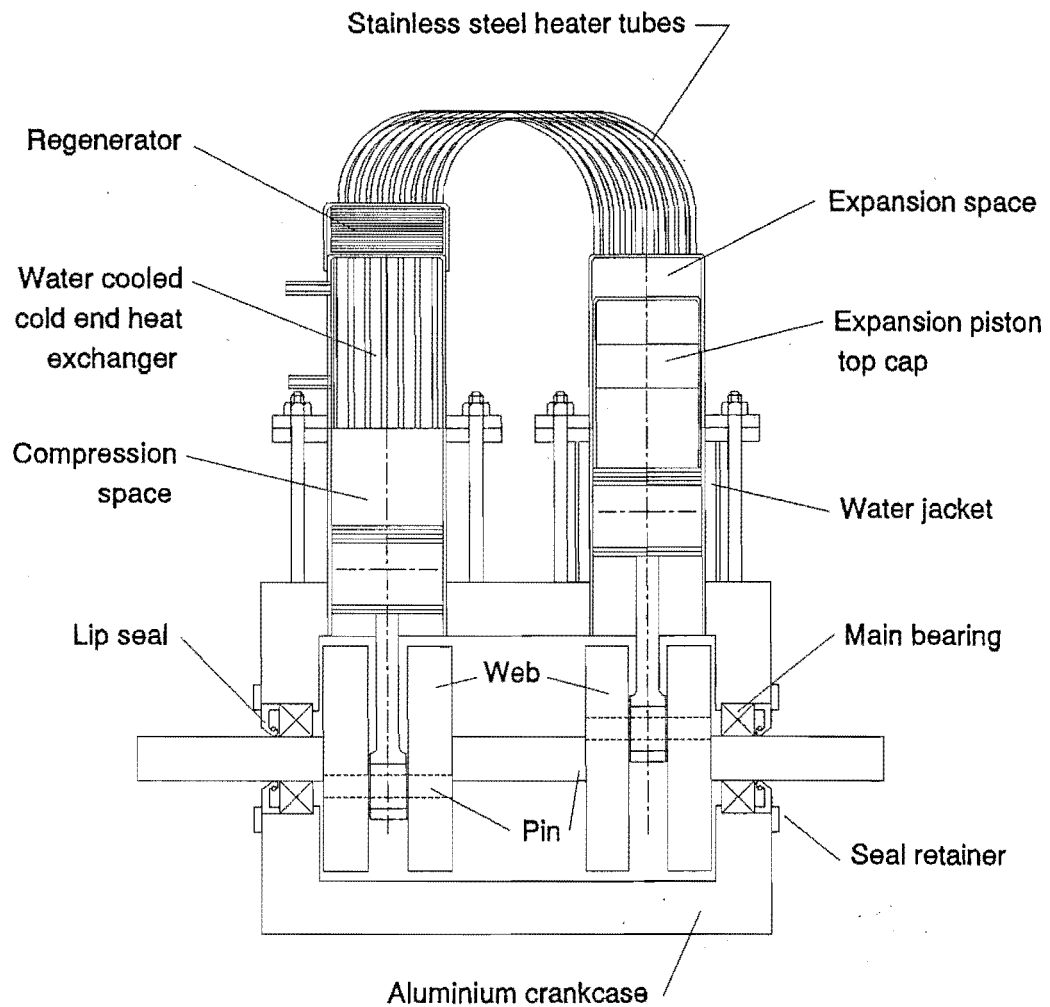


Figure 6.2 Sketch of DMC 2, a converted motorcycle engine.

At the time of designing this engine no decision had been made on the optimum engine configuration. The Department had a Philips 1002 C beta configuration engine and the gamma configuration was not popular for high power density engines so little additional experience could be taken from making either of these configurations. The alpha configuration is effectively one quarter of a four cycle double acting engine so manufacturing an alpha configuration offered experience for both engine types.

Motor cycle engines often have cranks which are pressed assemblies of webs and pins which can be easily dismantled and reassembled, (Clucas, 1992). A Suzuki twin cylinder two stroke engine was located which had cylinder mounted carburettors, a sealed crankcase and swept volume similar to that required for the SEBCY. Only the crankcase, crank, shaft seals and connecting rods were used. Pistons were fabricated from aluminium, PETP and PTFE. The heat exchangers were of tubular form and constructed as shown in Figure 6.2. A Primus LPG welding torch nozzle was used for the burner, which produced a fierce intense flame. A dynamometer was constructed from an automotive alternator which was belt driven from the driveshaft, experience with this led to the development of the combined starter alternator and dynamometer described in Sections 4.4 and 6.4.3. Only qualitative results were gained from this engine as it was realised that an engine closer to the final SEBCY design was required for simulation verification and other test work. The following lists conclusions drawn from this engine:

- It was difficult to obtain even heating on the tubular heat exchanger. During one test a heater tube burnt out.
- Reliable welding of the fine stainless steel heater tubes was difficult and time consuming.
- Burner roar and piston slap were the dominant engine noises.
- A stack of 150 mesh Stainless steel appeared to give the best regeneration.
- The circular construction of the regenerator housing caused considerable waste of the regenerator material and stacking the sheets was time consuming.
- Other regenerator materials tested which resulted in lower engine performance were:
 - (i) Steel wool, (cleaning scourers)
 - (ii) Brass wool, (cleaning scourers)
 - (iii) Kao wool
 - (iv) Various size meshes made from stainless steel or brass.
- A water jacket was required on the expansion cylinder to prevent overheating the expansion piston seal.

- Lip seals on the driveshaft were adequate up to 6 bar pressurisation. Regular lubrication was required and the power loss from these seals was not able to be measured with the equipment available at that time.
- Expansion piston seal leakage resulted in rapid deterioration of the seal due to high temperature gas flowing down past the seal.
- Extra flywheel mass was required to aid starting and reduce speed fluctuation. This was also important for stability of the dynamometer.
- When good piston seals were developed, the required engine starting torque was considerable to overcome the compression from a cold start.
- If the engine was stalled and immediately restarted, the required starting power was far less than from a cold start.
- Cyclic compression of the buffer space gas caused the crankcase temperature to increase. To reduce this power loss, extra buffer space was fitted, Figure 6.3.
- Piston seals proved to be the biggest problem.
- For an engine piston swept volume of 88 cm^3 and mean buffer space pressure 6 bar, the maximum speed was 2000 rpm and the maximum power recorded was 200 watts at 1200 rpm. The maximum sustainable power was 100 watts at 1200 rpm, (Clucas, 1992).
- The sustainable power was limited by heat transfer from the combustion gas to the heater head tubes.
- Engine efficiency was expected to be low, mainly due to the burner losses, so accurate thermal efficiency tests were not performed. The estimated thermal efficiency based on mass flow rate of fuel and shaft power was only 3 - 5%. Considerable improvements could have been made by optimisation of the heat exchangers and by preheating the combustion air.

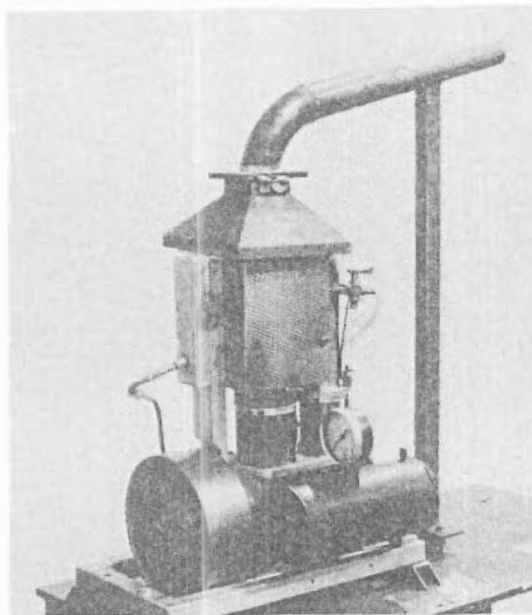


Figure 6.3 Photo of DMC 2 showing the added buffer space.

6.4 DMC 3

An experimental rig was required to test piston seals, test heat exchanger design, verify the simulation program, test the characteristics of load control by the alternator, and test the wobble yoke. One apparatus was designed and manufactured to meet all these requirements, Figure 6.4. The ancillary components which were tested are discussed in the appropriate Chapters, for example heat exchangers in Chapter 8. Photo 6.1 (a) shows DMC 3 fitted with heat exchangers.

6.4.1 Mechanism Housing

The foundation of the rig is the mechanism housing which was designed according to AS1210 (1989) for a maximum pressure of 20 bar. The base plate supports the main shaft bearings and has a seal cavity suitable for a Crane type 21 elastomeric bellows mechanical seal. The flywheel was fitted with a self aligning ball race bearing (a, Chapter 5), of which the offset radius (r_{ae} , Chapter 5) could be manually adjusted to allow stroke variation. Ports were provided in the

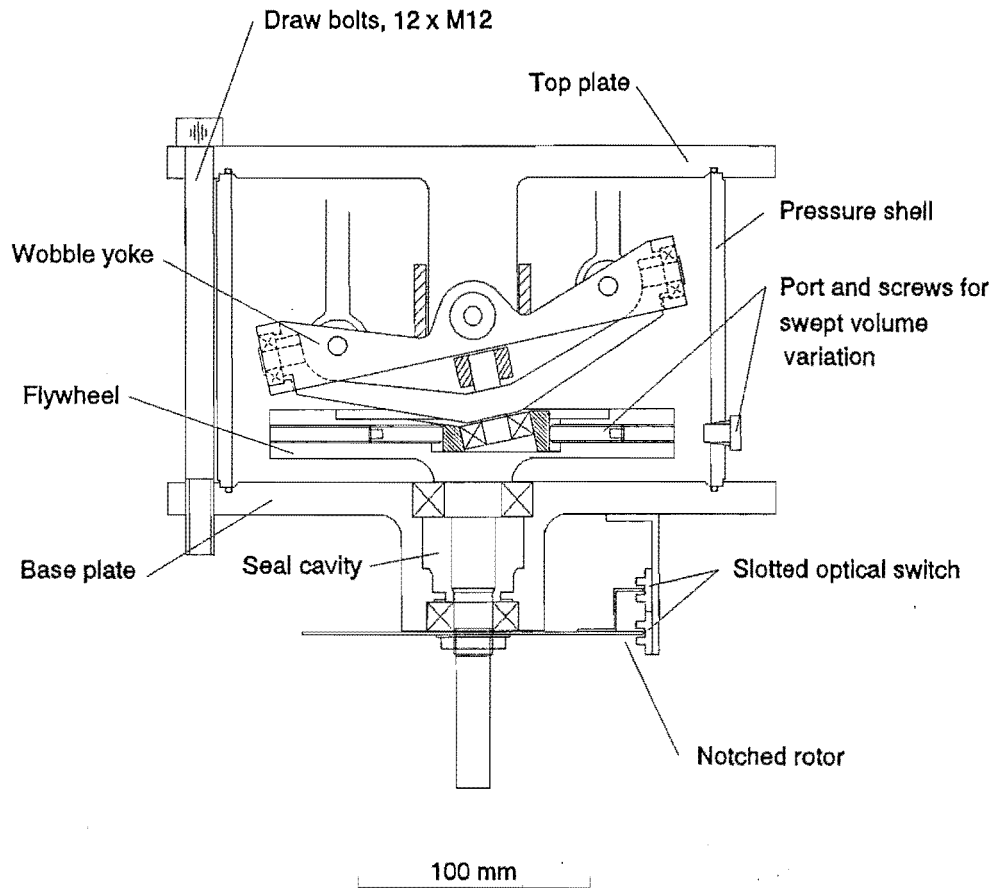


Figure 6.4 DMC 3 mechanism housing.

pressure shell to allow adjustment of the stroke without dismantling the engine. The main shaft bearings were sealed deep groove ball races, the upper bearing taking axial and radial loads. A rotor with 36 peripheral slots and one offset tang was keyed to the shaft. This provided 36 pulses at 10 degree intervals and one pulse every revolution from two slotted optical switches. This allowed determination of the driveshaft position and engine shaft speed. The ancillary components for heat exchanger and seal testing were attached to the top plate.

6.4.2 Motoring

For motoring tests a three phase, 0.37 kW, electric motor was directly coupled to the engine shaft, Figure 6.5. The electric motor housing was constrained from rotation by a custom made beam load cell which enabled determination of the driving torque. As an external drive is used in this situation a shaft seal was required. A Crane type 21 mechanical seal was chosen for this application. This seal has a spring loaded carbon rotary face and a ceramic stationary face. Oil lubrication was considered safe to use during motoring test as engine temperatures would be low compared to prime mover operation. The seal cavity above the seal was partially filled with light machine oil. This system worked extremely well, with no visible leakage evident over 30-40 hours motoring.

6.4.3 Dynamometer

For engine testing a hermetically sealed dynamometer was developed. It was considered that the hermetic seal losses on the output shaft would be an unknown quantity during engine testing and a dynamic hermetic seal was an item which would not be used on the SEBCY. So to eliminate this seal an automotive alternator sealed into the housing was used as a dynamometer, Figure 6.6. The alternator was directly coupled to the main shaft and was constrained from rotation about the shaft axis by the same beam load cell mentioned previously for motoring tests. As the slotted optical switches, alternator and load cell were now in the pressure vessel, the necessary wiring had to pass through the pressure wall. O-ring sealed fittings reliably accomplished this, Figure 6.6.

6.4.4 Engine Starter

The automotive alternator used for the dynamometer was too small to act as a starter motor. Hand cranking was also desirable for assembly and testing purposes. As there was no rotating shaft protruding the pressure vessel a starter was developed as shown in Figure 6.6. A sprag clutch was

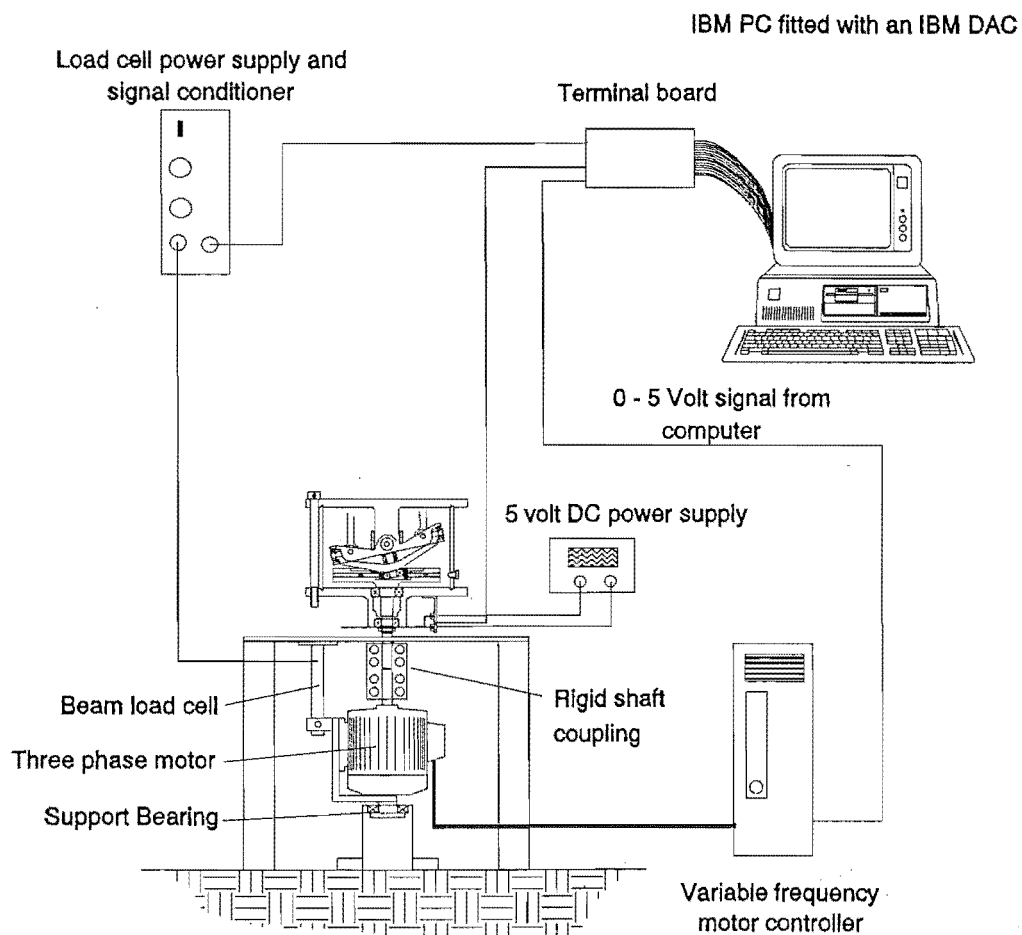


Figure 6.5 DMC 3 motoring apparatus.

used inside the pressure vessel to engage the starter shaft with the engine shaft. This allowed the starter shaft to rotate only when the starter was used. Due to the low rotational speed of the starter shaft, a grease packed O-ring seal was found to be adequate for the hermetic seal. A standard shaft, a grease packed O-ring seal was found to be adequate for the hermetic seal. A standard

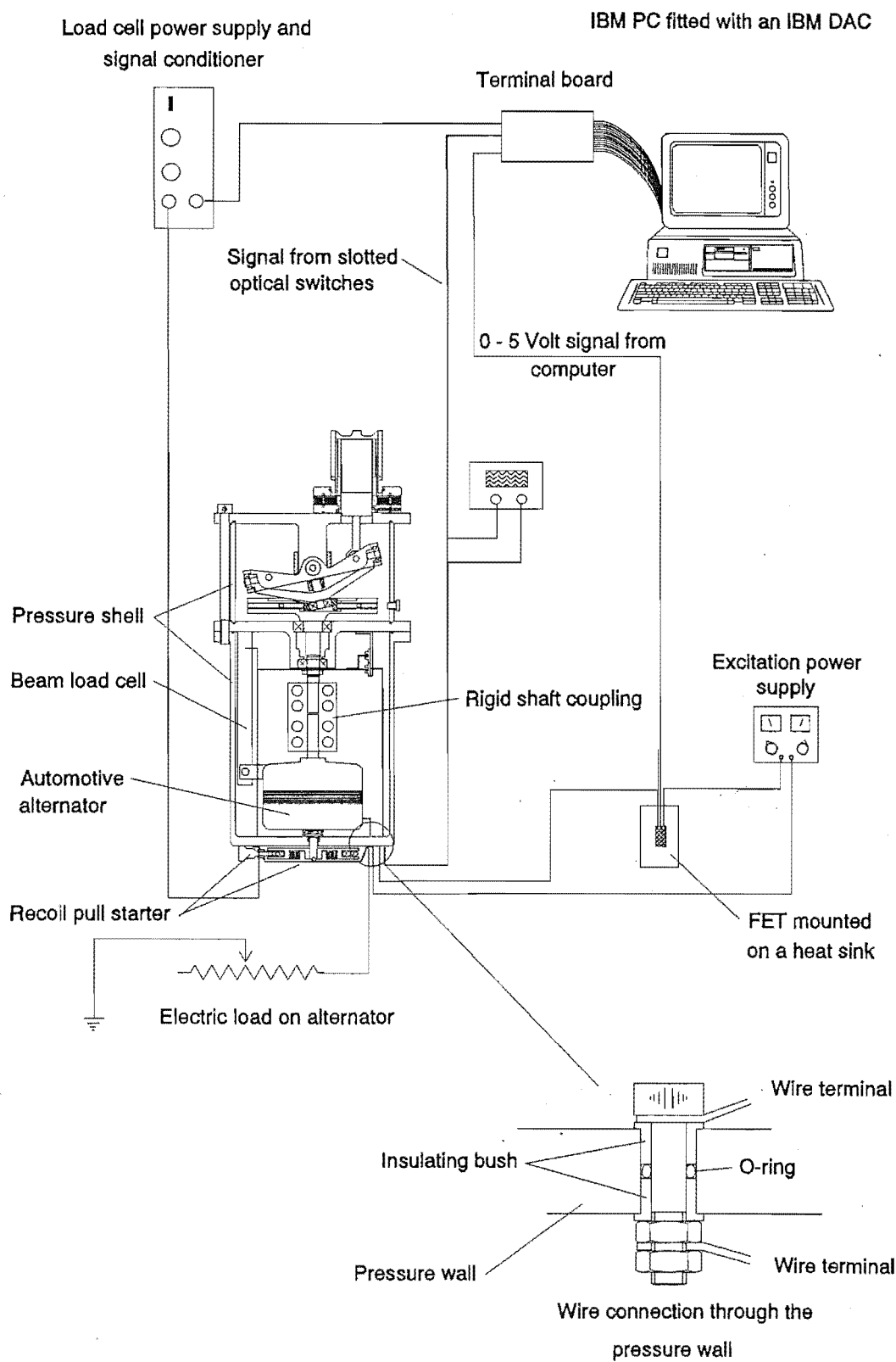


Figure 6.6 Hermetically sealed dynamometer for DMC 3 and the control equipment used.

recoil rope starter from a lawn mower was modified to give a convenient pull starter. This system worked extremely well and a similar design was used on the SEBCY, Chapter 9.

6.4.5 Data Acquisition and Engine Control

At the beginning of the project funds were limited for computer and data acquisition equipment. An IBM PC computer with an IBM DAC (data acquisition and control card) was borrowed from within the department. By current standards this equipment was primitive but by careful system design proved to be adequate for the purposes of this project. The most significant problem was the speed at which the DAC card could retrieve the data. Initially it was intended to trigger and scan data at 10 degree shaft intervals using the slotted optical switches. The speed of the DAC card was inadequate for this and two alternative methods were used.

- (a) For testing seal materials, load cell readings were required at $<10^\circ$ intervals. To achieve this the engine speed was determined by using the slotted optical switches and a rate of sampling was calculated to coincide with this speed. Sampling was triggered by the single pulse slotted optical switch and data was collected for several cycles. The consistency of data acquisition can be seen in a representative set of recorded data shown in Figure 6.7. The inertia of the flywheel and electric motor armature ensured the angular velocity was sufficiently constant during sampling.
- (b) For engine testing, sampling was required from one pressure transducer at 10 degree shaft intervals. This was to enable determination of mean cycle pressure, indicated power and heat exchanger pressure drop, Chapter 8. Sampling at the 10° shaft intervals was required to obtain reasonable accuracy. Due to non steady torque from the engine the method described above, (a), would not be accurate due to shaft angular velocity variation. Therefore a method of obtaining samples at known shaft angles was required. This meant three channels had to be scanned: (i) pressure transducer, (ii) slotted optical

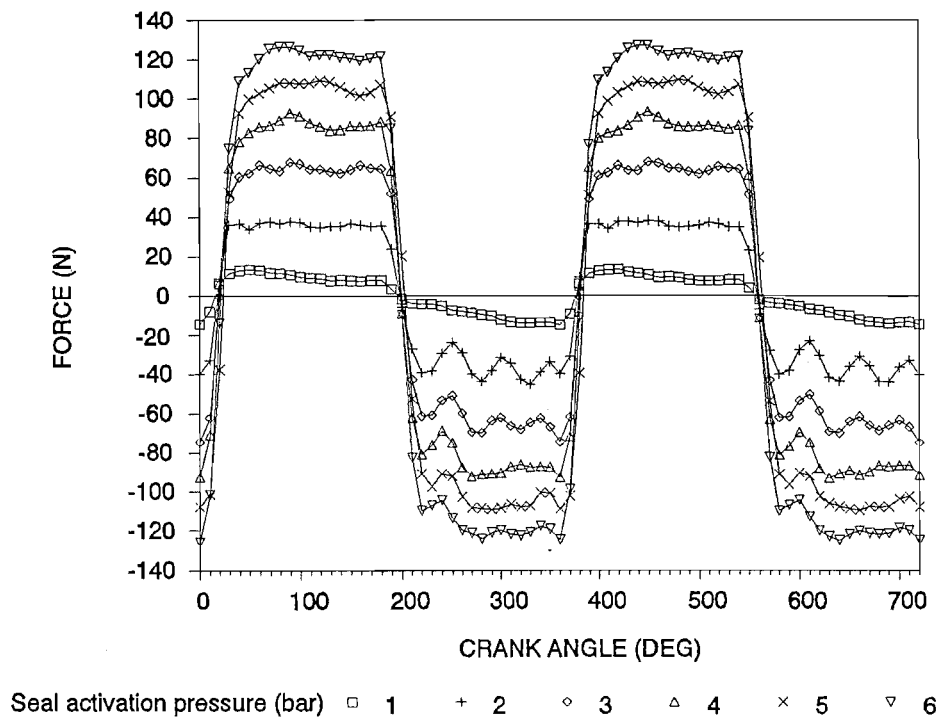
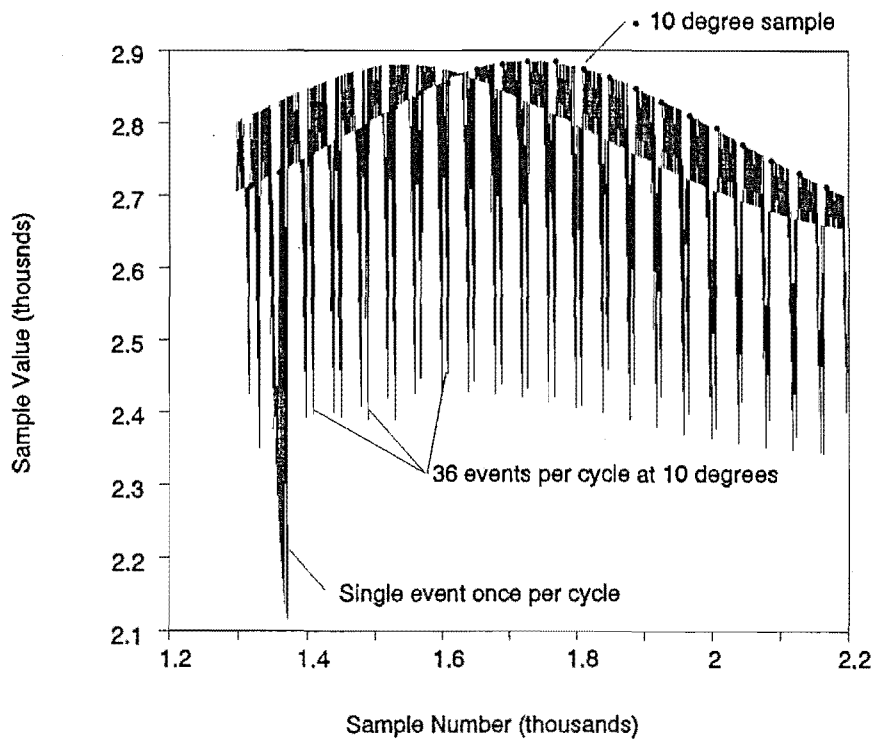
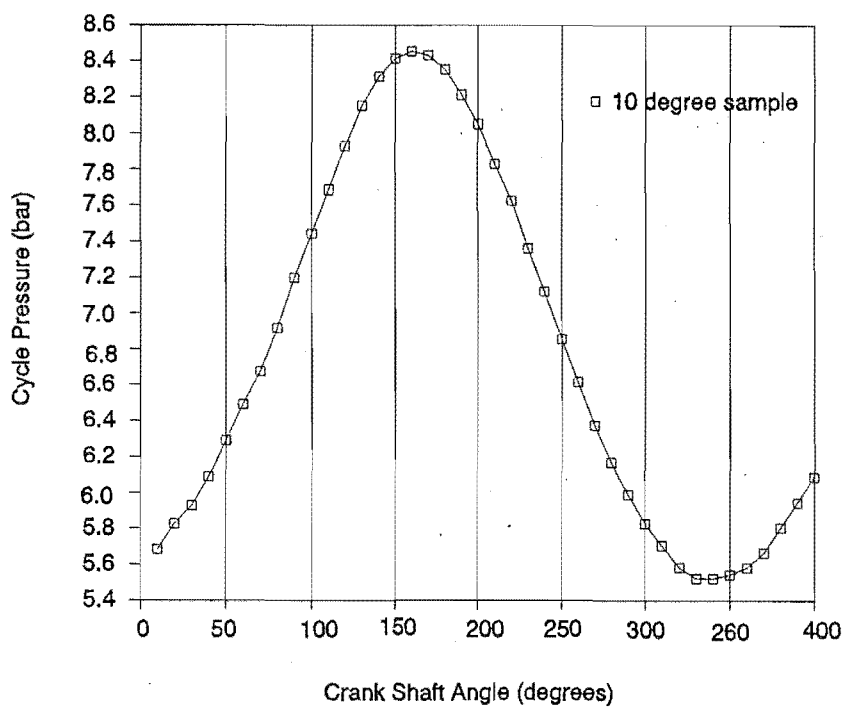


Figure 6.7 Representative data sampled by the data acquisition. Results show axial seal friction force for various interface pressure at 1250 RPM, refer to Chapter 7.

switch at 10° and (iii) slotted optical switch at 360° . But the DAC card could not scan 3 channels at the required sampling rate for normal engine speed but could sample one channel at $>12\,500$ sample/second. To utilise this feature the signal from the pressure transducer and the two slotted optical switches were added giving a signal as shown in Figure 6.8(a). The computer program then sorted the data to give a pressure signal as shown in Figure 6.8(b). Engine power was determined by $BP = T\omega$ where T , the engine torque, was measured by averaging the load cell reading over several cycles and ω was obtained from the slotted optical switches. As this reading was averaged and not cycle position dependent it was sampled directly following the pressure transducer at a more leisurely rate.



a.



b.

Figure 6.8 (a) Portion of a raw data signal read into the computer. (b) The resulting pressure curve after the raw signal had been processed. Note the angular consistency of the results.

6.4.6 Speed Control

For motoring tests the engine speed was determined by using the slotted optical switches and the DAC. To control the speed a Controlled Current Inverter three phase motor driver was used (GEC Ranger CCI 340). Due to variation of slip of the AC motor with variation of engine load a simple direct relationship between speed and voltage to the motor controller could not be given. By using a DAC analog output channel it was possible to control the motor speed with the computer giving a simple feedback control. This caused either a decrease, increase or no change of engine speed according to the measured shaft speed and the operator nominated speed.

For prime mover testing a method of electronic load governing was developed to control the engine speed, Figure 6.6. The alternator excitation was varied which altered the alternator power absorption which in turn modified the shaft speed. A DC 0 - 3 Amp power supply was used in conjunction with a IRFZ40 FET (field effect transistor). An analogue output from the DAC set the gate voltage of the FET which in turn set the current to the alternator excitation. This again formed a simple speed feedback control system. The FET had to be mounted to a large heat sink due to heat generation caused by resistance in the FET, (the value of the resistance was set by the gate voltage from the computer). Engine speed was measured, compared with the required speed and modified if required by the computer program. This worked very well but was time consuming due to the slow response time of the computer. The above method was used for speed control over long duration engine runs. For multiple increment engine tests manual control of the alternator excitation enabled much faster speed stabilisation between sampling. These two systems for load-speed control were very effective and a similar system was used on the SEBCY to control the engine shaft speed, Chapter 9.

6.5 DMC 4

As an aid for describing and demonstrating the Stirling engine, a low temperature engine based on the design by Senft (1991) was manufactured, Photo 6.1(b). The only significant difference to Senft's design is the piston seal. Senft used a graphite/glass piston/cylinder, a system not easily manufactured locally. A cup PTFE seal was developed using 0.2mm thick pure PTFE sheet. The manufacturing method was similar to that used on the DMC 1 engine. Whilst the engine performance was not as good as that reported by Senft the engine has run continuously for several months and has started and run from the heat of a human hand. Currently this engine is operating as part of a Stirling engine promotional display in the Department of Mechanical Engineering, The University of Canterbury.

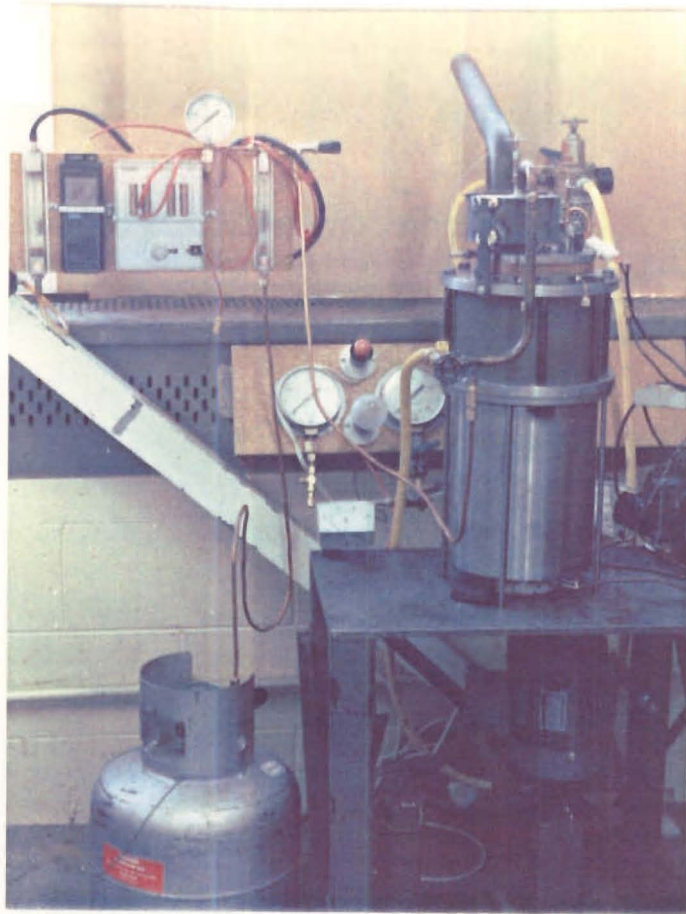


Photo 6.1 (a) DMC with heat exchangers fitted and dynamometer fitted. (b) Low delta T engine used for demonstrations.

7 Seals

7.1 Introduction

Many authors have commented on the lack of published seal design data for Stirling engines. This Chapter, in a modest fashion, adds the development work undertaken to meet the piston sealing requirements of the SEBCY.

Stirling Thermal Motors, (STM), (1990) stated that the three obstacles to mass production of automotive Stirling engines are:

- the integrated heater head;
- the sophisticated and complicated power control system ; and
- the seals for the reciprocating piston rods.

These obstacles also apply to production of the SEBCY. The heater head is dealt with in Chapter 8 and the problems associated with power control are alleviated with the use of swept volume variation^d, as utilised by the STM4-120 engine, (Meijer and Ziph, 1986) and by load control described in Chapter 9. This Chapter deals with the last obstacle, seals.

For each cylinder of a double acting engine there is a rod seal and a piston seal. By eliminating free lubricants from the mechanism housing, using air as the working fluid and pressurising the mechanism housing, the rod seal requirements are greatly reduced. For the SEBCY, piston seal

^d Volume variation for power control was not necessary on the SEBCY but the mechanism does allow this if necessary.

longevity is the most difficult to achieve, due to the higher local temperature, oscillating pressure differential, and larger seal circumference than the rod seal. Consequently this Chapter is primarily devoted to piston sealing.

In the early stages of this project, when most of the seal development work was performed, a twin alpha configuration (single acting) engine was intended for the SEBCY. Consequently some of the seal development work presented in this Chapter is applicable to a single acting alpha configuration engine. In single acting engines the pressure on one side of the seal is nearly constant at P_{buff} , and on the other side is the cyclic cycle pressure P_{cyc} . Minor preferential pumping of the seal ring can be tolerated in such an engine as it increases or decreases P_{mean} . For the double acting engine, however, the seal set is subjected to cyclic engine cycle pressure on both sides with a 90 degree phase difference. In this case preferential pumping is less desirable as leakage from one cycle adds to the mass of gas in the adjacent cycle thereby giving a different mean cycle pressure in each of the four cycles. When the individual cycle pressure is regulated, as in the Ford swash plate engine, this is not such a serious problem. But the complexity of cycle pressure regulation was unsuitable for the SEBCY. Therefore seals that do not preferentially pump were required.

7.2 Brief Stirling Engine Seal History

As seals have been a stumbling block to mass production, there has been considerable research and development devoted to seal design. It seems, however, that little detail of design procedures suitable for this project exists in the literature. This Section briefly summarises the existing Stirling Engine piston sealing technology.

During the early nineteenth century, leather washers soaked in oil provided the piston seal (Rizzo, 1985). Later in the nineteenth century cast iron rings were employed but still required some form

of fluid lubrication. Conventional piston ring design for internal combustion engines was used in the early Philips engines, and these required either grease or oil lubrication. This sealing method caused severe engine problems due to oil contaminating the heat exchangers and blocking the regenerator (Hargreaves, 1991). R. J. Meijer alleviated this problem in 1948 with the development of the Meijer groove in the top of the piston. This groove tended to transfer lubricants from above the piston back into the crankcase. This extended the time between overhauls to 1000 hrs for the Philips 200 W Type 19 engine, however, this piston seal design was still inadequate (Hargreaves, 1991). Many other seal arrangements were tested by Philips and their licensees. Their designs included close tolerance clearance seals, rolling sock seals, O-rings and various polymers in the form of sliding seals. Eventually a filled polytetrafluoroethylene (PTFE), Rulon[®] enabled dry running seals capable of withstanding the harsh environment in a Stirling engine with an acceptable seal life. Seal wear rates achieved were of the order of 0.06-0.09 mm/1000 hours. In 1978 and 1981 Philips published several papers on their seal developments the most relevant to this project are Eusepi et al, (1981) which investigates pumping rings and Ouwerkerk et al, (1981) which examines dry running piston rings. General Motors published details of their developments with neoprene, Rulon and roll sock seals, (Percival, 1974). To overcome the problem of preferential pumping caused by seal rings in double acting engines United Stirling used a two ring system on the 4-95 engine as shown in Figure 7.1, (West, 1986). The space between the two rings was held at the minimum cycle pressure. This caused the seal rings to be forced against only one face of the ring groove. This prevented oscillation of the ring in the groove and hence stopped preferential pumping. This could not be used on the SEBCY as no cycle pressure regulation was being used.

[®] A trade name of a filled PTFE material produced by Dixon, USA.

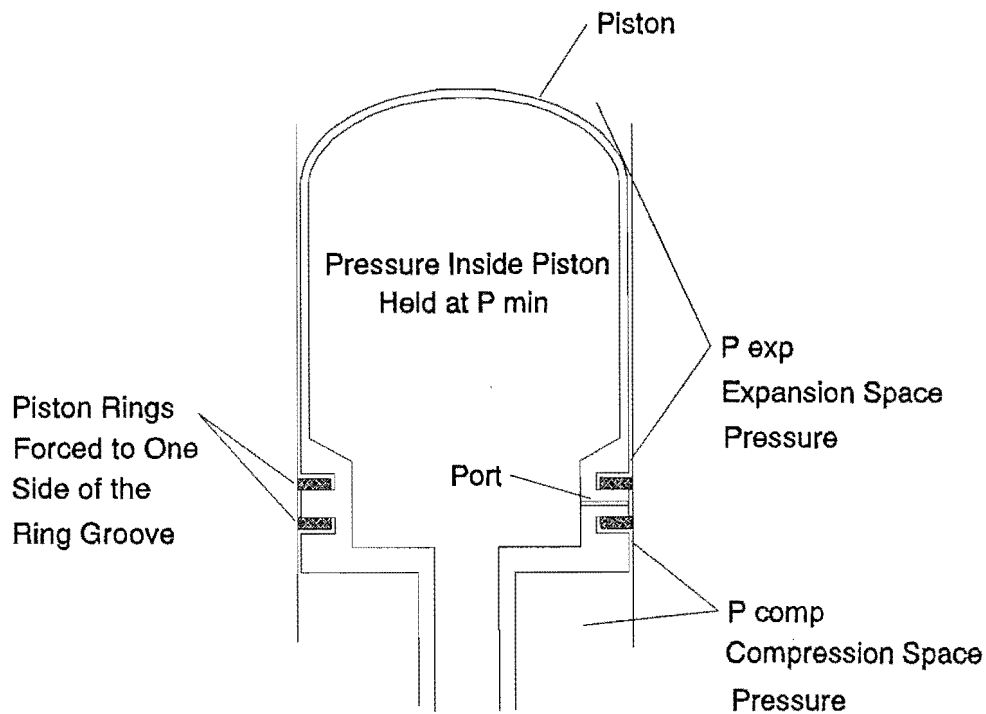


Figure 7.1 Piston seal system used by United Stirling in a double acting engine, (West, 1986)

7.3 Piston Seal Design Requirements

The seal system must:

- (a) Be capable of running reliably for 5000 hrs without added lubrication or maintenance.
- (b) Be able to withstand at least 150°C^f without breaking down due to thermal shock or numerous transient thermal fluctuations due to engine starting and stopping.

^f Estimate of the maximum seal interface temperature.

- (c) Be able to seal a pressure differential of up to 6 bar varying nearly sinusoidally.
- (d) Be mechanically efficient with low power loss due to friction.
- (e) Be resilient to thermal expansion and contraction.
- (f) Be of low cost to manufacture.
- (g) Not preferentially pump gas between the adjacent cycles.

7.4 Initial Seal Experience

During the first three months of this project the DMC 2 engine was manufactured to act as a proof of principle and a source of local practical experience with Stirling engine manufacture and characteristics. This engine design is described in greater detail in Chapter 6. Many seal configurations were tested with this engine, most with limited success. As was noted by Walker (1980) PTFE lip type seals would work well one day and then on the next day would not provide sufficient sealing to start the engine. Lip seals were fitted cold to DMC 2 with a slight interference which initiated the seal on the first start. When the engine was running, seal friction and heat conduction from the hot end caused the seal ring temperature to increase. PTFE has a higher rate of thermal expansion than the cylinder wall and having no ring gap, the seal ring permanently deformed (crept) and/or wore to the size of the cylinder. On cooling the higher rate of thermal expansion of the PTFE seal ring caused it to shrink more than the cylinder. Losing its interference it would not seal on the next start. To overcome this problem a steel expansion ring was fitted to the seal ring and this proved successful. After four years of intermittent use the engine still had compression and started reliably. Whilst this design was adequate for a proof of principle engine,

the life expectancy of the seal and the seal power consumption due to sliding friction was unknown.

It was decided that to produce a commercially viable system, further seal design experience was required. It was also considered that PTFE type lip seals had not been developed to their full potential for Stirling engines and there was scope for both experimental and theoretical research.

It was also noted that the design data for locally available PTFE was based on material tests at near ambient temperatures and for continuous unidirectional interface motion, rather than oscillatory. Therefore the use of this data for seal ring design was questionable.

Time limitations and resources precluded long duration seal testing of many different seal materials and configurations. It was decided that a seal, made from a suitable material, which was optimised for the lowest contact pressure while having permissible leakage, was most likely to survive the longest, provided the seal temperature was within acceptable limits. To aid determination of the minimum PV for sufficient sealing, a seal pre-loading system was sought which could modify the seal PV while the engine was running.

7.5 Seal Ring Material Testing and Selection

Many methods of controlling the seal interface pressure were examined and it was concluded that the only way to have uniform circumferential control over the seal PV was to use externally controlled hydraulic seal loading. Cylinder mounted seal rings were a practical way to achieve this, Figure 7.2. and 7.5

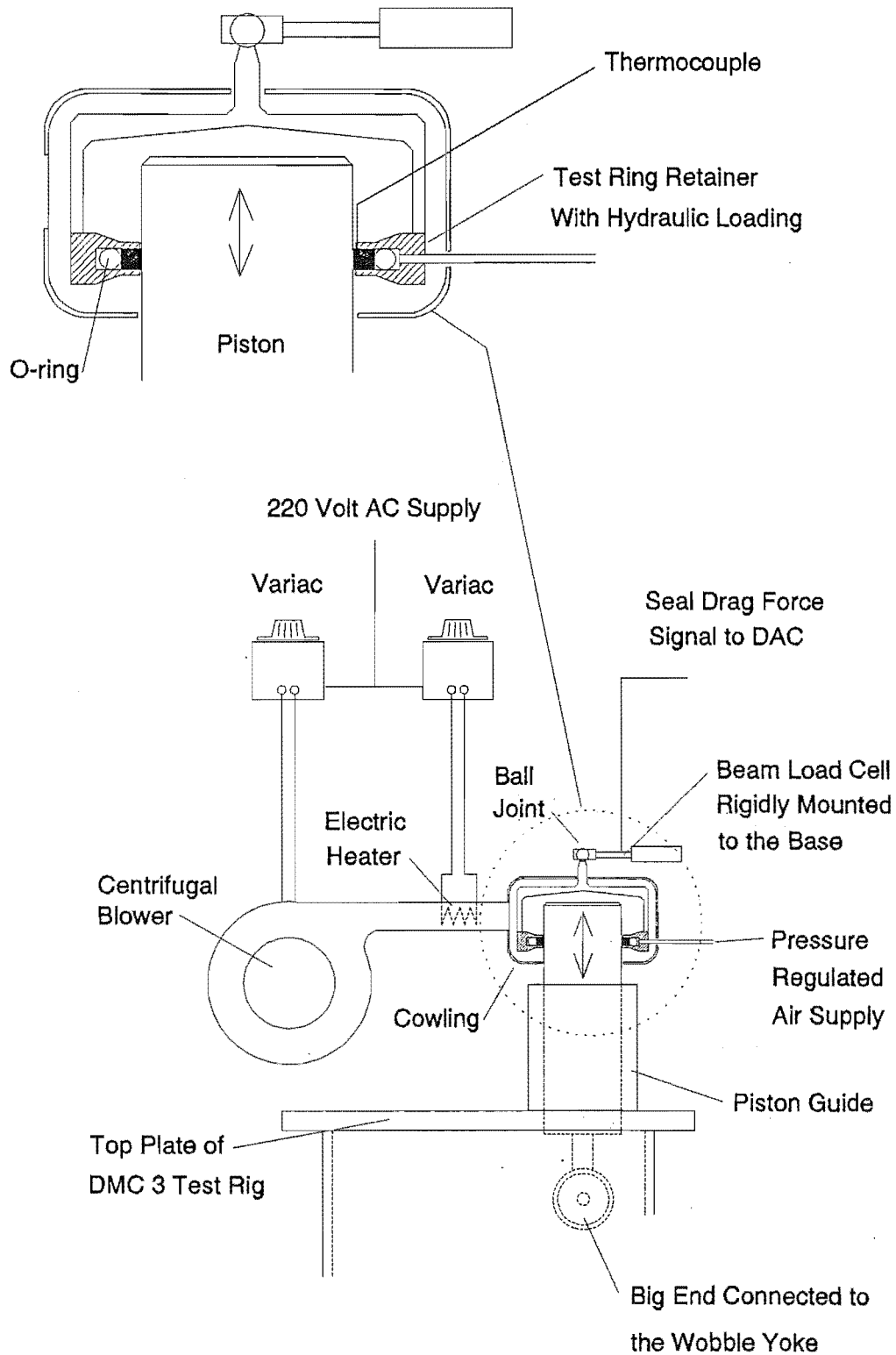


Figure 7.2 Test apparatus used for assessing seal materials. This apparatus was used in conjunction with the DMC 3 engine shown in Figures 6.4 and 6.5.

7.5.1 Materials

Texts on Stirling engines quote filled PTFE materials as being most suitable for dry running piston seal rings. These materials exhibit a low friction coefficient and an ability to operate at high temperatures. The most often referred material is Rulon, of which there are several grades which are made with a variety of unpublished performance enhancing fillers. Many attempts were made to obtain a suitable grade of this material but the cost was prohibitively expensive and it had to be imported on a minimum quantity basis. Locally sintered materials at around one tenth of the price of Rulon were readily available. A decision was made to attempt to use the locally sintered materials and if they proved unsuccessful Rulon could be used in production engines when bulk purchasing could reduce the seal material cost per engine. This was a dubious decision as General Motors had changed from Rulon when developing seals for the GPU-3 engine. Percival (1974) describes how their Rulon sales representative moved to an opposition company and General Motors were persuaded to buy his new proprietary product. The new material, which the engineers believed to be Rulon, gave wear rates an order of magnitude higher than Rulon. When the problem was finally realised, Rulon was again exclusively purchased.

7.5.2 Measurement of Material Characteristics

Initially attempts were made to measure both leakage and friction during a single test. It was found, however, that pressure oscillations in the rig adversely influenced the friction force measurements.

The rig was later converted to measure solely material performance characteristics, for example the coefficient of friction for various ring PV and interface temperatures, Figure 7.2. Once suitable materials had been selected from these results and the relevant design parameters had been established the rig was converted back to the original design and leakage tests were performed.

7.5.3 Friction Power Loss Measurement

The object was to determine the coefficient of friction of locally manufactured materials for various PV and operating temperature under oscillatory motion similar to the piston motion of the prototype SEBCY. The data obtained could then be used to verify simulations of the effects on engine performance of different seal designs. By determining the seal drag in units of force for a known velocity and interface pressure, the instantaneous coefficient of friction and related power consumption was derived. The interface pressure was controlled pneumatically by a regulated compressed air supply, Figure 7.2. The motoring speed was set by the operator to either 800 or 1250 rpm (For the initial motoring tests the motor speed was controlled by a variac which gave a limited speed range. The motor controller was later modified to a variable frequency electronic system Section 6.4.2. Due to the stroke used, 23 mm, the interface velocity was similar to that finally used in the prototype engine when the rig operated at 1250 RPM).

Having the seal ring externally mounted meant a very light aluminium ring retainer could be used and this was mounted to the rig solely via a load beam with a bridge strain gauge system. The signal from the load beam was amplified, displayed on an oscilloscope and recorded using the computer DAC system. The piston position and velocity was determined as described in Section 6.4.5. This system provided adequate results for this project. For more advanced studies of seal ring friction more sophisticated load measuring equipment would be required. Examples of such equipment are given by Ouwerkerk (1981) and Smith (1991). It was found that at higher PV and temperature the seal ring went through severe "stick - slip" at the ends of the stroke. This induced vibration in the load beam. Consequently the load beam required careful design to ensure this induced vibration was not near the beam's natural frequency. The system natural frequency was checked using an accelerometer before use.

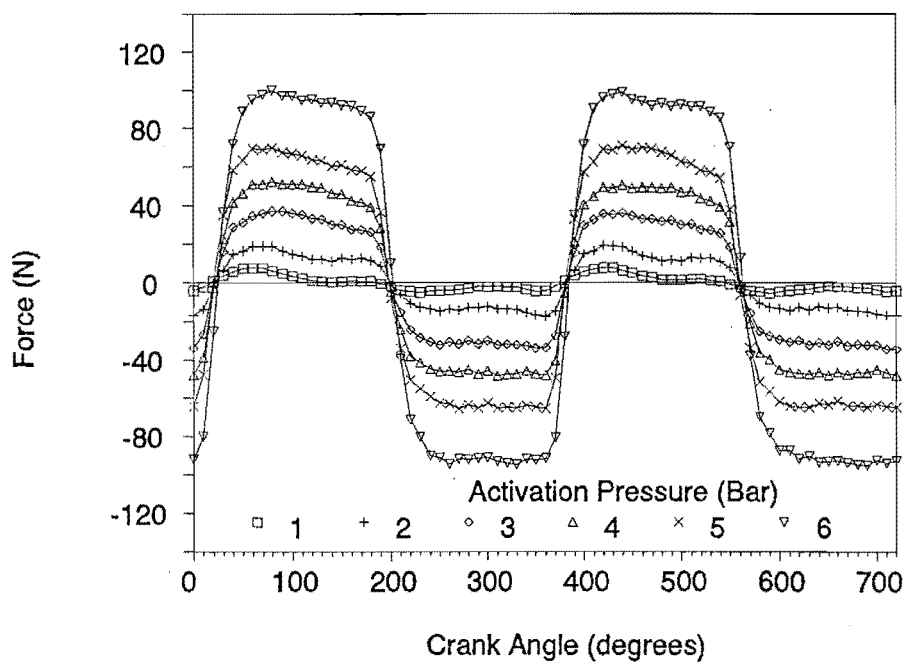
7.5.4 Seal Heating

It was necessary to operate the test ring at temperatures comparable to the operating conditions in the prototype engine. Heated air was supplied to a cowling which surrounded the test ring holder and piston, Figure 7.2. The two variacs which controlled the air blower and air heater element were used to regulate the seal/piston temperature. A thermocouple was fitted into a small hole drilled in the side of the test ring, Figure 7.2. The operator was able to read the seal temperature and adjust the two variacs accordingly. This method enabled data readings to occur within 2 degrees of the desired temperature. Slow thermal response, complicated by seal ring heat generation, made this a time consuming procedure.

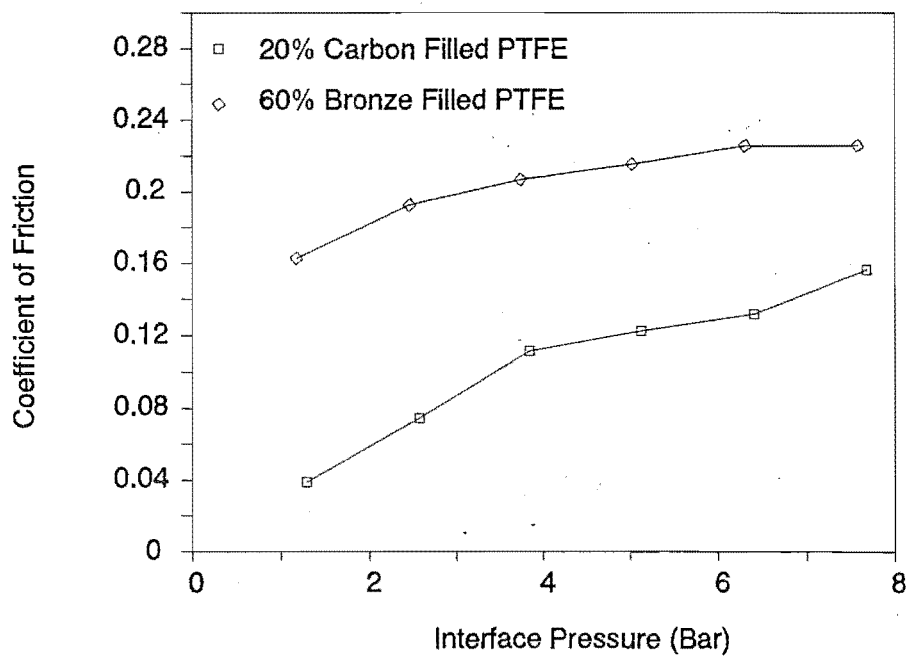
7.5.5 Results of Seal Material Testing

Three types of filled PTFE were tested. The filler and percentage mass of filler in each material were: Carbon 20%, Bronze 60% and Glass 30%. Pure PTFE was briefly tested, but this showed had an unacceptably high wear rate as was expected.

Figures 7.3 and 7.4 give examples of the data obtained for each test. These results are for 20% Carbon filled PTFE operating at 150° C and 1250 RPM. Figure 7.3(a) shows the seal friction force for various seal activation pressures. It was noted from this result that PTFE rings do not exhibit the sharp spikes at the end of the stroke like internal combustion piston rings, Smith (1991). Figure 7.3(b) shows that the coefficient of friction for filled PTFE materials is not constant. Therefore when simulating the seal friction force the coefficient of friction should be related to the instantaneous seal/piston interface pressure. Figure 7.4(a) shows the instantaneous seal ring power consumption, as expected the power peaks at the maximum piston velocity and is zero at the ends of the stroke. Figure 7.4(b) shows the average power consumption over one cycle. Due to the non-linear coefficient of friction the power is also non-linear when graphed versus the interface pressure.

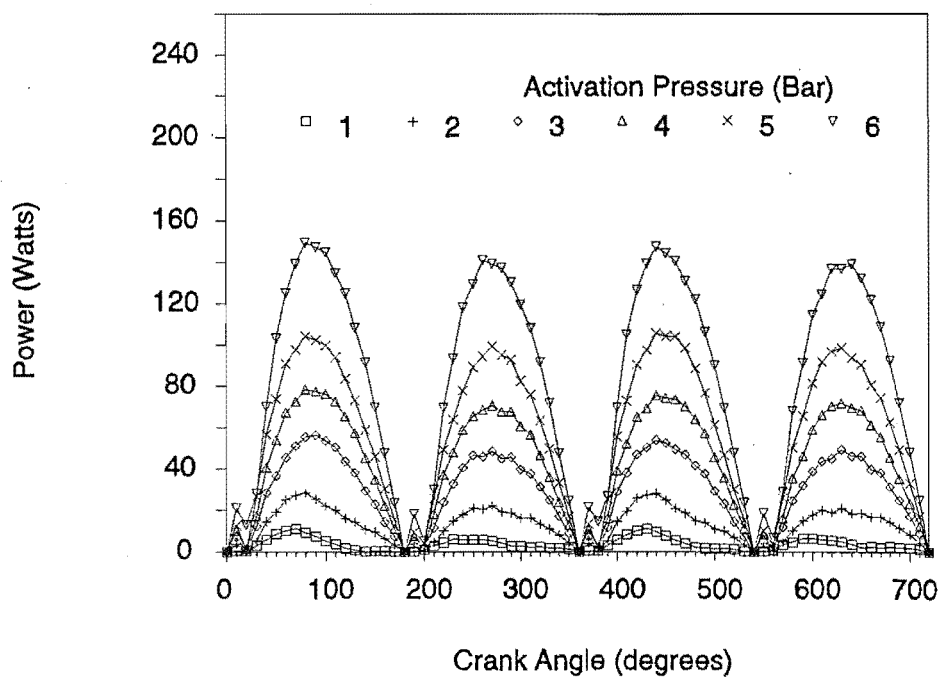


a.

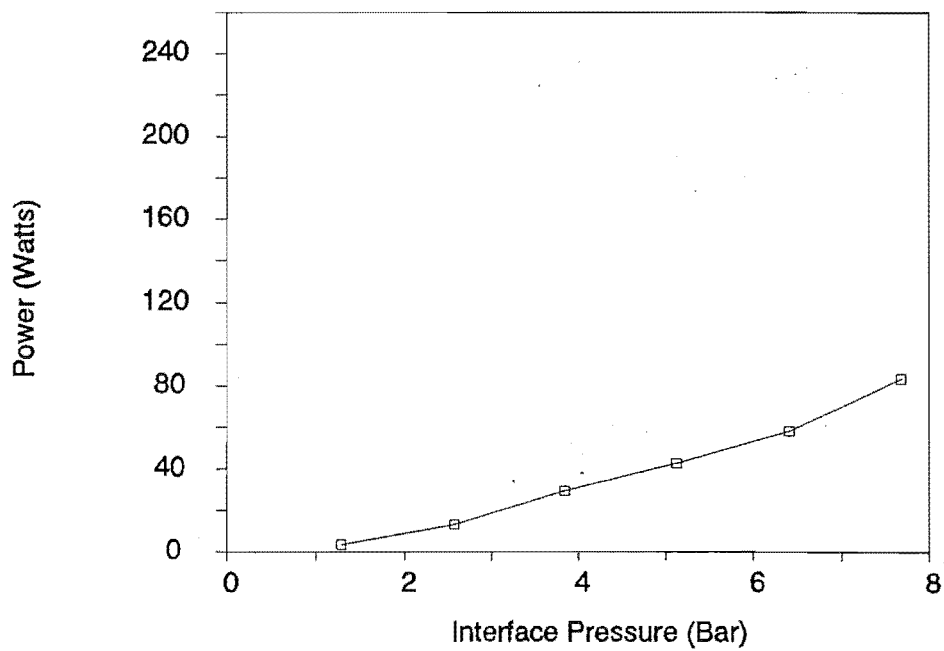


b.

Figure 7.3. Example of seal material test data. (a). Instantaneous friction force. (b). average coefficient of friction.



a.



b.

Figure 7.4 Example of seal material test data. (a) Instantaneous power consumption. (b). Average cycle power consumption.

PTFE with 20% carbon filler showed the best performance overall and was chosen for use in the SEBCY prototype.

PTFE with 60% Bronze filler gave higher power consumption due to having a higher coefficient of friction. One set of results of the coefficient of friction for this material is shown in Figure 7.3(b) as a comparison.

7.6 Cylinder Mounted Seals For Engine Use

It was decided cylinder mounted seal were also suitable for use in an engine application, Figure 7.5. Some of the advantages over piston mounted seals include:

- The seal ring is encapsulated on three sides by the water cooled cylinder allowing good heat dissipation from the seal ring.
- Thermal expansion of non-split seal rings relieves the seal/piston interference.
- On cooling the seal will contract onto the piston which ensures sealing on the next start.
- The cylinder does not need to be bored to a high tolerance and suitable surface for the seal to run against.
- The cylinder does not need to be made of any special material for wear resistance. For example a material of high thermal conductivity such as aluminium can be used instead of wear resistant steels with lower thermal conductivity.
- The piston can be a thin shell with the external diameter finished to act as the mating seal face.
- Accurate finishing of the external surface on the piston may be less expensive than an internal bore.
- The piston design is suited to using ceramic pistons in future engine developments.
- For split seals the seal gap decreases as the seal wears, thereby reducing seal leakage.

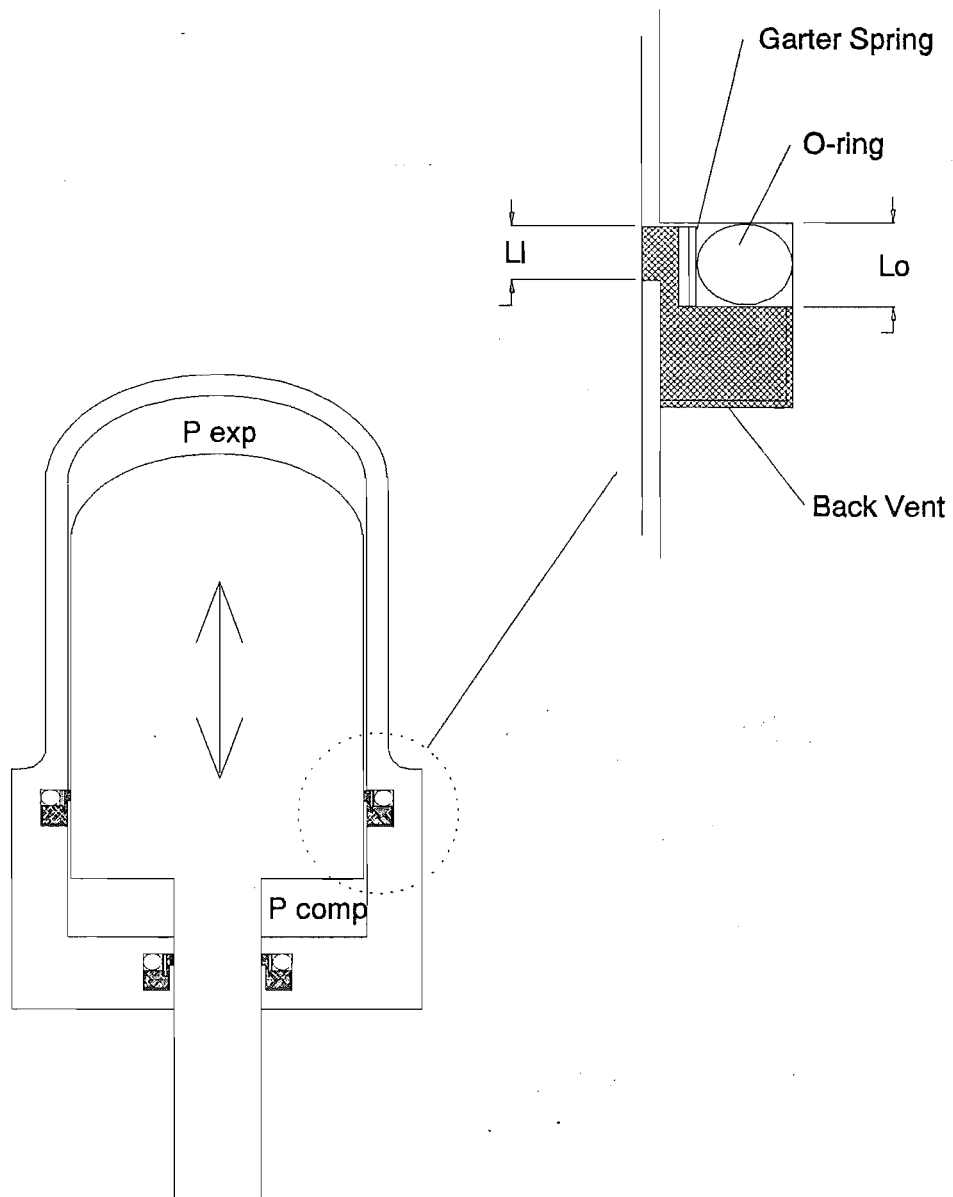


Figure 7.5 Cylinder mounted seal arrangement.

- Simple garter type springs can be used to preload the seal as they would be in tension and would provide even compressive loading on the seal ring.

A disadvantage of this system is the piston surface (seal interface) is being cooled by the working fluid rather than the heat going directly to the cooling water through the cylinder wall. The cylinder mounted seal is therefore more suited to single acting engines where the piston skirt can be cooled internally by the buffer space working fluid. For example the alpha configuration test engine, DMC 3, described in Chapters 6 and 8.

Cylinder mounted seals are essentially large diameter rod seals. There has been considerable research and development on rod seals, but mainly devoted to hermetic seals for helium and hydrogen charged engines, and this does not directly relate to the requirements of this project.

7.7 Seal Simulation.

To investigate the effects of seal leakage, preferential pumping, wear, thermal expansion and seal material characteristics on the Stirling engine, a computer program was written which updates the cycle pressure at 10 degree shaft intervals and determines the corresponding working fluid leakage over that interval. The cycle mass of gas, seal hydraulic loading and seal wear is then updated and the engine mean pressure and power is recalculated. This routine was iterated over 10 000 engine cycles (6 minutes operation at 1500 RPM) for four seal ring configurations either split or non-split. As this procedure required such a large number of iterations, the Schmidt analysis for an alpha configuration was used as it has closed form solutions and the ability to calculate the cycle pressure at given shaft angles. The model included thermal expansion, seal ring wear and seal ring stiffness. The computer code is listed in Appendix B.

7.7.1 Seal Preferential Pumping

It was mentioned that preferential pumping on the piston seal was detrimental to engine performance in double acting engines. It is shown below that preferential pumping can be used to control the mean cycle pressure and hence the engine power. This is possible on the rod seal for double acting engines and the piston seals of other configurations.

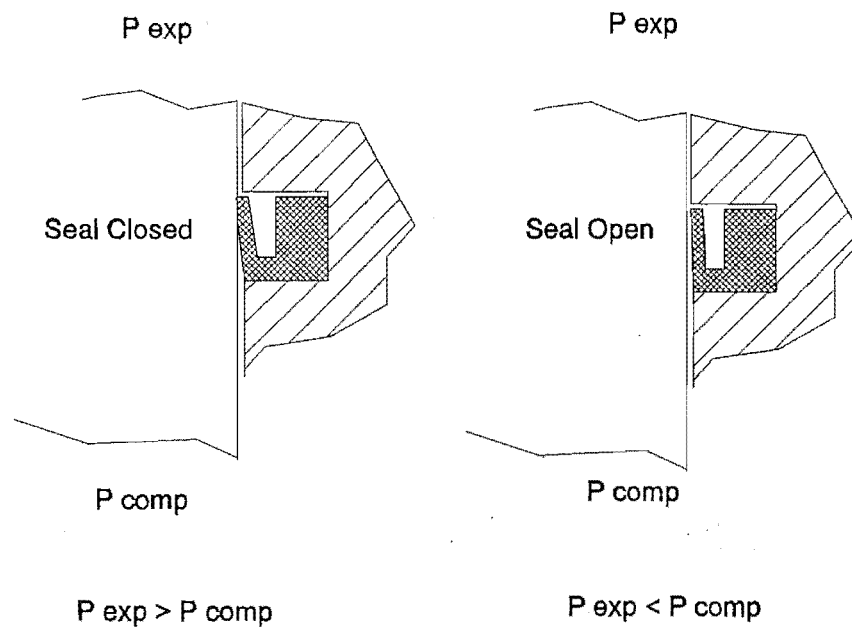


Figure 7.6. The effect of reversing the pressure differential across a lip type seal.

Lip type seals can act as non-return valves, Figure 7.6. Consequently the mean cycle pressure can be elevated above the buffer space pressure, P_{buff} , or in the case of the SEBCY above the mechanism housing pressure which is 10 bar. A desirable case is obtained when the minimum cycle pressure is equal to the buffer space pressure because: (a) the power output is a maximum due to the highest mean cycle pressure and (b) the pressure load on an alpha, beta and gamma

configuration's piston(s) would not reverse each cycle. If $P_{\text{mean}} = 4/3 P_{\text{min}}$, (Walker, 1980) then preferential pumping could give a significant power increase, Equation 4.5.

The Philips 1002C engine used two cast iron piston rings, similar to those used in an internal combustion engine. A port in the wall of the cylinder at the bottom of the stroke was used equalise the minimum cycle pressure and the buffer space pressure. When the piston opened this port at BDC the cycle pressure was near its minimum value. Consequently the mean cycle pressure would be well above the buffer space pressure.

This pressure variation due to preferential pumping is of major concern to free piston engine designers as it causes the piston and/or the displacer to drift to one end of the cylinder. To overcome this problem, porting is also used to equilibrate the pressures and ensure the piston or displacer remain in their correct mean positions, (Walker and Senft, 1985).

Due to pumping effects most engines would not have buffer space pressure equal to the mean cycle pressure and therefore determination of the actual mean cycle pressure requires an indicator or pressure transducer. This adds to the confusion over the use of the Beale and West equations: was the mean pressure used from various engines to determine the West number, Section 4.9.6, the actual mean pressure or the buffer space pressure?. As indicated above this can have dramatic consequences on the power predicted by the West formula, Equation 4.5.

7.7.2 Seal Leak Paths

Clearance seals have only one leak path, between the cylinder wall and the piston. Depending on the design, contact type seals can have several leak paths these include: (i) between the sliding faces, (ii) around the back of the seal and (iii) through the ring gap if the seal is split. As the seal types modelled are sealed from leaking around the back side, Figure 7.5, only leakage between the sliding surfaces is modelled.

7.7.3 Seal Simulation Results

Four seal types were examined, Figure 7.7. The hydraulic seal loading for each type was determined by Equations 7.1 to 7.5.

Type 1.

$$P_{close} = P_{act} \quad (7.1)$$

Type 2.

$$P_{close} = P_{act} - \frac{P_{cycle} + P_{buff}}{2} \quad (7.2)$$

Type 3.

$$P_{close} = \frac{P_{act} L}{l} + \frac{P_{cycle} L}{l} - P_{buff} \frac{(L-l)}{l} - \frac{(P_{cycle} + P_{buff})}{2} \quad (7.3)$$

Type 4.

$$\text{If } P_{cycle} > P_{buff}$$

$$P_{close} = P_{act} + P_{cycle} - \frac{(P_{cycle} + P_{buff})}{2} \quad (7.4)$$

$$\text{If } P_{cycle} < P_{buff}$$

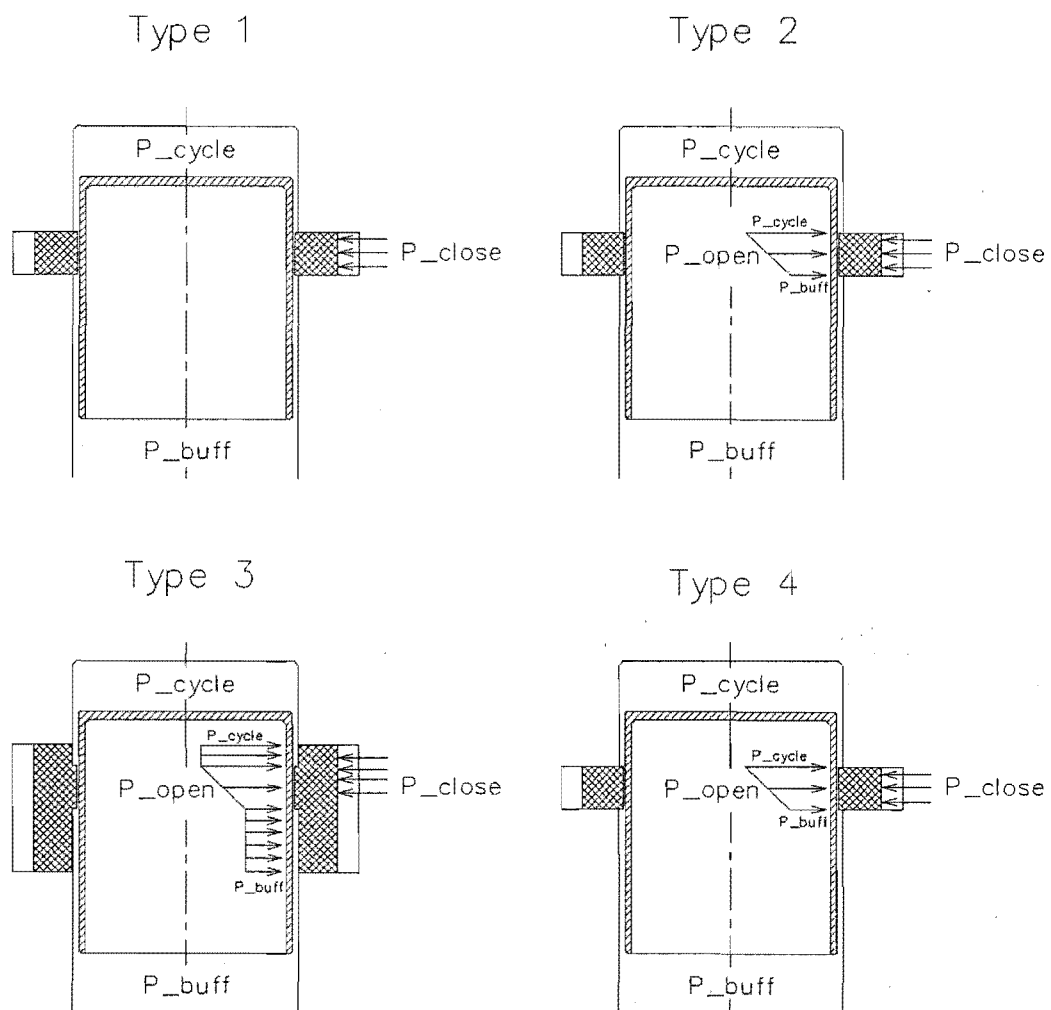
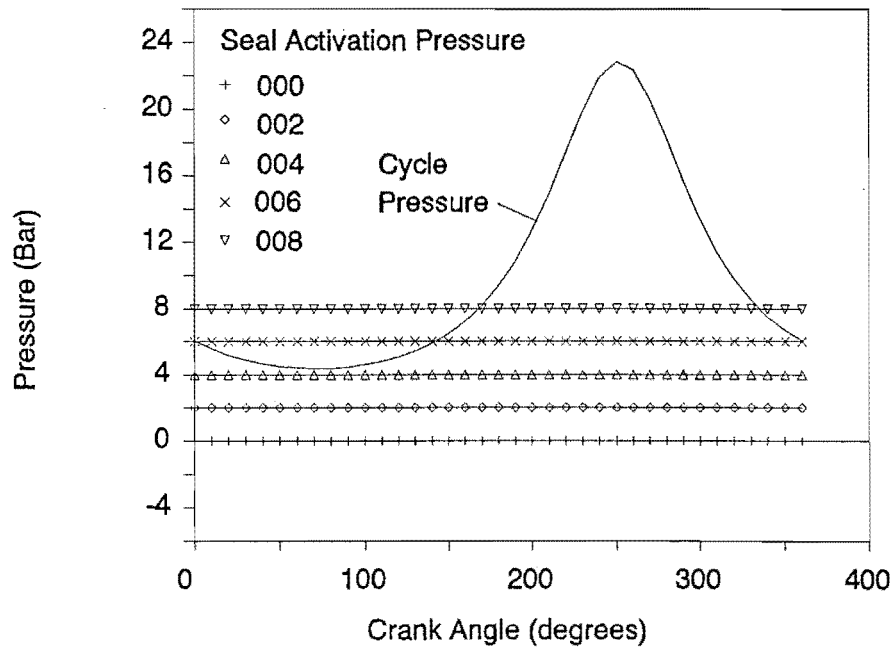


Figure 7.7 Seal types modelled. Ranging from the simplest Type 1 to the most realistic, Type 4.

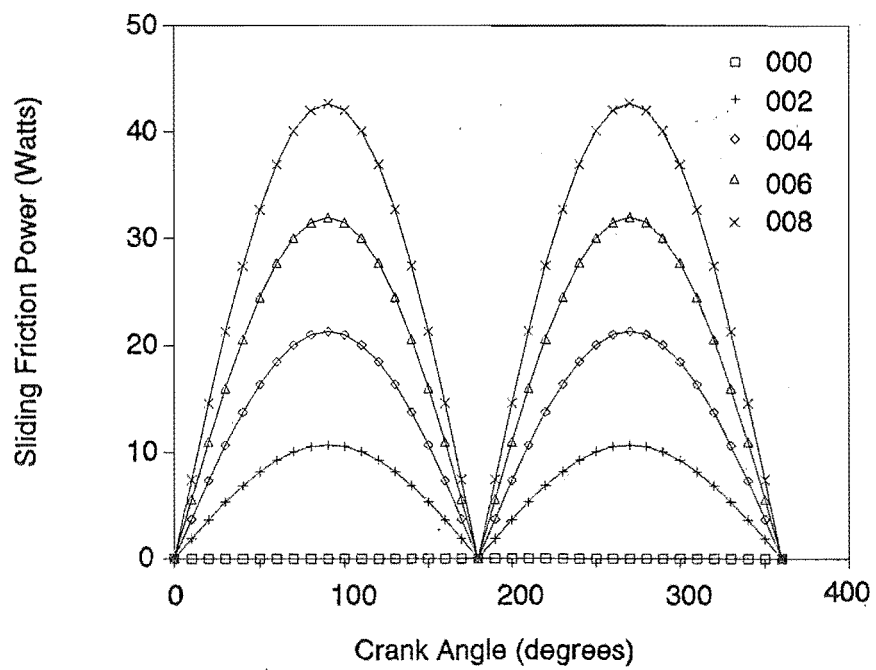
$$P_{close} = P_{act} + P_{buff} - \frac{(P_{cycle} + P_{buff})}{2} \quad (7.5)$$

The Type 1 split seal is identical to the seal testing described in Section 7.5. In this case there is no opening pressure and the seal/piston interface pressure is solely due to the activation pressure. The simulated seal power consumption is shown in Figure 7.8. Figure 7.8(a) shows the cycle pressure over one shaft revolution and the corresponding seal hydraulic loading pressure. As there is no cycle induced hydraulic loading, this pressure is constant over the cycle. Figure 7.8(b) shows the corresponding friction power, as can be seen the form of the results are very similar to Figure 7.4(a) from the experimental results.

The Type 4 non-split ring was the most relevant. This ring was subjected to both closing and opening hydraulic pressures and pressure differential reversal during one shaft revolution. In this case the seal activation pressure simulates a garter type spring applying an even pressure load around the circumference of the seal. Examples of the graphical output from the seal simulation for a Type 4 non-split ring is shown in Figures 7.9 and 7.10. This seal type was the most similar to the seal used for the SEBCY DMC 5 engine. It should be noted, however, that this analysis was only for single acting engines. (The analysis for double acting engines is considerably more complex due to leakage from one cycle affecting the adjacent cycle. Therefore all four cycles need to be modelled simultaneously while modelling both the piston and rod seals. This is feasible but was not considered necessary to achieve the objectives of this project. Hence a simpler modelling technique was used which is described in Section 7.9). Figure 7.9(a) shows the cycle pressure and the corresponding seal hydraulic loading. A pressure differential reversal occurred due to the cycle pressure P_{cyc} going below the buffer space pressure P_{buff} , 10 Bar. Despite this the seal hydraulic loading was always positive. It can be seen that the seal pressure loading follows the cycle pressure variation which is important for long seal life and low friction power loss. Figure 7.9(b) shows the seal leakage over one shaft revolution for the tenth cycle after starting the engine. For low activation pressure the seal leakage is considerable. The most notable feature being the

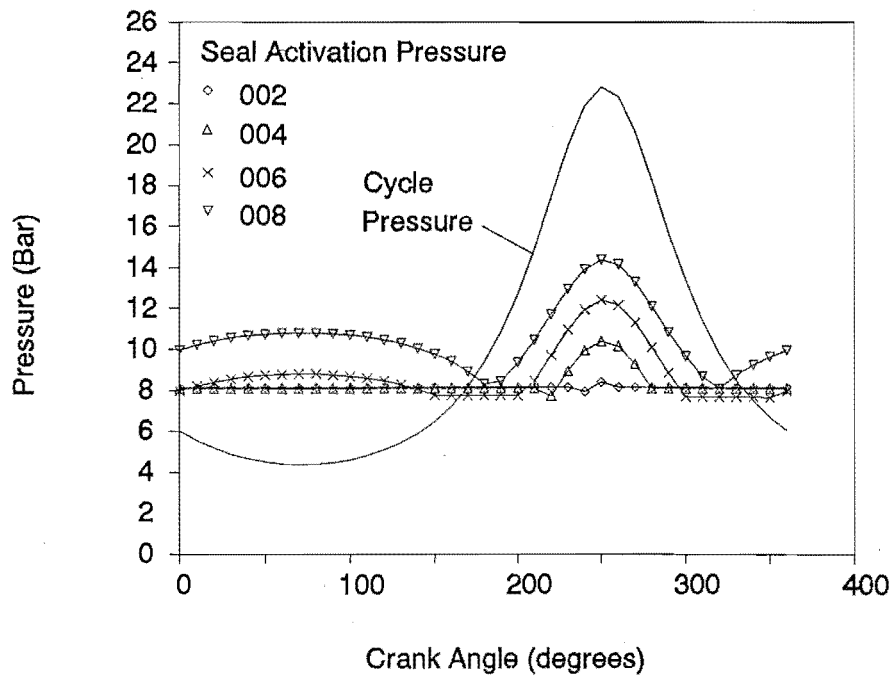


a.

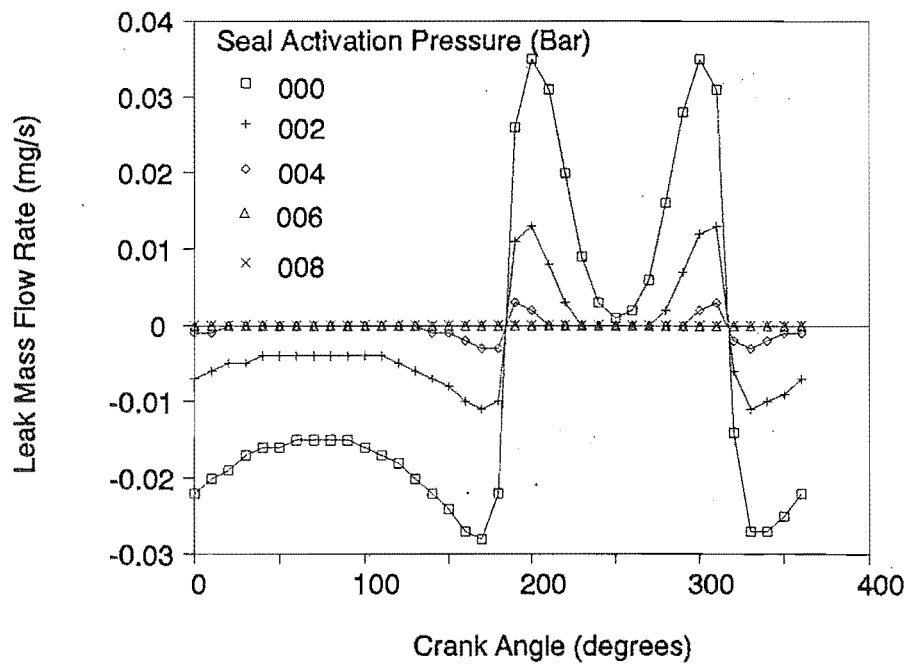


b.

Figure 7.8. Type 1 seal analysis. (a). Cycle pressure and seal activation pressure over one shaft revolution. (b). Resulting seal ring friction power.

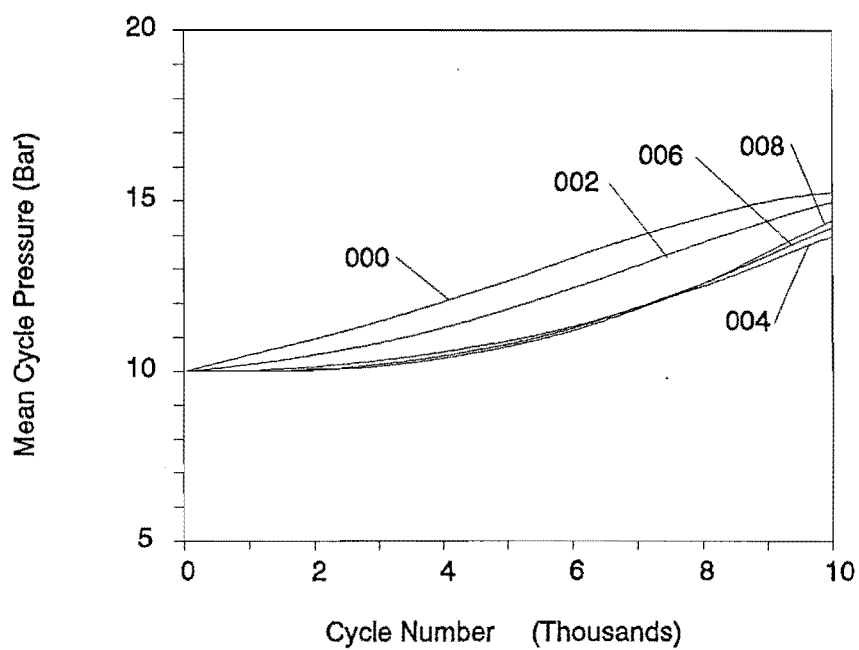


a.

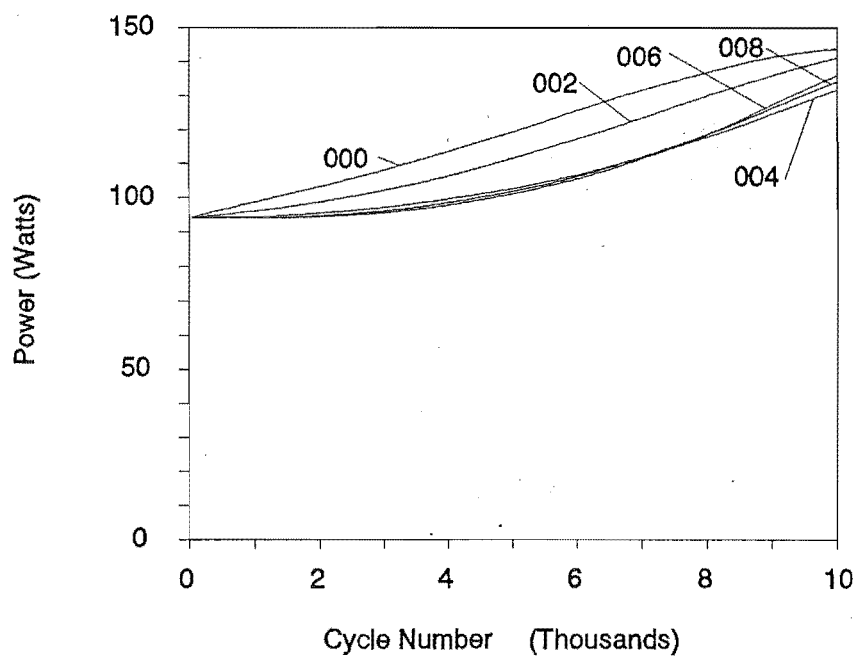


b.

Figure 7.9 Type 4 seal analysis. (a). Cycle pressure and the seal hydraulic closing pressure for one shaft revolution. (b). Resulting seal leakage.



a.



b.

Figure 7.10 Type 4 seal analysis. (a) Variation of the mean cycle pressure for various seal activation pressure over 10 000 cycles. (b). Resulting engine indicated power due to the mean pressure variation (thermodynamic and friction losses not included).

dominant negative mass flow which indicates more gas is flowing into the cycle than leaving. Therefore the seal is preferentially pumping gas into the cycle. After 10 000 cycles the negative mass flow was considerably reduced due to P_{min} approaching P_{buff} . Figure 7.10(a) shows the resulting change in the mean cycle pressure over 10 000 cycles. For zero activation pressure the mean cycle pressure increases rapidly and stabilises when P_{min} becomes close to P_{buff} . At higher activation pressure the rate of pumping is much lower and the rate of pressure rise is slower. In this case an accelerated wear rate has been applied which has accelerated the rate of pressure rise for 6 and 8 Bar after about 5 000 cycles. This is due to the seal wearing and the seal ring stiffness results in a larger seal/piston gap over parts of the cycle. A flaw in this simulation was seal creep was not included which would undoubtedly have beneficial effects to counteract seal/piston clearance due to wear over the life of the engine. Figure 7.10(b) shows the resulting power rise due to the increased mean cycle pressure. Thermodynamic and seal friction effects are not included in this calculation.

The basis for a useful seal design tool has been described in this Section. It should be noted that limitations exist in the computer code, some of which have been briefly mentioned. Experimental results described later in this Chapter do support the general trends shown. There is considerable scope for further development of this computer code as a useful seal design tool and it is recommended that a Postgraduate project should address this task.

7.8 Cylinder Mounted Seals in Operation

DMC 3 was fitted with pressure activated cylinder mounted seals to investigate their actual performance. Figure 8.9 shows the seal and heat exchanger arrangement. Note the ports used to supply compressed nitrogen gas to activate the two seals. Figure 7.11 shows a typical set of results for variation of the expansion piston seal activation pressure. The activation pressure on the compression piston seal was held constant at a pressure which was known to give complete

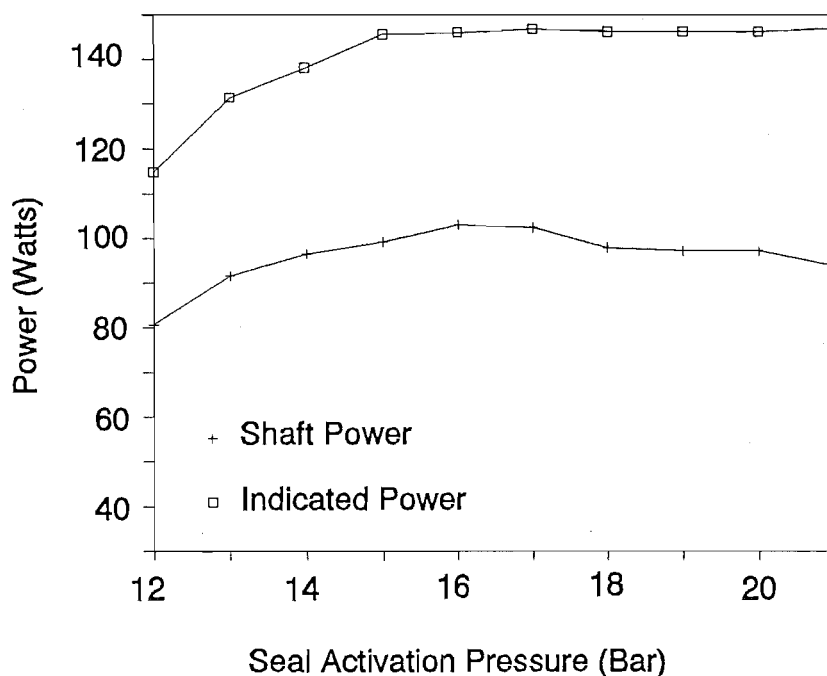


Figure 7.11 Variation of indicated power and shaft power for seal activation pressure. Engine shaft speed was 1500 RPM and the mechanism housing pressure was 10 Bar.

sealing over the entire cycle. Referring to Figure 7.11, at low activation pressure the seal was leaking and the indicated power was low. This was as expected due to the seal design causing gas leakage from the cycle, thereby reducing the mass of gas in the cycle and correspondingly reducing the work done. As the activation pressure was increased, both the indicated and shaft power increased due to progressively less seal leakage. Above approximately 15 Bar the indicated power ceased to increase, this was due to the seal being closed for the entire cycle. As no leakage could occur above this pressure the area of the PV diagram must remain constant. The shaft power, however, decreases above this critical pressure. This is due to the additional friction power loss of the seal caused by the increased seal/piston interface pressure. This result clearly shows that there is an optimum activation pressure which will give both the maximum indicated and maximum shaft power. Utilising the external seal activation system in practice can allow the operator to tune the seal to optimum conditions. It may also be possible to determine

the optimum spring loading required of the garter spring on the lip seal for situations where hydraulic activation is not practical. This system was also very valuable during the heat exchanger performance testing described in Chapter 8. By optimising the seal activation pressure, piston seal leakage from the cycle could be eliminated, thereby ensuring the indicated power measurements were not influenced by seal leakage.

This seal system demonstrated other interesting phenomena. For example, the engine could be started with no activation pressure. But the engine would only run for around 30 seconds and then stop. It was found that to restart the engine immediately the activation pressure had to be applied. This phenomena can be explained by examining the thermal characteristics of the seal. When the engine started for the first time the seal was cold and therefore shrunk onto the piston and would seal. After running for several seconds the seal temperature would increase and expand off the piston. This caused hot air from the expansion space to leak down past the seal causing the seal temperature to rise at a faster rate until the leakage rate was sufficient to prevent the engine from operating.

7.9 Seal Design for the SEBCY

No literature has been found relating to the use of cylinder-mounted single lip seals in double acting engines. The design difficulty is mainly due to cycle pressures at 90 degree phasing acting on each side of the seal which causes a reversal of the pressure differential. For normal lip seals this would tend to close the seal for say a positive pressure differential ($P_{exp} > P_{comp}$), Figure 7.6, and open the seal for a negative pressure differential ($P_{exp} < P_{comp}$). To overcome this, the seal shown in Figure 7.5 was developed. Figure 7.5 gives the most basic form of the design. By variation of the critical dimensions the seal could be tuned for optimal performance, Figure 7.12.

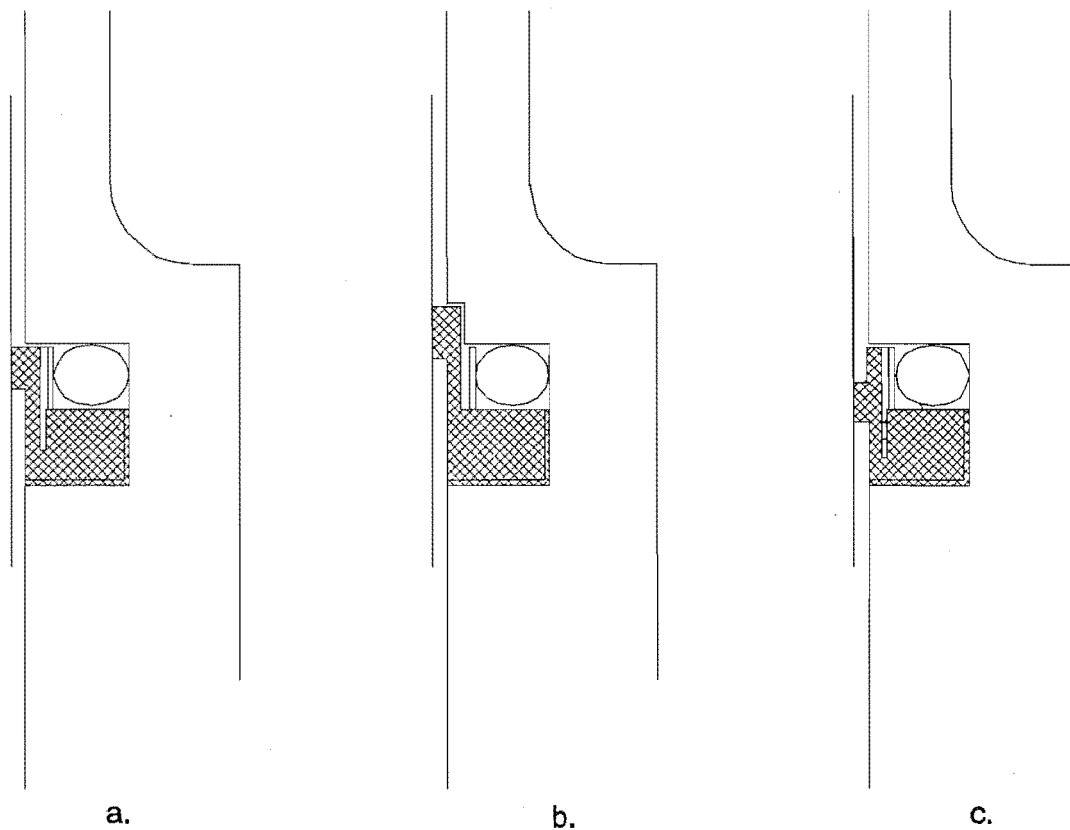


Figure 7.12 Possible variations of the seal design which could enhance the performance by optimising the seal pressure loading to suit the application. Seal (a) was initially used in DMC 5.

7.9.1 Single Lip Cylinder Mounted Piston Seal for Double Acting Engines

Referring to Figure 7.5 the design concepts are:

- There is only one lip in contact with the piston.
- The ring is positively sealed around the back by one O-ring.
- The large area of the seal body is pressed against the cylinder block for heat dissipation.

- A garter type spring puts slight positive closing load on the seal, being in tension the force on the seal is uniform and the spring rate is very low.
- The O-ring is in compression axial to the piston. Consequently the axial force on the seal ring keeps it from oscillating in the ring groove.
- The lip design causes the seal to close for a positive pressure differential.
- The seal ring is vented around the back by small channels, Figure 7.5. This allows the pressure from the compression space to act on the O-ring causing a positive seal closing load when the pressure differential is negative. This is the key feature of the design.

This design was successfully used for the initial tests of the SEBCY DMC 5 prototype engine.

7.9.2 Simulation of the Seal Pressure Loading

The SEDA⁹ spreadsheet program, described in detail in Chapter 8, includes seal simulation procedures and some key results obtained from this software are presented below. For determining the seal hydraulic loading the Schmidt analysis was used for the reasons outlined in Section 7.7. The engine parameters are the same as those used in Section 5.5.

The closing pressure is calculated according to Equation 7.6. This simple simulation only examines the hydraulic seal loading and does not include effects due to temperature and material stiffness.

In Figures 7.13, 7.14 and 7.5 P_{exp} refers to the expansion space pressure in cylinder one. P_{comp} refers to the compression space pressure in cylinder one. Delta P refers to the instantaneous pressure difference across the seal $P_{exp} - P_{comp}$. Figure 7.13(a) shows the instantaneous pressures P_{exp} , P_{comp} and Delta P over one engine cycle. It can be seen that there is a 90 degree phase difference between P_{exp} and P_{comp} . It can also be seen that the pressure differential reverses during the cycle, this would tend to open a conventional lip seal, Figure 7.6. Figure 7.13(b) shows the seal closing pressure with and without back venting on the seal. It can be seen

⁹ Stirling Engine Design Aid

For $P_{\text{exp}} > P_{\text{comp}}$

$$P_{\text{close}} = \frac{\left(-\frac{(P_{\text{exp}} + P_{\text{comp}}) L_I}{2} + P_{\text{exp}} L_o - P_{\text{comp}} (L_o - L_I) \right)}{L_I}$$

7.6

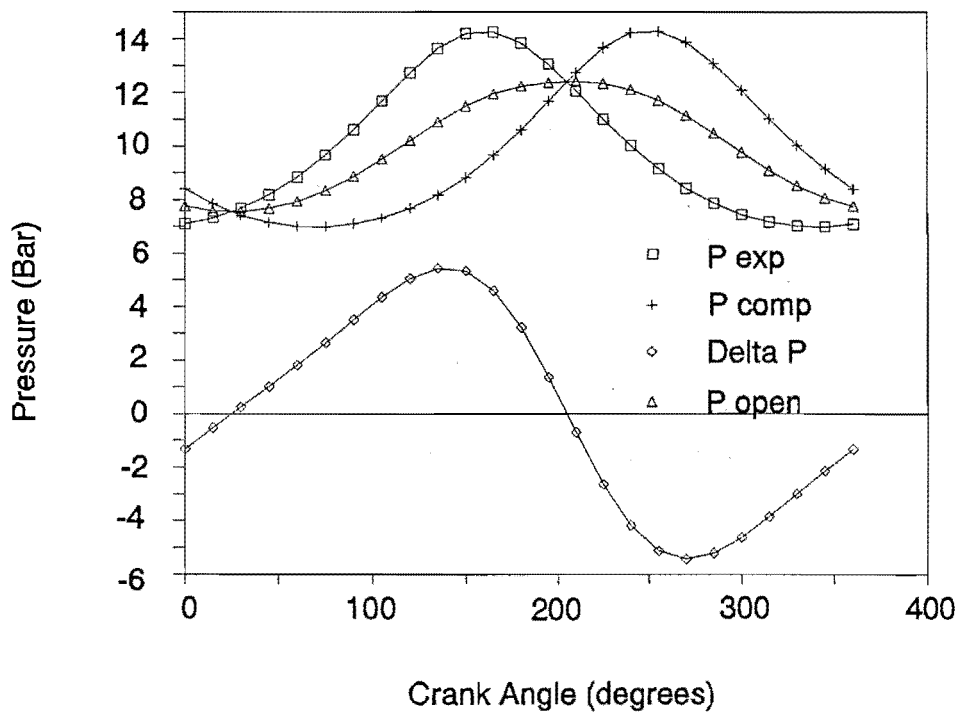
For $P_{\text{exp}} < P_{\text{comp}}$

$$P_{\text{close}} = \frac{\left(-\frac{(P_{\text{exp}} + P_{\text{comp}}) L_I}{2} + P_{\text{exp}} L_o - P_{\text{comp}} (L_o - L_I) + (P_{\text{comp}} - P_{\text{exp}}) L_o \right)}{L_I}$$

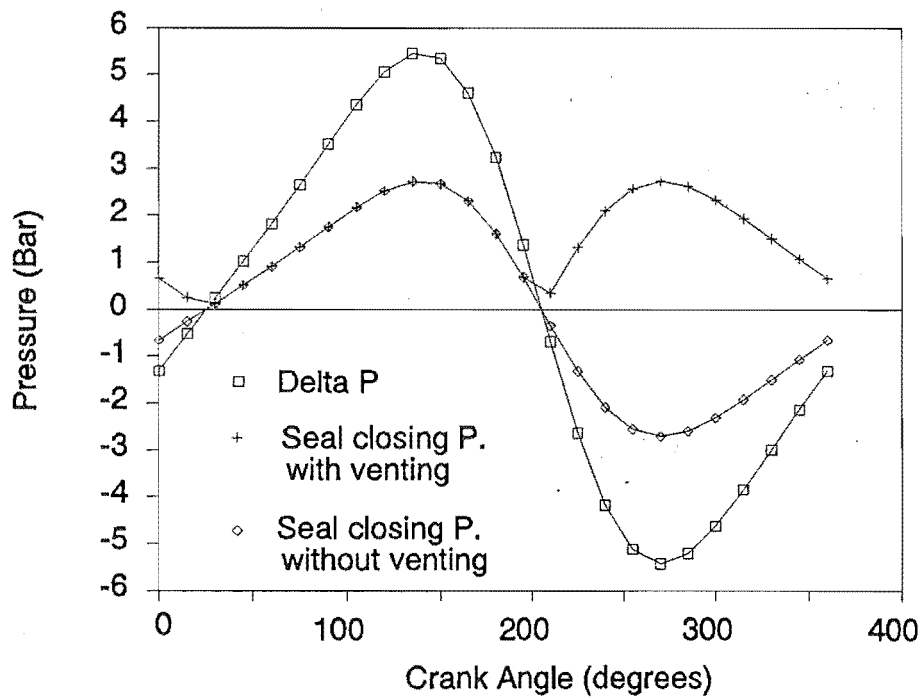
from Figure 7.13(b). that in the case where L_I (defined in Figure 7.5) is equal to L_o and the seal is back vented that there is always a positive closing hydraulic pressure. If the seal was not back vented there would be negative closing pressure and the seal would open. When L_I and L_o are equal the maximum magnitude of the closing pressure is equal for both positive and negative pressure differential. If L_I is decreased the magnitudes of the closing pressure changes as shown in Figure 7.14. This result confirms that it should be possible to design the seal geometry to suit the application.

7.10 Conclusions From Chapter 7

- The sealing problem associated with Stirling Engines has been alleviated by using a dry pressurised mechanism housing.



(a.)



(b.)

Figure 7.13 Cylinder mounted lip seal characteristics. (a). Cycle pressures and pressure differential across the seal. (b). Seal closing pressure with and without seal back venting.

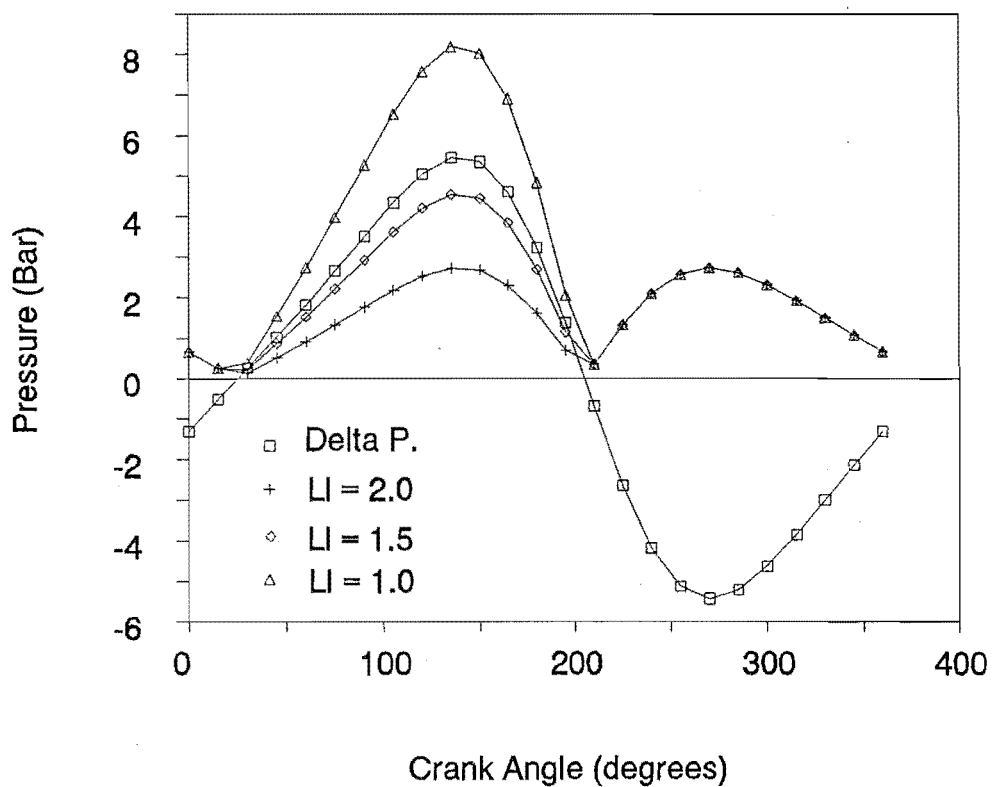


Figure 7.14 Seal closing pressure when $L_1 = 2, 1.5$ and 1 for $L_0 = 2$.

- Preferential pumping by the piston seals in the SEBCY can cause a variation of working fluid mass between the four cycles of double acting engines. As the power is proportional to the cycle pressure this would cause different power output from each cycle and torque fluctuations.
- 20% Carbon filled PTFE offered the best performance from the locally available materials.
- A simulation program, Appendix B has been developed to analyze an engine's performance variation due to seal pumping, thermal expansion and wear over 10 000 cycles.

- Cylinder mounted seals were fitted to DMC 3 and DMC 5. The resulting performance shows promise for this type of seal in production engines.
- The geometry of the seal is critical due to the seal lip pressure loads.

8 Heat Transfer System

8.1 Introduction

The heat exchangers of the Stirling engine are undoubtedly the most critical and expensive components (Urieli and Berchowitz, 1984). The Carnot efficiency ($\eta = 1 - T_K/T_H$) shows that any temperature drop in the heat transfer processes decreases the engine efficiency and the fundamental equation for convective heat transfer ($Q = h_{\text{conv}} A \Delta T$) shows that to reduce the temperature drop for a given rate of heat transfer, either the wetted area or the heat transfer coefficient must be increased. Increasing the wetted surface area and heat transfer coefficient, however, can be detrimental to the engine power due to increasing dead volume and/or flow losses. Prior to manufacturing a well designed Stirling engine it is generally necessary to optimise the heat exchangers for a specific application using computer programs, (Organ, 1991).

There are several published computer codes for 2nd and 3rd order analyses of the Stirling Cycle (Martini 1982, Urieli and Berchowitz, 1984) there are also several commercially available codes and many in-house codes. Development of new code and enhancement of existing code is the subject of many research projects in institutions where adequate facilities for experimental verification of the code is possible. To expedite the design and development process it was decided to utilise an existing published code which could be customised and would allow dimensional optimisation of the heat exchangers. Urieli and Berchowitz (1984) listed a computer code suitable for isothermal, adiabatic and quasi-steady flow nodal analysis. This code was customised to suit the SEBCY project and was subsequently used to optimise the test engine, DMC 3, and the prototype

DMC 5 heat exchangers. The following Sections outline the code, optimisation techniques, results from the computer analysis, and test results from DMC 3 used to verify the computer code.

8.2 Quasi Steady Flow Model, QSFM

This Section includes extractions of necessary theory for a basic understanding of the Quasi-Steady Flow Model from the text by Urieli and Berchowitz (1984). The reader is directed to this reference for more detailed theory and the Fortran listing.

8.2.1 Non-steady flow

At the time Urieli and Berchowitz developed this code the majority of published compact heat exchanger design techniques were based on the assumption that steady flow conditions prevailed. In the Stirling Cycle the flow conditions are always changing and at some time the flow is in opposite directions at either end of the heat exchangers (Walker, 1980). To overcome this lack of design data Urieli and Berchowitz developed the Quasi-Steady Flow model based on the assumption that at each increment in the cycle, steady flow conditions prevail and the existing data and equations could be used.

8.2.2 The Model

Prior to the development of the QSFM, Urieli and Berchowitz developed the adiabatic model which would not allow optimisation of the heat exchanger dimensions due to holding the heater and cooler gas temperatures at a constant temperature equal to the heat exchanger wall. This is not suitable due to thermal resistance between the wall and the gas. That is, the gas temperatures can be substantially different to the wall temperature. The QSFM was selected for the heat exchanger optimisation because it determines the flow and heat transfer characteristics in the heat exchangers. If further work is to continue at the University of Canterbury a more recent validated code should be purchased eg. GLIMPS or Marwiess (Stirling Machine World, 1992).

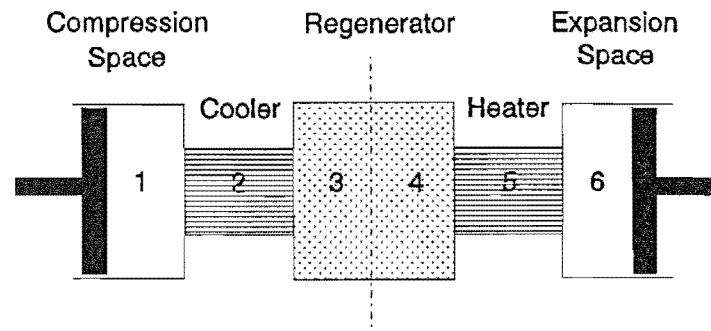


Figure 8.1 Minimum cell division for the QSFM.

The QSFM is now defined with reference to Figure 8.1. The engine is broken up into a minimum of 6 cells or nodes; compression, cooler, regenerator/2, regenerator/2, heater, and expansion space. The energy equation for each cell can be generalised in the form of:

$$\begin{aligned} & \{\text{rate of heat transfer into the cell}\} - \{\text{rate of heat generation}\} + \{\text{net enthalpy into the cell}\} \\ & = \{\text{rate work done on the surroundings}\} + \{\text{rate of increase of internal energy in the cell}\} \end{aligned}$$

Based on this equation Urieli and Berchowitz derived 40 equations, 13 of which are simultaneous differential equations, Appendix C. A consistent set of initial conditions was determined from the designer's input conditions and the solution was obtained using the 4th order Runge-Kutta method. Convergence was achieved when the regenerator residual heat Q_r at the end of the cycle was zero. Running on a Micro Vax computer the average solution time was close to four minutes.

Several modifications and additions were made to the published code, they were:

- Stability checking and modification of the time step if necessary. Optimisation routines require a large number of simulations so the routine must be robust and able to operate unattended. To set the time step small enough to ensure reliable operation for all engine variants would make the optimisation extremely slow. It was noted that when the simulation went unstable, certain temperatures would rapidly increase. Node temperatures were monitored and if instability was detected the time step was decreased and the simulation continued. This simple method proved very reliable. The initial time step value was set according to previous experience to give stable solutions for a typical set of variables. Some engine variants could not be solved, for example if the regenerator cross sectional area was too small. In such cases the simulation aborted and went to the next optimisation variable.
- External heat transfer conditions. The original code held the heater and cooler wall temperatures at a constant temperature nominated by the designer. For some simulations some extra code was added to include the external heat transfer conditions, for example the designer could nominate the burner gas temperature and the gas-to-head heat transfer coefficient.
- Optimization routine. This addition is discussed in detail in Section 8.3.
- Volume variations according to the wobble yoke kinematics. The kinematic equations derived in Chapter 5 were included.
- Inclusion of fin efficiency. The flat plate cold end heat exchanger developed was thermodynamically modelled by treating the plates as fins and using conventional fin heat transfer theory given by Holman (1981).

- The code was linked to a Spreadsheet program to allow easy pre and post processing of the large volumes of data produced by the QSFM. This work is described in the following Section.

8.2.3 Designer - Computer Interface

The computer code as given was written in a format which was very easy to follow format. This suited a wide variety of applications. This format allowed easy customising of the program, particularly with regard to pre and post data processing. A Spreadsheet program, SEDA^h, was developed which allows the engine designer to develop the engine using first and second order analyses. When the designer is satisfied the model is suitable the third order (more time consuming) analysis can be selected. The spreadsheet program formats and writes an input file for the QSFM containing the 27 variables necessary to describe the engine. The compiled executable QSFM is then run external to the Spreadsheet program. When completed the QSFM writes a data file containing the computed data for one engine cycle. This data is then retrieved by the SEDA program and graphic output can easily be generated and edited. A full set of graphs produced by SEDA is given in Appendix C.

8.3 Heat Exchanger Optimisation

Figure 8.2 shows the general procedure used to optimise the heat exchangers for DMC 3 and DMC 5.

Twenty seven engine variables are passed to the QSFM from SEDA which define the engine and its heat exchangers, Table 8.1. This gives a possible optimisation problem with twenty seven

^h Stirling Engine Design Aid

Stirling Engine Optimization

1. Define the Problem
What are the objectives?
2. Select suitable modelling technique
which will give the objectives with suitable
accuracy whilst including all significant effects
3. Check the simulation results
Do they seem reasonable?
4. Reduce the number of variables from:
General knowledge
Literature
Previous experimentation
Manufacturing constraints
Geometry constraints
5. Perform a grid search to
ensure the optimization
starts near an optimum.
(most optimization routines
will only find a local optimum)
6. Select a suitable optimization routine
that will accommodate the function
and constraints
7. Optimize the problem
8. Check the optimization

Figure 8.2 Typical optimisation technique used to design the prototype engine.

dimensions. The variable field was reduced substantially by: previous calculations, published recommendations, manufacturing constraints, geometry constraints and the designer's preference. The variable field was reduced to six for the final engine optimisation.

There are a number of optimisation techniques generally used in engineering, Figure 8.3, but few meet the requirements for Stirling engine optimisation which is in the category of numerical, multidimensional and constrained. Some of the routines were surveyed. The following Sections report the evaluation.

A problem with Stirling Engine optimisation is that there is more than one objective function, that is, power, efficiency, volume, weight and cost all need to be optimised. To determine an algorithm to combine all the factors for all the possible objective functions would be a significant problem. An optimisation method that avoided this difficulty were sought.

Variable Number and Description	Value
1. Compression space clearance volume (cm ³) =	5
2. Compression space swept volume (cm ³) =	22.04
3. Expansion space clearance volume (cm ³) =	3
4. Expansion space swept volume (cm ³) =	25.13
5. Phase angle (degrees) =	90
6. Hot end fin gap (mm) =	0.35
7. Hot end fin width (mm) =	135
8. Hot end fin length (mm) =	50
9. Hot end fin number (mm) =	1
10. Hot fin material conductivity (W/mK) =	16
11. Hot end external heat transfer coef. (W/m ² K) =	20
12. Cold end fin gap (mm) =	0.3
13. Cold end fin width (mm) =	8
14. Cold end fin length (mm) =	40
15. Cold end fin number (mm) =	20
16. Cold fin external area (mm ²) =	0
17. Cold fin conductivity (W/mK) =	360
18. Cold end external heat transfer coef. (W/m ² K) =	15
19. Internal regenerator diameter (mm) =	42
20. External regenerator diameter (mm) =	52
21. Regenerator length (mm) =	30
22. Regenerator porosity =	0.8
23. Regenerator wire diameter (mm) =	0.04
24. Mean cycle pressure (Bar) =	10
25. Hot end temperature (K) =	1023
26. Cold end temperature (K) =	323
27. Engine shaft rotational speed (RPM) =	1500

Table 8.1 Variables passed to the QSFM. Values shown are for DMC 5

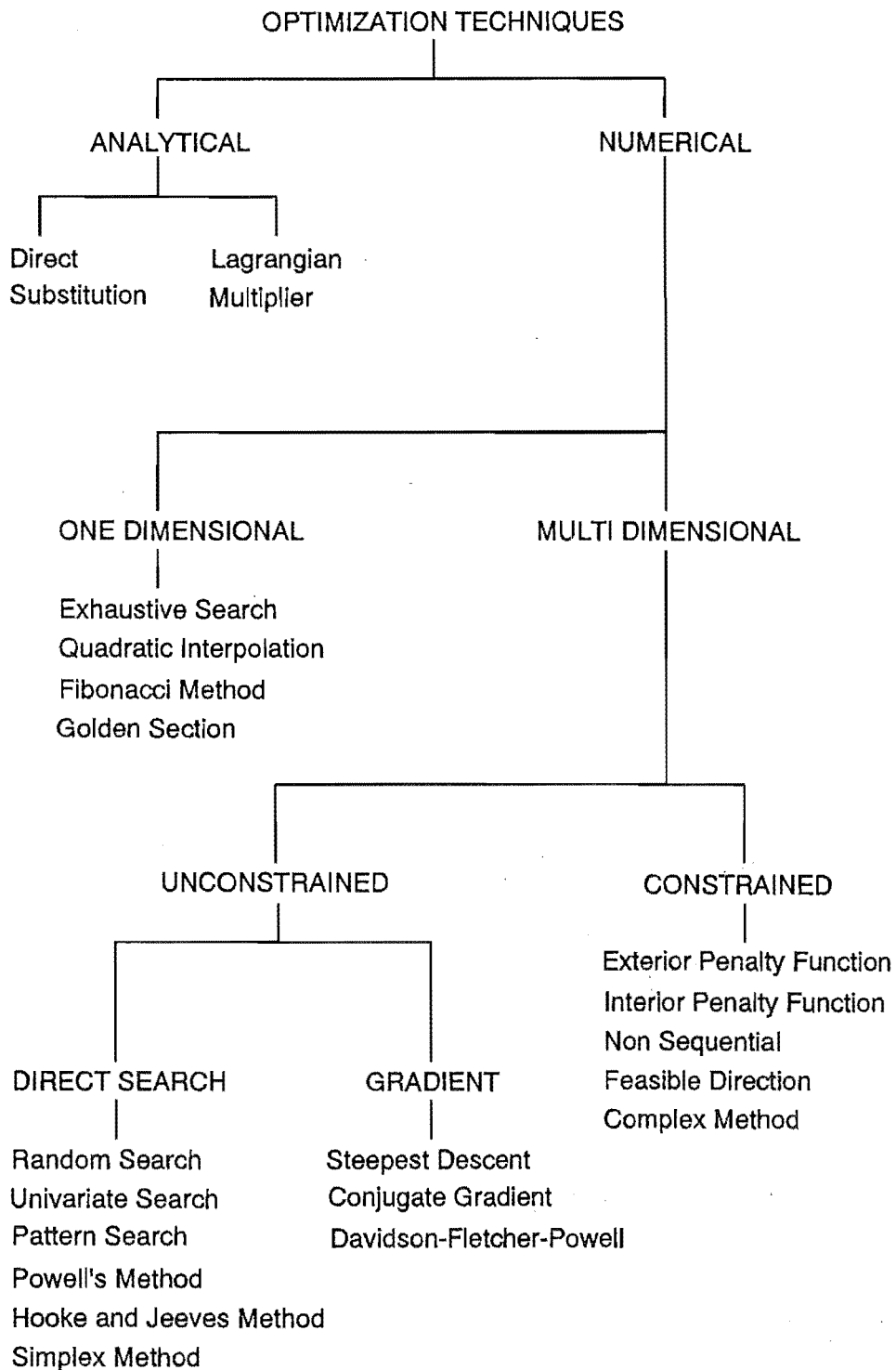


Figure 8.3 Optimisation techniques. Heat exchanger optimisation for a Stirling engine requires a numerical, multi-dimensional and constrained technique, after Venkatarathnam (1991).

8.3.1 Steepest Ascent Techniques

These techniques often follow a vector of the variables which gives the greatest change of a single objective function. It is possible, however, to optimise to a local peak which may not be the overall maximum. A routine available on the NAG Fortran subroutine set, (NAG, 1991) was tested which used this technique but was very slow and unreliable. The simple routine given in Figure 8.4 was also tested. This routine described followed a rise of engine power up to a set point then maximised the engine efficiency while maintaining the desired power. Generally when close to an optimum solution an increase of power or efficiency would result in a decrease of the other. Each variable was initially varied $\pm 20\%$ and then returned to its original value and the modified variable which produced the best result after all had been tested was modified permanently and the process repeated. When no positive change to the efficiency occurred the overall process was repeated with each variable varied by 15% and this routine was repeated until the percentage change was reduced to 1%. Figure 8.5 shows the variation of power and efficiency with respect to optimisation progression. The step changes in percentage change of the variable are very noticeable. Also note the rapid rise in engine power then stabilisation to the set point followed by a gradual increase of engine efficiency. This technique was not finally used because it only alters one variable at a time and consequently could only find a local optimum. That is, a simultaneous change of many variables may find a greater optimum.

8.3.2 Grid Search

The most reliable method of determining an optimum solution is a simple search of all possible combinations of each variable within specified limits and steps. This technique is the easiest to program, requiring only two lines of code per variable but is the most time consuming to run. Most engine development programs are of the order of months and often years before hardware is actually made so there is sufficient time to run such long programs. For example, the optimisation routine of the SEBCY heat exchangers took several minutes to program, more than a week to

Simple Optimization Technique

Only suitable for preliminary reduction

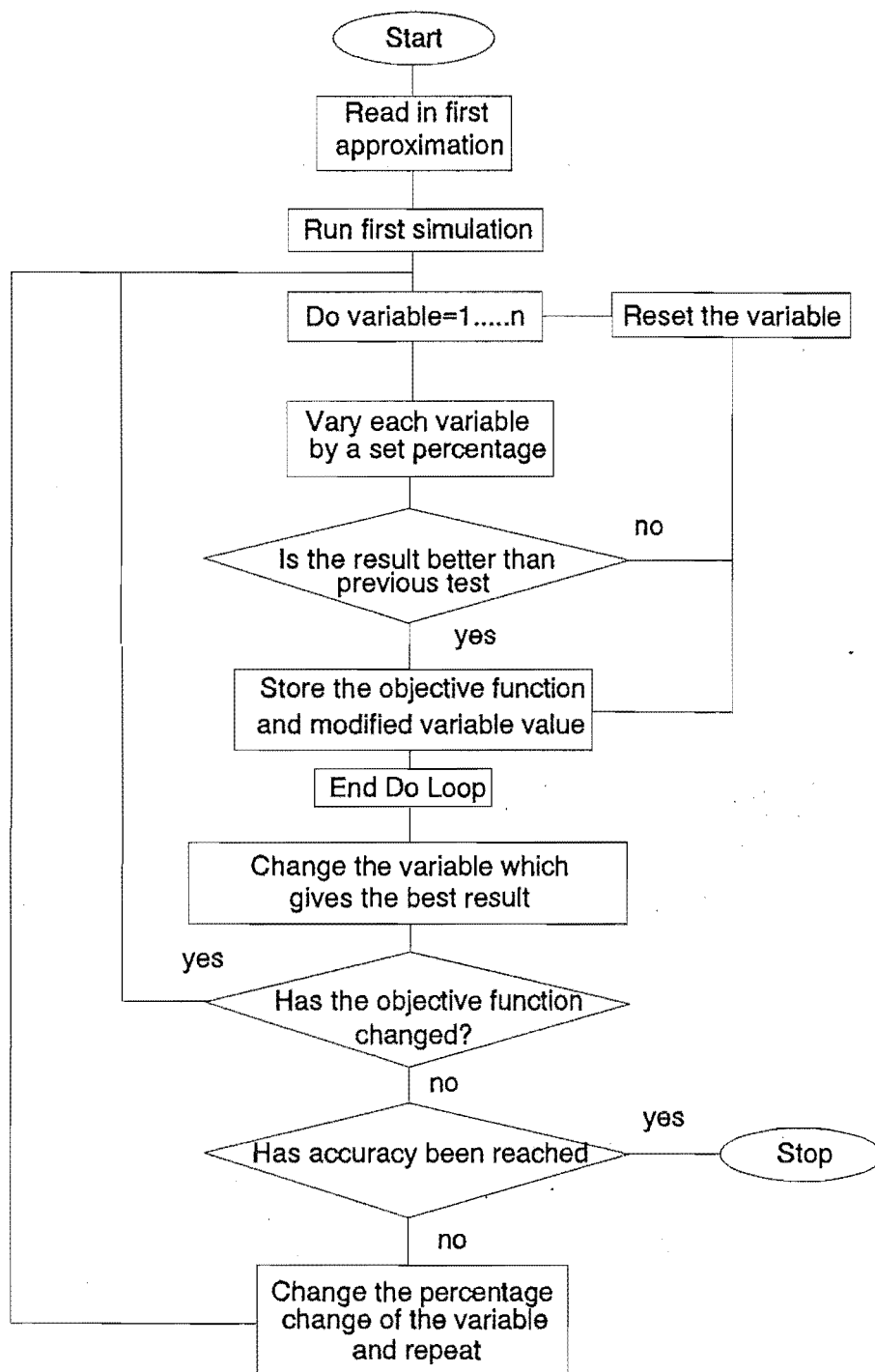


Figure 8.4 A simple optimisation technique initially developed but not used for the final optimisation.

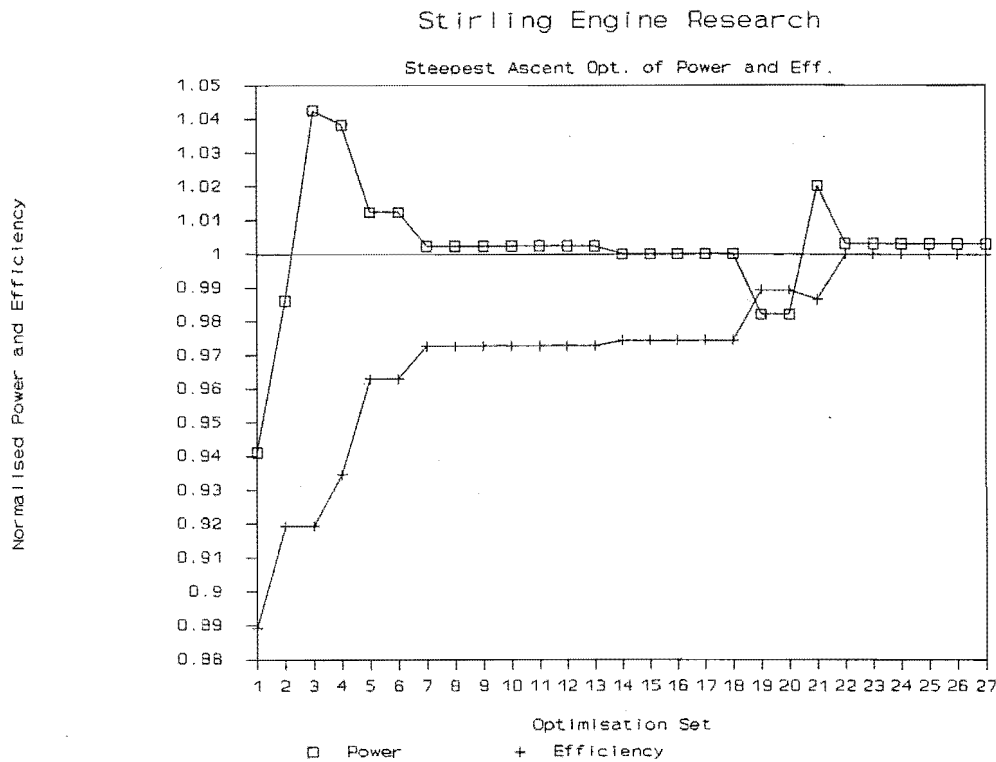


Figure 8.5 Steepest ascent optimisation. Normalised power and efficiency vs. optimisation set.

process but covered all the possible combinations and was totally reliable. The steepest ascent methods, however, took several weeks programming and testing and then several days to run and the results could not be relied on for the reasons given in Section 8.3.1. It is also possible to arrive at an absolute peak which with a small change of one variable could cause a dramatic drop of the objective function, Figure 8.6. Stirling engine design is by no means an exact science and the chance of having this one variable exact for the life of the engine may be unlikely. It is more desirable to arrive at an optimum that is the crest of a mound, Figure 8.6. The grid search technique can give many results with similar results and the designer can make a choice of which combination of variables is most suitable. This technique was finally chosen to optimise the heat exchangers.

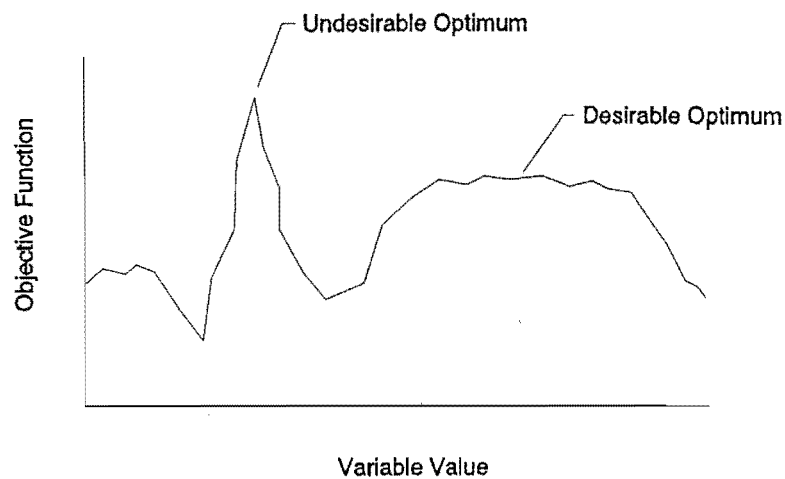


Figure 8.6 Example of desirable and undesirable optimums for a single dimension optimisation.

The several thousand results from the grid search were stored in a file and selection of the optimum was achieved by running a separate program which selected and sorted the variable combinations which gave the power and efficiency within a desired range. The optimum combination of variables was then chosen from a group of 20-30 combinations. It was found that many of the sorted combinations had similar variable combinations. This ensured that the chosen combination was on the crest of a mound. A demonstration grid search was performed and the results obtained are given in Table 8.2. In this case five variables were varied. 1296 simulations were performed which took two days to process on a VAX computer. The results shown are those that met the designers criteria as shown in the left hand column. In practice the designer would select a combination of variables, from this list, that he/she deemed suitable. The bottom two rows shows the combination that gave the greatest power and the greatest efficiency respectively. It should be noted that for maximum power the efficiency is low and for maximum efficiency the power is low.

Optimisation Criteria	Sim. Number	BP	Eff	Hot Gap	Fin Width	Fin Gap	Fin Length	Fin Thick.	
		(Watts)		(mm)	(mm)	(mm)	(mm)	(mm)	
Optimised Power and Efficiency BP > 500 W and Eff > 57.5 %	55	507	57.72	0.2	10	0.25	50	0.65	
	56	502	58.02	0.2	10	0.25	50	0.65	
	73	503	58.18	0.2	10	0.25	50	0.65	
	128	503	57.7	0.25	10	0.25	50	0.65	
	145	506	57.73	0.25	10	0.25	50	0.65	
	703	508	57.94	0.2	10	0.25	50	0.95	
	704	502	58.2	0.2	10	0.25	50	0.95	
	721	504	58.3	0.2	10	0.25	50	0.95	
	775	508	57.62	0.25	10	0.25	50	0.95	
	776	503	57.78	0.25	10	0.25	50	0.95	
	793	506	57.93	0.25	10	0.25	50	0.95	
	794	501	58.19	0.25	10	0.25	50	0.95	
	BP Max. W	289	523	55.85	0.3	10	0.25	50	0.65
Eff Max. %	378	342	64.54	0.2	20	0.35	50	0.65	

Table 8.2 Example set of results from a grid search.

8.3.3 Optimisation Verification

To verify that an optimum had been reached and that no variable change could produce a dramatic positive change in the main objective functions a separate set of simulations was run where each variable was changed between 50% and 150% at 5% intervals, (100% being the optimised variable dimension). The power and efficiency was then normalised by dividing by their respective values by the optimised power and efficiency.

By graphing these results it was possible to see if the variable was optimised and how strong the objective functions were with respect to that variable. See for example Figures 8.7 and 8.8. High and low slopes indicate strong and weak functions respectively. If the slopes of power and efficiency are not opposite, that is, not negative and positive or vice versa, then an optimum has not been reached. For example, if increasing the value of a variable would increase both power and efficiency then an optimum had not been reached. The figure for phase angle, Figure 8.7 bottom left, is of interest as it shows a distinct optimum phase angle for maximum power at 90 degrees, an increase of phase angle, however, would produce a drop in power and a gain in efficiency. The figures for swept volume, Figure 8.7 middle, are of little value in the optimisation because it is known that an increase of swept volume will cause an increase of power, it is interesting, however that an increase in the expansion space swept volume would also cause an increase in efficiency. That is, both power and efficiency curves have a positive slope. Figure 8.8 shows that in engine design, concentration to detail on the cold end can be beneficial. That is the slopes of the curves for the cold end are much steeper than the hot end figures.

8.4 Heat Exchanger Design, Testing and Simulation Verification

To test the heat exchangers and verify the simulation program a test engine DMC 3, was manufactured, Section 6.3. A sectioned view of the heat exchanger and piston design is given in Figure 8.9 and the assembled engine is shown in Photo 6.1.

8.4.1 Description of DMC 3's Heat Exchangers

DMC 3 was an alpha configuration engine with dimensions to give similar power and performance equivalent to one quarter of the final prototype engine, DMC 5. This enabled heat exchanger testing with approximately one quarter of the components to be manufactured. As the double acting engine is a combination of four alpha configuration engines the heat exchanger layout is

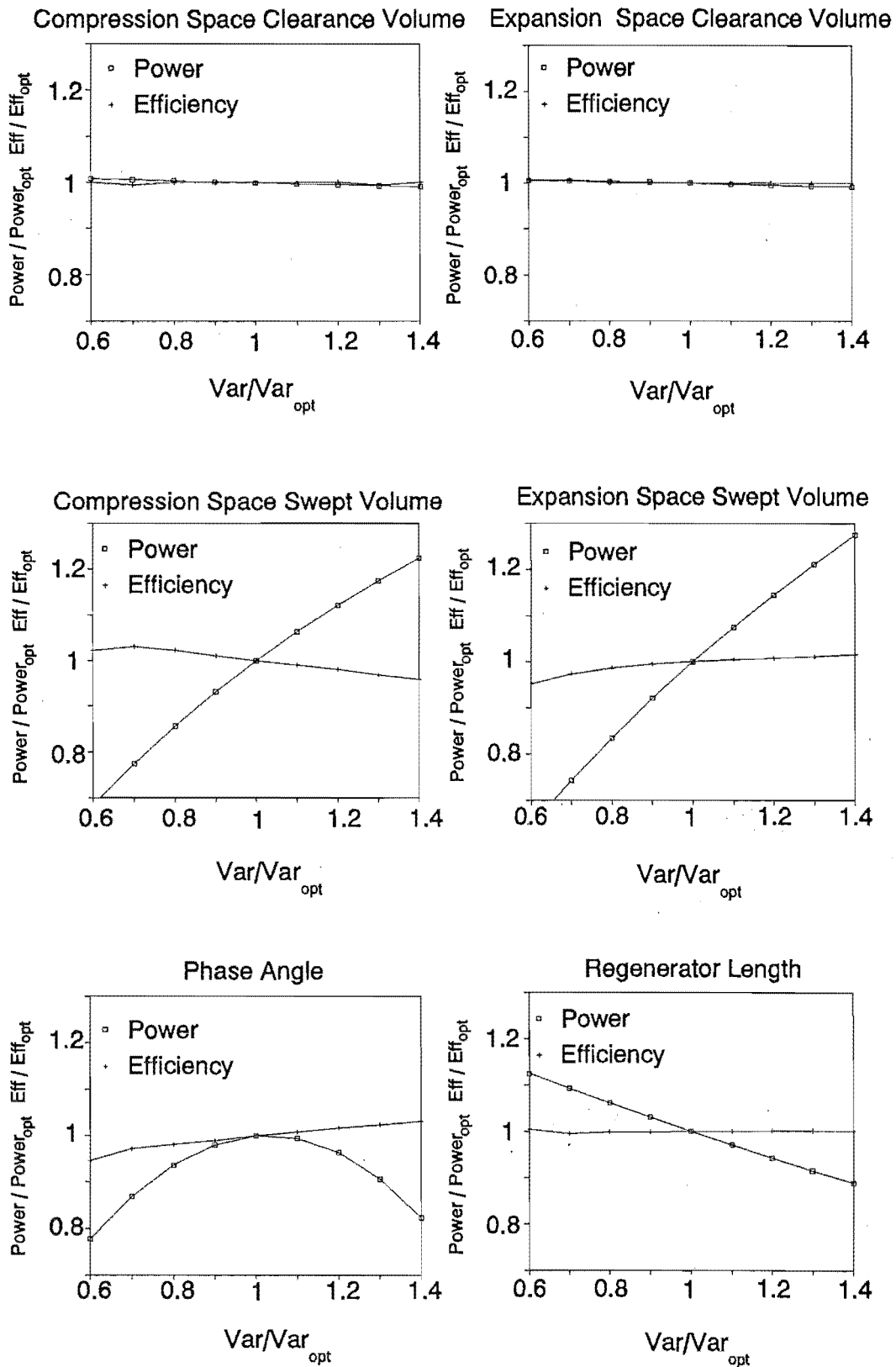


Figure 8.7 Examples of the optimisation verification curves.

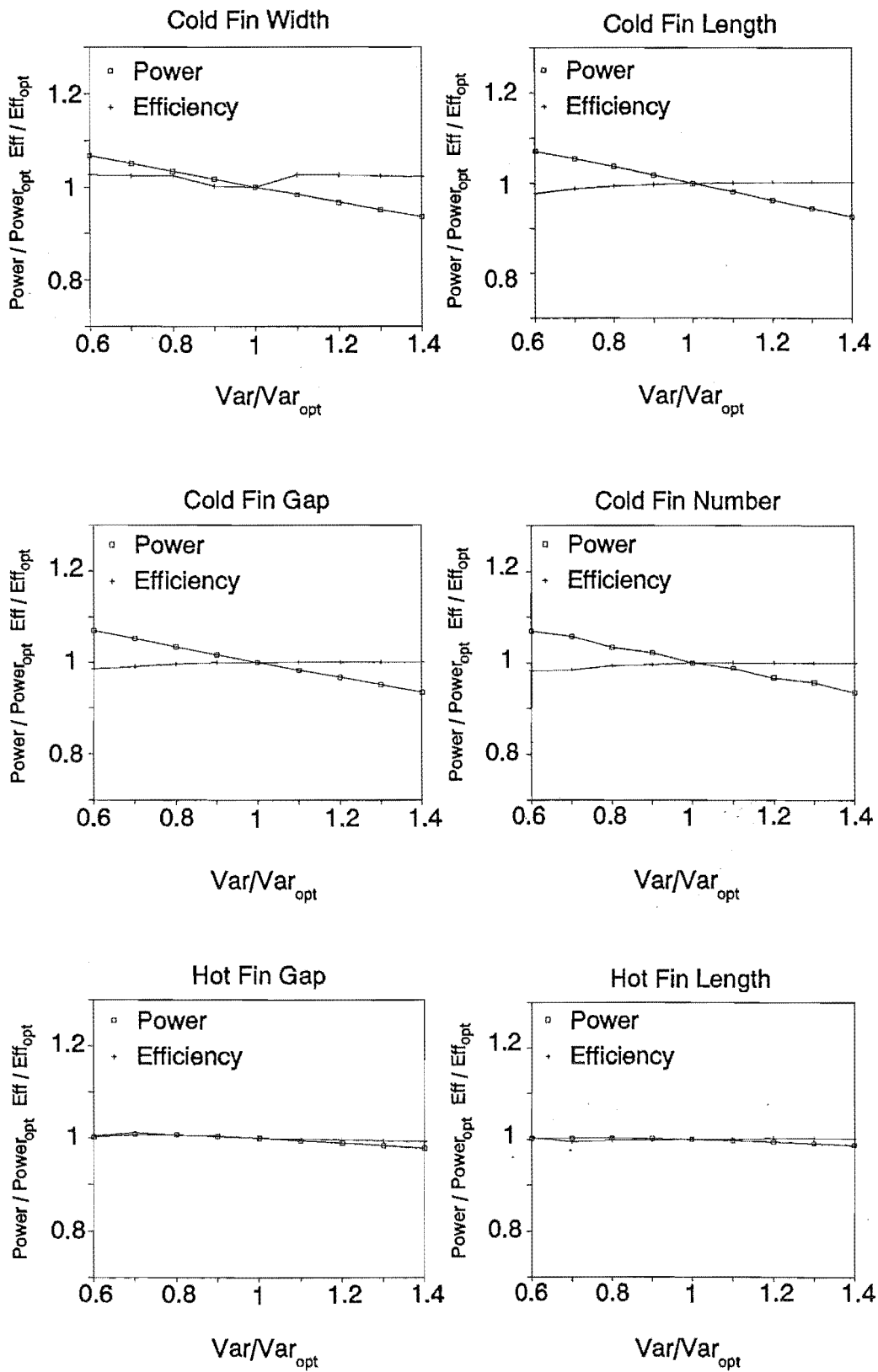


Figure 8.8 Examples of the optimisation verification curves

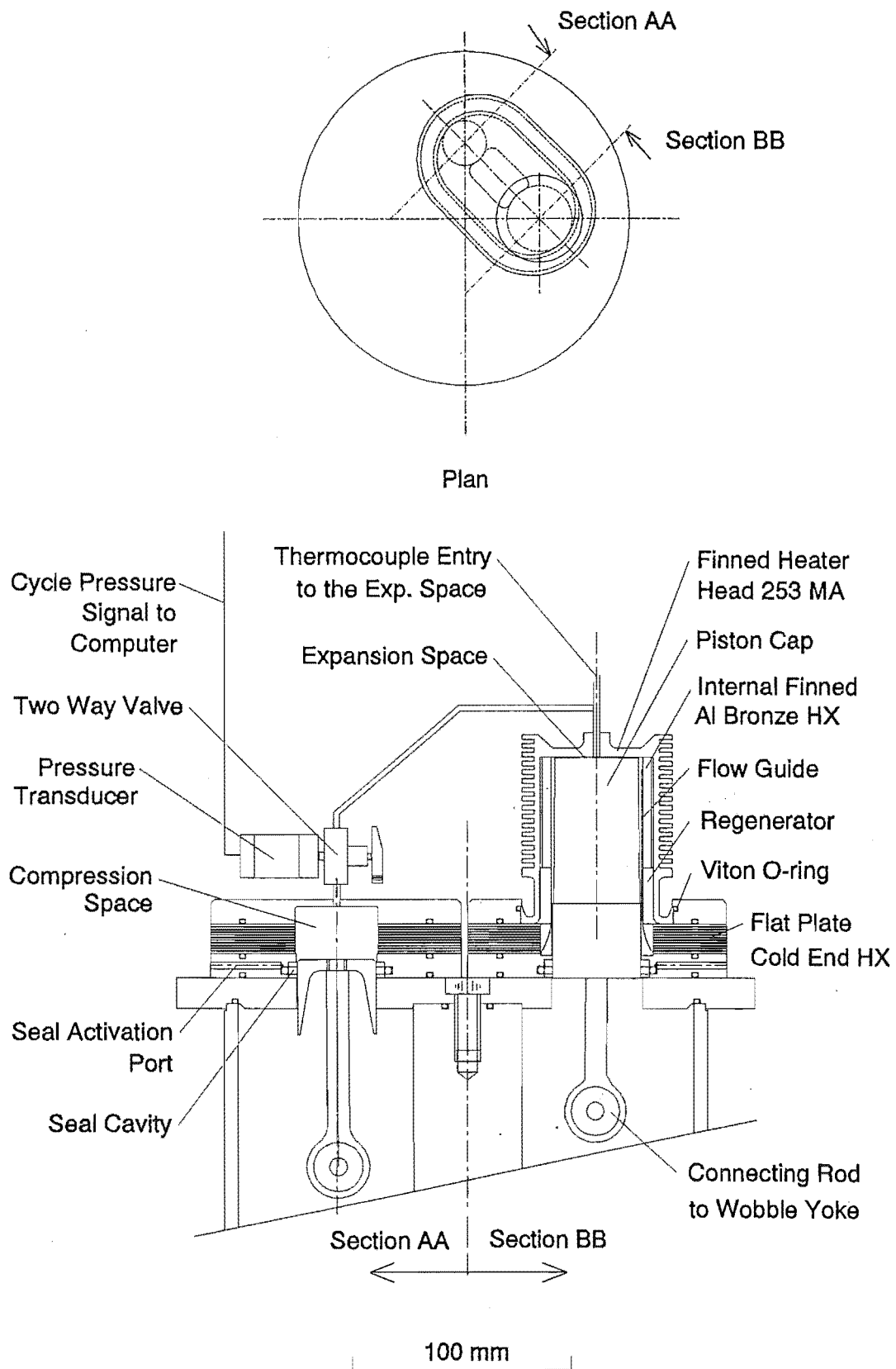


Figure 8.9 Cross section of DMC 3 heat exchangers, pistons and seal cavities.

very similar. The main difference is the lack of a piston rod seal and an additional piston seal on the compression space piston.

The heat exchangers were designed and optimised using the techniques described in the previous Sections.

The finned heater head was made from Avesta 253 MA heat resisting stainless steel, Section 4.6.2. This was circumferentially finned on the outer surface and bored parallel on the inner surface. An aluminium bronze internally finned sleeve, similar to that used by Philips (de Brey, 1947), was initially press fitted into the bore of the finned heater head to act as the metal-working fluid heat exchanger. The purpose of this was to give a high heat transfer area with a low dead volume. The fine fins were manufactured by a custom manufactured 0.35 mm thick high speed steel hack saw blade. A jig was manufactured to index and guide the blade. One hundred slots, 3.5 mm deep were cut. The press fit required to ensure a low temperature drop between the stainless steel and aluminium bronze only lasted for the first engine run. The difference of thermal expansion of the two materials caused the aluminium bronze to yield at the higher temperature and on cooling the interference was lost. To overcome this the aluminium bronze sleeve was split along the axis and the stainless steel flow guide was used to press it against the heater head.

The stainless steel flow guide ensured that the working fluid passed through the annular hot end heat exchanger and the regenerator.

The regenerator cavity was annular and easily accessible for testing various regenerator packings.

One of the design difficulties with alpha configuration engines is transporting the working fluid between the expansion and compression cylinders while incurring a low dead volume penalty. Additionally the cold end heat exchanger requires a large wetted surface area. A cold end heat

exchanger in the form of stacked plates was developed to meet both of these requirements. The copper plates were machined on a CNC milling machine to the form shown in Figure 8.10. To minimise dead volume the working fluid exhausts directly into the compression space from the heat exchanger channel. Using this manufacturing method gives considerable flexibility over the entry and exit shape to ensure low loss. This feature was not fully utilised and optimisation of the entry/exit shape would be another worthy project. A suitable jointing compound was found which enabled the plates to be assembled and disassembled to allow variation of the number of flow ducts. Two sets of plates were manufactured, one set with two working fluid ducts and the other with only one duct. This allowed various combinations giving between 12 and 24 ducts.

The piston seals were externally activated and cylinder mounted as described in Chapter 7. The compression piston was rigidly fixed to the piston rod. This was to allow examination of the effects of the slight angular oscillation of the piston caused by the wobble yoke bearing, d , following a slight arc. This was very convenient due to the piston not requiring guides. As the expansion piston was much longer the same technique was not feasible due to the increased dead volume required and the rotational inertia of the piston about the seal. Therefore a gudgeon bearing was fitted to the expansion piston. This required piston guides to ensure straight line piston motion.

8.4.2 Engine Data Measurement and Recording

The measurement of engine shaft power and piston position was described in Section 6.4.

K type thermocouples were fitted: in the combustion space, to the external finned surface of the heater head, in the expansion space, in the compression space, in the inlet water and in the outlet water. Tests were made with thermocouples in the regenerator and heat exchangers but they proved unreliable and were not used.

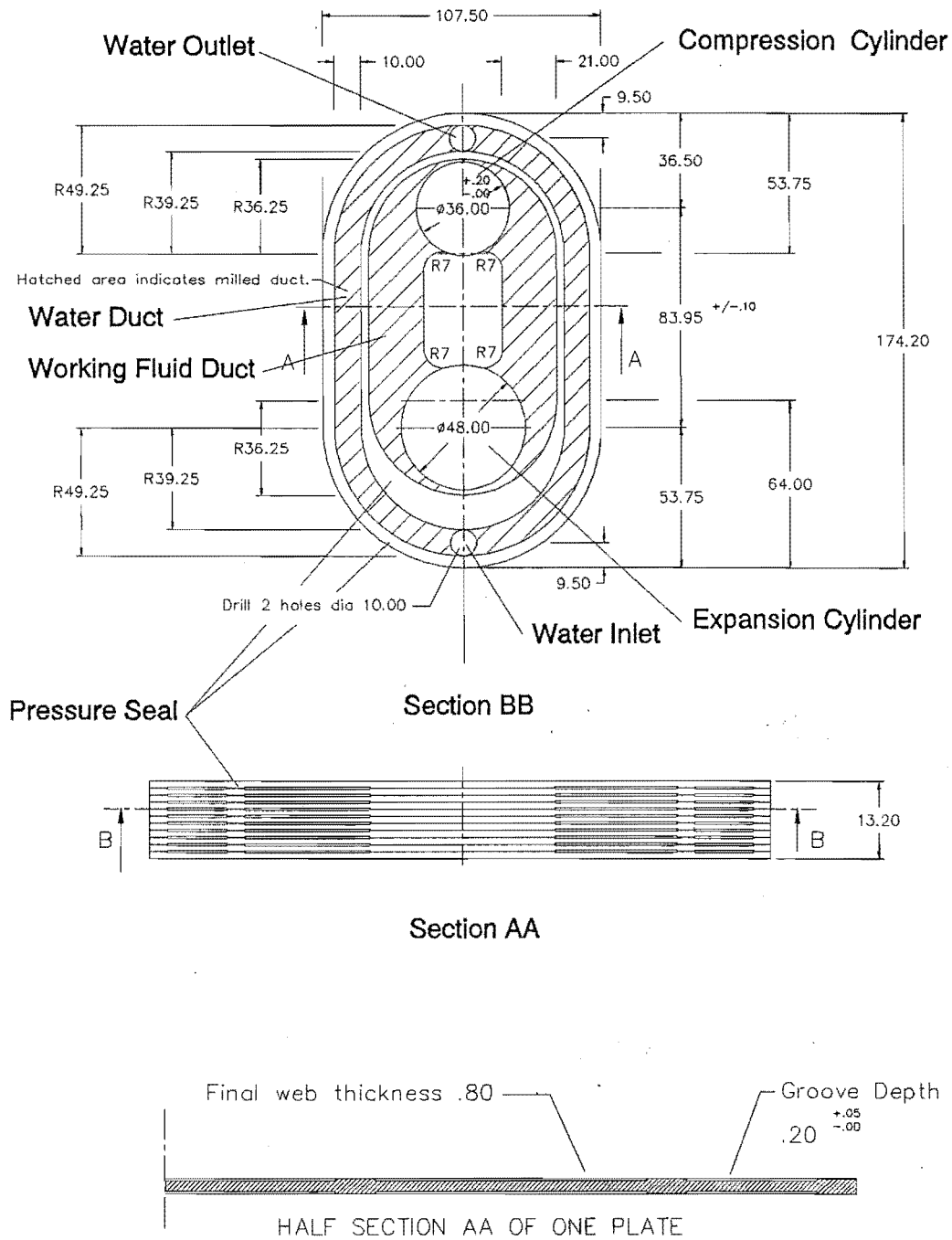


Figure 8.10 Stacked plate cold end heat exchanger for DMC 3.

Pressure regulators and Bourdon tube gauges were used to control the seal activation pressure, the buffer space pressure, the LPG supply pressure and the combustion air supply. It was desired to measure the pressure drop through the heat exchangers. To achieve this a SENSYM, (SENSYM, 1991) pressure transducer was connected to the expansion and compression space via a two way valve, Figure 8.9. When the operator was satisfied that the engine had stabilised, cycle pressure measurement was requested from the computer. The operator first set the two way valve to the compression space and the computer recorded and stored the cycle pressure P_{comp} for one shaft revolution. The operator then set the two way valve to the expansion space and the cycle pressure P_{exp} was measured and recorded. The difference between the two pressures gave the pressure drop through the heat exchangers. At the start of each engine run the pressure transducer calibration was checked.

The fuel flow rate was measured by a calibrated micrometer needle valve. Cooling water and combustion air flows were measured by gas flow meters.

Engine speed control was by adjustment of the excitation to the dynamometer. This could be done either manually or automatically by the computer.

While engine tests were being performed the computer continually monitored and displayed the shaft speed, shaft power, minimum cycle pressure P_{min} , mean pressure P_{mean} , maximum cycle pressure P_{max} and $P_{max} - P_{min}$. This enabled the operator to select the best time for recording the engine data and to ensure the engine was stabilised and operating correctly. Using this technique it was possible to set P_{mean} to within 0.1 Bar of the required pressure before taking the readings.

All readings were entered into the computer and immediately processed and stored. This enabled the operator to check the results before adjusting the engine parameters for the next measurement.

8.4.3 Results From DMC 3 Tests

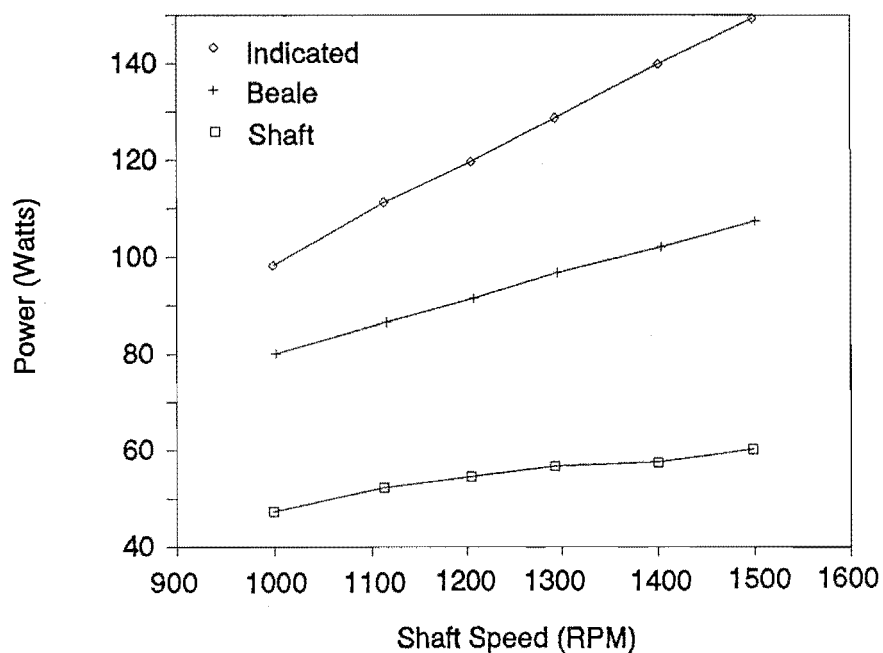
Twenty two sets of six recorded readings were taken. Reporting all these results is not relevant to reporting the development of the SEBCY so only necessary results are given below.

A typical set of readings is shown in Table 8.3 and Figure 8.11-8.12.

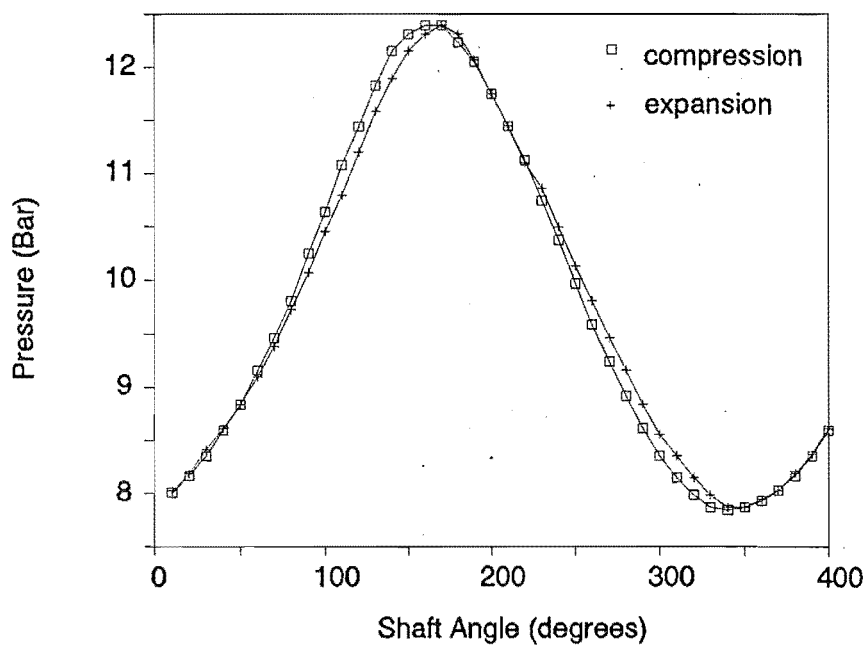
File Number	500	501	502	503	504	505
Date	31192	31192	31192	31192	31192	31192
Time	9.28	9.32	9.38	9.42	9.57	10.05
Buffer Pressure (Bar)	8.4	8.4	8.4	8.4	8.4	8.4
Ambient Pressure (Bar)	1.007	1.007	1.007	1.007	1.007	1.007
Water Flow Rate (kg/s)	0.02	0.02	0.02	0.02	0.02	0.02
Gas Mass Flow Rate (gm/s)	0.053	0.051	0.0549	.054	0.055	0.057
Air Vol Flow Rate (m ³ /s)	0.77	0.77	0.77	0.78	0.78	0.78
Air/Fuel Ratio	29.9	31.1	28.8	29.4	28.9	27.9
Exp. Seal Act Press (Bar)	15	15	15	15	15	15
Comp. Seal Act Press (Bar)	15	15	15	15	15	15
Required RPM	1000	1100	1200	1300	1400	1500
Actual RPM	998	1113	1205	1293	1401	1498
Min.Cycle Pressure (Bar)	7.88	7.94	7.92	7.94	7.86	7.88
Mean Cycle Pressure (Bar)	10.04	10.08	10.06	10.1	10.01	10.05
Max.Cycle Pressure (Bar)	12.3	12.38	12.38	12.44	12.38	12.38
Max-Min Cycle Pressure (Bar)	4.42	4.44	4.46	4.51	4.53	4.51
Shaft Power (Watts)	47.23	52.25	54.43	56.61	57.06	60.27
Torque (Nm)	0.452	0.448	0.431	0.418	0.368	0.384
West Power (Watts)	77.2	86.4	93.3	100.6	108.1	115.9
Indicated Power (Watts)	98.33	111.3	119.69	128.61	139.91	149.38
Work (J/cycle)	5.91	6.00	5.96	5.96	5.99	5.98
Work Comp. (J/cycle)	-1.51	-1.49	-1.51	-1.53	-1.48	-1.49
Work Exp. (J/cycle)	7.42	7.49	7.47	7.50	7.47	7.47
W/WE*100 (%)	79.6	80.05	79.76	79.52	80.14	80.00
Indicated Efficiency (%)	48.03	46.95	45.48	44.01	38.64	40.34
IP/Heat in*100 (%)	4.03	4.73	4.73	5.08	5.44	5.61
Carnot Cycle Efficiency (%)	73.02	73.01	72.96	73.00	73.07	73.00
Fuel Heating Value (Watts)	2440	2351	2529	2529	2574	2663
Thermal Efficiency (%)	1.94	2.22	2.15	2.24	2.10	2.26
Combustion Efficiency (%)	19.81	21.82	20.70	21.43	21.92	22.35
Burner Heat Loss (Watts)	1956	1837	2006	1987	2009	2068
Heat Absorbed By Head (Watts)	483	513	523	542	564	595
Net Thermal Efficiency (%)	9.7	10.1	10.4	10.4	9.5	10.1
Heat to Water (Watts)	-436	-460	-469	-485	-510	-534
Exp. Swept Vol (cm ³)	22.75	22.75	22.75	22.75	22.75	22.75
Comp. Swept Vol (cm ³)	17.41	17.41	17.41	17.41	17.41	17.41
Head Temperature (°C)	800	800	798	800	803	801
Exp. Temperature (°C)	800	788	783	780	786	779
Exhaust Temperature (°C)	643	638	641	628	655	657
Comb. Temperature (°C)	878	868	875	877	886	889
Water in Temperature (°C)	13.8	13.8	13.8	13.8	13.7	13.7
Water out Temperature (°C)	19.1	19.4	19.5	19.7	19.9	20.2
Fuel Temperature (°C)	20.4	20.6	20.7	20.5	20.0	19.8
Comp. Temperature (°C)	26.6	26.8	26.8	26.8	27.4	27.4
Atmos. Temperature (°C)	18	19	19	18	18	18

Table 8.3 Typical sample of recorded and calculated data from one set of results.

Note. Combustion and exhaust temperatures are low due to the location of the thermocouples

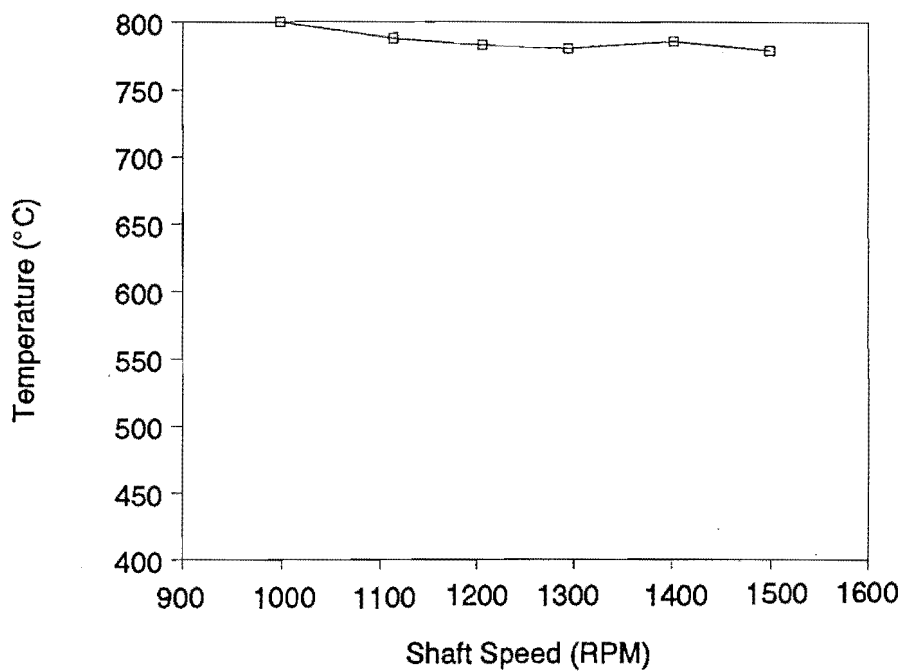


a.

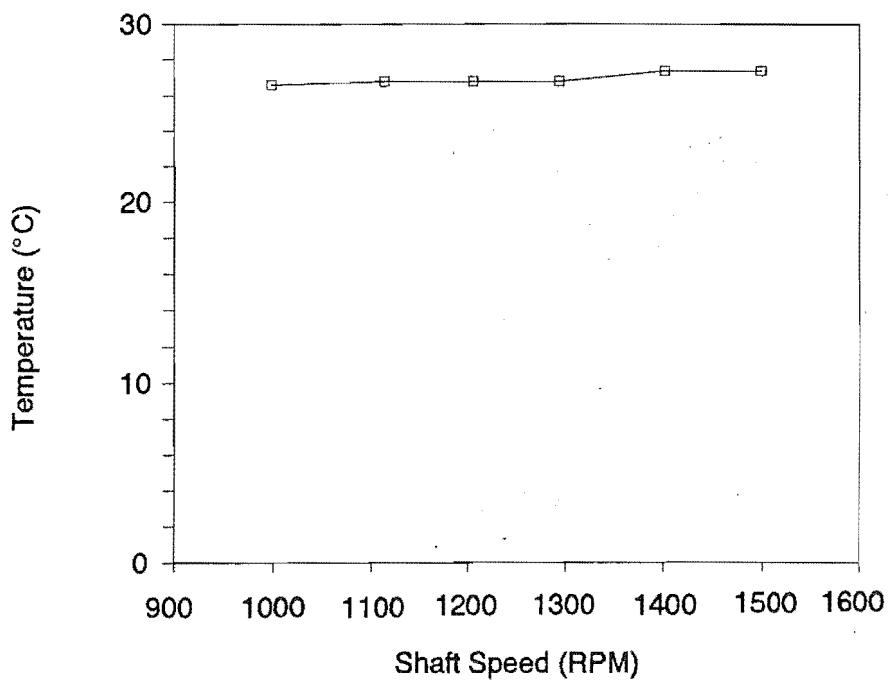


b.

Figure 8.11 Test results from DMC 3. (a). Measured indicated and shaft power compared with the power calculated by the Beale equation. (b). Compression and expansion space cycle pressure.



a.



b.

Figure 8.12 Mean expansion and compression space temperatures. Measured in the space with a thermocouple.

The results shown in Figures 8.11 and 8.12 were created during a group of tests to examine the effect of the heater head temperature. In this case the head temperature was held at 800 °C. Figure 8.11(a) shows the indicated and shaft power for 1000 to 1500 RPM. The indicated power is nearly linear. The shaft power, however, is not linear and is considerably less than the indicated power. This mainly due to the seal activation pressure being set to a level to ensure minimal leakage during the cycle. Consequently the mechanical efficiency is low due to the high seal friction. Consider though, if the mechanical efficiency were 70%, a realistic value for a small low power engine, then the shaft power at 1500 RPM would be 105 Watts. Consider also, if four of these cycles were operating, then the shaft power would be 420 Watts, which is well above the required design power of 350 Watts. During all the testing of DMC 3 the maximum continuous shaft power obtained was 109 Watts. The power calculated by the West equation, Equation 4.5, is also shown on Figure 8.11(a) for a comparison. Figure 8.11(b) shows the measured cycle pressure in the compression and expansion cylinders. The heat exchanger pressure drop was determined from the difference between the two curves. Figure 8.12 shows the expansion and compression space mean temperature over the range of speeds. As expected there was a temperature drop and increase for the expansion and compression spaces respectively. This is due to the increased rates of heat transfer causing increasing temperature drops in the heat exchangers.

Figure 8.13 shows a comparison between measured and simulated indicated power. The results are for various swept volumes which could be adjusted by the mechanism shown in Figure 6.4. A correlation factor of 0.85 was required to correct the simulation. This is often required with Stirling engine simulations (Martini, 1983). Once applied the simulation results followed the measured results surprisingly well which is a credit to the writers of the code Urieli and Berchowit.

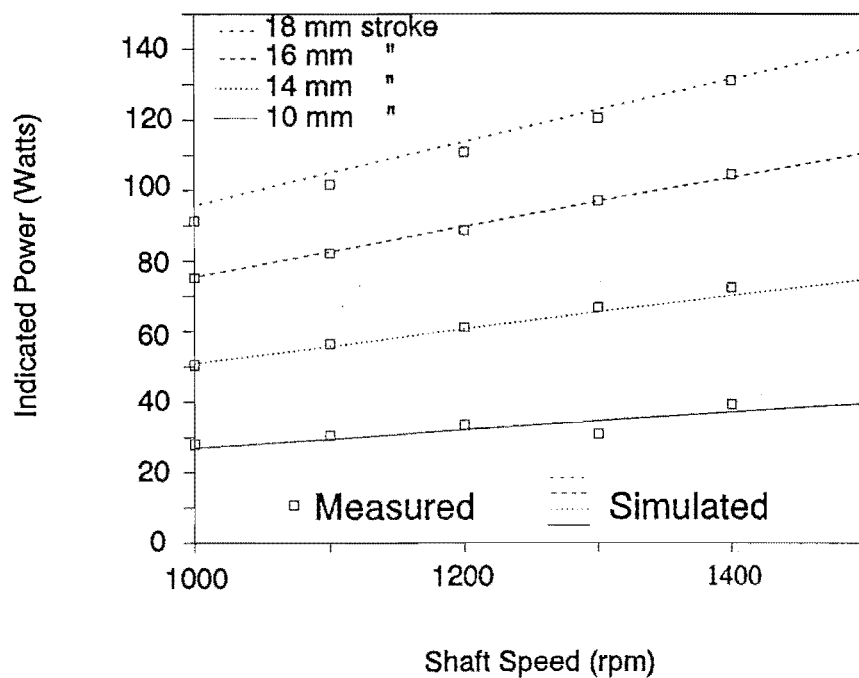


Figure 8.13 Measured and simulated indicated power for various stroke lengths.

As the engine performed so well with the fine finned aluminium bronze heat exchanger on the hot end, Section 8.4.1, Figure 8.9, it was decided to remove the finned aluminium bronze insert and replace it with another insert that would create a small concentric annular gap between it and the 253 MA heater head. If this gave sufficient heat transfer, the manufacturing costs of the hot end heat exchanger could be dramatically reduced. Creating a narrow annular passage for the working fluid, it would cause the working fluid to be in direct contact with the heated head. After simulating the performance, an insert was manufactured to allow the gap to be increased after each test. Gaps of 0.2 mm to 0.6 mm were tested. The results are compared with the finned insert in Figure 8.14. It can be seen that with a 0.5-0.6 mm gap that the results are similar to that of the finned insert. The rapid decline of power with speed for the 0.2 mm gap is mainly due to the high pressure drop.

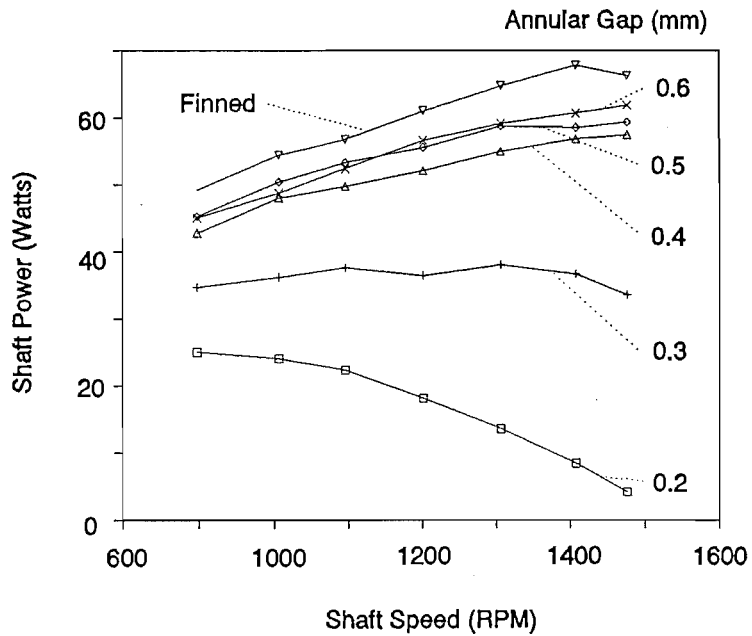


Figure 8.14 Shaft power for various hot end annular gaps compared with the finned insert.

8.5 Conclusions from Chapter 8

- While driving a mechanism designed for four pistons and with experimental equipment fitted, DMC 3 produced the desired power.
- The most reliable optimisation technique is the simple grid search.
- The QSFM compared well with the experimental results from DMC 3. A correlation factor of 0.85 was required for the indicated power.
- The stacked plate cold end heat exchanger gave good performance and could be used with confidence on the prototype engine.

- High performance was obtained from a simple annular gap hot end heat exchanger. This design is much cheaper to manufacture and more reliable than the fine finned insert. By optimising the critical dimensions this design could be made adequate for the SEBCY.
- From all tests performed on DMC 3, the best overall performance was obtained using conditions and dimensions very close to that predicted by the optimisation.

9 SEBCY Prototype Design, DMC 5.

The design solutions presented in this Chapter are a very small percentage of the possible solutions. To present all the variations investigated throughout the duration of this project would fill several volumes, so for the sake of brevity the chosen design is discussed and where appropriate, possible alternatives are compared.

Several design philosophies were adopted to make the engine easy to produce, easy to assemble and disassemble, perform the required task, marketable and be able to be manufactured using standard workshop equipment. They were:

- Avoidance of welded components, particularly in the heated zone.
- Use of O-rings on pressure joints and avoidance of the use of gaskets and gasket compounds. Use of the latter can make engine stripping and cleaning very tedious.
- Use of commercial shielded bearings to reduce manufacturing costs and to improve the engine reliability.
- Design of components with manufacturing techniques in mind. For example, where possible use castings.
- Allowance of disassembly of the mechanism and alternator while leaving the pistons and heat exchangers intact.
- Aesthetically pleasing design.
- The system should not have dangerous exposed rotating components.
- The external surfaces should be clean and free from wires, fittings or other items which look unprofessional or untidy.

9.1 Component Design

This Section describes the design features and manufacturing techniques used to manufacture DMC 5. The following begins at the bottom of the engine and works up.

The assembly and production drawings for the SEBCY prototype manufactured are given in Appendix DMC 5.

Photos 9.1(a) and (b) show DMC 5 assembled and disassembled respectively.

9.1.1 Wobble Yoke And Alternator Housing

The mechanism housing was designed to withstand internal pressurisation up to 15 bar and to hold this pressure for the life of the engine. Whilst the design pressure was 10 bar, this allowed tests to be performed at greater pressure. Since the unit was initially designed primarily for the Australasian market the Australian standard AS 1210 SAA Unfired Pressure Vessel Code, (AS1210, 19), was used to specify the minimum Sections of the housing. The New Zealand pressure vessel code was limited in terms of materials and detailed design.

LM25 (AP601) aluminium alloy with T6 temperⁱ was selected for its high strength, corrosion resistance, thermal conductivity and suitability for high volume production casting processors. This is a material which is often used in industry for similar engineered components, for example engine blocks and engine manifolds.

The alternator was shown in Section 4.4 to be around 60% efficient at maximum output (200 W electric). Hence around 150 watts needs to be absorbed and dissipated by the alternator casing.

ⁱ Solution heat treatment at 536 C for 12 hours and artificially aging at 150 C for 3 hours

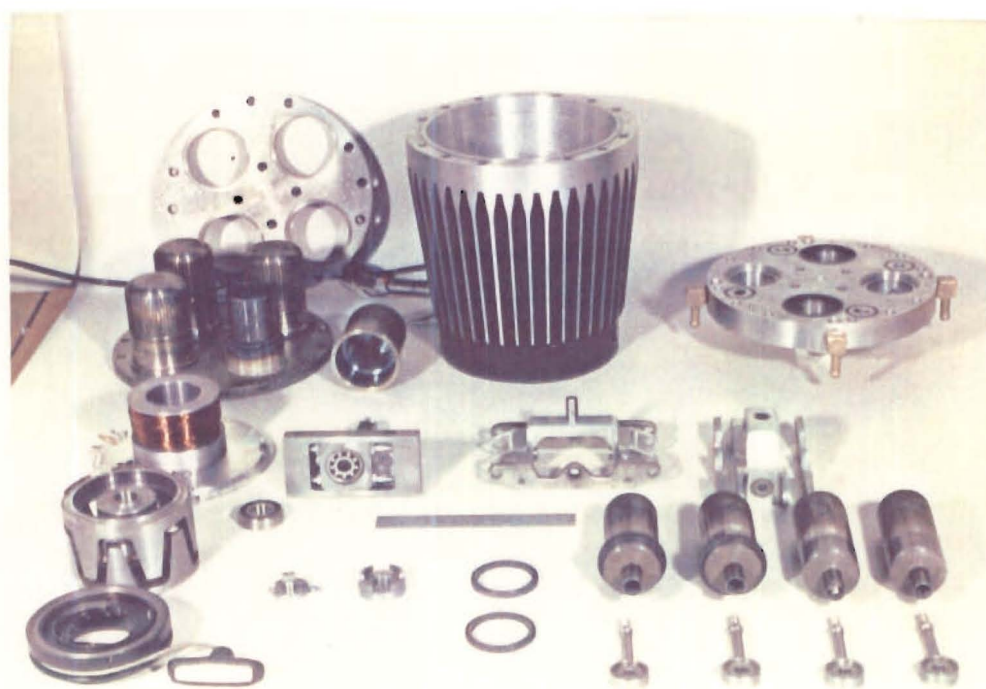


Photo 9.1 DMC 5 (a). Assembled (b). Dissassembled

(The mechanism housing was sealed and there was no flow of air through the alternator as in an automotive application). The heat generated in the alternator should be dissipated to the internal surface of the casing by convection and conduction at a sufficient rate to ensure the electronic components and bearing temperatures would not exceed reasonable temperature limits. The heat would then be transferred from the casing to the air and surroundings by radiative and convective heat transfer and to the cooling water by conduction and convection. The large external surface of the casing had to be finned to enhance heat transfer to the ambient air. Casting or fabricating fins were the two main manufacturing options. Fabricated fins were considered an added expense with the possibility of unreliable attachment to the casing. Cast fins are the cheapest to produce once the pattern has been made. The form shown in Drawing DMC 5-2 was selected for the casting. Longitudinal fins offered many advantages over circumferential fins including: natural convection, aesthetically pleasing appearance, exposed surface area, and pattern release from the sand mould. The final form of the prototype casing is shown in Photo 9.1(a). The roots of the fins were painted black and the tips left unpainted, this gives a very attractive appearance to the engine. Longitudinal fins required that the engine was mounted with the axis vertical, this allowed greater air movement, aided by buoyancy effects of the heated air. Also with the axis vertical the piston mass is not resting on the piston guides or seals. This design of housing also suits forced convection. A fan driven by an output engine shaft would blow air up the fins in the case of a direct air cooled engine, that is without a secondary cooling loop. The assumption that the 150 watts could be dissipated proved correct during the final prototype testing.

The number and depth of fins was determined from the required surface area given by Equation 9.1 to dissipate 150 Watts. For housing and ambient air temperatures of 60 and 30 °C respectively and an overall external heat transfer coefficient $h_{\text{overall}} = 20 \text{ W/m}^2\text{k}$ (Holman, 1981) between the casing and the ambient air. The required surface area was 0.208 m^2 and this area was easily accomplished by 40 fins of the geometry shown in Drawing DMC 5-2.

$$q_{diss} = h_{overall} A_{casing} (T_{amb} - T_{casing}) \quad (9.1)$$

The minimum radial wall thickness was finally specified by practical manufacturing constraints suggested by the foundry (AS1210 specifies a minimum thickness for a cast aluminium alloy of only 2.5 mm by calculation, and later states the minimum thickness of any wall should be 6 mm or greater). The heavier wall thickness, 10 mm, was selected to allow for possible radial misalignment of the mould when performing the sand casting. Other casting techniques such as shell moulding or investment casting would be preferable for production runs which would allow better dimensional accuracy and material consistency to allow the wall thickness to be reduced to 6 mm.

Photo 9.2(a) shows the successive manufacturing steps used for producing the mechanism housing. Firstly a wooden pattern was turned with ample machining allowance, Drawing DMC 5-1. A second aluminium pattern was cast from the wooden pattern. The aluminium pattern then had the fin profile machined around its periphery, Drawing DMC 5-1, and finally the mechanism housing was cast from this pattern. The large riser was used to hold the housing for machining and was finally parted off, leaving a housing without blemishes from gripping, Drawing DMC 5-2.

Before use the housing was hydrostatically tested at 20 bar.

Wiring and other ports were machined and the alternator stator was then fixed into the housing using a retaining compound Loctite 601.

9.1.2 Manual Starter

Should there be insufficient charge in the battery to perform an automatic electric start the operator would be signalled on the control panel that a manual start should be performed. For manual starting the operator must impart rotary motion to the flywheel and a design difficulty

arises due to the engine being hermetically sealed with no rotating shafts leaving the pressure shell. There are many possible designs to accomplish this and the one selected is similar to that successfully used on DMC 3 and is shown in Photo 9.2(b) and Drawings DMC 5-3 and 5-4. To operate, the user simply pulls the starter cord which rotates the shaft entering the casing driving a sprag clutch to engage the engine shaft. When the speed of the engine exceeds the rotational speed of the starter shaft, the sprag clutch will disengage and the operator should release the starter cord. The rope would then recoil. Since the starter shaft only rotates during manual starting and at low angular velocity a simple O-ring seal was found to be adequate for the dynamic housing/shaft seal. This starting system was selected for its simplicity, ease of operation, single handed reliable operation, and compact layout. A magnetic drive is another possibility. Similar to that used on magnetic drive pumps, this would allow a completely hermetically sealed unit. The extra mass, volume and complexity of such a system was considered unnecessary in this case. The Philips 1002C engine used a rope starter but required the operator to wind on the rope. This was considered inappropriate for this engine and a recoil rope starter was designed. The clock spring rewinds the rope after use, Photo 9.2(b). This system proved to be very effective and very easy to use.

9.1.3 Alternator

For low manufacturing costs, a standard automotive alternator could have been used. The standard aluminium alternator casings would have to be replaced to allow convenient mounting in the mechanism housing and the integral voltage regulator and brushes would have to be replaced. The stationary field coil design, Figure 3.7, eliminates the need for brushes and slip rings providing the following advantages:

- It has less friction loss.
- It gives no arcing from slip rings. This can cause radio interference and could ignite accumulated fumes in the mechanism housing.

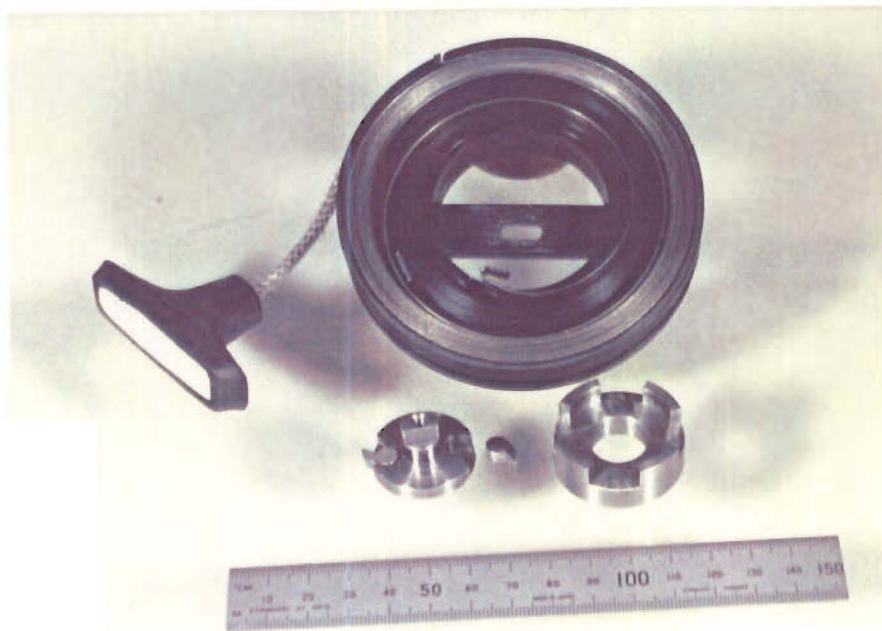
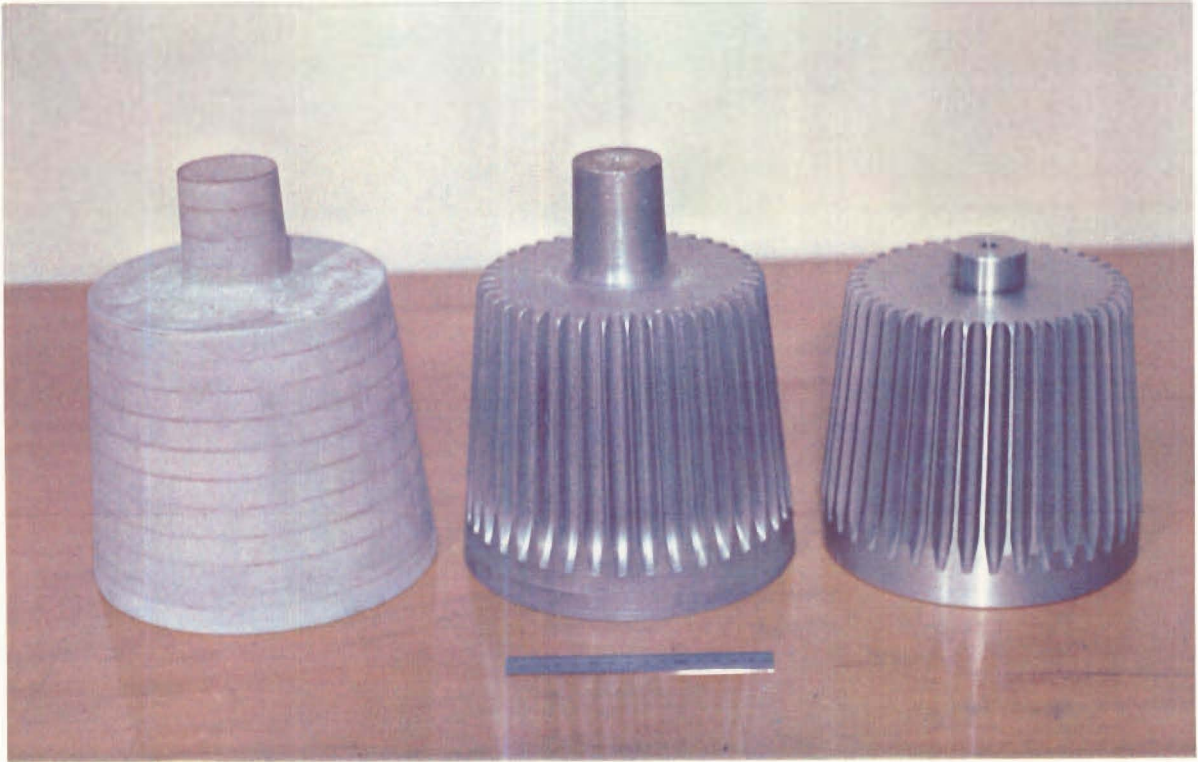


Photo 9.2 (a). Manufacturing steps of the mechanism housing. Left to right, wooden pattern, aluminium pattern, finished housing. (b). Recoil manual starter components.

- It has no brushes which could wear and require maintenance.
- It gives off no abrasive dust from wearing brushes.
- Brushless alternators are preferred by yacht owners and selecting this type would aid marketing.

There are also several disadvantages with using the stationary field coil alternator, these include:

- There are extra air gaps for the magnetic flux to pass through. Due to requiring greater excitation current to maintain the magnetic field strength, the alternator efficiency is slightly reduced.
- The required machining tolerances are tighter. This increases the manufacturing costs.
- The requirement of small air gaps between the stationary and rotating components causes greater aerodynamic loss.

Despite these disadvantages, the stationary field coil alternator was selected as it met safety and reliability criteria. Photo 9.3 shows the manufactured alternator components.

9.1.4 Alternator Stator

Development and manufacture of a new stator was not desirable for cost and tooling reasons. A standard Bosch U-KK-14V 30/70A alternator stator was used since it met the electrical requirements.

9.1.5 Alternator Rotor

Ideally the rotor components should be made from a steel with high magnetic permeability such as a silicon steel but a suitable grade was not readily available at the time of manufacture. BS 1020 steel (Commercial Bright) was the closest substitute. To enhance the permeability of the BS 1020 steel the components were rough machined annealed and then finished. The North-South poles are joined by a non-magnetic ring, Drawing DMC 5-6. In an alternator with slip rings the poles are joined by the rotor shaft, Figure 3.5.

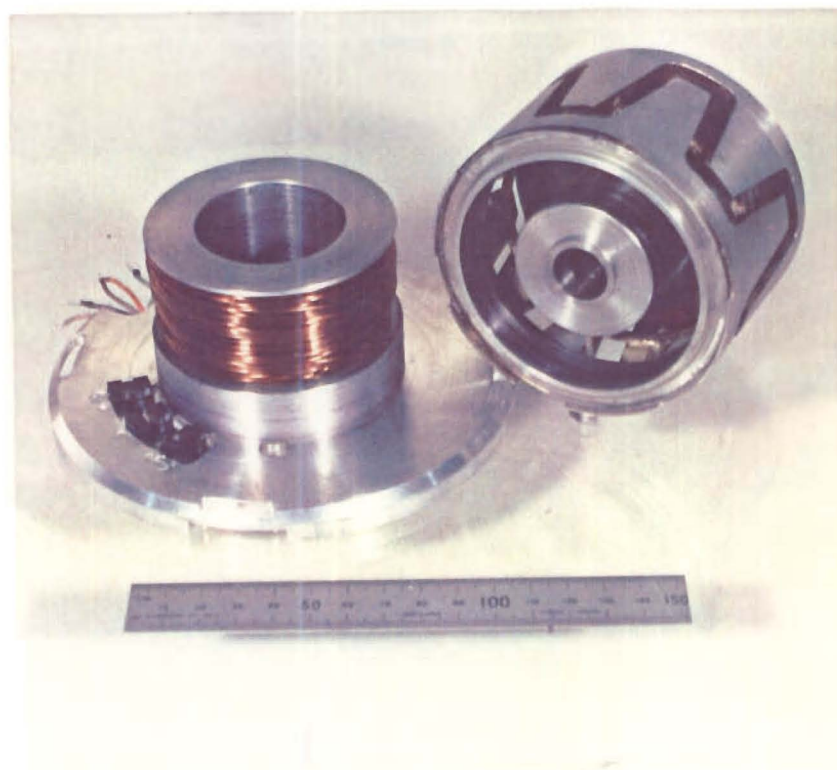
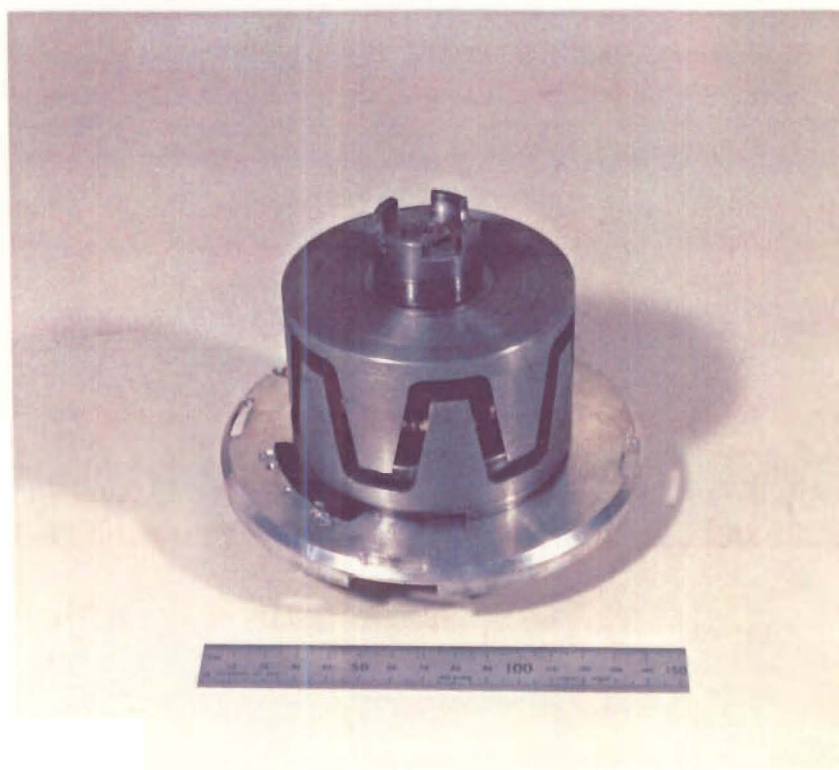


Photo 9.3 Alternator components. Top assembled, bottom disassembled.

9.1.6 Alternator Field Coil

This is simply a coil of copper wire wound onto the field coil carrier, Drawing DMC 5-5. The magnetic flux generated by the coil passes through the field coil carrier, poles and stator.

9.1.7 Driveshaft

The alternator shaft is also the driveshaft of the engine, this makes the engine more compact, more reliable and reduces the number of components.

Connecting the wobble yoke eccentric bearing to a standard automotive alternator shaft, in such a way as to allow easy disassembly and a compact engine, posed several difficult design problems. This was another reason for manufacturing a new stationary field coil alternator.

The driveshaft, DMC 5-9 was fabricated from BS 4140 steel bar and a rectangular mild steel block. This block was recessed for the eccentric wobble yoke bearing and mounting pads for the balance weights were machined on its side faces.

9.1.8 Driveshaft Bearings

The two driveshaft bearings were 6003.2ZR, (FAG, 1984), shielded ball races. The upper bearing is sandwiched between the base plate and the field coil carrier. This bearing supported both radial and axial shaft load. The lower bearing fitted into the housing with axial freedom to allow for axial misalignment and thermal expansion of the assembly.

9.1.9 Eccentric Bearing

As shown in the previous Chapters, swept volume variation is desirable for engine power control. Whilst this was not necessary for the SEBCY, provision was made to adjust the swept volume manually. The DMC 5 eccentric bearing was a self aligning double row ball race, 1200 TV (Fag,

1984), which was mounted at the required angle in a rectangular collar which fitted the recess in the drive shaft, Section 9.1.7. The recess was machined to allow the bearing position to be manually adjusted by four screws to set the engine swept volume (within the limits of the angular misalignment of the self aligning ball race). For production units, a shielded deep groove ball bearing would be fitted directly into the driveshaft at the required angle to reduce manufacturing costs.

9.1.10 Driveshaft Lock Nut

The driveshaft bearing inner races and alternator rotor were clamped to the shaft by a lock nut which also served as the dog for the manual starter clutch, Photo 9.2(b), Drawing DMC 5-4.

9.1.11 Base Plate

The three slotted optical switches, SOSs, required for the electric starter were mounted into the base plate, Photo 9.4(a), Drawing DMC 5-11. The alternator rotor had six slots suitably machined around its periphery which activated these switches. The switches and slots were positioned to ensure that at any driveshaft angle only one switch was on. The base plate was mounted to the mechanism housing by 4 cap screws. The screw holes in the base plate were circumferentially slotted to allow timing the switches to the stator. For production engines the rectifier diodes would also be mounted on the base plate. For experimental reasons the diodes and starting FET's were mounted externally on DMC 5. This required that the wires from the stator, slotted optical switches and excitation field windings all had to pass through the pressure wall. To seal these wires through the housing wall Devcon Epoxy resin was used. This worked well during engine testing and was much simpler and more compact than the system used on DMC 3, Figure 6.6.

9.1.12 Wobble Yoke, General.

On first inspection, refer Photo 9.4(a), the wobble yoke appears complex and difficult to manufacture. However, when the wobble yoke is broken down into its individual items, Photo

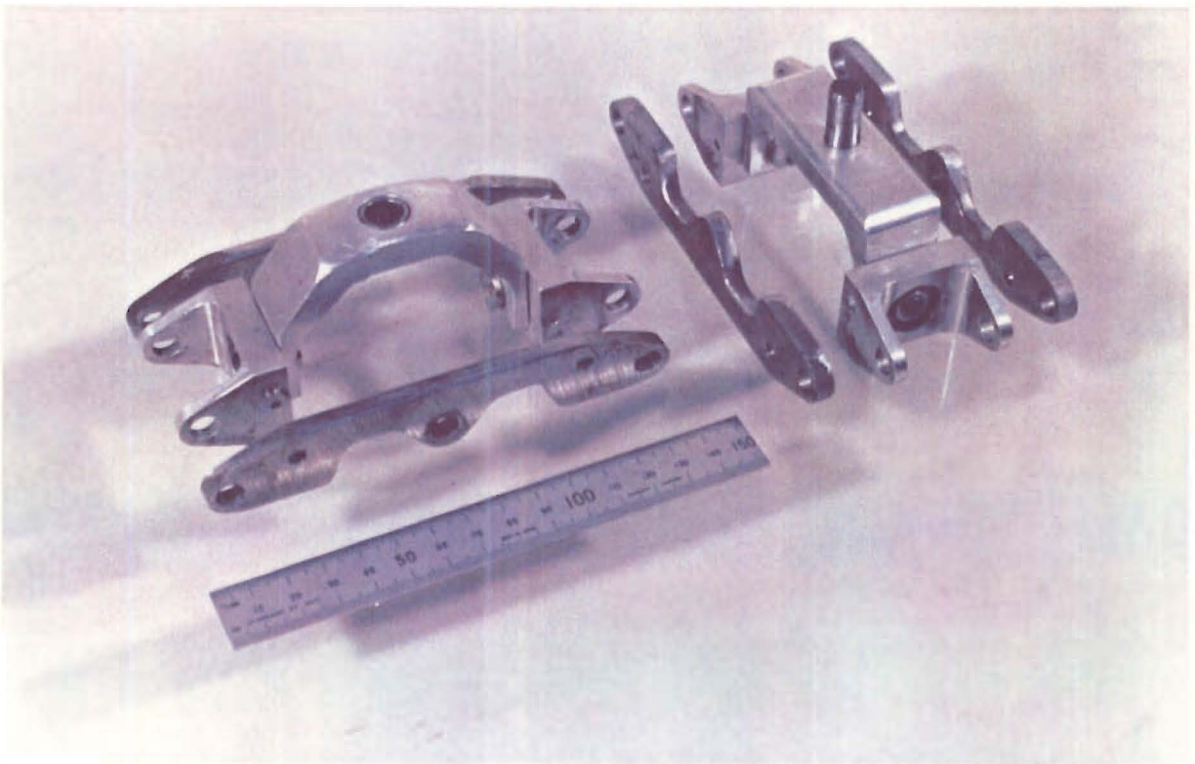
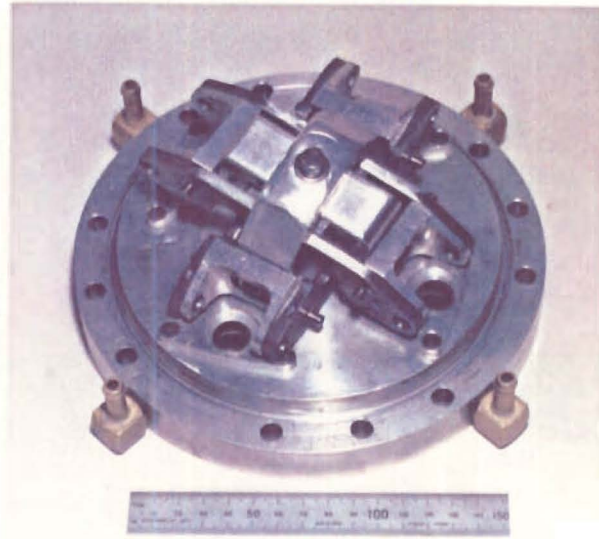


Photo 9.4 Wobble Yoke. (a) Assembled. (b) Disassembled

9.4(b), it can be seen that it is suitable for both small number and mass production techniques, with each giving equivalent performance. The manufacturing facilities available dictated the design chosen for DMC 5. One bearing size was selected for all the main wobble yoke bearings. This has the advantages of only having to carry one stock item, bulk purchasing price reduction, and one machining dimension for the bores and shafts. These advantages reduce the overall manufacturing costs.

The bearing size selected, 608.2ZR, (FAG, 1984), was based on the highest loaded bearing which is bearing, c, Figure 5.3. As the bearings only have small angular oscillations, $> +/- 10$ degrees, the static load rating, C_o , for the bearing was used, (FAG, 1984).

9.1.13 Wobble Yoke Nutating Pin

The nutating pin was made from hardened and tempered BS 4340 steel. The pin was pressed into the upper yoke and acted as a needle roller bearing journal for the lower yoke, Section 9.1.14. A tapered lead was machined on the lower end of the pin to aid assembly of the wobble yoke and heat exchanger unit to the mechanism housing and eccentric bearing.

9.1.14 Wobble Yokes

The yokes were machined from aluminium 5251 flat on a CNC mill, Drawings DMC 5-14 and 5-15. The beam-yoke bearing, (bearing, c, Figure 5.3), was mounted on the inner side of the connecting rod bearing (bearing d Figure 5.3). This gave a compact mechanism design and a greater pitch radius of the cylinders. The latter is advantageous by: giving low wobble yoke angle, giving low piston side load, and allowing a suitable cold the end heat exchanger design. The lower yoke had a needle roller bearing fitted which runs on the nutating pin, Section 9.1.13, giving the required degree of freedom between the two yokes. A plain bush was initially tested in this location, but it produced a slight tapping noise at high engine load. The needle roller bearing gave no further problems.

9.1.15 Wobble Yoke Beams

Each of the two beams were fabricated from two side plates and two end blocks. The two beam side plates were initially machined from 5 mm thick aluminium 5086 H32 flat on a CNC milling machine, Drawing DMC 5-12. One of these beams failed by fatigue failure after 15 hours running, Section 9.3.4. They were subsequently replaced with 6 mm thick medium tensile steel BS 1040. It is recommended that optimisation of the beam material and shape should take place before production begins. There are many ways to produce the beams and the option selected depended on the manufacturing methods which were available. The two beam sides are identical for both yokes so only one setup was required and a mass production technique such as stamping could be used. The ends of the four beams were also identical, Drawing DMC 5-13, so again a mass production technique requiring one setup could be used. Alternatively, the complete beams could be cast and machined. Again the two beams are identical, requiring only one mould and one setup for machining.

9.1.16 Wobble Yoke Pivot Block

This part supports the main wobble yoke pivot bearings, b, Figure 5.3. In a production engine this would be cast with the cylinder block in one item. For the DMC 5 this part was manufactured from aluminum square bar, Alloy 6005, and was fitted to the cylinder block by one M10 cap screw, Drawing DMC 5-16. This pivot block takes the engine torque reaction so a matching square recess was machined in the cylinder block which keyed the pivot block in the correct orientation to the cylinders.

9.1.17 Cylinder Block

This was machined from solid aluminium bar, Alloy 2011, for the prototype but would be cast for production engines. As the seals are cylinder mounted the cylinder walls did not require special wear resistant coatings or finishing. All static seals are O-rings to allow easy dismantling and reassembly during engine testing. Ten M8 cap screws, around the engine periphery, joined the

heat exchangers, cylinder block and the mechanism housing. Four more M8 cap screws, in the centre of the engine join the heat exchangers and cylinder block. This arrangement allowed the heat exchangers and cylinder block to be removed from the mechanism housing while still joined. 10 mm diameter ports are machined to the bottom of each cylinder which act as the working fluid transfer ports, Drawing DMC 5-18. This added dead volume to the engine, and was a required detrimental compromise for using cylinder mounted seals, and the flat plate heat exchanger on a double acting engine design. This port was not required on DMC 3, an alpha configuration engine. A pressure relief valve was also designed into the cylinder block.

Cooling water ports in the cylinder block provided the connection between the water supply/return tubes and the flat plate heat exchanger. The four fittings shown protruding from the cylinder block, Photo 9.4(a), would be replaced by four tubes fitted into the housing cooling fins to give a clean exterior to production engines.

Space is available in the cylinder block for a small cycle pressure driven diaphragm pump for circulating the cooling water. This, however, was not fitted in the DMC 5 engine.

9.1.18 Piston Seals

A single lip type seal manufactured from 20% carbon filled PTFE was fitted to each cylinder. On starting the engine would run for 10 - 300 seconds and then stop. It was discovered that the lip was increasing in temperature and expanding off the piston. This caused massive seal leakage and the engine would stop. Resting for several minutes the seal would cool and shrink onto the piston again, allowing the engine to be restarted. A thin aluminium ring was later fitted around the lip of the seal, this prevented the lip expanding off the piston. The improvement in engine performance was astonishing. This technique would not be suitable for production. It is intended that a garter type spring would be used as shown in Figure 7.5.

9.1.19 Pistons

Using cylinder mounted seals, the piston need only be a cylindrical shell, Drawing DMC 5-19. Being of a double acting design, there is also the requirement for a piston rod seal. The piston rod displacement at bearing, d, Figure 5.3, was only 0.4 mm off the line of stroke therefore the piston side loading was negligible and the angular displacement of the joint, f, Figure 5.3, was less than one degree. This allowed a flexure joint between the piston and connecting rod to be used, Section 9.1.21. Because the connecting rod oscillated slightly an extension to the piston was designed to run in the rod seal. This created another important advantage of the cylinder mounted seals: due to the fixed distance between the rod seal/guide and piston seal/guide the piston was very stable despite the slight moment caused by the piston-connecting rod flexure joint. The top end of the piston requires heat resistant material and the lower end wear resistant. For this reason the piston cap was made from a suitable grade of stainless steel and filled with a light castable insulation material. The wall of the piston cap was very thin, 0.5 mm, to reduce longitudinal thermal conduction. The piston inner cavity was vented to the mechanism housing to reduce the pressure differential across the thin wall. The piston cap was fixed into the piston base with Loctite 601, a high temperature retaining compound. The piston base-piston cap lapped joint was designed to withstand the longitudinally induced shear by the pressure difference between the piston inner and the expansion space. This joint gave no problems during engine testing.

9.1.20 Rod Seal

The rod seals were similar in design to the piston seals, although their operation is slightly different. The rod seals should act as a pumping ring to increase the mean cycle pressure. Therefore when the cycle pressure is lower in the compression space than the mechanism housing pressure, the seal should leak. An O-ring was fitted to prevent leakage around the back of the seal.

9.1.21 Connecting Rod-Piston Flexure Joint

Many bearing joints were examined but few met the design requirements, these were:

- The piston had to be assembled to the connecting rod from above the cylinder block, after the piston base was assembled to the piston cap. This did not allow access to the piston base or piston interior during assembly.
- The joint had to accommodate a displacement of the lower connecting rod bearing d (Figure 5.3), of 0.4 mm from the line of stroke. Therefore, the longer the connecting rod, the less the angular displacement required of the flexure joint. The length is, however, limited by the overall size of the engine and the temperature that the flexure joint can operate. (The temperature of the top of the piston cap is close to the expansion space temperature. Heat will be transferred down through the piston and the joint used must be resilient to this high temperature environment).
- The joint must be cheap to manufacture.

The design chosen is shown in Drawing DMC 5-19. The joint is essentially two Viton O-rings held between two collets which are attached to the connecting rod. The upper collet had a female thread to match the connecting rod and was held to the piston by two bend over tabs, thus the upper collet was fitted to the piston prior to the piston cap being fitted. With the connecting rod in place in the cylinder and the lower collet and O-ring on the connecting rod the piston was lowered onto it and screwed until the collets locked. This system worked very well and was very easy to assemble. The O-rings were made from Viton to withstand the high temperature in the piston cavity. During the engine testing one O-ring failed but this was due to misalignment during assembly.

9.1.22 Cold End Heat Exchanger

Like DMC 3 this engine has a stacked flat plate heat exchanger. The manufacturing method was, however, quite different. To mechanically machine 10 plates each of 0.9 mm thick copper would be very time consuming and costly. A manufacturing method was required that did not require expensive tooling, such as press tools. Chemical machining was an obvious choice. A local printed circuit board manufacturer was found who had suitable equipment and was employed to produce the plates. The procedure was as follows:

1. A full size photographic image was made of Figure 9.1.
2. This image was used to apply the Photo-Resist material to the square 0.9 mm thick copper plates on both sides.
3. A chemical etchant was evenly sprayed on the side of the working fluid and cooling water passages at different angles until the correct passage depth was obtained, 0.35 mm.
4. The plates were then inverted and sprayed on the reverse side which had only the shape of the through holes exposed. This was continued until all holes and outer shape had broken through.
5. The Photo-Resist was scrubbed off the plates.
6. The plates were tinned to prevent corrosion and enable reliable assembly of the plates.

This process took the plain copper squares and produced a heat exchanger plate free of burrs and did not require any form of finishing, Photo 9.5(a). Whilst the process was expensive for this one-off operation, automation and considerable cost reduction is feasible.

The plates of the DMC 3 engine were able to be sealed using Silicon based sealant, as all pressure joints were adequately clamped. To obtain suitable flow paths, the pressure joints of the DMC 5 engine could not be adequately clamped and adhesive jointing was required. Many gasket compounds were tested, but all failed. A solder cream is manufactured for surface mounted

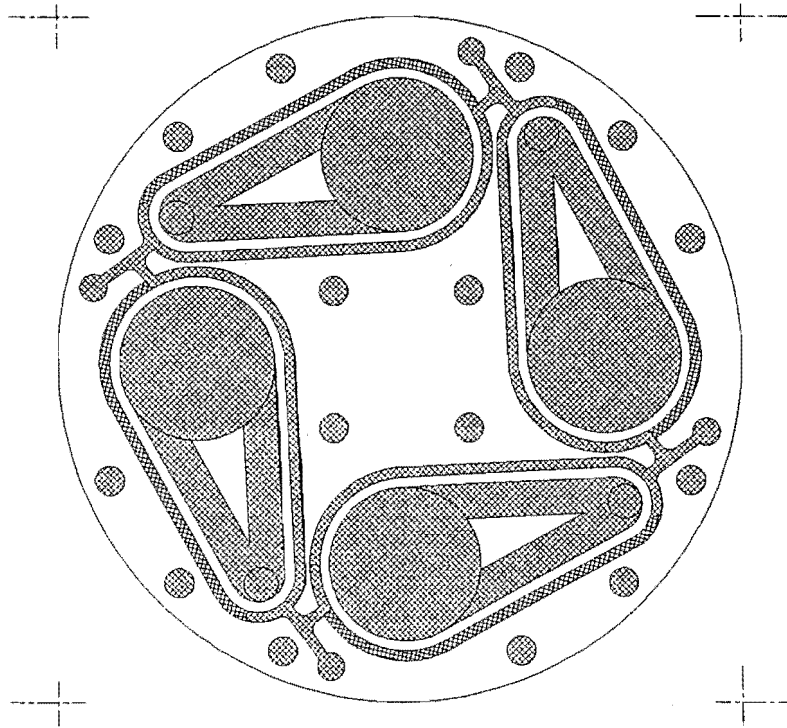


Figure 9.1 Pattern used to create a photographic image, hatched areas were blackened.

components in the electronics industry. This material is a paste which has small particles of tin, silver, and lead emersed in a flux. This solder paste was screen printed onto the copper plates and the plates were assembled. The unit was then heated at 210°C for 20 minutes, which was sufficient temperature and time for the solder to "reflow" on all joints.

Unlike the alpha configuration DMC 3, the working fluid passages could not exhaust directly into the cylinder and a transfer port was required. This compromised the design by adding extra dead volume. In the early stages of this project investigations were made on machining fine annular fin heat exchangers such as that used on the Philips 1002 C engine, (de Brey, 1947), approximately 100 slots were required 3 mm deep and 0.2mm - 0.4mm wide. By far the most accurate method was wire cutting (spark erosion). Estimates of around \$700 per cylinder were obtained from the local operators. This price precluded even prototype manufacture and the flat plate heat exchanger

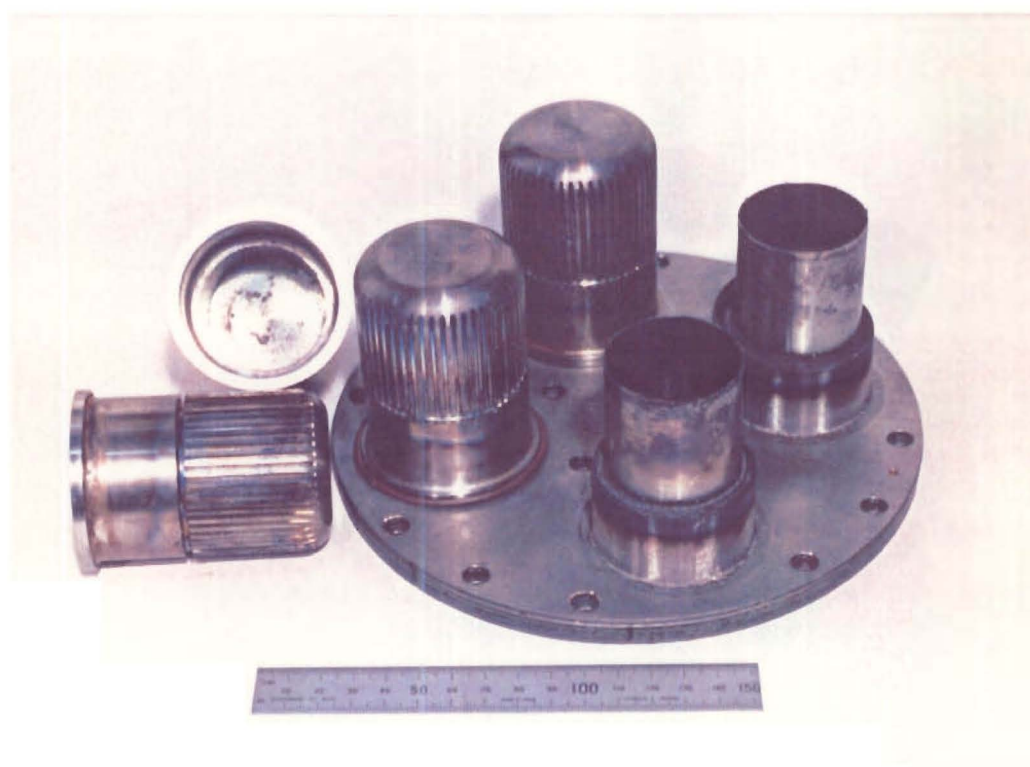
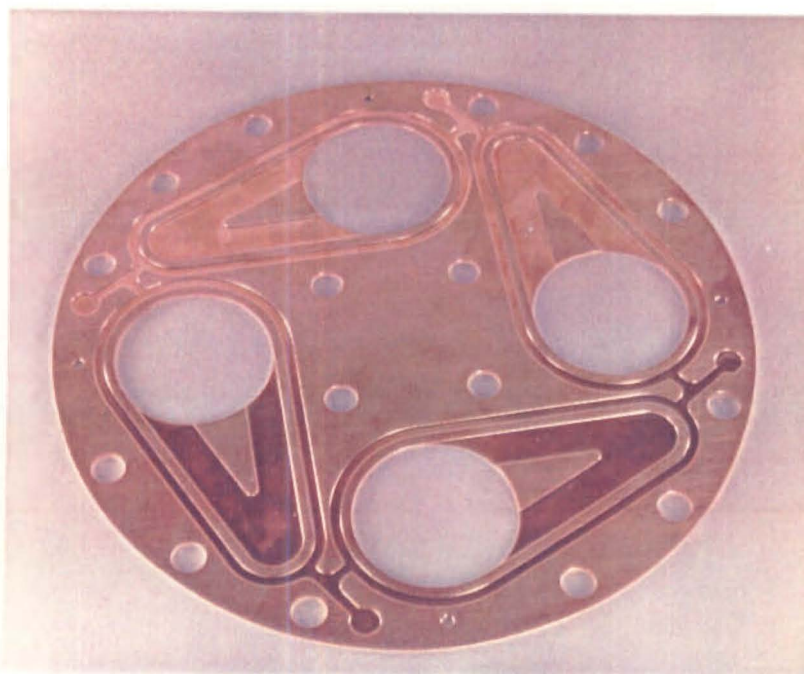


Photo 9.5 Heat Exchangers. Top: etched copper plat for the cold end heat exchanger. Bottom: Heat exchanger partly assembled.

was developed. In the last few months of this project another estimate was obtained for \$30-40 per cylinder. This makes wire cut heat exchangers a likely candidate for production. A transfer port would still be required but sealing the plates of the flat plate heat exchanger would be avoided.

9.1.23 Regenerator

Annular regenerators similar to that used on DMC 3 were manufactured, Photo 9.5(b). To improve engine efficiency the length was increased from 25 mm to 30 mm as suggested by the optimisation routine. Each regenerator used a 6.5 m strip of 150 mesh stainless steel. To avoid purchasing 6.5m of material, a 1 m square was purchased and torn into 30 mm wide strips. Seven strips were then spot welded together and wrapped onto the flow guide. Photo 9.5(b) shows the regenerators and hot end heat exchangers partially fitted to the cold end heat exchangers. Note the discolouration due to the temperature variation through the regenerator. A concern with using wrapped regenerator material is bubbles occurring during wrapping which can allow gas to avoid the flow through the tortuous mesh. By unwrapping the regenerator it was possible to see by the discolouration that the flow was very even. Whilst the performance of this regenerator may not be as effective as the more traditional stacked mesh screens, this method of manufacture was very cheap and simple to manufacture.

9.1.24 Hot End Heat Exchanger and Cylinder Head

Like DMC 3, the heads were machined from heat resistant AVESTA 253 MA solid bar, Drawing DMC 5-23. It was anticipated that the heads should be investment cast for production units. The heads were designed to have external fins, but for initial tests they were not machined. During testing the high head temperature could not be maintained at the design power for the unfinned head. This indicated that both an improved burner and an externally finned head were required, as anticipated. Fins were machined into the head as originally designed and burner insulation was improved. This enabled the design power to be met for continuous service. Tests on DMC 3 indicated that fins were unnecessary for the working fluid heat exchanger. To reduce

manufacturing costs a simple annular gap heat exchanger was manufactured. The flow guide which passed through the regenerator caused the gas to pass the internal surface of the heated head before exhausting into the expansion space. This appeared to work well during the engine testing but a thermocouple should be fitted to measure the mean working fluid temperature in the expansion space to determine the effectiveness of this heat exchanger. This is an attractive design due to the low manufacturing costs. Extra wall thickness was allowed for fitting an internal finned annular insert. But like the DMC 3 engine, difficulty attaching the finned block to give suitable heat transfer may introduce added complexity and costs.

9.1.25 Initial LPG Burner For Engine Testing

For engine testing it was desirable to have known fuel and air flow rates therefore it was more effective to use the compressed air supply for the combustion air than a naturally aspirated burner. Initially the mixing tube and plenum chambers were fabricated from mild steel and 0.4 mm slits were cut to form the burner nozzles. The burner was designed for combustion to occur on the lower half of the head and the exhaust gases to pass through an annular gap between the cast refractory cap and the top half of the heater head, Photo 9.6(a).

9.1.26 LPG Burner For Production Engines

Fabricating the burner from steel was very tedious and time consuming, a process which would be too costly when producing the engines commercially. Considerable development of manufacturing techniques for casting the complete heater in one operation was performed. Many refractory materials were tested and the most promising was Thermo Sil Air Fine. This is a castable refractory material. The advantage over many of the other materials tested was its fine grain size and structural strength. The fine grain size allowed the castable material to form around the small diameter burner nozzles. Lost wax casting techniques were developed which would enable all four plenum chambers, the mixing tube, burner nozzles and combustion chambers to be cast in one operation. A similar technique was used to manufacture the burner/insulator shown in Figure 9.2.

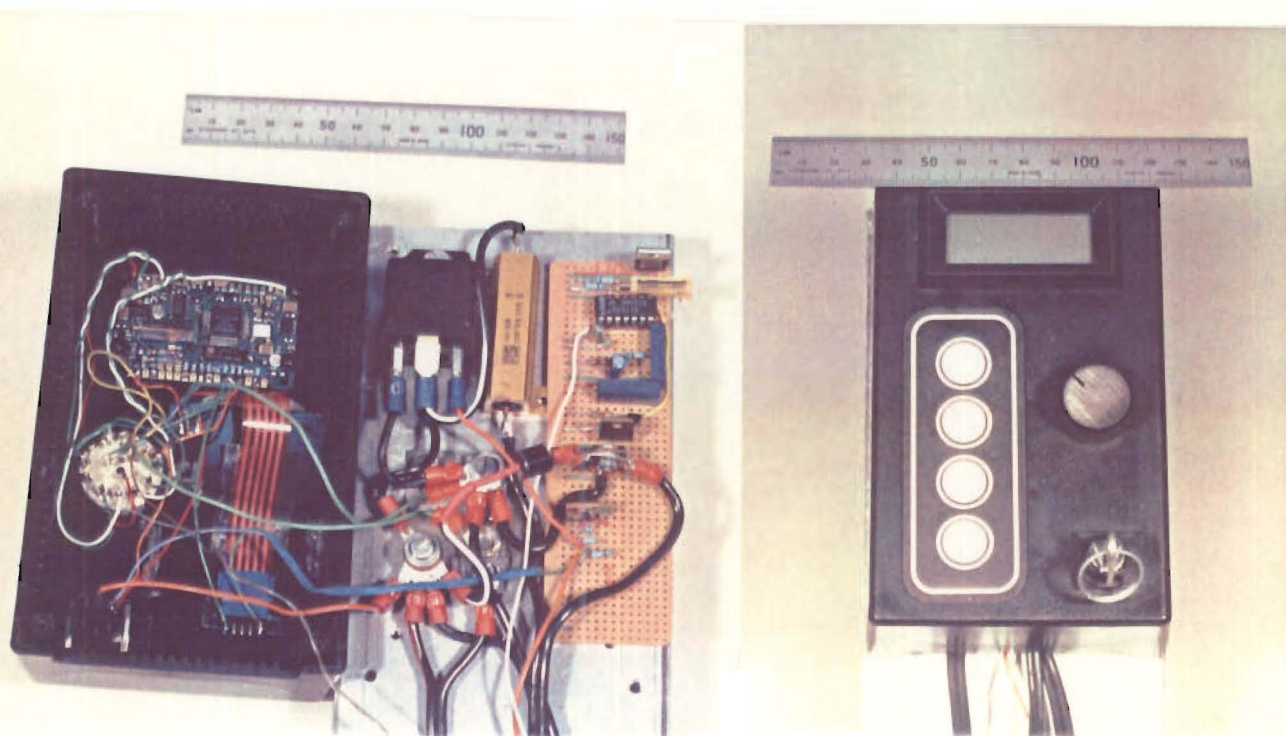


Photo 9.6 (a). First burner used on DMC 5 with ceramic caps and steel burner rings. (b). Remote control panel. Left, preliminary circuit showing the starting solenoid and voltage regulator.

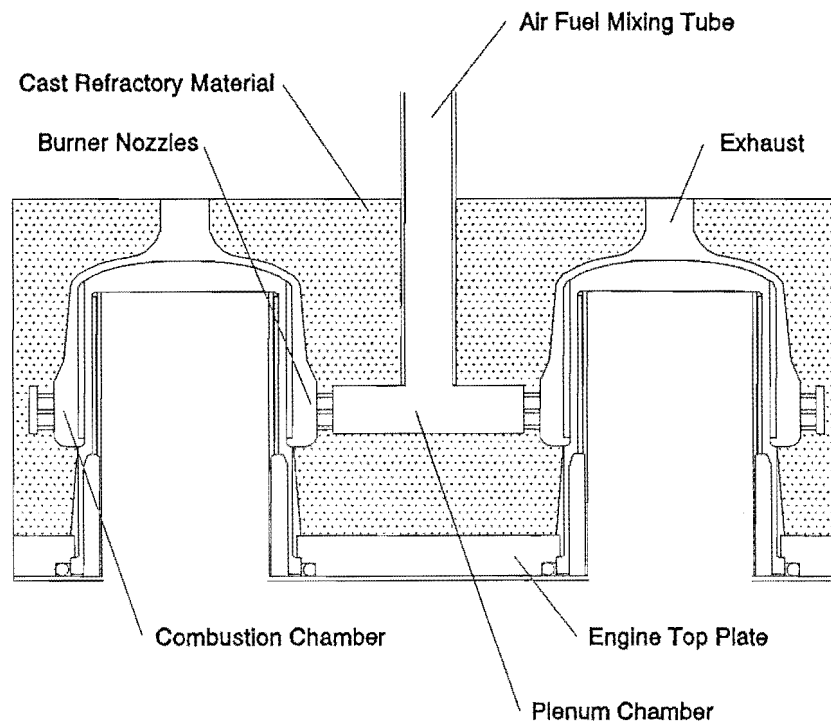


Figure 9.2 Cross section of the cast refractory burner/insulator.

9.1.27 Burner Capacity.

Referring to Figure 9.3. The required power output is 200 Watts and the estimated efficiency is 10%, based on a survey of similar engines. Therefore, the heat input to the system by the LPG is 2 000 Watts. From Appendix A the lower calorific value is 95 MJ/m^3 or 46 MJ/kg , therefore $21 \times 10^{-6} \text{ m}^3/\text{s}$ or $43 \times 10^{-6} \text{ kg/s}$ of fuel is required. One kilogram of fuel should last 6.4 hours, assuming the engine runs for 8 hours per day on average, a 9 kg container (average size for New Zealand) should therefore last around one week.

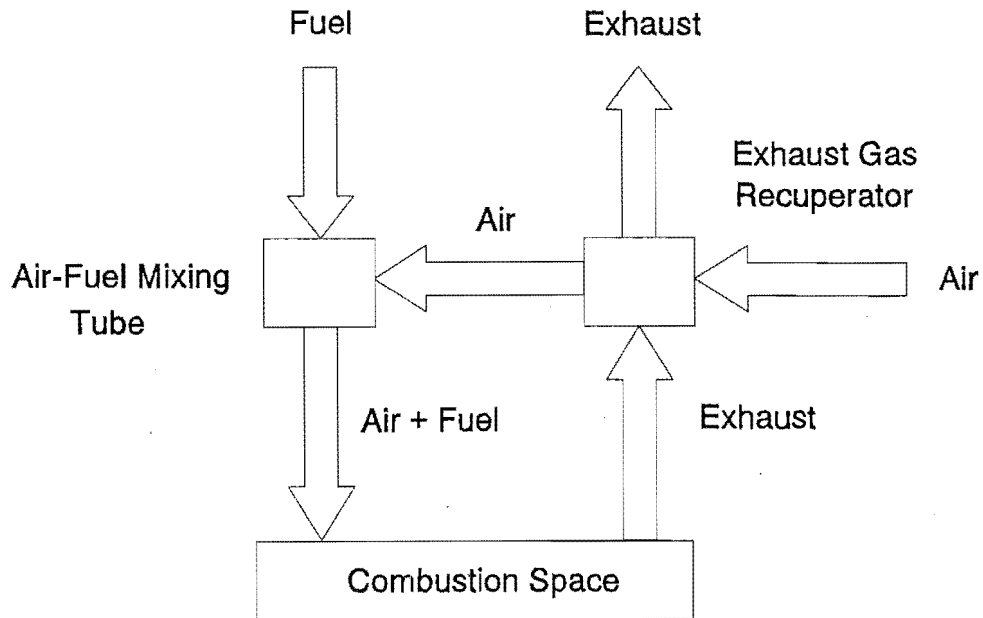


Figure 9.3 Flow diagram of the recommended burner for the SEBCY.

From Appendix A the theoretical air requirement is 26.19 m^3 per m^3 of fuel at 15°C and 101.325 KPa . Using one jet and venturi the air-fuel mix is distributed to the combustion space by a mixing tube and a plenum chamber surrounding the head.

At 15°C and allowing 20% excess air the total volumetric flow rate in the venturi is:

$$1.2 \times 26.19 \times 21 \times 10^{-6} + 21 \times 10^{-6} = 680 \times 10^{-6} \text{ m}^3/\text{s}$$

The auto-ignition temperatures are 450°C and 405°C for propane and butane respectively, so 405°C must not be achieved in the venturi and distribution system. Assuming 200°C is achieved by the air preheater the volumetric flow rate is:

$$680 \times 10^{-6} \times 473/288 = 1.11 \times 10^{-3} \text{ m}^3/\text{s}$$

The jet venturi system can be designed similar to a standard Meker burner (Gaydon, 1970) although inverted and positioned down the axis of the engine, Figure 9.2.

9.1.29 Exhaust

For the exhaust gas leaving the heater head at 1023 K, assuming the exhaust temperature is similar to the head temperature for maximum heat transfer, the volumetric flow rate is:

$$680 \times 10^{-6} \times 1023 / 288 = 2.415 \times 10^{-3} \text{ m}^3/\text{s}.$$

Or by conservation of mass:

$$m_{\text{air}} = 660 \times 10^{-6} \times 1.2 = 792 \times 10^{-6} \text{ kg/s and } m_{\text{gas}} = 43 \times 10^{-6} \text{ kg/s}$$

By addition the mass flow rate of combustion products is $835 \times 10^{-6} \text{ kg/s}$.

This simple analysis enabled a test burner to be designed and manufactured for initial engine testing.

9.2 SEBCY Electronic Control System

Recent advances in automotive electronics have enabled complex engine controls to be performed by a single integrated circuit. During this project it was intended to build up logic circuits with transistors and other required components which would ultimately have been complicated and less effective than using an integrated circuit. Another project has been initiated to develop an engine management package based on this IC. Therefore sufficient electronic equipment was developed to demonstrate the engine and obtain sufficient data to allow design of the control system. This Section describes the control system requirements and other necessary electronic equipment.

9.2.1 Basic Circuit Design

To be an effective system there must be minimal attention required from the operator. Ideally when boarding the craft an ignition key would be turned on and the SEBCY would take over the battery management until the ignition key was switched off at the end of the sailing trip.

9.2.2 Pilot Light

To ensure combustion of all gas at the engine a pilot light should remain on while the SEBCY is activated. Therefore to start the engine the solenoid valve to the main gas supply can be activated. When suitable combustion is occurring the solenoid valve would be held open by a thermocouple current, (this system is typically used on domestic gas heaters). A vent at the bottom of the SEBCY cabin should exhaust to the atmosphere, as LPG is more dense than air it can be contained in a cup shaped space, such as a yacht hull.

9.2.3 Battery Charge Determination, SEBCY Starting and Stopping

Battery terminal voltage could be used to determine when the SEBCY should be started. For example, when the voltage drops below a set point, approximately 12 Volts, for more than one minute the SEBCY should be activated.

Overall charging efficiency drops as the battery acceptance current drops when the battery is approximately 85% charged. At this stage the power output ($\text{Power} = \text{Volts} \times \text{Amps}$) could be determined. Once below a certain threshold, approximately 100 Watts for more than one minute, the SEBCY could be shut down.

There is potential here for a very interesting optimisation project on the best start and stop thresholds to give the optimum overall efficiency. Particularly when the preheating required to start the SEBCY is included.

9.2.4 Electric Starting

One of the novel features of the SEBCY is the ability to use the alternator as a starter motor. This was possible by switching the neutral star point of the three phase alternator to positive and in the correct sequence connecting each phase to negative, Drawing DMC 5-26. There are several ways to achieve the correct sequencing of the switching to ensure the motor has high torque and starts in the correct direction. The most effective system developed and used on DMC 5 was switching high current (60 A) FETs with SOSs. Three slotted optical switches were mounted to the base plate of the engine at 20 degree increments. Six equally spaced circumferential slots were machined in the alternator rotor which switched only one FET on at anyone time. The SOSs could be timed to match the stator ensuring a high torque, even when stalled. The major difficulty encountered was finding FETs which would accommodate the high current. Eventually Philips TOP (temperature overload protected) FETs were obtained and these worked without fault. Attempts were made to use Hall effect transistors instead of the SOS but the high magnetic fields surrounding the rotor gave unreliable operation. An undergraduate project is currently in progress to remove the SOSs entirely by detecting the back EMF in the stator windings to give the rotor position. No FETs could be found that could operate with the high current between the neutral point and the + 12V battery terminal. To overcome this a Bosch automotive lighting solenoid was used. When either the operator or the engine management system performs an electric start a 12 V supply is given to a FET which activates the starting solenoid, the SOSs, and excites the alternator. As a protection to the starting FETs and the solenoid, a resistor is placed in series with the star point, this limits the current through the FETs and solenoid to around 40 A. For a 12 volt supply the power supplied is therefore 480 W. The available torque was not easily measurable but the system did start the engine without difficulty under normal operating conditions. This system proved to be very successful and further developments should continue.

9.2.5 Engine Speed Control and Voltage Regulation

Controlling the power output from a Stirling Engine can often require a complex control system, (Walker, 1980). During the charging period from 50% to 85% of the battery Ah rating full excitation could be used. This may however cause the engine to run at slower than optimum speed. The load on the engine is related to the alternator excitation which would be so adjusted to control load. To achieve this a LM2917 frequency to voltage converter was used to modify the voltage feeding the Zener diode, Figure 3.6 and Drawing DMC 5-26. That is, if the engine frequency were low the voltage to the Zener diode would be increased until the excitation was low enough to allow the engine to come back up to optimum speed. Likewise if the engine frequency were too high the voltage to the Zener diode would be decreased causing the excitation to increase which in turn increases engine load and decreases the engine speed. The engine frequency was taken from one of the alternator phases. The frequency to voltage converter, LM2917, detects the periodic change of voltage and gives a voltage proportional to the frequency. Applying a suitable voltage divider to the output gave a voltage in the correct range for controlling the Zener diode. As this system changes the charging voltage, suitable damping is required to prevent "hunting" of the engine which would cause changes of intensity of lights powered by the battery. Changes of electrical load on the battery also causes variation of the battery voltage, the system described can accommodate this.

9.2.6 Control Panel

The SEBCY engine unit is likely to be concealed in a locker or engine compartment. To allow easy access to the electronic controls and monitoring system the control panel was made remote to the engine. The control panel, Photo 9.6(b), had a back lit LCD display that showed voltage, current, engine speed and head temperature. Also on the control panel was a four position switch to select the feature to be displayed on the LCD display, an ignition key and a set of sealed diaphragm switches. One of the diaphragm switches was used to perform a manual electric start.

9.3 SEBCY Testing

On completion and assembly of the engine and ancillary equipment, basic engine tests were performed. The procedures and results are discussed in this Section.

9.3.1 Alternator Motoring Tests

An extension shaft was made to replace the lock nut on the driveshaft. With the manual starter removed the driveshaft could be externally driven. The SEBCY was set up in a variable speed lathe as shown in Figure 4.3 and the alternator performance was tested. The test rig and condensed results are shown in Photo 9.7(a) and Figure 9.4 respectively. Figure 9.4(a) shows that the optimum efficiency occurs between 1400 and 1500 RPM. 1500 RPM was the speed for which the heat exchangers were optimised. Figure 9.4(b) shows that the variation of power or load on the engine is very steep between 0 and 20 Watts excitation power when driven at 1500 RPM. This feature enabled engine load control by varying the excitation power, Section 9.2.5. It was concluded that the load levels off above 20 Watts excitation due to saturation of magnetic flux in the rotor components.

9.3.2 Engine Motoring Tests

With the engine completely assembled and before the engine was operated as a prime mover, it was motored over in the lathe as described in Section 9.3.1. This allowed gradual speed increase and was used to identify possible engine faults early. The only required adjustment was to the piston stroke to prevent the pistons touching the cylinder head, this was easily accomplished using the swept volume control. Following unloaded motoring (at atmospheric pressure) tests, water cooling was applied and the mean cycle pressure was gradually increased to 15 bar. The engine showed favourable signs of working as a heat pump as expected.

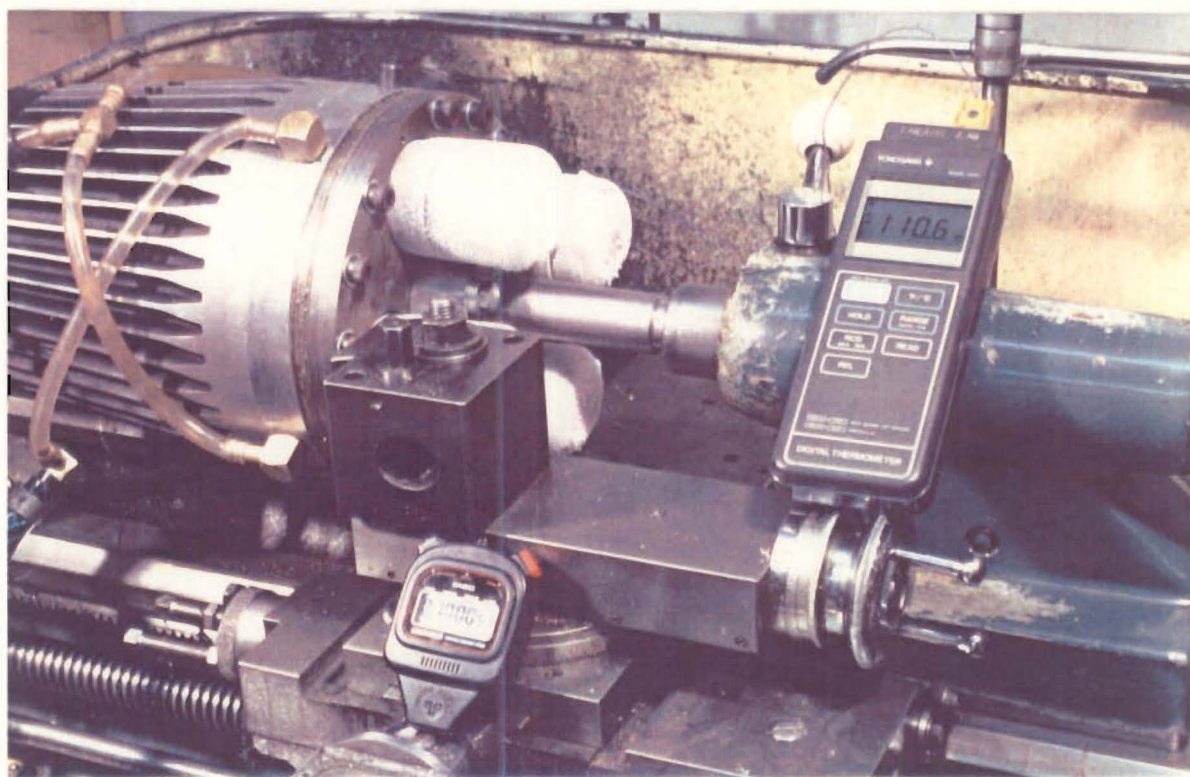
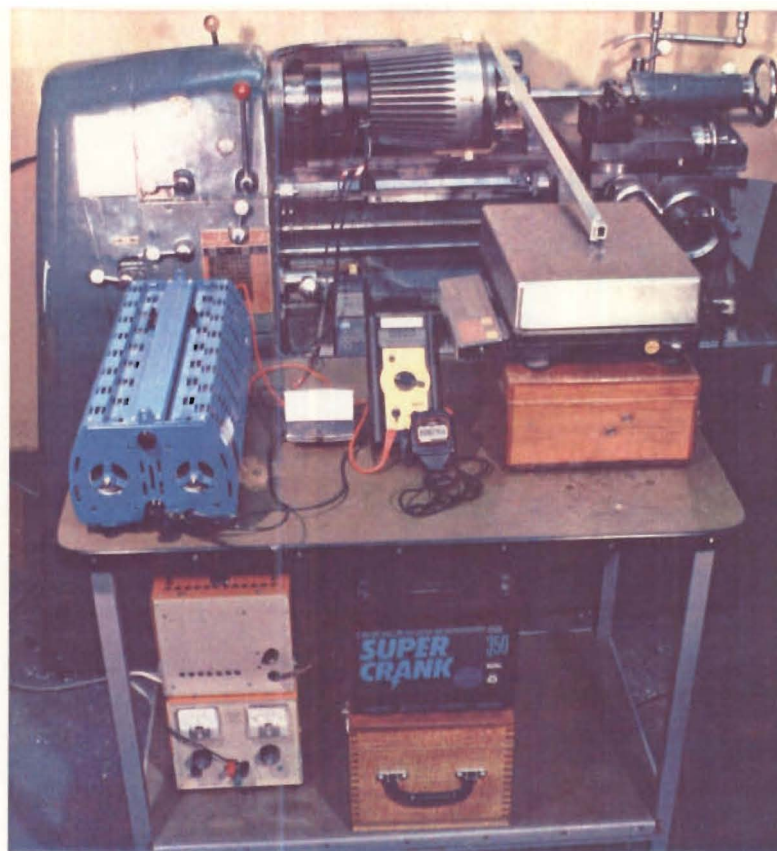
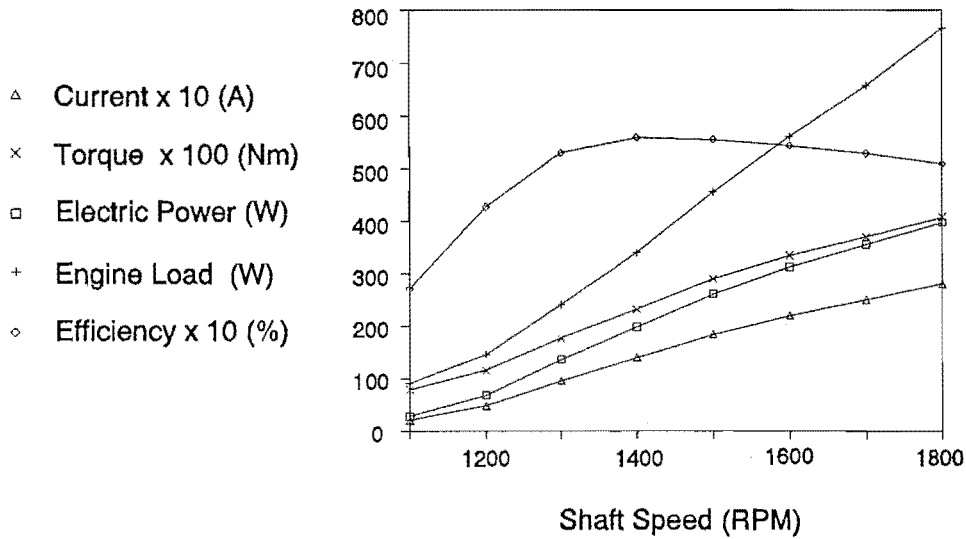
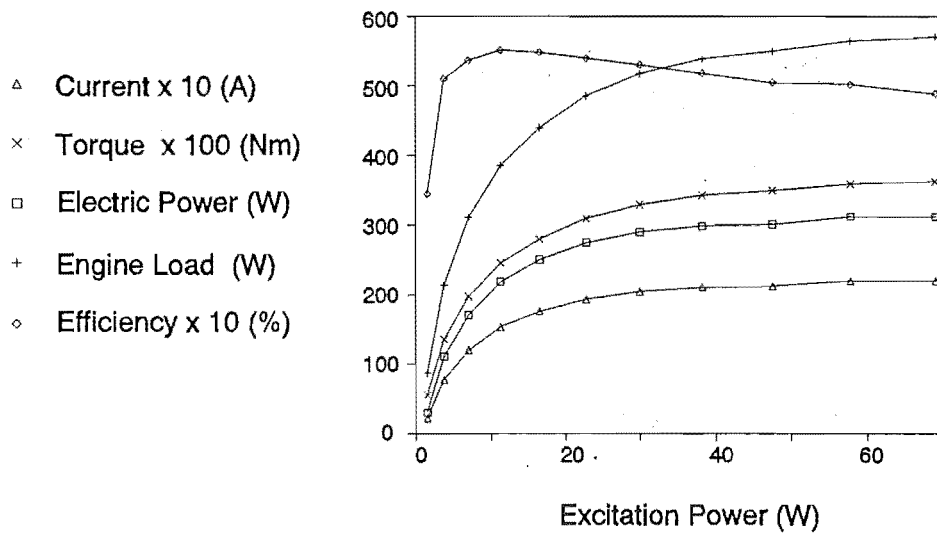


Photo 9.7(a) DMC 5 set up in a variable speed lathe for driving tests. (b) Ice formed on the heater heads after driving the engine for 10 minutes.



a.



b.

Figure 9.4 Stationary field coil alternator characteristics. (a) Excitation set to maintain 14.2 volts.

(b) Speed constant at 1500 RPM.

9.3.3 Driven Tests

Tests were performed on DMC 5's ability to work as a heat pump (refrigerator). The engine was set up in the lathe as before. The heads were exposed to the atmosphere as shown in Photo 9.7(b). The head temperature was recorded at 30 second intervals for the engine operating at 10 Bar mechanism housing pressure and 1500 RPM, this was continued for 10 minutes. The engine was then left overnight to allow the heater heads to return to the atmospheric temperature. The next day the engine was driven in reverse for the same period and conditions as before. The temperature time profile from these tests is shown in Figure 9.5.

9.3.4 Prime Mover Testing

For the first engine tests, the engine would only run for 10-300 seconds and then stop rapidly. The rapid slowing of the engine speed indicated seizure of the seals. Seal testing, described in Chapter 7 showed that tight seals which were overheated became very sticky and required considerable power for motoring. Based on these results the seal clearances were increased. Surprisingly this made the engine run for shorter times. It was then realised that the heating of the seals caused the lip to expand to a point where the sealing effect was suddenly lost and the engine stopped. As hydraulic seal activation was not included in this engine a thin, 0.3 mm, aluminium band was fitted around the lip to limit the thermal expansion. This cured the stopping problem but the power output was still low, (30-40 W). Aluminium bands were then fitted to the rod seals. This completely changed the characteristics of the engine, and it now felt lively to turn over by hand. The engine test following this modification gave a continuous electrical power of 110 W, and for a short period the design power of 200 W was exceeded (a maximum electrical power of 250 W was measured). During these tests the heater head was not insulated and there were no external fins on the head. Fins and insulation were subsequently provided, Figure 9.2. This modification allowed the engine to run continuously at its design power.

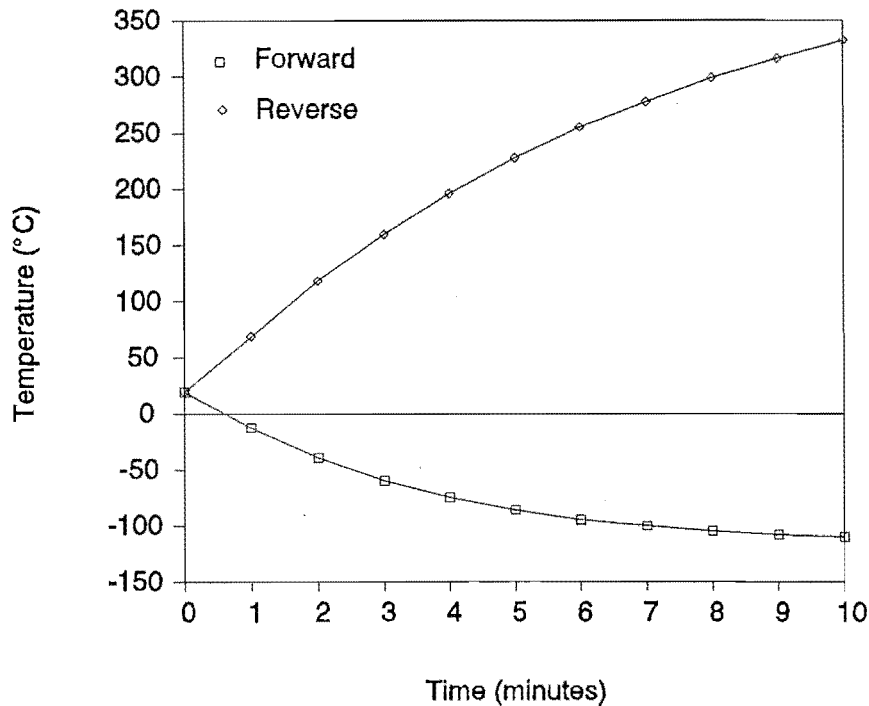


Figure 9.5 Temperature-time plot for DMC 5's heater head when driven forward and reverse.
(At 1500 RPM, 10 Bar mechanism housing pressure and 0.0625 l/s water flow at 13.6 °C)

After running for 10 hours as a prime mover the engine was stripped for inspection. It was found that one of the wobble yoke side plates had broken, Figure 9.6. Prior to the engine being stripped down it was running well and without excessive noise. However, the break appeared to have been present for some time, evident by the wear on the fracture surfaces. It seemed very odd that sufficient stress was on the beam to cause failure but not sufficient to cause damage to the rest of the mechanism or even produce noticeable changes in engine noise. The fracture surface showed the characteristic fatigue failure patterns when viewed by eye. But when viewed under a microscope there appeared to be inclusions in the material. Calculations of the stress in the beam side plate were repeated and indicated the aluminium should be satisfactory. The continued use of a material prone to fatigue failure was questioned. To remedy this fault medium tensile steel BS 1040 beams were manufactured and fitted. These increased the inertia loads on the mechanism but gave no further trouble. The engine was run for a further 8 hours and then stripped for a

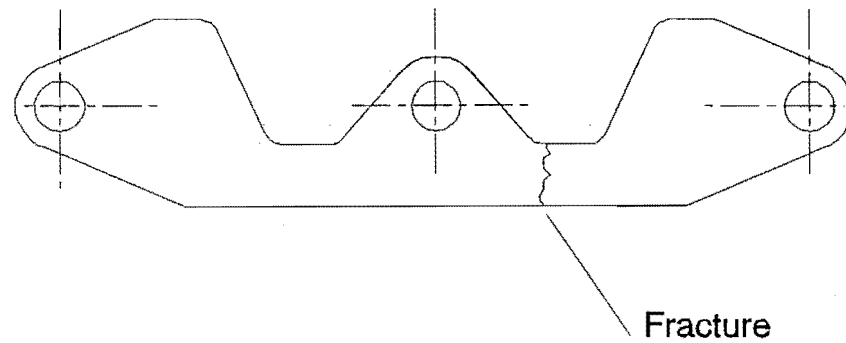


Figure 9.6 Wobble yoke beam side plate broken after 15 hours operation.

general examination. The engine showed no adverse signs of deterioration so it was reassembled for final engine testing for this project.

9.4 Conclusions for Chapter 9

- Overall the engine design has been very successful.
- The engine alternator met and at times exceeded its design specification of 200 Watts electric power.
- Engine speeds in excess of 3 000 RPM were recorded. The engine accelerated very fast 0-2 000 RPM in less than one second.
- The engine worked well as a heat pump, either cooling or heating.

- The manual pull starter worked well. It was convenient to use and reliable.
- The converted alternator starter performed both operations very well.
- The alternator efficiency was 2%-5% lower than the original Bosch alternator due to using unsuitable materials and more air gaps in the magnetic field path.
- The engine was very quiet. Burner noise was dominant, it was often difficult to detect whether the engine had started.
- Accurate dynamic balance weights had not been fitted but the engine balance was very good.
- The cylinder mounted seals worked well but further endurance testing is required. Rulon material should be tested. It appears seals will still be the life limiting component.
- The piston-connecting rod flexure joints showed no obvious deterioration, but further endurance testing is required.
- The flat plate cold end heat exchangers worked well but manufacturing costs may require that other designs be investigated further.
- The wrapped regenerators worked well and were cheap to manufacture compared to contemporary methods.
- A technique has been developed for casting the complete burner in one operation from an insulation material.

- A burner suitable for applying heat to the head for initial testing was manufactured but the efficiency of the burner was very low. There is still work to be done to develop an efficient and reliable burner-air preheater assembly.
- The electronics worked as required but are still in a very preliminary form.
- For the initial testing of DMC 5 the overall efficiency was only 3 to 5%. It should be noted, however, that the burner was very inefficient. It is expected that the efficiency would increase to above 10% with a suitably optimised burner and air pre-heater. This efficiency would be well above that of a large diesel running solely to charge the batteries.

10 Conclusions and Recommendations

10.1 Conclusions

In 1993 there are still no Stirling Engine prime movers in mass production. This project and many others have shown that the technology exists to manufacture engines that will perform the tasks for which they have been designed. The Stirling Engine attracts many enthusiasts, academics and engineers with its promise of quiet, efficient and vibrationless operation. Yet, ask a member of the general public about a Stirling Engine and few can offer an intelligent reply. So where has all the research and development taken the Stirling Engine? The time has long passed when the engineers and researchers should have changed caps to sales and marketing engineers and taken the Stirling Engine to the general public, potentially the biggest market. A Battery Charger for Yachts is just one of many ideal applications for the Stirling Engine. Throughout the duration of this project many other ideal applications have been identified which have enormous commercial potential. The key to commercial success will not be found in the laboratory, but it will be found in successful marketing. Consequently the next phase of this project will involve marketing the SEBCY and its derivatives in both the Southern and Northern hemispheres.

This design-oriented project has concentrated on creating a viable system for a market that was known to exist and that has a high public profile. A Stirling Engine Battery Charger system has been successfully developed. The objectives set at the beginning of the project have been achieved and some have been exceeded. Whilst an operational system could have been produced by using existing technology, several novel design features have been presented. These include:

a wobble yoke mechanism; a stacked flat plate cold end heat exchanger; a combined starter alternator and cylinder mounted piston seals.

Design of the prototype required substantial analytical and computer modelling to justify the design decisions. The QSFM was used with a grid search optimisation to suggest the heat exchanger dimensions. Prior to this it was required to verify the simulation. This was accomplished using an Alpha configuration engine with similar heat exchangers to the prototype engine.

A key feature of the design is the ability to scale the engine while maintaining the same basic design. This makes it more commercially attractive for an investing company. This design feature enables parametric design to be programmed. With this it should be possible to produce engines to order on a small or large batch size. This ideally suits manufacturing in New Zealand. The SEBCY was intended to be the smallest in a range of engines which could reach 20 kW with the present design layout or greater powers with more sophisticated heat exchangers.

Some authors have stated that the Beta configuration engine is the most suitable for small engines. By following strict design aid guidelines it was shown that a double acting configuration is the most suitable in this application and is likely to be so for larger engines also. This design makes the most of as many as possible of the benefits the Stirling Engine has to offer.

Other than the overall design, the most notable development in this project has been the invention of the Wobble Yoke mechanism, for which a provisional Patent has been granted. This mechanism offers many advantages over previous wobble or swash plate type engine mechanisms. The most significant advantage is the ability to use standard cheap prelubricated and sealed bearings which eliminates the need for free lubricants in the mechanism housing. This, along with a pressurised housing greatly alleviates the rod sealing problems previously associated with Stirling Engines. The

Wobble Yoke is not only suited to the Stirling Engine and other variations and applications have been identified.

A cylinder mounted seal system has been developed which enables a single lip type seal to be used in situations where there is a pressure reversal across the seal. A computer program was developed which simulates the seal behaviour and its implications on the Stirling Engine performance. Results obtained from the theoretical model predicted the phenomena experienced on the experimental test engine.

The heat transfer system which was optimised by a computer simulation program gave the required engine indicated power. The stacked flat plate heat exchanger was successful but other manufacturing techniques should be investigated.

The basic components of a fully automated engine/battery management system have been developed and tested. The initial performance was very promising and warrants further development.

The combined starter alternator system shows considerable promise for meeting both power generation and engine starting needs. This lets the engine be very compact and cheaper to manufacture than a system with separate components.

An easy to use Stirling engine design aid has been developed in the form of a spreadsheet program. This program enables the designer to use 1st, 2nd and 3rd order simulations. The enormous quantities of data generated from the simulations are presented in graphical form which is easily edited. A difficulty with specially compiled programs is the inflexibility of post-processing the data, for this, the spreadsheet is ideal.

10.2 Recommendations

The engine has been shown to work as required and it is now time to enter the second phase of the project which is endurance testing. Requiring more computer control equipment and engine components this is likely to be a more expensive process than manufacturing the prototype. It is recommended that the author now embark on publicising the engine and seeking commercially interested companies to fund the endurance testing work.

An adequate burner for initial engine testing has been developed. A more reliable and efficient burner is required. This is by no means an insignificant task. Some of the features required are: a pilot light; error checking; an air preheater; easy conversion to alternative LPG mixtures and self regulation.

Design and development of a 3 kW system is recommended. This would have many applications such as: holiday home power and hot water supply; hybrid electric car; quiet domestic generators.

The base code for a seal design simulation program has been developed. There are limitations, which were identified and there is scope for another interesting project to further develop and test this code.

SEDA is a very user friendly Stirling engine design aid. The program should be updated to include other engine configurations which would make it a valuable tool for preliminary engine design. This program could also be the basis for the parametric engine design software.

Seal longevity is still likely to be the life limiting component in the engine and further work on seal development is required. Other materials such as Rulon should be tested and in different configurations to that used on DMC 5. External pressure loading of the seals was useful for the

experimental rig and DMC 5 has been designed to accommodate this feature. It is also recommended that this be tested and that full instrumentation be fitted to DMC 5 including cycle pressure measurement. The annular hot end heat exchanger has given adequate results but tests with fins should be performed to evaluate the compromise in efficiency.

The wobble yoke offers considerable promise and should be applied to other applications. Accurate dynamic balance weights have not been fitted to DMC 5 and this should be done before the endurance testing. Some abrasive insulation material entered the mechanism housing during a test and is likely to have contaminated the grease in the bearings. It is recommended that the mechanism bearings be replaced before endurance testing begins.

Further validation of the software used is required. This requires a fully instrumented engine which is also required for complete engine testing. This would be a major task requiring sophisticated technical equipment including instantaneous temperature measurement equipment.

In view of the very promising results achieved with the four cycle double acting configuration, it is recommended that this be pursued as the basis for further research and development in the Department of Mechanical Engineering, The University of Canterbury.

References

Avesta (8524), *Avesta 253 MA, UNS S30815, Stainless and Heat Resisting Steels*. Avesta AB, S-77401 AVESTA, Sweden.

AS1210 (1989), *SAA Unfired Pressure Vessel Code*

Benvenuto,G. Farina,F. (1991), *Possible Marine Applications of Combined Cycle Power Plants Including A Stirling Engine* 5th International Stirling Engine Conference, Dubrovnik

Bartolini,C. (1991), *Development of Monocylinder B-Type Small Size Stirling Engine*. Proceedings of the 5th International Stirling Engine Conference. Yugoslavia.

Bosch. (1985), *Alternators*.

Bragg,J.H. (1878), *Winnebago Combines Stirling Technology with Unique Motor Home Design*. 1978 Society of Automotive Engineers, Inc.

Brey,H.de;Rinia, H. and Weenen,F.L.van (1947), *Fundamentals for the Development of the Phillips Air Engine*. Volume 9, Philips Technical Review.

Calder,N. (1990), *Boatowner's Mechanical and Electrical Manual*, Nautical Books, A. & C. Black Ltd, London.

Cambell,C. (1941), *The Axial Engine* Automobile Engineer

Chiang,C.H. (1988), *Kinematics of Spherical Mechanisms*. Cambridge University Press, Cambridge.

Clucas,D.M.;Raine,J.K. and Tucker,A.S. (1992), *A Stirling cycle battery charger for yachts*. Proc. IPENZ Annual Conference, vol.2, pp351-362, N.Z.

Clucas,D.M and Raine,J.K (1992), *Post Graduate Stirling Cycle Research in New Zealand* Stirling Machine World, March.

Crouch,A. and Pope,V.C.H, (1982), *The Design and Development of a 40 kW Stirling Engine and its Applications* Stirling Engines - Progress Toward Reality, Institute of Mechanical Engineers

Doige,A.G. and Walker G. (1986), *Dynamics of the Ross-Stirling Engine*. Proceedings of the 4th International Conference on Stirling Engines, Italy.

FAG, (1984), *Standard Programme*.

Fauvel,O.R. and Walker, G. (1986), *A Flexure Joint for Use in Ross-Linkage Engines*. Proceedings of the 4th International Conference on Stirling Engines, Italy.

Finkelstein T. (1959), *Air Engines* The Engineer, CCVII

Flynn,G.;Percival,W.H. and Heffner,F.E. (1960), *GMR Stirling Thermal Engine: Part of the Stirling Engine Story - 1960 Chapter*. SAE Annual Meeting, Detroit, Michigan, U.S.A.

- Gaydon, A.G. and Wolfhard, H.G. (1970), *Flames: Their Structure, radiation and temperature*. Chapman and Hall LTD., London.
- Hannah, J. and Stephens, R. (1982), *Mechanics of Machines*. Edward Arnold (Publishers) Ltd., London.
- Hargreaves, C.M. (1991), *The Philips Stirling Engine*. Elsevier.
- Holman, J.P. (1981), *Heat Transfer*. McGraw Hill.
- IECEC (1992), *27th Intersociety Energy Conversion Engineering Conference Proceedings*.
- ISEC (1984), *Proceedings of the 2nd International Conference on Stirling Engines*. China.
- ISEC (1986), *Proceedings of the 3th International Stirling Engine Conference*. Italy.
- ISEC (1988), *Proceedings of the 4th International Stirling Engine Conference*. Japan.
- ISEC (1991), *Proceedings of the 5th International Stirling Engine Conference*. Yugoslavia.
- ISEC (1993), *Proceedings of the 6th International Stirling Engine Conference*. The Netherlands.
- Kirkley, D.W. (1962), *Determination of the Optimum Configuration for a Stirling Engine*. Volume 4, Journal Mechanical Engineering Science.
- Li, X. (1988), *Design of the Low Power Stirling Engine- Possible Application to Irrigation in Rural Areas of China* PhD Thesis, University of Reading
- Mansoor, K. (1984), *Air Charged Stirling Engines*. PhD Thesis, University of Reading
- Martini, W.R. (1983), *Stirling Engine Design Manual*. Martini Engineering, Washington.
- Meijer, R.J. (1979), *Prospects of the Stirling Engine for Vehicular Propulsion*. Volume 31, Philips Technical Review.
- Meijer, R.J. (1986), *Design Philosophy, Design and Preliminary Test of a New Stirling Energy Conversion Unit*. Proceedings of the 3th International Stirling Engine Conference. Italy.
- Meijer, R.J and Ziph. (1979), *A Variable Angle Wobble Plate Drive for a Stroke Controlled Stirling Engine* Proceedings of Intersociety Energy Conversion Engineering Conference, 799258.
- Nag (1991), *The NAG Fortran Library Manual Mark 15*. Volume 4, NAG.
- Nakesch, M. (1960), *Internal Combustion Engine with Swash Plate Drive* United States Patent, 2940325.
- Nilsson, H. and Gummesson, S. (1988), *Air-independent Stirling-engine-powered Energy Supply System for Underwater Applications*. Marine Applications of the Stirling Engine, the Institute of Marine Engineers, London, U.K.
- Organ, A.J. (1991), *Intimate Thermodynamic Design of the Stirling Engine Gas Circuit Without the Computer*. Proceedings of the Institute of Mechanical Engineers.

- Ouwerkerk, C. and Theeuwes, G. (1981), *Leakage and Friction of Different Dry-Running Piston Rings*. Proceedings of 9th International Conference on Fluid Sealing, Netherlands.
- Pahl, G. and Beitz, W. (1988), *Engineering Design A Systematic Approach*. Springer Verlag.
- Percival, W.H. (1974), *Historical Review of Stirling Engine Development in the United States from 1960 to 1970*.
- Reader, G.T. (1991), *The Brothers Stirling and their Engines*. Proceedings of the 5th International Stirling Engine Conference. Yugoslavia.
- Reader, G.T. and Hooper, C. (1983), *Stirling Engines*. E and F Spon, London.
- Rice, G. (1992), Private Communication.
- Rizzo, J.G. (1985), *Modelling Stirling and Hot Air Engines*.
- Rogers, G.F.C. and Mayhew, Y.R. (1983), *Engineering Thermodynamics Work and Heat Transfer*. Longman Group Limited, U.K.
- Ross, A. (1977), *Stirling Cycle Engines*. Solar Engines, Phoenix.
- Senft, J.R. (1982), *A simple Derivation of the Generalized Beale Number*. Proceedings, 17th IECEC.
- Senft, J.R. (1991), *An Ultra Low Temperature Differential Stirling Engine* Proceedings of the 5th International Stirling Engine Conference. Yugoslavia.
- Sensym (1991), *Solid-state Sensor Handbook*. Sensym, INC., U.S.A.
- Sier, R. (1987), *A History of Hot Air and Caloric Engines*. Argus Books, London.
- Sier, R. (1991), *The Stirling Engine Robert or James?* Proceedings of the 5th International Stirling Engine Conference. Yugoslavia.
- Smith, E.H.; Clarke, D.G. and Sherrington, I. (1991), *The Measurement of Piston Assembly Friction in a Motored Engine*. IMechE C433/031.
- STM (1990), *Breakthrough in Energy Conversion*. Stirling Thermal Motors, Inc. U.S.A.
- Urieli, I. and Berchowitz, D.M. (1984), *Stirling Cycle Engine Analysis*. Adam Hilger, Bristol.
- Venkatarathnam, G. (1991), *Matrix Heat Exchangers* PhD Thesis. IIT Kharagpur.
- Walker, G. (1973), *Stirling Cycle Machines*. Clarendon Press, Oxford
- Walker, G. (1980), *Stirling Engines*. Oxford Press.
- Walker, G. (1979), *Elementary Design Guidelines for Stirling Engines*. SAE 799230
- Walker, G. and Senft, J.R. (1985), *Free Piston Stirling Engines, Lecture Notes in Engineering*.
- Walker, G.; Fauvel, O. and West (1986), *The Martini Memorial Volume* The University of Calgary.

Walker,G. and Fauvel,R. (1986), *Applications For Stirling Engines - A Personal View*. Proceedings of the 3th International Stirling Engine Conference. Italy.

Walker,G.;Reader,G.;Fauvel,O.R. and Bingham,E.R. (1993), *The Stirling Alternative*. Department of Mechanical Engineering, The University of Calgary, Canada.

Walker,G.;Scott,M.J. and Bingham,E.R (1991), *Ross-Stirling Silent Boat Engine* Proceedings of the 5th International Stirling Engine Conference. Yugoslavia.

Weenen,F.L. van (1947), *The Construction of the Philips Air Engine*. Volume 9, Philips Technical Review.

Wehr,R.D (1932), *Internal Combustion Engine*. United States Patent, 1886770.

West,C.D. (1981), *Theoretical Basis for the Beale Number*. Proceedings, 16th IECEC, American Society of Mechanical Engineers.

West,C.D. (1986), *Principles and Applications of Stirling Engines*. Van Nostrand Reinhold Co. New York.

Young,A.P.;Griffiths.L (1980), *Automobile Electrical and Electronic Equipment*. Newnes and Butterworths.

Yu,Z. and Lee,T.W. (1986), *Kinematic Structural and Functional Analysis of Wobble Plate Engines* Journal of Mechanisms, Transmissions and Automation in Design, ASME,

Ziegler,J.A (1985), *Axial Piston Macine Having Double Acting Pistons and a Rotary Control Valve* United States Patent, 4491057.

Ziph,B. and Meijer,R.J (1981), *Variable Stroke Power Control for Stirling Engines* Society of Automotive Engineers, 810088.

Appendix A

Composition		Ideal Gas Density (kg/m ³) at 15°C and 101.325kPa	Relative ^a Density Ideal Gas (Air = 1)	Specific Volume (m ³ /kg) at 15°C and 101.325 kPa	Calorific ^b Value at 15°C and 101.325 kPa Net		Theoretical ^c Combustion Requirement of Air m ³ /m ³
Weight %	Vol. %				MJ/m ³	MJ/kg	
Propane		1.865	1.5219	0.5362	86.42	46.34	23.81
90/10	92.3/7.7	1.911	1.5592	0.5233	88.42	46.27	24.36
80/20	84.3/15.7	1.958	1.5979	0.5107	90.50	46.22	24.93
70/30	75.1/24.3	1.998	1.6304	0.5005	92.22	46.15	25.40
60/40	66.7/33.3	2.062	1.6831	0.4850	95.07	46.11	26.19
50/50	57.2/42.8	2.119	1.7291	0.4719	97.54	46.03	26.82
40/60	47.2/52.8	2.178	1.7775	0.4591	100.14	45.98	27.58
30/70	36.5/63.5	2.242	1.8293	0.4460	102.92	45.91	28.34
20/80	25.1/74.9	2.309	1.8845	0.4331	105.89	45.86	29.16
10/90	12.9/87.1	2.382	1.9436	0.4198	109.06	45.78	30.03
n-Butane		2.458	2.0060	0.4068	112.41	45.73	30.95

a: i.e. at 15° C and 101.325 kPa.

b: Where gas is 'Liquid' at 15° C and 101.325 kPa, calorific values are based on Ideal gas volumes.

c: i.e. for stoichiometric air-fuel mixture. Air assumed 21% O₂, 79% N₂.

Table A1 Properties of gaseous propane / n-butane mixtures

Appendix B

PROGRAM SEAL

C Seal Analysis Program

C By. D. M. Clucas

```

REAL T,ALPHA,DELTA,W,S,R,M,VO,TC,TE,STROKE,BORE,
& PI,PHI,THETA,MT,P,VT,RHO,VLEAK,MLEAK,RPM,
& OMEGA,FREQ,L,LIP,SEALID,SEALIDORIG,SEALOD,
& CLEARANCE,WORNSEALID,ORSEALID,PER

```

```

REAL PVEXP,PVCOMP,POWEREXP,POWERCOMP,PINTERFACE,
& VELEXP,VELCOMP,VELEXPABS,VELCOMPABS,WEAR,SEALNU,PISTNU,
& WEARRATE,SEALLOAD,K1,K2,L1,L2,PISTE,SEALE,M1,M2,M3

```

```

INTEGER INC,NCYC,K

```

```

CHARACTER*30 FNAME,FULLFNAME,SPLIT,TYPE,PACTFNAME

```

C INPUT USER CODES

501 FORMAT(A)

```

PRINT*,'INPUT SEAL TYPE 1,2,3,4 '
READ(*,501)TYPE

```

```

PRINT*,'SPLIT SEAL Y/N '
READ(*,501)SPLIT

```

```

C PRINT*,'INPUT ACTIVATION PRESSURE bar '
C READ(*,*)PACT
C PRINT*,'INPUT ACTIVATION PRESSURE bar '
C READ(*,501)PACTFNAME

```

```

PRINT*,'TEST CODE EG. 012 '

```

```

READ(*,501)FNAME

```

```

DO 1000 PACT=0,8E5,2E5

```

```

IF(PACT .EQ. 0)PACTFNAME='00'

```

IF(PACT .EQ. 2E5)PACTFNAME='02'
IF(PACT .EQ. 4E5)PACTFNAME='04'
IF(PACT .EQ. 6E5)PACTFNAME='06'
IF(PACT .EQ. 8E5)PACTFNAME='08'

PI=3.1415927
INC=10
NCYC=10000

C GAS PROPERTIES FOR AIR

M=28.96
R=287.1

C ENGINE DIMENSION

STROKE=.020
BORE=.040
W=.9
TC=300
TE=1000
S=.1
PBUFF=10.0E5
RPM=1500

C CALC ENGINE PARAMETERS

VO=PI/4*BORE**2*STROKE
T=TC/TE
PHI=90*PI/180
OMEGA=RPM*2*PI/60
FREQ=RPM/60

C SEAL/PISTON DATA

SEALTEMP=100
SEALID=.0400
SEALLEN=.0015
SEALTHICK=.0015
SEALOD=SEALID+2*SEALTHICK
SEALE=1352E6
SEALALPHA=10.3E-5
SEALNU=.2
LIP=.005
L=.0015

PISTTEMP=50
POD=.040
PID=.037
PISTE=200E9
PISTNU=.3
PISTALPHA=16.5E-6

FRICCOEF=.18
WEARRATE=5E-9

```

FULLFNAME(1:2)='SA'
FULLFNAME(3:3)=TYPE
FULLFNAME(4:4)=SPLIT
FULLFNAME(5:5)=' '
FULLFNAME(6:8)=PACTFNAME
FULLFNAME(9:9)='.'
FULLFNAME(10:12)=FNAME.

```

C CALC SEAL DIMENSION AFTER THERMAL EXPANSION ASSUME ORIG T=20 C

```

SEALOD=SEALOD+SEALOD*SEALALPHA*(SEALTEMP-20)
SEALID=SEALID+SEALID*SEALALPHA*(SEALTEMP-20)

```

```

PISTOD=POD+POD*PISTALPHA*(PISTTEMP-20)

```

C CALC PISTON/SEAL CLEARANCE

```

CLEARANCE=(SEALID-PISTOD)/2
PRINT*, 'LEAK GAP (mm)', CLEARANCE*1E3

```

C DETERMINE LAME CONSTANTS

```

R1=SEALID/2
R2=SEALOD/2

```

```

RADIAL=((R2**2)/(R2**2-R1**2))*(1-(R1**2/R2**2))
HOOP=((R2**2)/(R2**2-R1**2))*(1+(R1**2/R2**2))

```

C DETERMINE LAME SEAL INTERFACE PRESSURE CONSTANTS

```

R3=POD/2
R4=PID/2

```

```

K2=(1/R3**2-1/R4**2)
L2=(R3**2-R4**2)

```

C SCHMIDT CONSTANTS

```

A=(T**2+W**2+2*T*W*COS(PHI))**.5
B=T+W+2*S
DELTA=A/B
MT=B*M*VO*(1-DELTA**2)**.5*PBUFF/(2*R*TC)
C=2*R*TC*MT/(M*VO)
THETA=ATAN((W*SIN(PHI)/(T+W*COS(PHI))))
Y=2*R*TC/(B*M*VO*(1-DELTA**2)**.5)

```

```

PM=PBUFF
WORNSEALID=SEALID

```

C OPEN OUTPUT FILE

```

OPEN(UNIT=7,FILE=FULLFNAME)

```

```

WRITE(7,900)
WRITE(7,900)

```

```
WRITE(7,900)
WRITE(7,900)
```

C WRITE ENGINE PARAMETERS TO FILE

```
WRITE(7,850)STROKE*1E3,BORE*1E3,VO*1E6,W,TC,TE,T,S,
& PBUFF*1E-5,RPM
850 FORMAT(1X,2F8.3,2F8.2,2F8.0,2F8.2,1F8.2,1F8.0)
```

```
WRITE(7,900)
WRITE(7,900)
```

C WRITE INITIAL SEAL PARAMETERS

```
WRITE(7,860)SEALTEMP,SID*1E3,SEALID*1E3,SEALLEN*1E3,
& SEALTHICK*1E3,SEALOD*1E3,SEALE*1E-9,SEALALPHA*1E6,
& SEALNU
860 FORMAT(1X,10F10.3)
```

```
WRITE(7,900)
WRITE(7,900)
```

C WRITE PISTON PARAMETERS

```
WRITE(7,870)PISTTEMP,POD*1E3,PISTOD*1E3,PISTE*1E-9,PISTALPHA*1E6,
& FRICCOEF,DHORIZ*1E3,CLEARANCE*1E3
870 FORMAT(1X,8F10.3)
```

```
WRITE(7,900)
WRITE(7,900)
WRITE(7,900)
```

K=0

DO 90 I=0,NCYC*360,INC

ALPHA=I*PI/180

C CALC SCHMIDT EQUATIONS FOR MEAN PRESSURE, TOTAL VOLUME, PRESSURE AND DENSITY

```
PM=MT*Y
VT=(VO/2)*(B+A*COS(ALPHA-THETA))
P=(C/B)/(1+DELTA*COS(ALPHA-THETA))
RHO=MT/VT
```

C CALC PRESSURE DROP ACROSS SEAL, P TO PBUFF POSITIVE

PD=P-PBUFF

C CALC PISTON VELOCITY

```
VELEXP=-STROKE/2*OMEGA*SIN(ALPHA)
VELCOMP=-STROKE/2*OMEGA*SIN(ALPHA-THETA)
```

C CALC ABSOLUTE PISTON VELOCITY

```

VELEXPABS=(VELEXP**2)**.5
VELCOMPABS=(VELCOMP**2)**.5

```

C CALC CLOSING PRESSURE

```

IF(TYPE .EQ. '1')PCLOSE= +PACT
IF(TYPE .EQ. '2')PCLOSE=PACT-(P+PBUFF)/2
IF(TYPE .EQ. '3')PCLOSE=PACT*LIP/L-P*LIP/L-PBUFF*LIP/L-(P+PBUFF)/2
IF(TYPE .EQ. '4' .AND. P .GE. PBUFF)PCLOSE=PACT+P-(P+PBUFF)/2
IF(TYPE .EQ. '4' .AND. P .LT. PBUFF)PCLOSE=PACT+PBUFF-(P+PBUFF)/2

```

C CHECK IF SEAL IS WORN OUT

```

IF(SEALOD-WORNSEALID .LE. 0)THEN
PRINT*, 'SEAL WORN OUT'
GOTO 1000
ENDIF

```

```

IF(SPLIT .EQ. 'Y')GOTO 80

```

C CALC SEAL RADIAL DISPLACEMENT BASED ON LAME EQUATIONS FOR NON SPLIT

```

R1=SEALOD/2
R2=WORNSEALID/2

STRESSHP=-PCLOSE*(R1**2+R2**2)/(R1**2-R2**2)
SEALID=WORNSEALID+WORNSEALID*(STRESSHP-SEALNU*PCLOSE)/SEALE

```

C CALC NEW CLEARANCE AFTER CLOSING PRESSURE

```

CLEARANCE=(SEALID-PISTOD)/2

```

C CALC INTERFACE PRESSURE FOR SPLIT OR IF NO CLEARANCE

```

80 IF(SEALID .LE. PISTOD .OR. SPLIT .EQ. 'Y')THEN
CLEARANCE=0.000000000001

```

```

IF(SPLIT .EQ. 'Y')THEN
PINTERFACE=PCLOSE
GOTO 100
ENDIF

```

C CALC INTERFACE PRESSURE

```

C PINTERFACE=- (SEALID-PISTOD)*SEALE/PISTOD

```

```

PINTERFACE=(PCLOSE/SEALE*(POD/(2*SEALTHICK)-SEALNU))/
& (1/PISTE-PISTNU/PISTE+POD/(2*SEALTHICK*SEALE)-SEALNU/SEALE)

```

```

IF(PINTERFACE .LE. 0)THEN
PVEXP=0
PVCOMP=0
POWEREXP=0
POWERCOMP=0
SEALLOAD=0
WEAR=0

```

```

CLEARANCE=.001
GOTO 110
ENDIF

```

C CALC PV AND FRICTION POWER CONSUMPTION

```

100 PVEXP=PINTERFACE*VELEXPABS
PVCOMP=PINTERFACE*VELCOMPABS
POWEREXP=VELEXPABS*FRICCOEF*PINTERFACE*PI*PISTOD*L
POWERCOMP=VELCOMPABS*FRICCOEF*PINTERFACE*PI*PISTOD*L

```

C CALC INTERFACE LOAD, DISTANCE TRAVELLED BY PISTON AND CALC SEAL WEAR

```

SEALLOAD=PINTERFACE*PI*PISTOD*L
DIST=(((STROKE/2)*((1+COS(ALPHA))-
& (1+COS(ALPHA-INC*PI/180))))**2)**.5
WEAR=WEARRATE*DIST*SEALLOAD
WORNSEALID=WORNSEALID+(WEAR/(PI*PISTOD*L))*1E-3

```

```

GOTO 200

```

```

110 ENDIF

```

C ZERO CONTACT THEREFORE WEAR, PV AND POWER ARE ZERO

```

PVEXP=0
PVCOM=0
POWEREXP=0
POWERCOMP=0

```

C CALC LEAK VOLUME, MASS AND TOTAL MASS OF LEAKAGE DURING THE INC.

```

200 VLEAK=(((PD**2)**.5*4*CLEARANCE)/(98*RHO*L)**.5*PD/(PD**2)**.5
MLEAK=RHO*VLEAK*(PI/4)*(2*CLEARANCE)**2
MLEAK=MLEAK/(FREQ*(360/INC))

```

C CALC REMAINING MASS OF GAS IN CYLCLE

```

MT=MT-MLEAK

```

C FOR FIRST CYCLE OUTPUT RESULTS

```

IF(I .GE. 3600 .AND. I .LE. 3600+360)THEN
WRITE(7,810)I,P*1E-5,PCLOSE*1E-5,CLEARANCE*1E3,MT*1E6,MLEAK*1E6,
& PINTERFACE*1E-5,PVEXP*1E-6,PVCOMP*1E-6,POWEREXP,POWERCOMP
810 FORMAT(1X,I6,2F10.2,1F8.5,2F12.3,5F8.2)
ENDIF

```

```

IF(I .EQ. 360+3600)THEN
WRITE(7,900)
WRITE(7,900)
ENDIF

```

C WRITE CYCLE NUMBER, MEAN PRESSURE AND WORN SEAL ID


```
IF(J .EQ. NCYC*360/200)THEN
  K=K+NCYC/200
  WRITE(7,800)K,PM*1E-5,WORNSEALID*1E3,0.15*VO*FREQ*PM
  WRITE(*,880)K,PM*1E-5,WORNSEALID*1E3,0.15*VO*FREQ*PM
880  FORMAT(1X,'CYCLES COMPLETED= ',I6,3F10.3)
  J=0
  ENDIF

  J=J+INC

90  C=2*R*TC*MT/(M*VO)

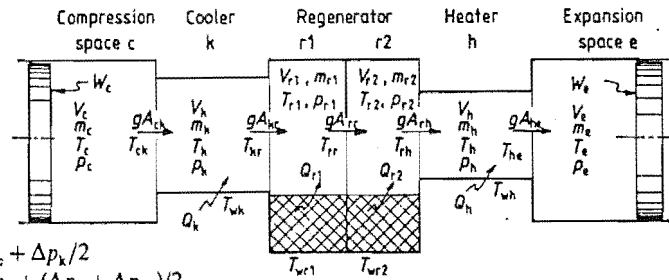
800  FORMAT(1X,I6,3F10.3)
900  FORMAT(1X,' ')

1000 CLOSE(UNIT=7)

  END
```

Appendix C

This Appendix gives the Quasi Steady Flow Model equation set and the graphical output SEDA produces from the results of the QSFM.



$$p_k = p_c + \Delta p_k / 2$$

$$p_{r1} = p_k + (\Delta p_k + \Delta p_{r1}) / 2$$

$$p_{r2} = p_{r1} + (\Delta p_{r1} + \Delta p_{r2}) / 2$$

$$p_h = p_{r2} + (\Delta p_{r2} + \Delta p_h) / 2$$

$$p_c = p_h + \Delta p_h / 2$$

Pressures

$$m_c = M - (m_c + m_k + m_{r1} + m_{r2} + m_h)$$

Expansion space mass

$$T_c = p_c V_c / (R m_c)$$

$$T_k = p_k V_k / (R m_k)$$

$$T_{r1} = p_{r1} V_{r1} / (R m_{r1})$$

$$T_{r2} = p_{r2} V_{r2} / (R m_{r2})$$

$$T_h = p_h V_h / (R m_h)$$

$$T_c = p_c V_c / (R m_c)$$

Gas temperatures

$$T_{rk} = 1.5 T_{r1} - 0.5 T_{r2}$$

$$T_{rr} = 0.5 (T_{r1} + T_{r2})$$

$$T_{rh} = 1.5 T_{r2} - 0.5 T_{r1}$$

Regenerator interface temperatures

$$\text{If } gA_{ck} > 0 \quad \text{then } T_{ck} \leftarrow T_c$$

$$\text{otherwise } T_{ck} \leftarrow T_k$$

Conditional

$$\text{If } gA_{kr} > 0 \quad \text{then } T_{kr} \leftarrow T_k$$

$$\text{otherwise } T_{kr} \leftarrow T_{rk}$$

interface

$$\text{If } gA_{rh} > 0 \quad \text{then } T_{rh} \leftarrow T_{rh}$$

$$\text{otherwise } T_{rh} \leftarrow T_h$$

temperatures

$$\text{If } gA_{hc} > 0 \quad \text{then } T_{hc} \leftarrow T_h$$

$$\text{otherwise } T_{hc} \leftarrow T_c$$

$$DW = p_c DV_c + p_e DV_e$$

$$DQ_k = h_k A_{wsk} (T_{wk} - T_c)$$

$$DQ_{r1} = h_{r1} A_{wgr1} (T_{wr1} - T_{r1})$$

$$DQ_{r2} = h_{r2} A_{wgr2} (T_{wr2} - T_{r2})$$

$$DQ_h = h_h A_{wsh} (T_{wh} - T_h)$$

Energy

$$DT_{wr1} = -DQ_{r1} / c_{mr}$$

$$DT_{wr2} = -DQ_{r2} / c_{mr}$$

Regenerator matrix temperatures

$$DQ = DQ_k + DQ_{r1} + DQ_{r2} + DQ_h$$

$$V = V_c + V_k + V_{r1} + V_{r2} + V_h + V_e$$

$$Diss = Diss_k + Diss_{r1} + Diss_{r2} + Diss_h$$

$$Dp_c = [R(DQ - Diss) - c_p DW] / (c_v V)$$

Compression space pressure

$$Dm_c = (p_c DV_c + V_c Dp_c / \gamma) / (RT_{ck})$$

Compression space mass

$$gA_{ck} = -Dm_c$$

$$gA_{kr} = (c_p gA_{ck} T_{ck} - DQ_k - c_v V_k Dp_c / R - Diss_k) / (c_p T_{kr})$$

$$gA_{rr} = (c_p gA_{kr} T_{kr} - DQ_{r1} - c_v V_{r1} Dp_c / R - Diss_{r1}) / (c_p T_{rr})$$

$$gA_{rh} = (c_p gA_{rr} T_{rr} - DQ_{r2} - c_v V_{r2} Dp_c / R - Diss_{r2}) / (c_p T_{rh})$$

$$gA_{hc} = (c_p gA_{rh} T_{rh} - DQ_h - c_v V_h Dp_c / R - Diss_h) / (c_p T_{hc})$$

Mass flows

$$Dm_k = gA_{ck} - gA_{kr}$$

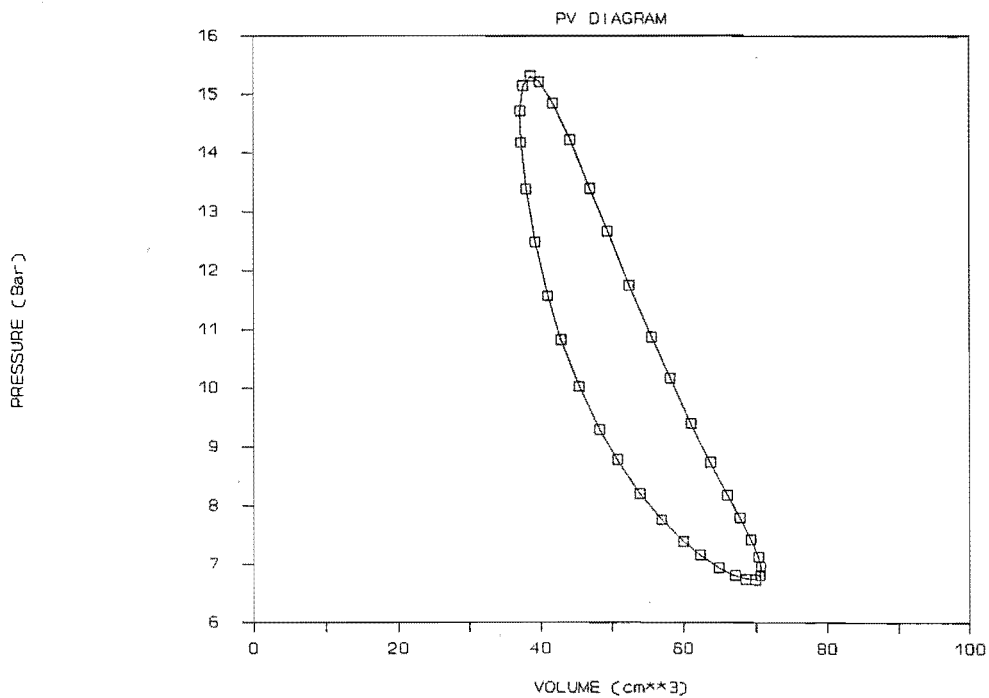
$$Dm_{r1} = gA_{kr} - gA_{rr}$$

$$Dm_{r2} = gA_{rr} - gA_{rh}$$

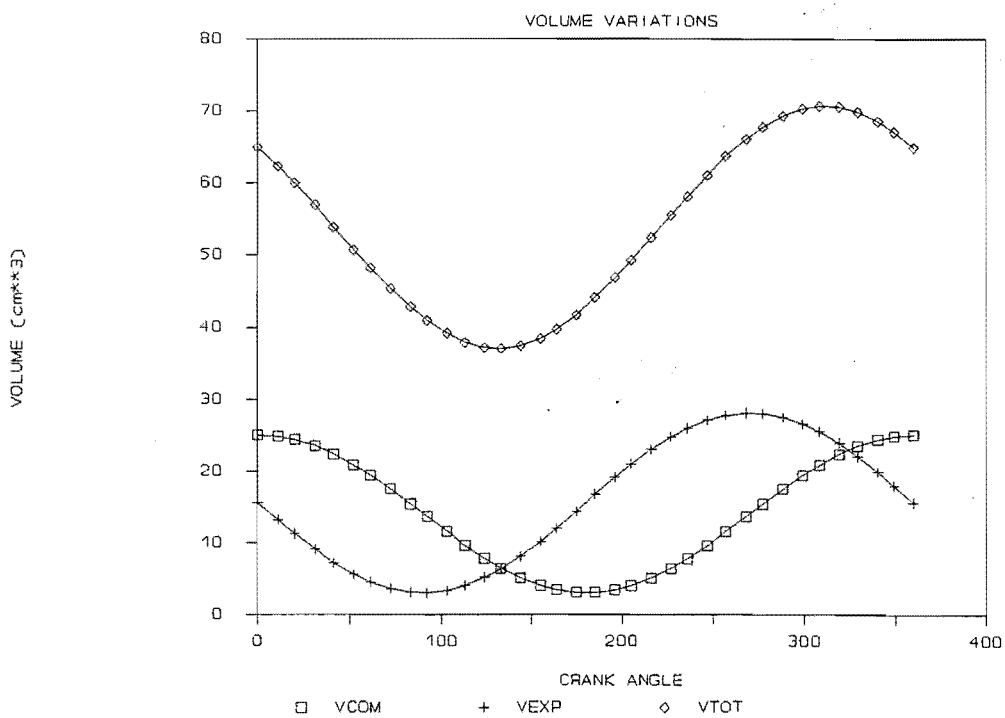
$$Dm_h = gA_{rh} - gA_{hc}$$

Masses

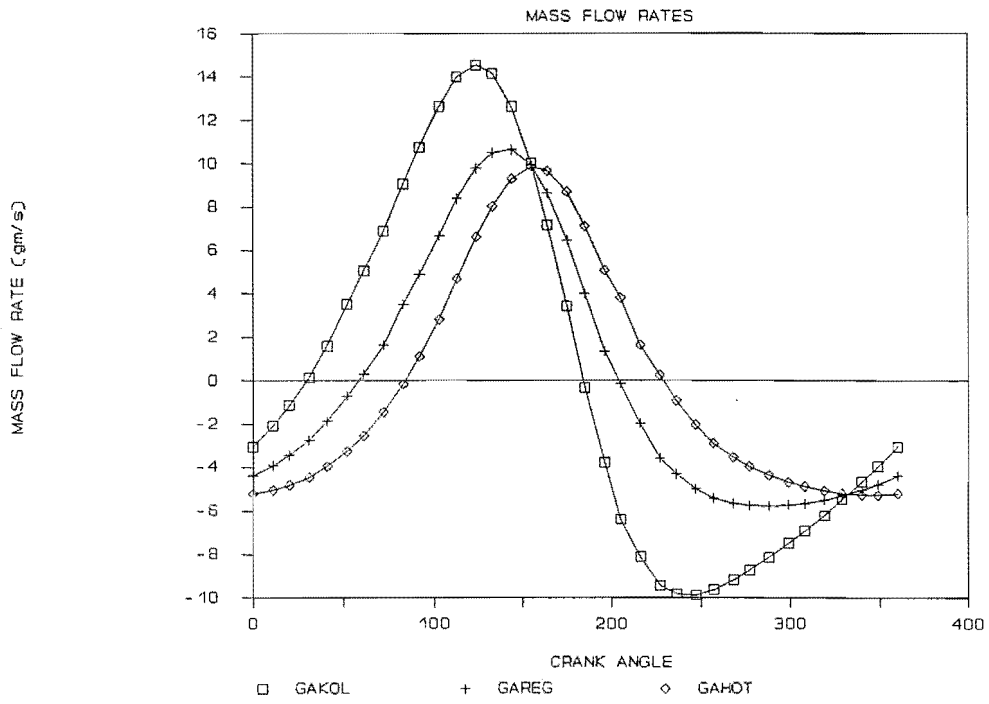
STIRLING CYCLE ENGINE ANALYSIS



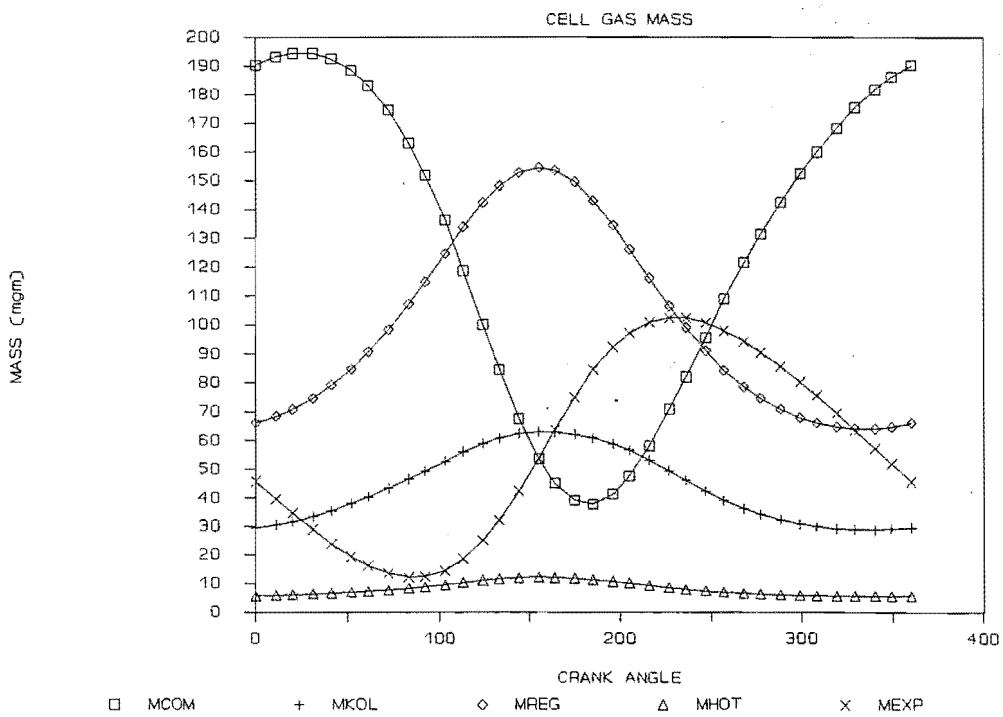
STIRLING CYCLE ENGINE ANALYSIS



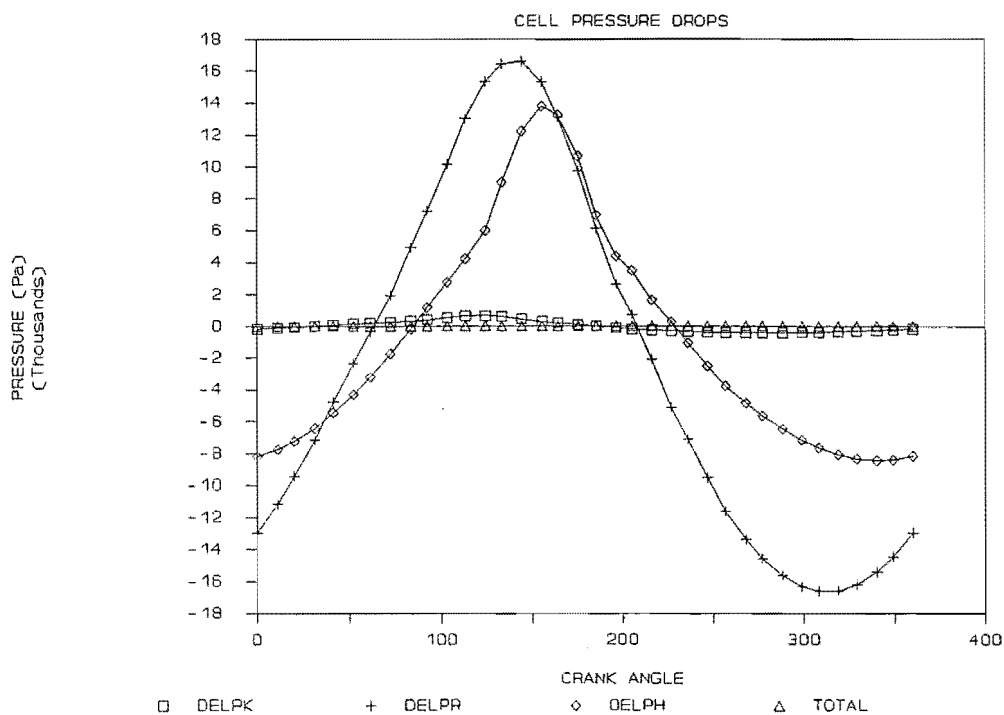
STIRLING CYCLE ENGINE ANALYSIS



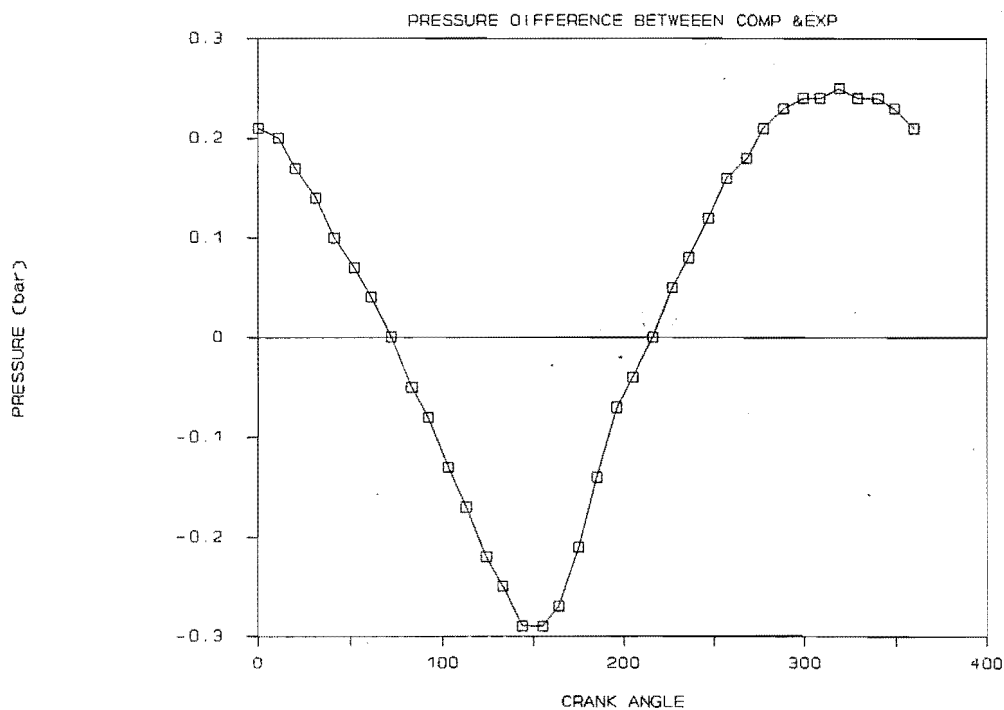
STIRLING CYCLE ENGINE ANALYSIS



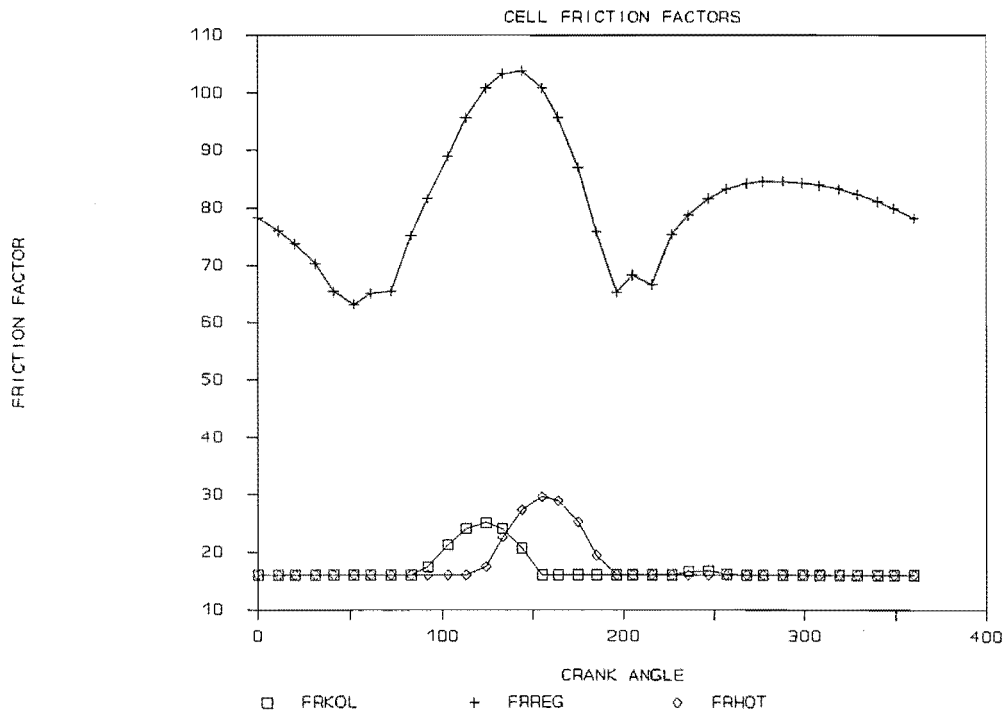
STIRLING CYCLE ENGINE ANALYSIS



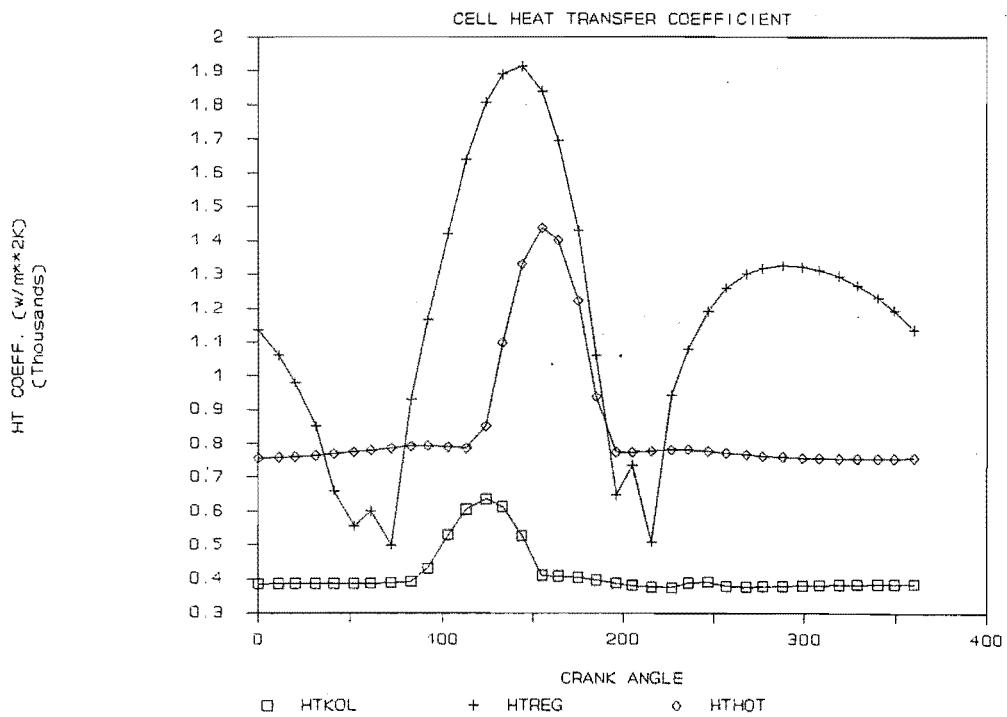
STIRLING CYCLE ENGINE ANALYSIS



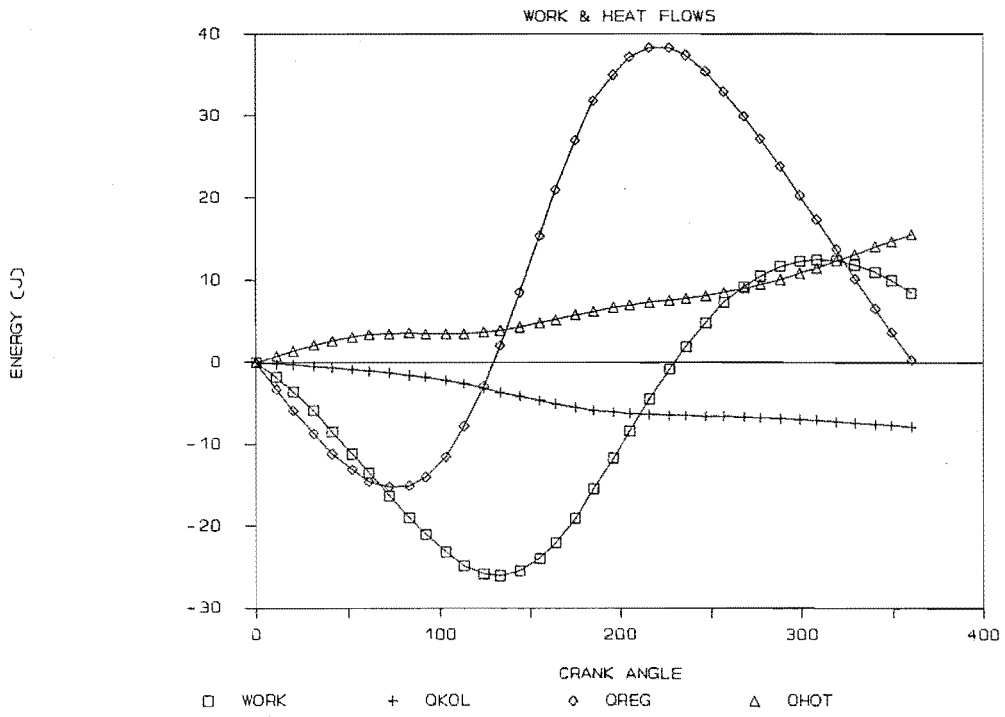
STIRLING CYCLE ENGINE ANALYSIS



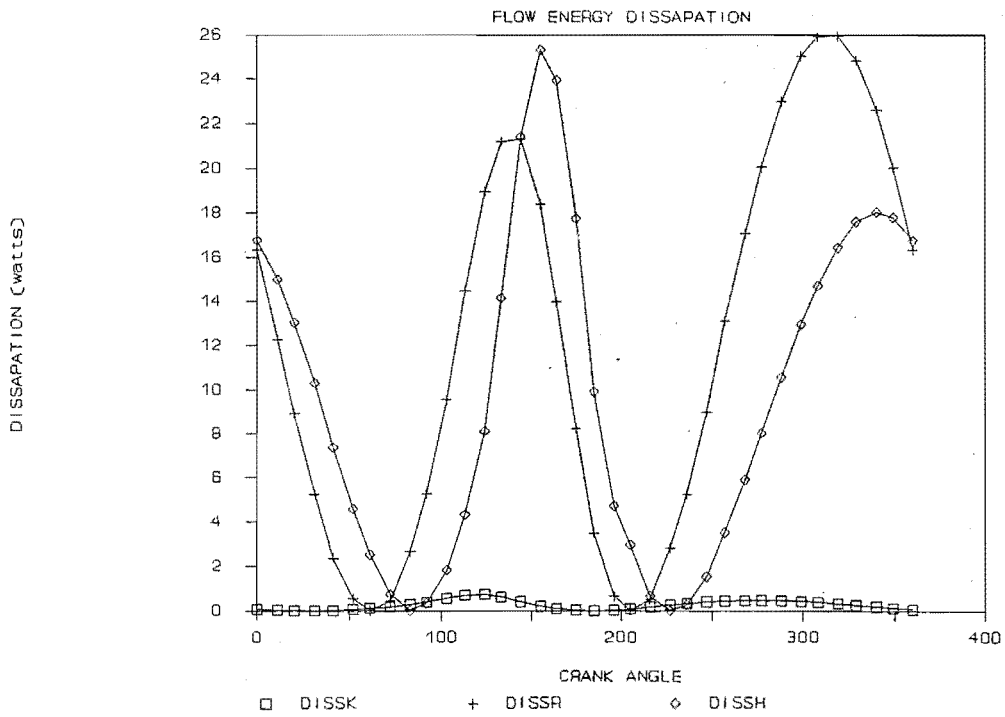
STIRLING CYCLE ENGINE ANALYSIS



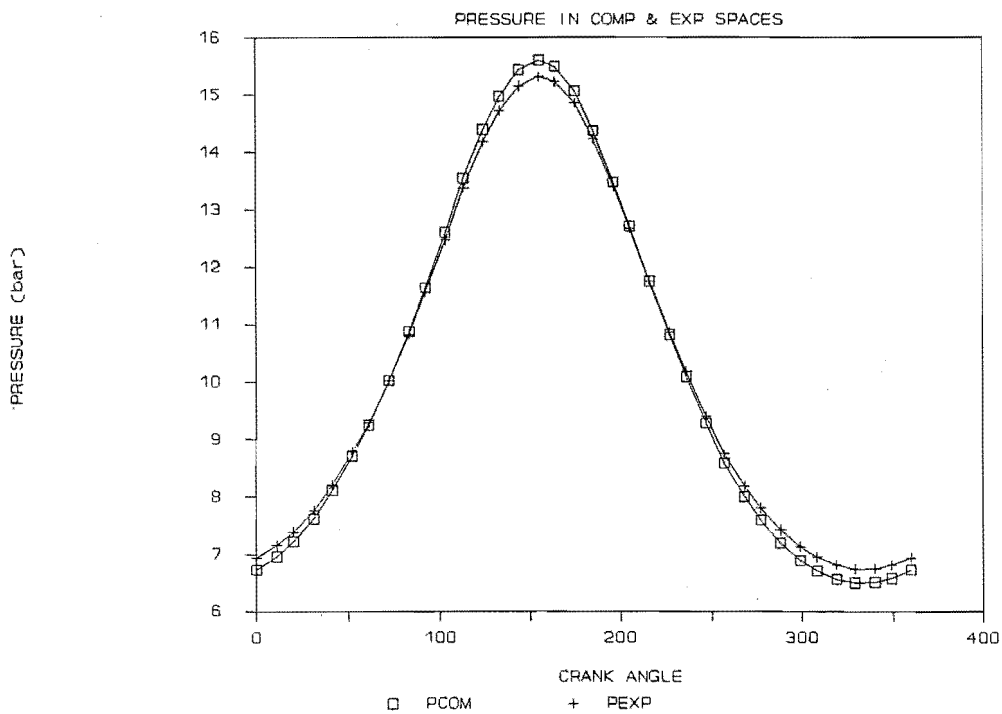
STIRLING CYCLE ENGINE ANALYSIS



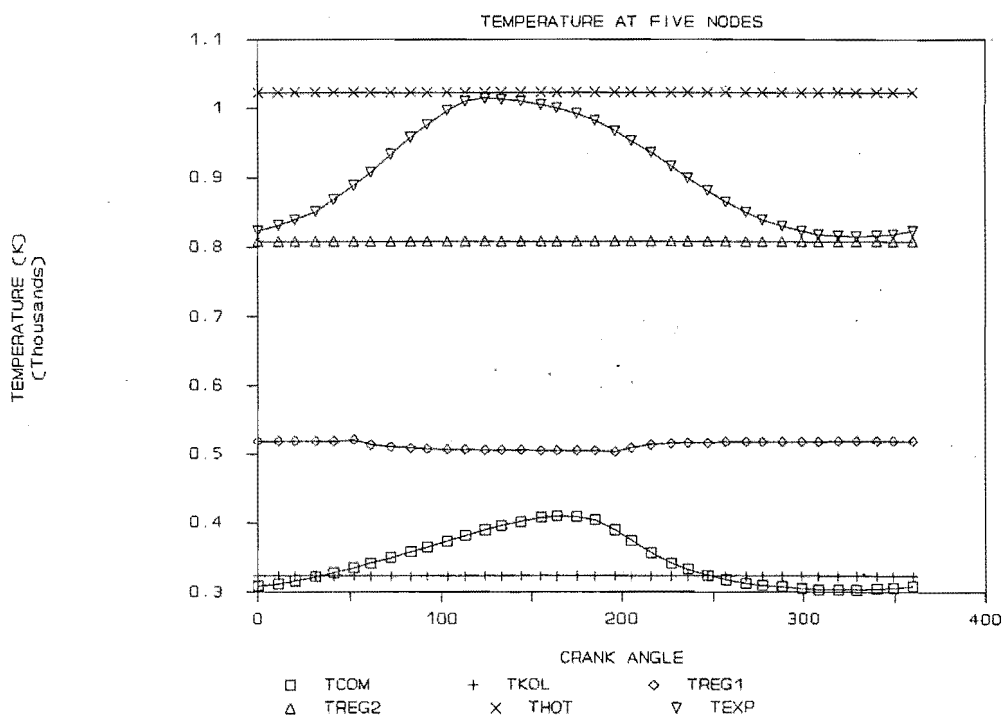
STIRLING CYCLE ENGINE ANALYSIS



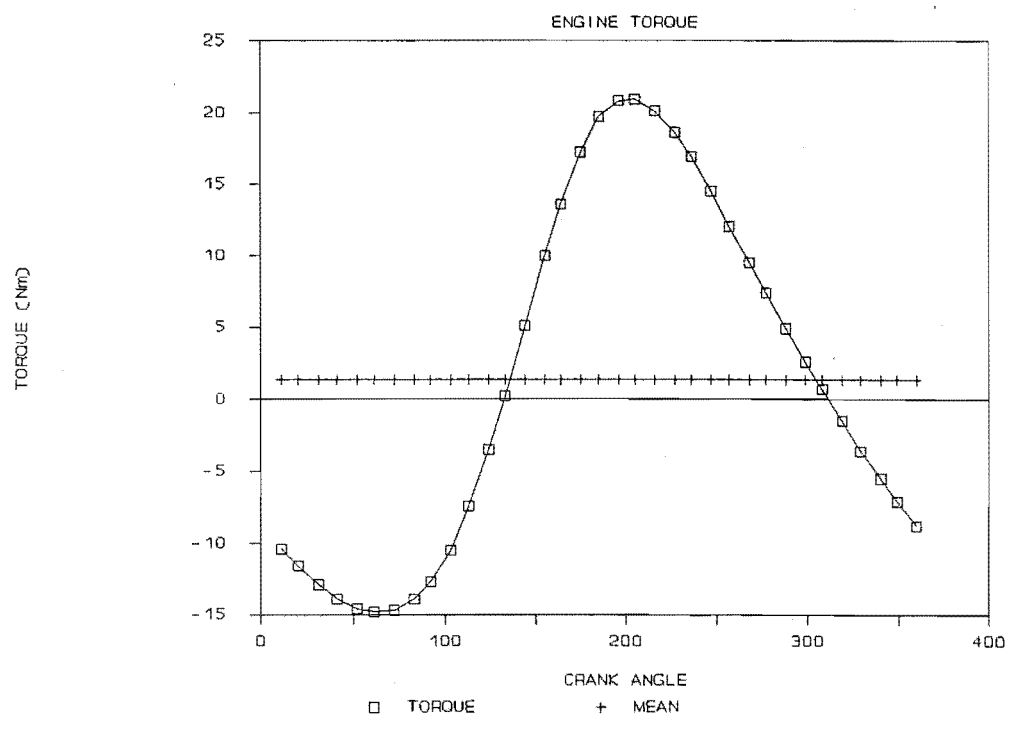
STIRLING CYCLE ENGINE ANALYSIS



STIRLING CYCLE ENGINE ANALYSIS

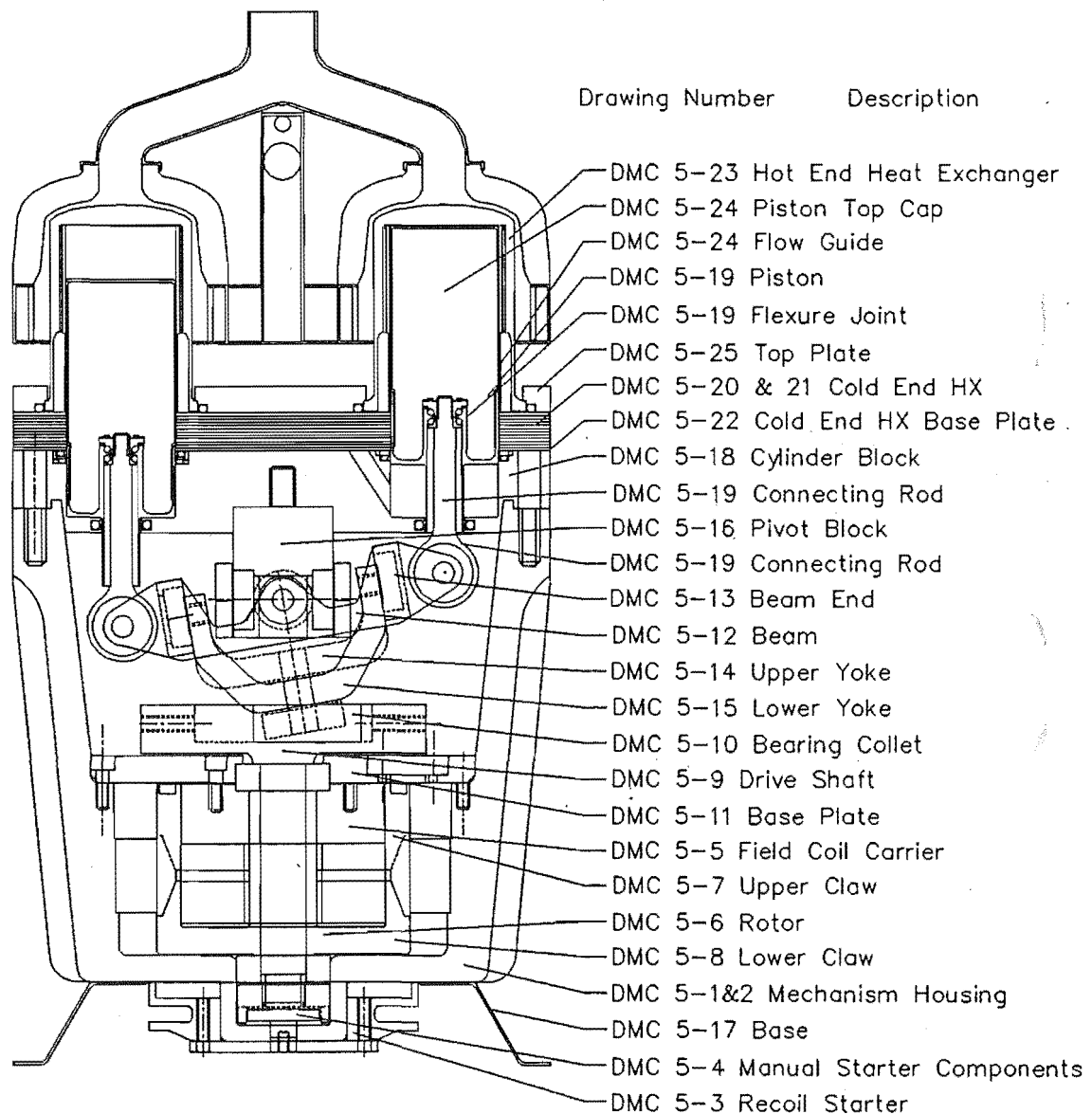


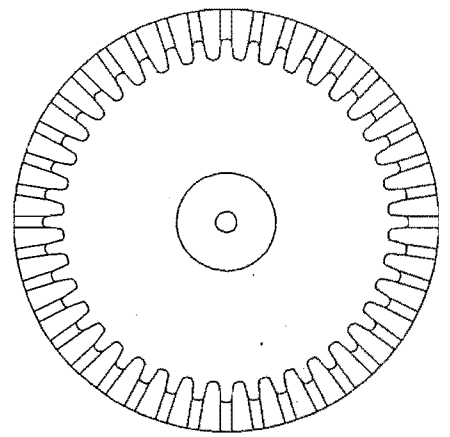
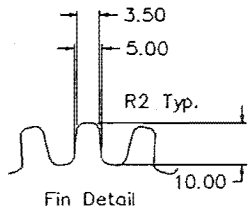
STIRLING CYCLE ENGINE ANALYSIS



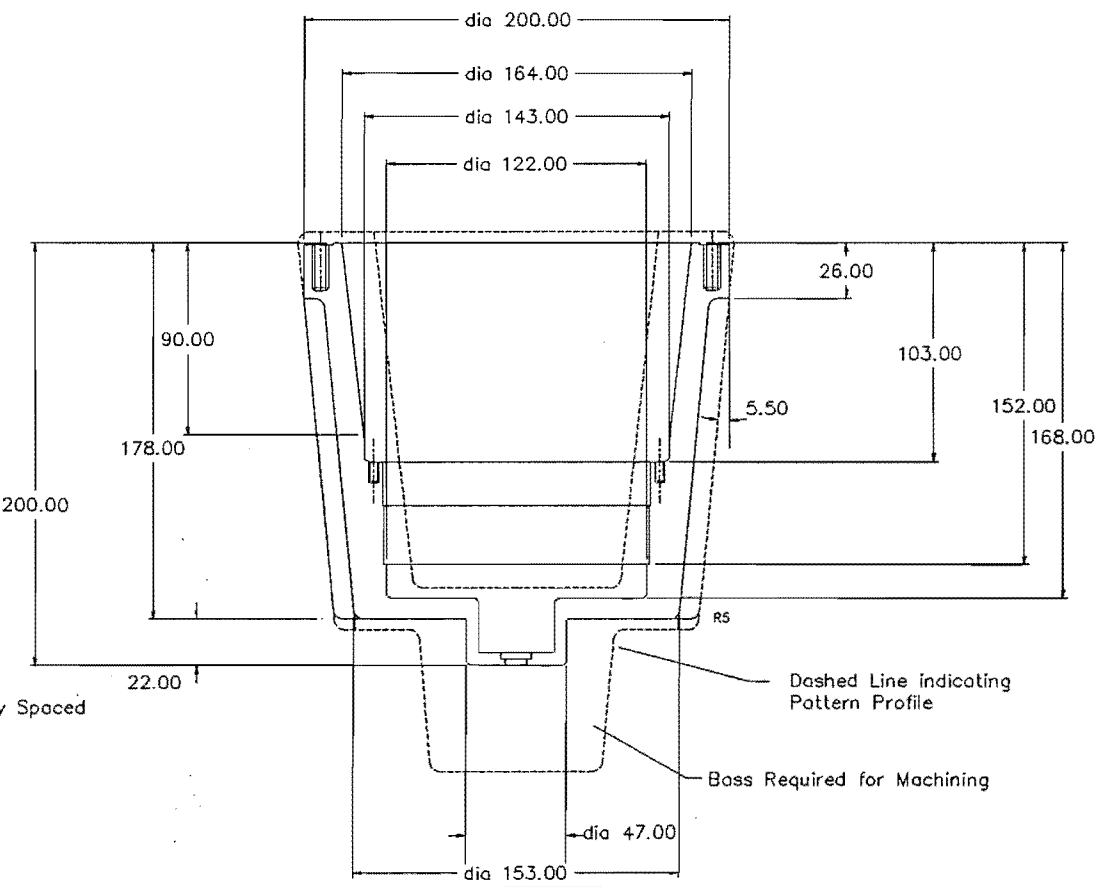
Appendix DMC 5

This Appendix gives the manufacturing drawings for DMC 5. The following pages are numbered according to the number of the drawing on that page. The figure below gives a cross section of the assembled engine.





40 Fins Evenly Spaced
Fin Detail

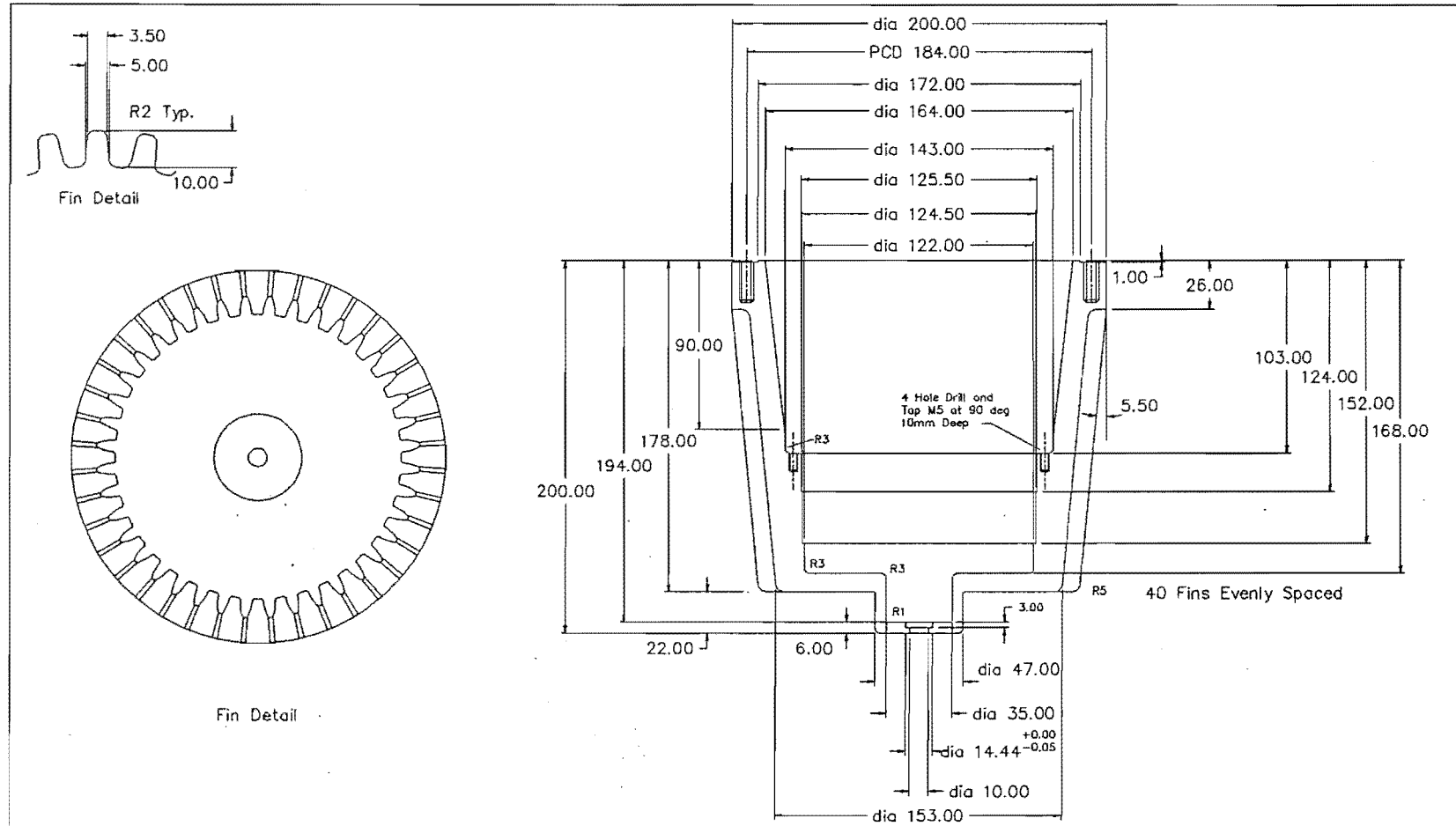


Dashed Line indicating Pattern Profile

Boss Required for Machining

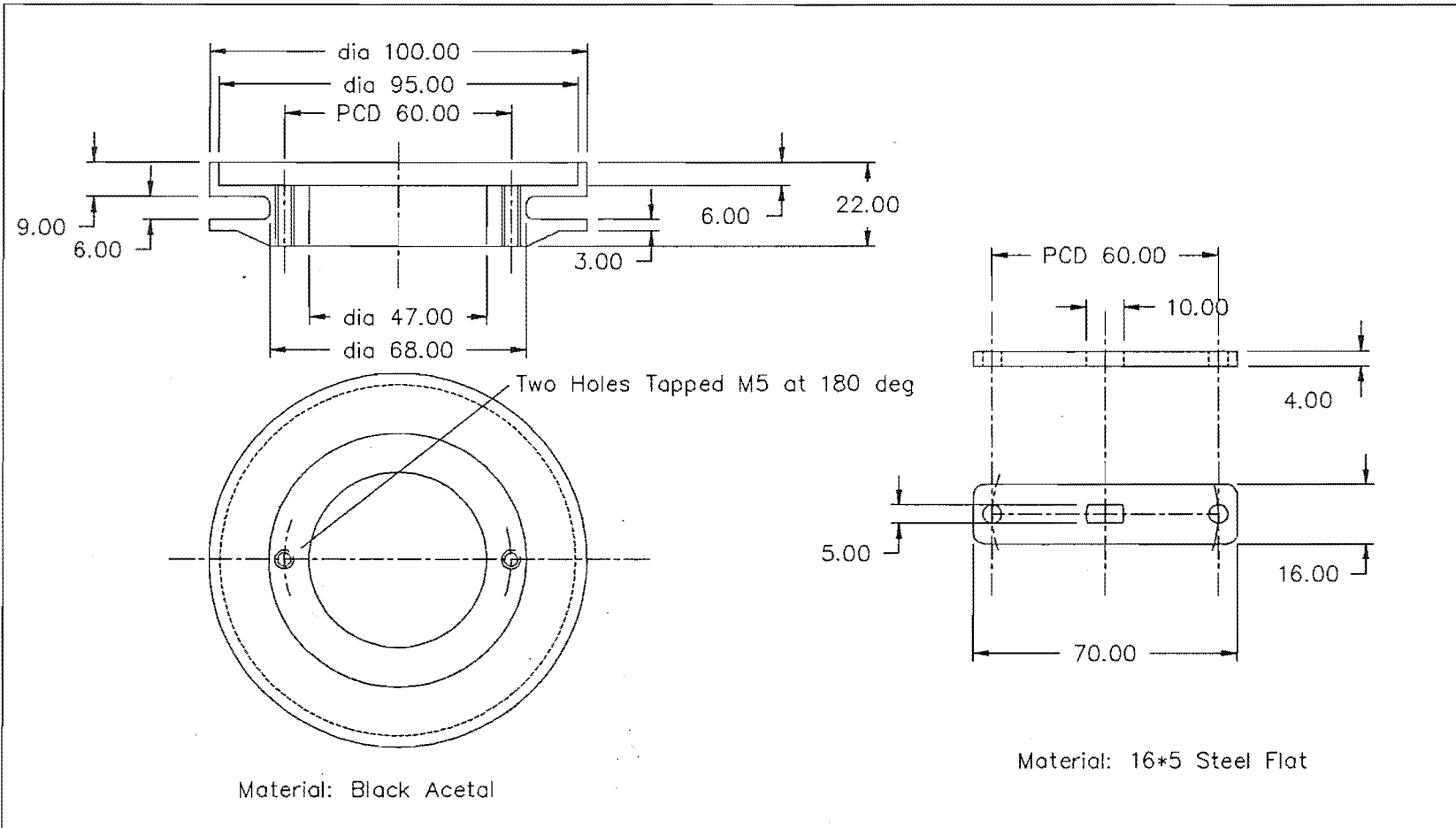
Do Not Scale.	Material. Cast Aluminium	Base Tolerance.	Scale.
Title. C.Case Pattern	Stirling Engine Research		Dwg. No. DMC 5-1

DMC 5-1

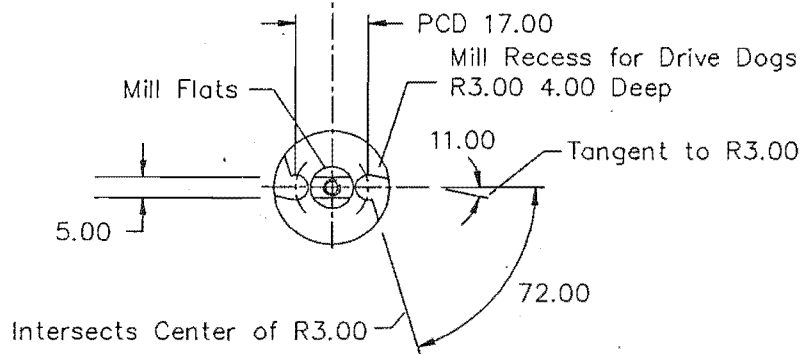
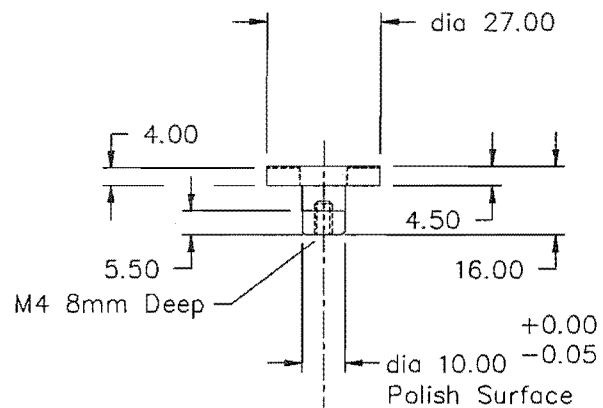


Do Not Scale.	Material. Al. LM25 T6	Base Tolerance.	Scale.
Title. Crank Case	Stirling Engine Research		Dwg. No. DMC 5-2

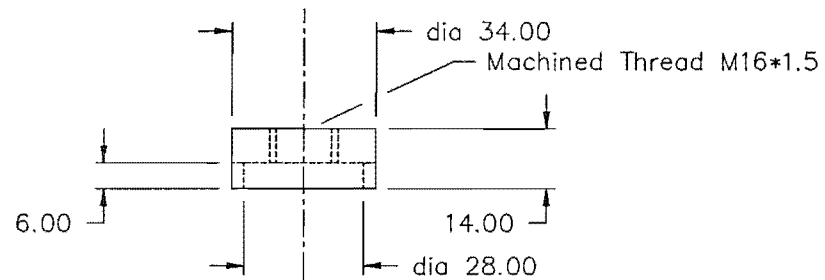
DMC 5-2



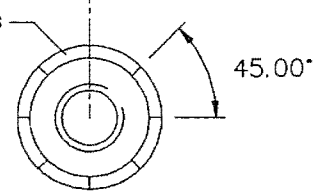
Do Not Scale.	Material.	Base Tolerance.	Scale.
Title. Recoil Starter	Stirling Engine Research		Dwg. No. DMC 5-3



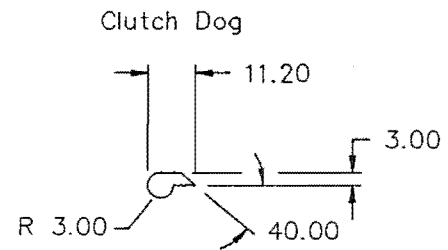
Manual Starter Drive Shaft



Material: 4340 Steel

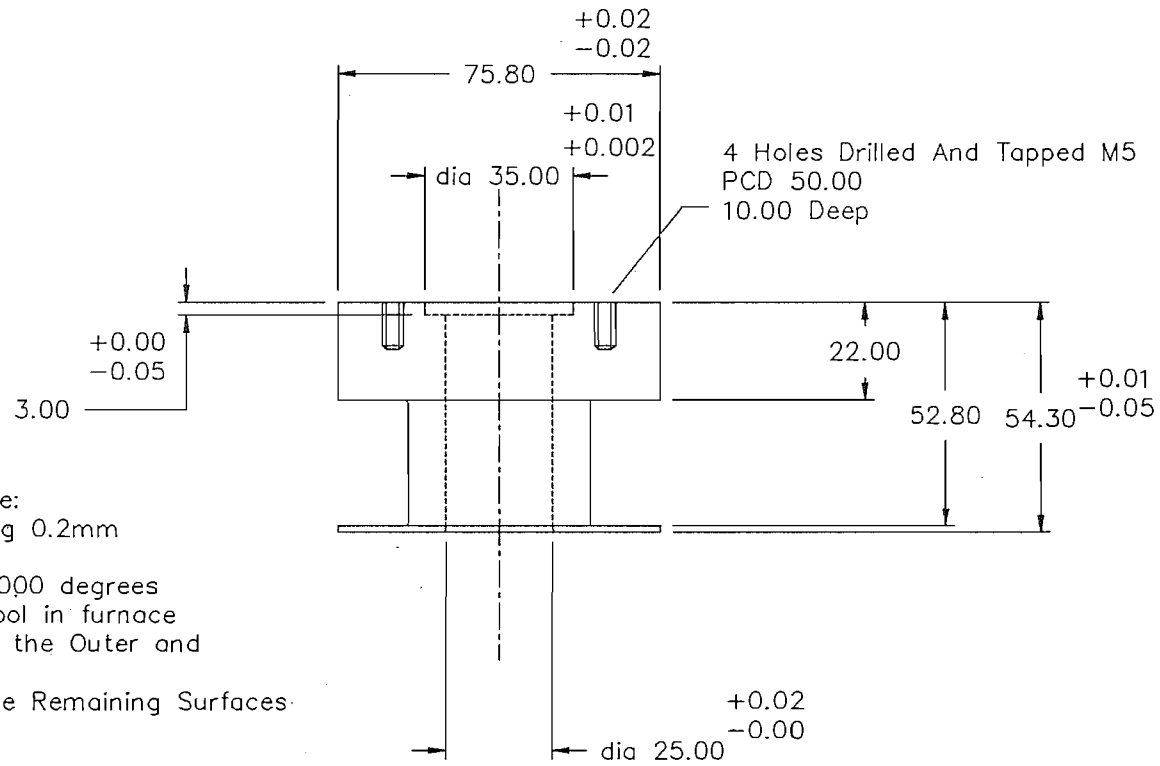


Castle Nut



Material: 4340 Steel
Surface Grind 4.00 Thick

Do Not Scale.	Material.	Base Tolerance.	Scale.
Title. Recoil Starter Parts	Stirling Engine Research		Dwg. No. DMC 5-4



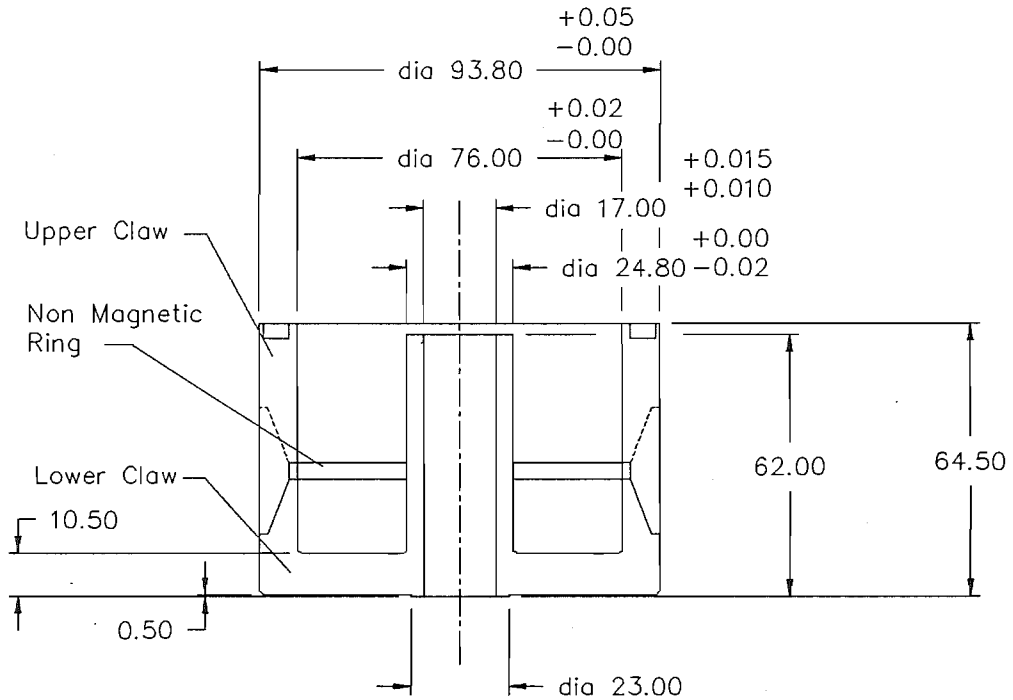
- Machining Procedure:
1. Rough Out Leaving 0.2mm on all Surfaces
 2. Anneal at 950-1000 degrees for one hour and cool in furnace
 3. Cylindrically Grind the Outer and Inner diameters
 4. Finish Machine the Remaining Surfaces

Radius All Corners R0.8

Do Not Scale.	Material. 1018 Steel	Base Tolerance.	Scale.
Title. Field Coil Carrier	Stirling Engine Research		Dwg. No. DMC 5-5

Manufacturing Procedure:

1. Rough machine the two claw pieces. Finish all milling operations for the claws and slots.
2. Anneal at 950-1000 deg for 1 hour and slow cool in the furnace.
3. Finish machine the spigot surfaces for the connecting ring
4. Assemble and easyflow the two claw pieces together.
5. Finish all surfaces to match the dimensions on this drawing.

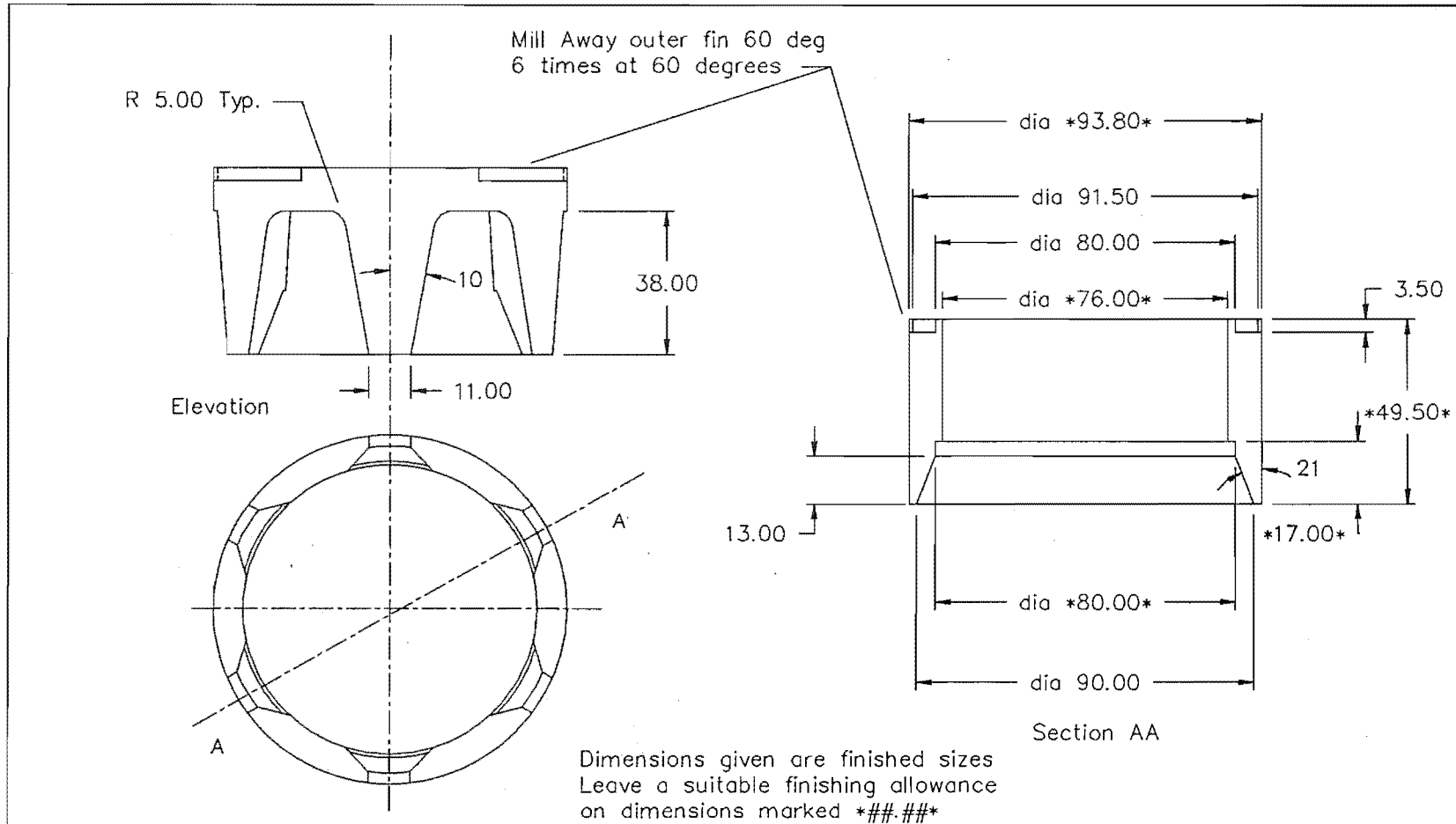


Radius All Corners R0.8

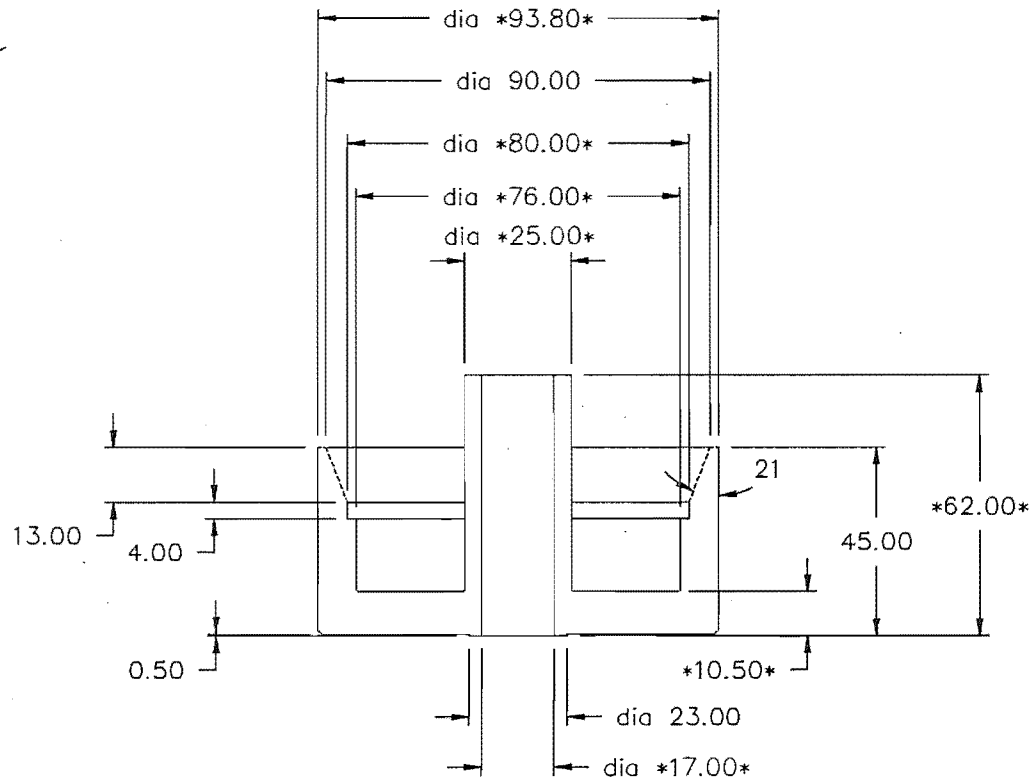
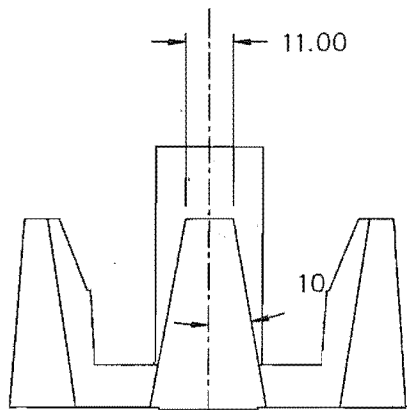
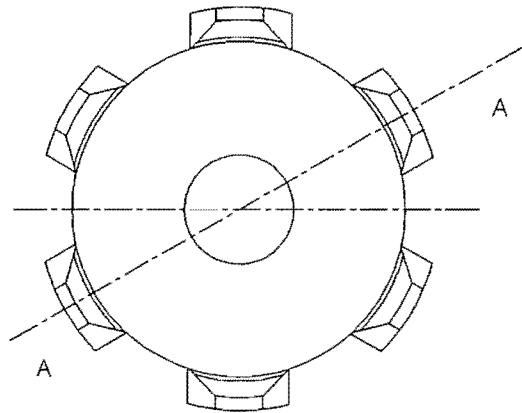
This drawing gives the critical dimensions which must be obtained after easyflowing the components together.

Where possible cylindrically grind otherwise machine and emery.

Do Not Scale.	Material. 1018 Steel	Base Tolerance.	Scale.
Title. Field Rotor 1 of 3	Stirling Engine Research		Dwg. No. DMC 5-6

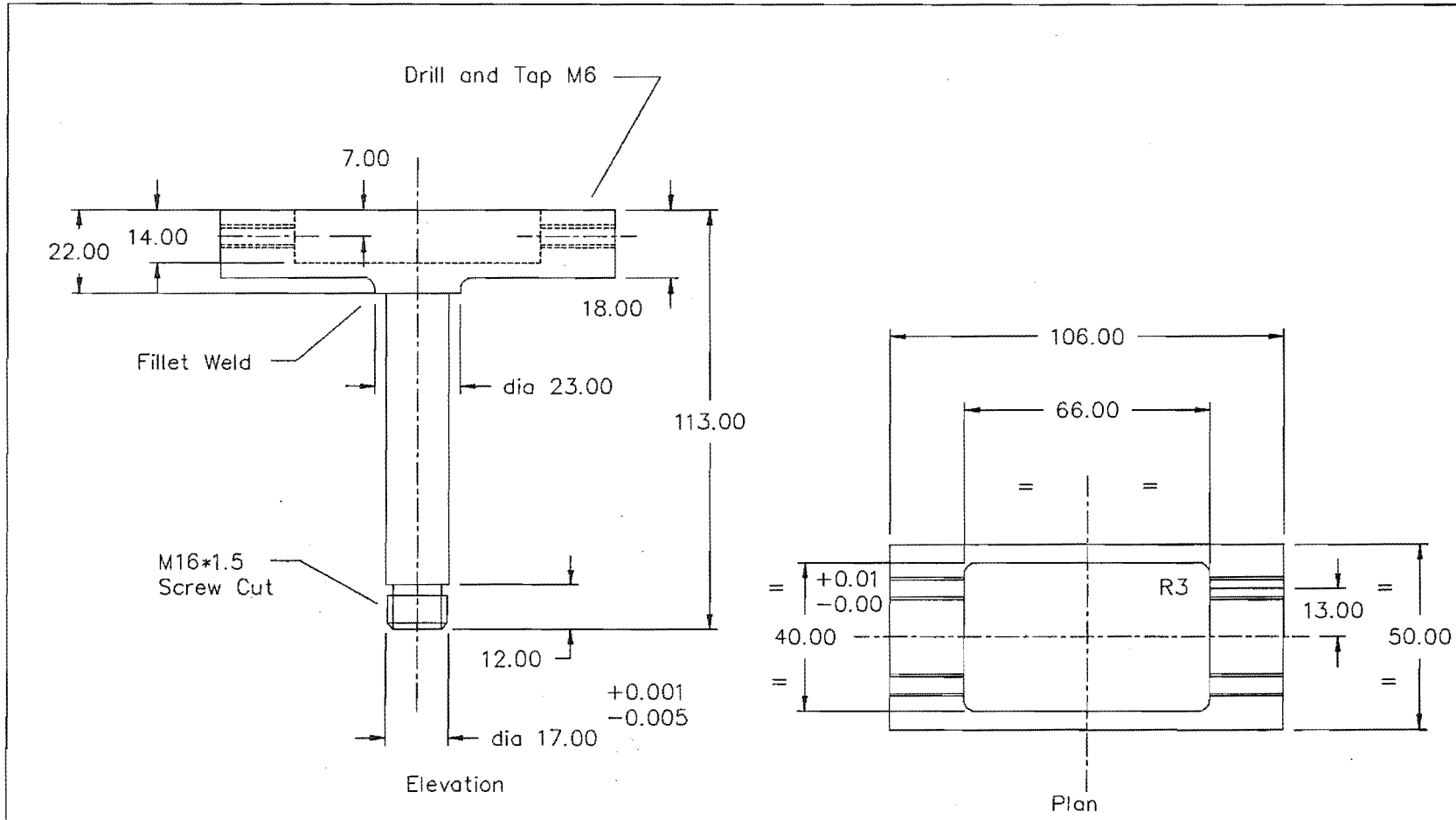


Do Not Scale.	Material. 1018 Steel	Base Tolerance.	Scale.
Title. Upper Claw 2 of 3	Stirling Engine Research		Dwg. No. DMC 5-7

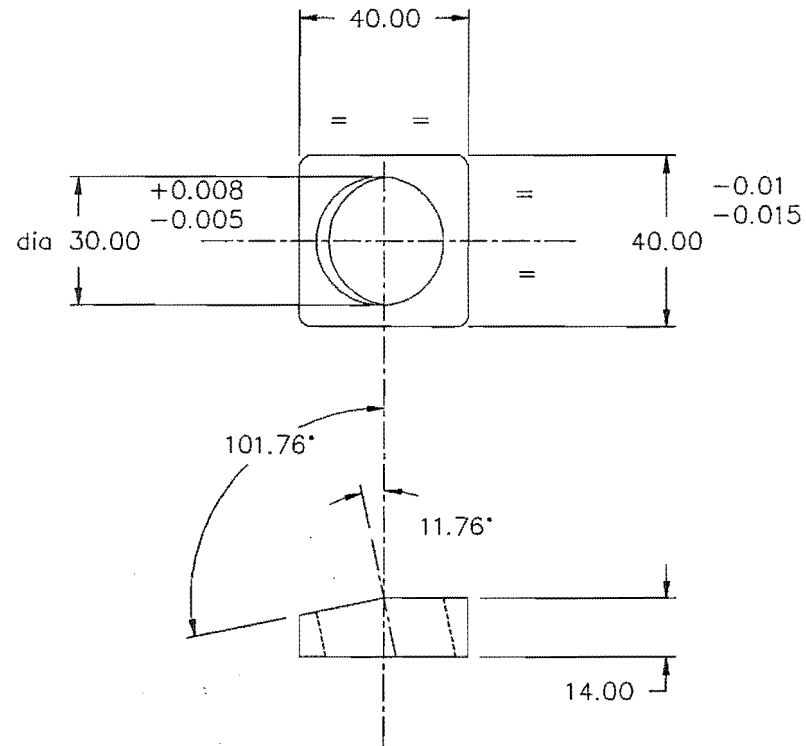


Dimensions given are finished sizes
 Leave a suitable finishing allowance
 on dimensions marked *##.##*

Do Not Scale.	Material. 1018 Steel	Base Tolerance.	Scale.
Title. Lower Claw 3 of 3	Stirling Engine Research		Dwg. No. DMC 5-8

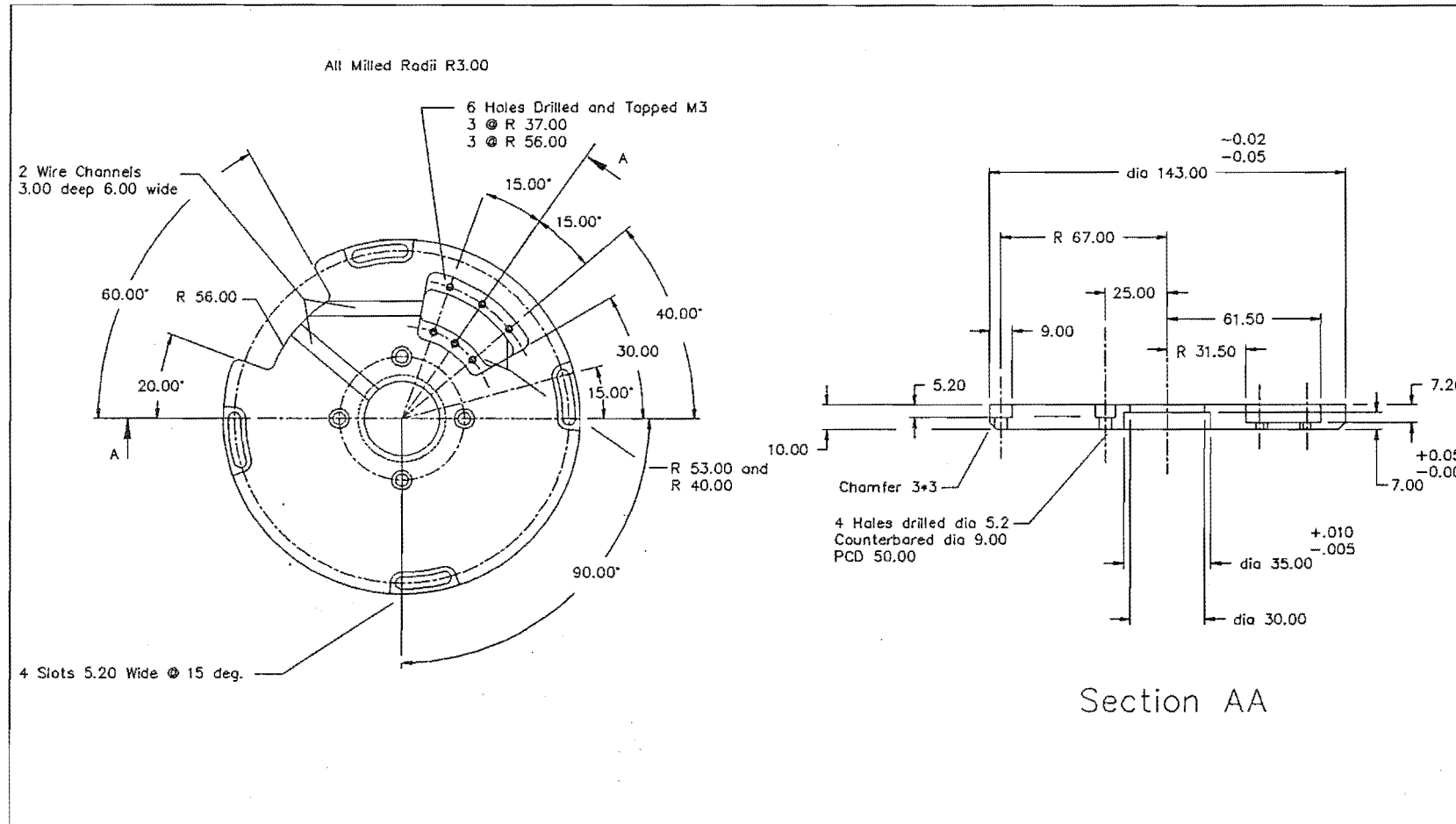


Do Not Scale.	Material. 1020 Steel	Base Tolerance. +/- 0.1	Scale.
Title. Drive Shaft	Stirling Engine Research		Dwg. No. DMC 5-9

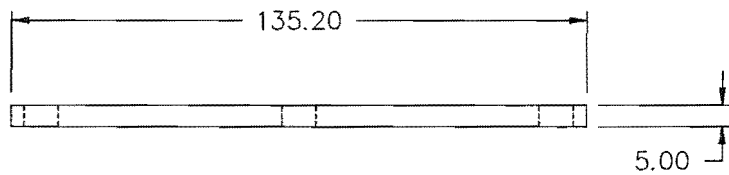


Do Not Scale.	Material. 1018 Steel	Base Tolerance. +/- 0.1	Scale.
Title. Bearing Block	Stirling Engine Research		Dwg. No. DMC 5-10

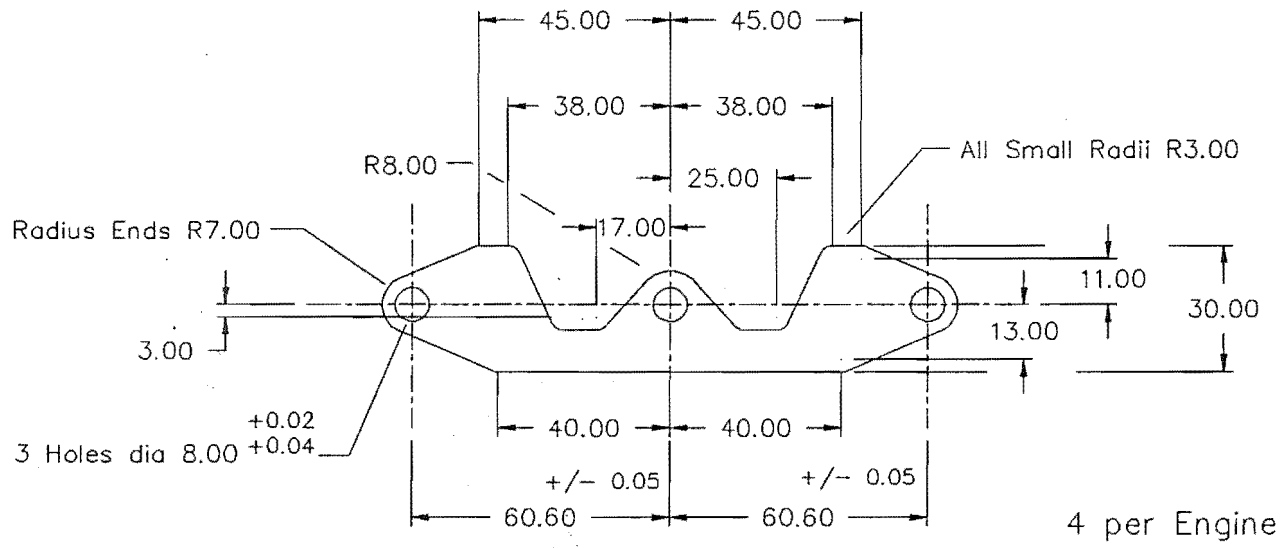
DMC 5-10



Do Not Scale.	Material. Al 5251/5454	Base Tolerance.	Scale.
Title. Base Plate	Stirling Engine Research		Dwg. No. DMC 5-11



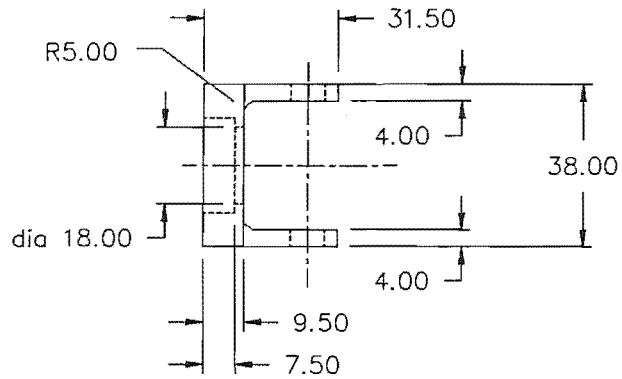
Plan



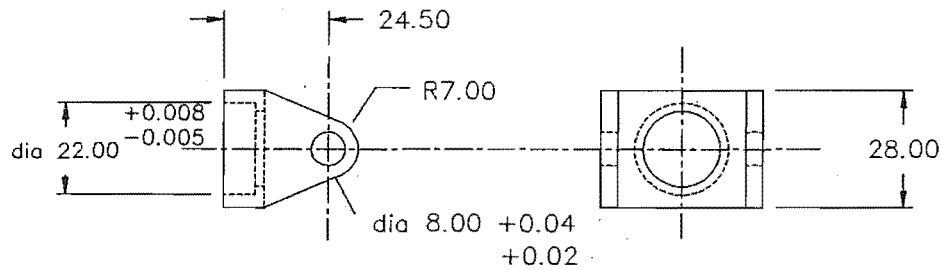
Elevation

Do Not Scale.	Material. Al. 5086 H32	Base Tolerance. $\pm .2$	Scale.
Title. Beam	Stirling Engine Research		Dwg. No. DMC 5-12

DMC 5-12



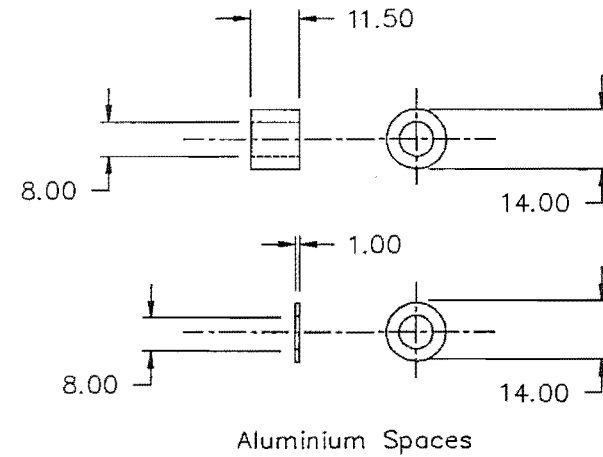
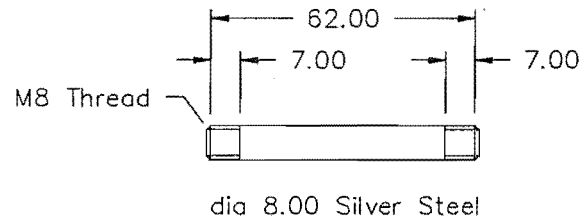
Plan



Elevation

End Elevation

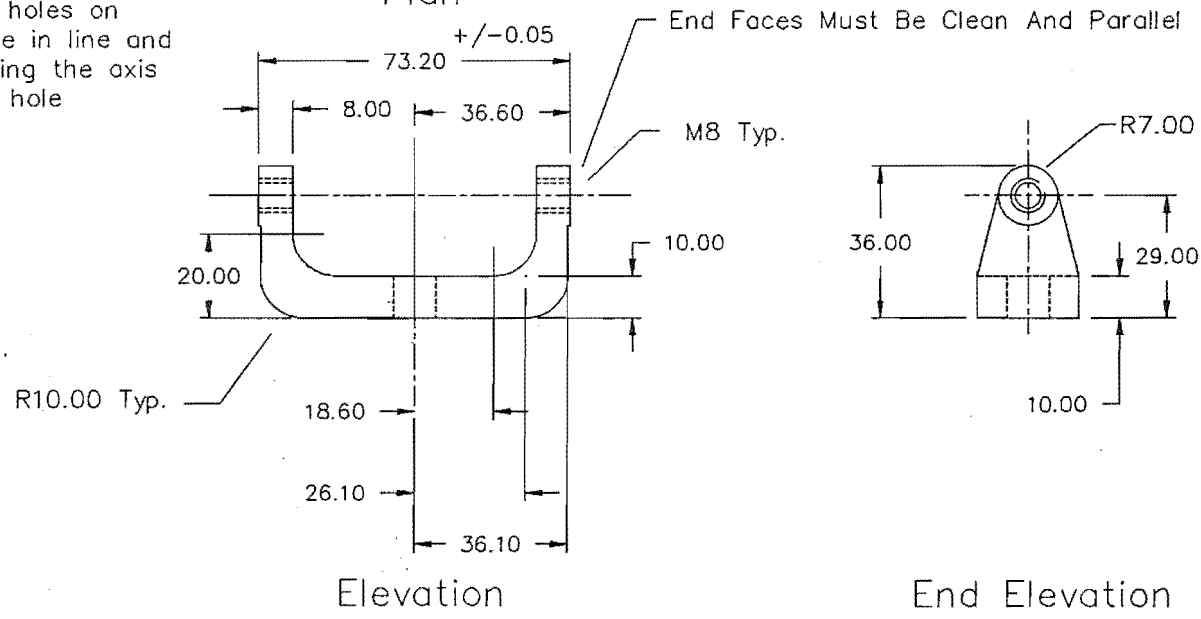
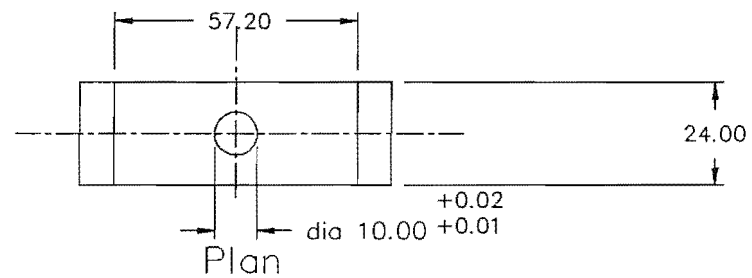
Material: 38.1*38.1 Aluminium 6351 T6
Square Bar



4 per Engine

Do Not Scale.	Material.	Base Tolerance. +/- 0.10	Scale.
Title. Beam End	Stirling Engine Research		Dwg. No. DMC 5-13

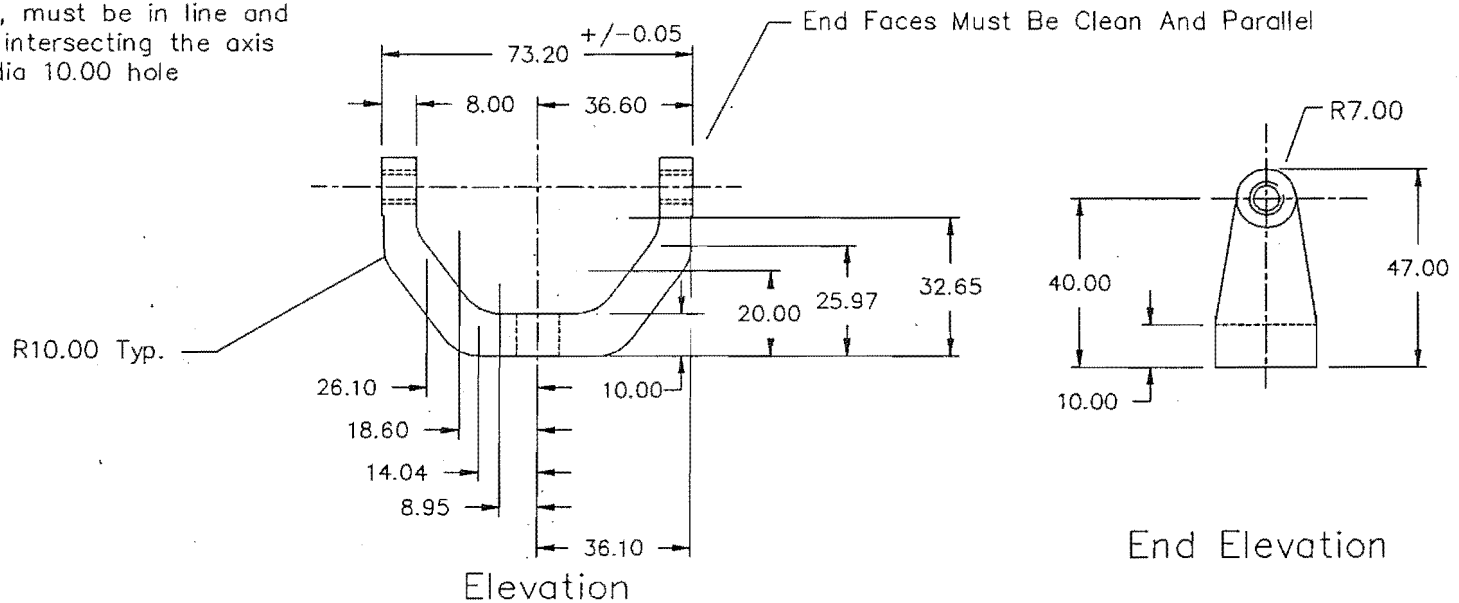
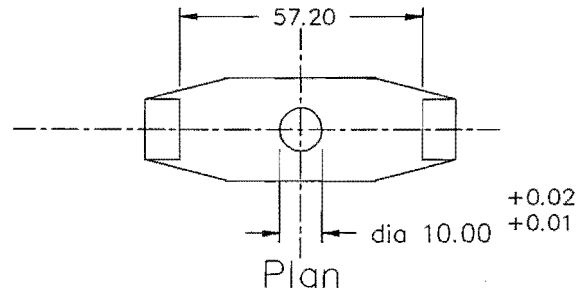
Mirror about vertical axis
 Drill and tap M8 holes on
 machine, must be in line and
 on axis intersecting the axis
 of the dia 10.00 hole



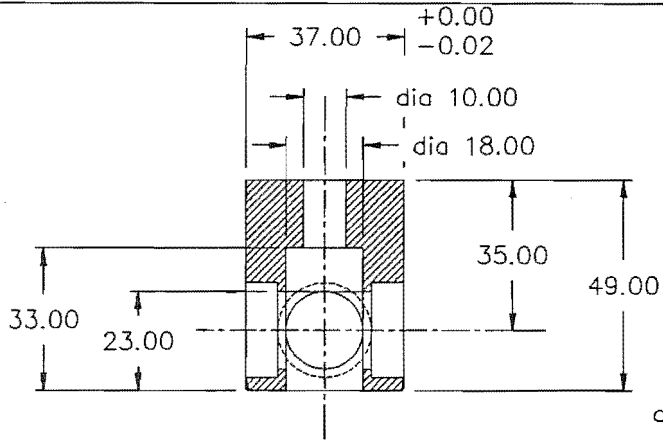
Do Not Scale.	Material. Al. 5251/5454	Base Tolerance.	Scale.
Title. Upper Yoke	Stirling Engine Research		Dwg. No. DMC 5-14

DMC 5-14

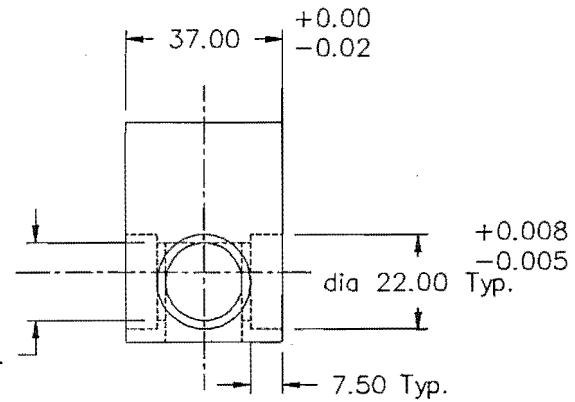
Mirror about vertical axis
 Drill and tap M8 holes on
 machine, must be in line and
 on axis intersecting the axis
 of the dia 10.00 hole



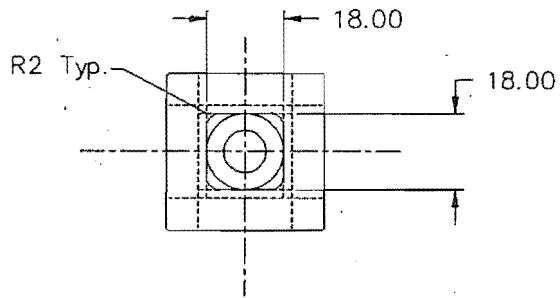
Do Not Scale.	Material. Al. 5251/5454	Base Tolerance.	Scale.
Title. Lower Wobble Yoke	Stirling Engine Research		Dwg. No. DMC 5-15



Section AA

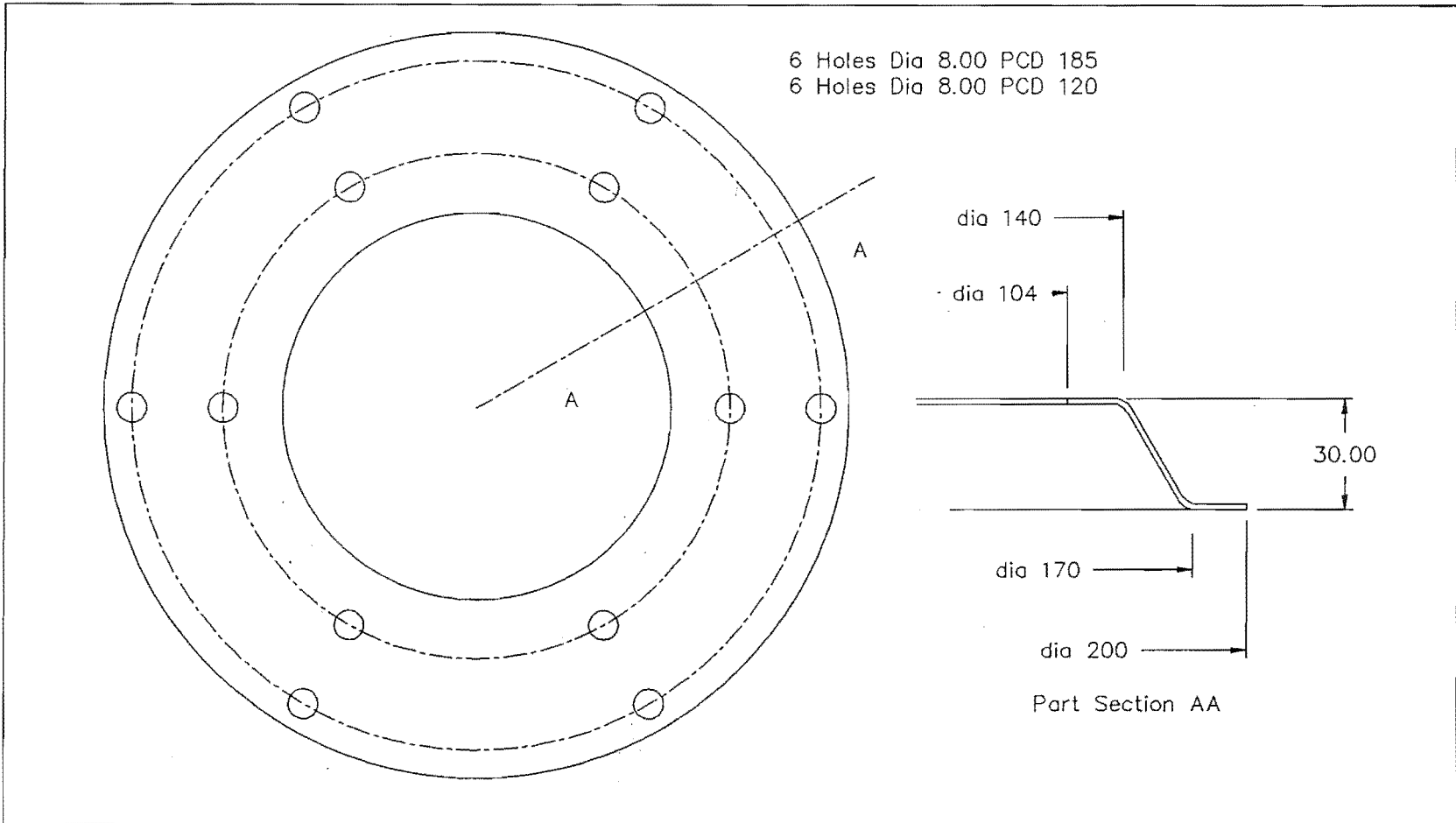


End Elevation



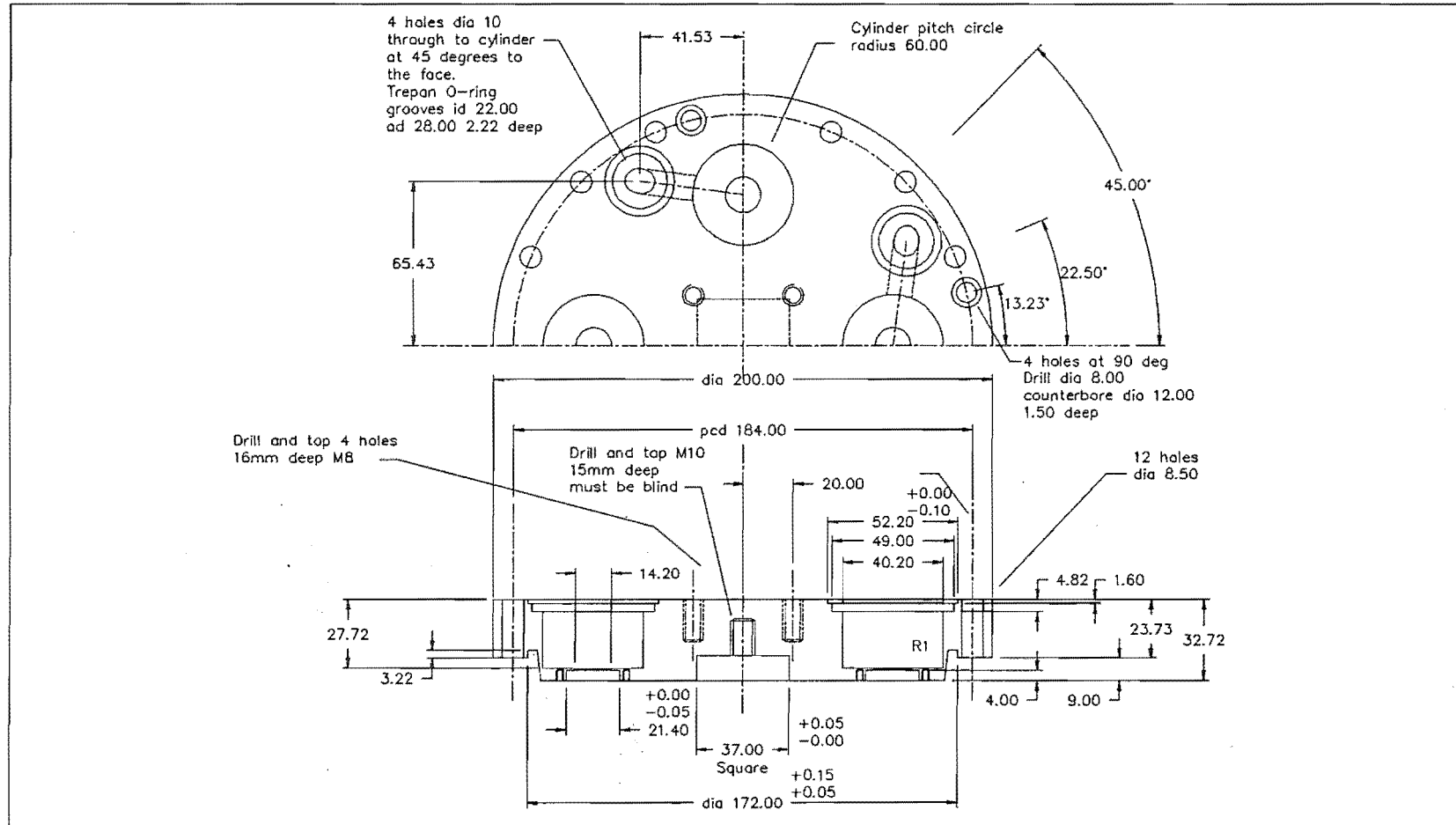
Plan

Do Not Scale.	Material. 38.1*38.1 Al 6351	Base Tolerance. +/- 0.1	Scale. 1:1
Title. Pivot Block	Stirling Engine Research		Dwg. No. DMC 5-16



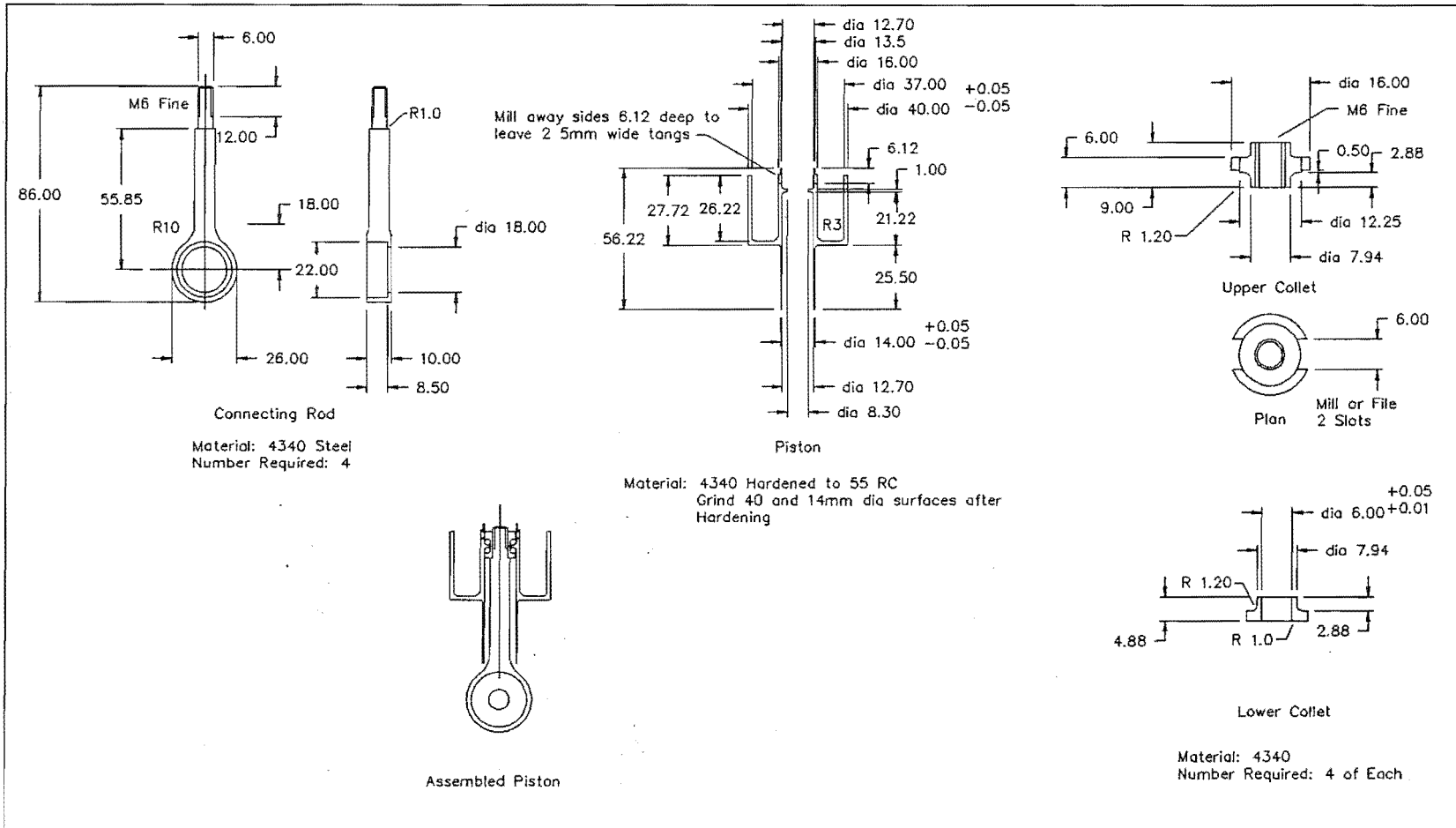
Do Not Scale.	Material. 1/16" Mild Steel	Base Tolerance.	Scale.
Title. Base	Stirling Engine Research		Dwg. No. DMC 5-17

DMC 5-17



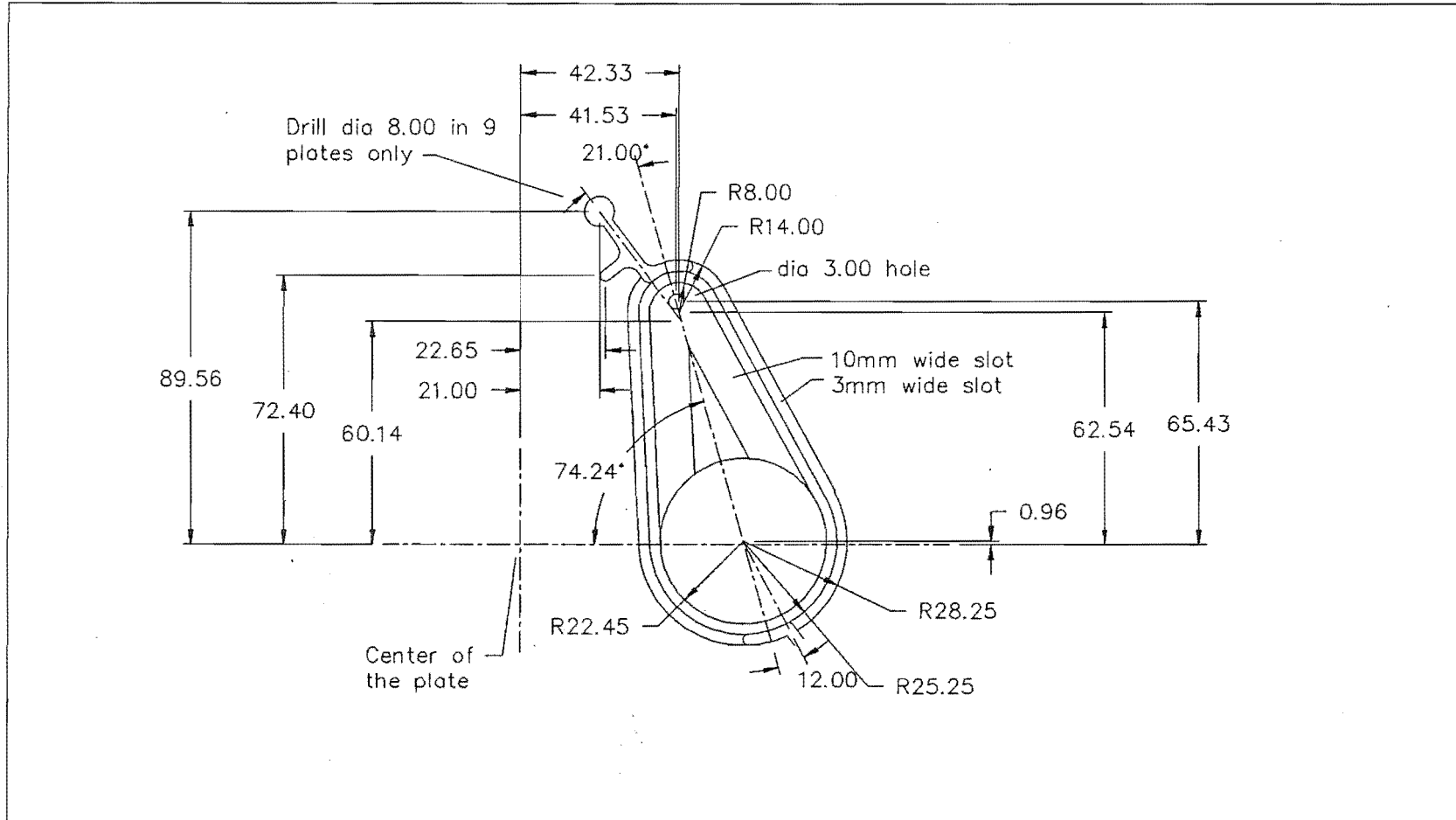
Do Not Scale.	Material.	Base Tolerance.	Scale.
Title. Cylinder Block	Stirling Engine Research		Dwg. No. DMC 5-18

DMC 5-18

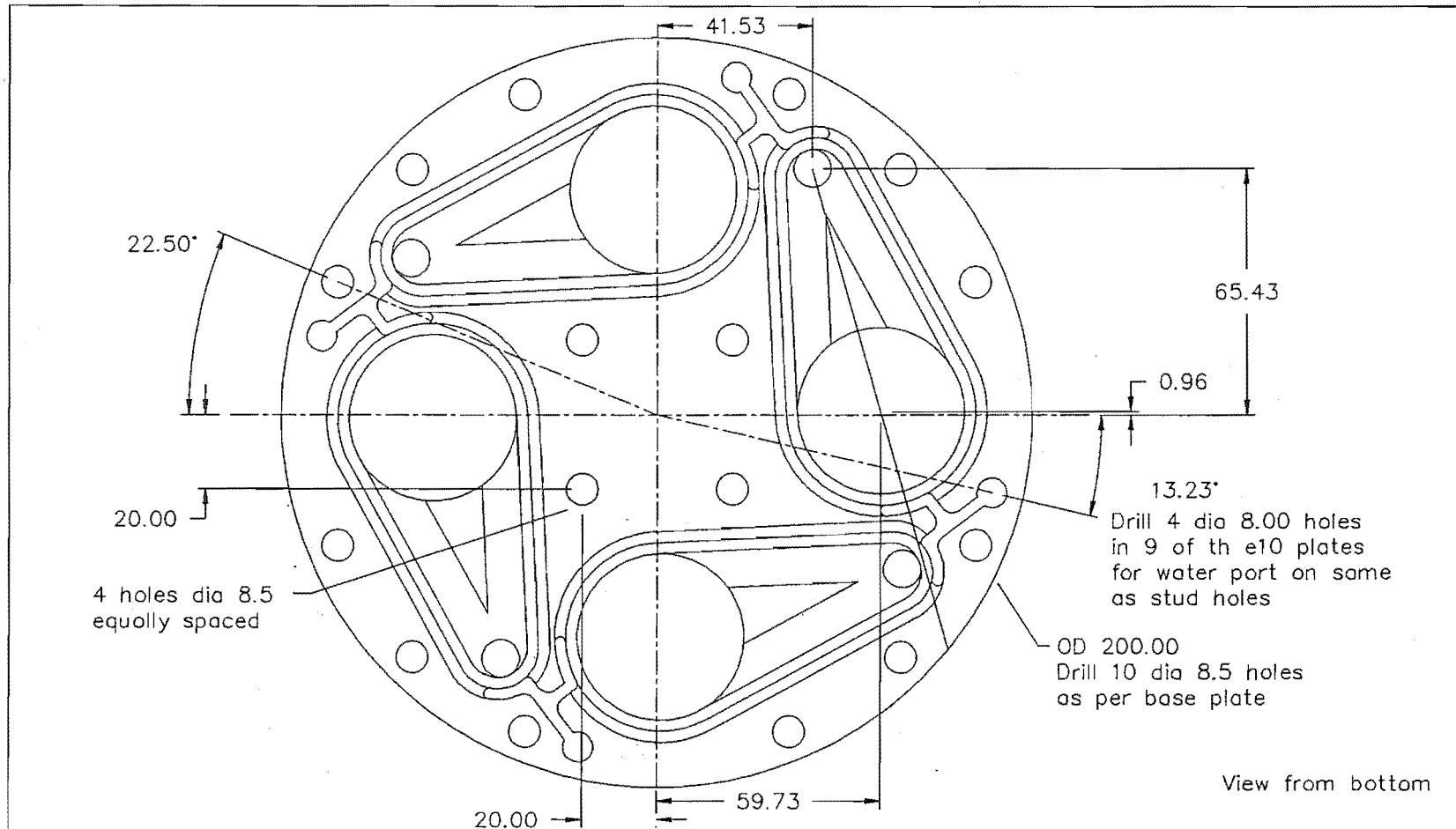


Do Not Scale.	Material.	Base Tolerance.	Scale.
Title. Piston Assem.	Stirling Engine Research		Dwg. No. DMC 5-19

DMC 5-19

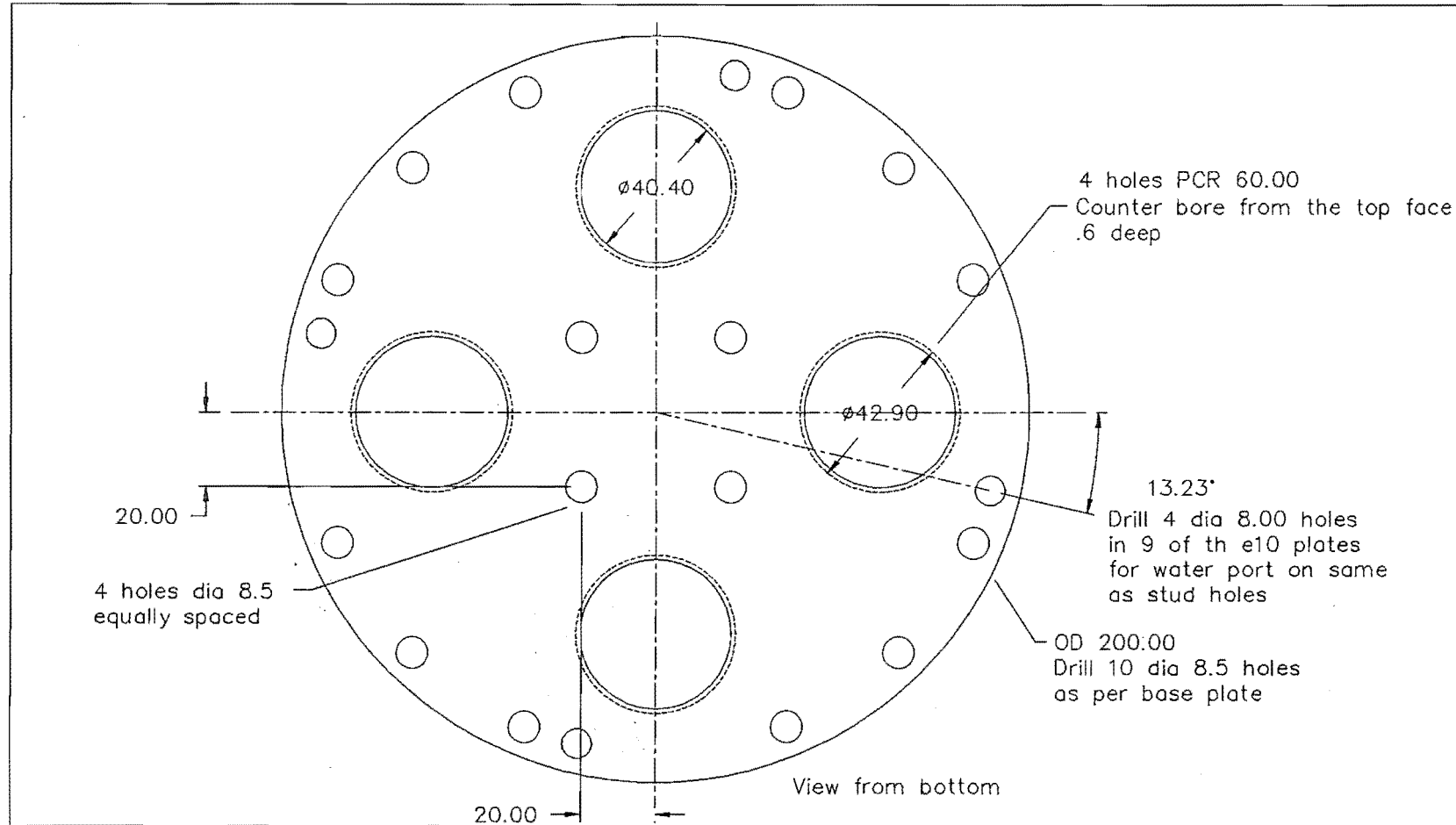


Do Not Scale.	Material. 253 MA	Base Tolerance.	Scale. 1:1
Title. Cold End HX	Stirling Engine Research		Dwg. No. DMC 5-20

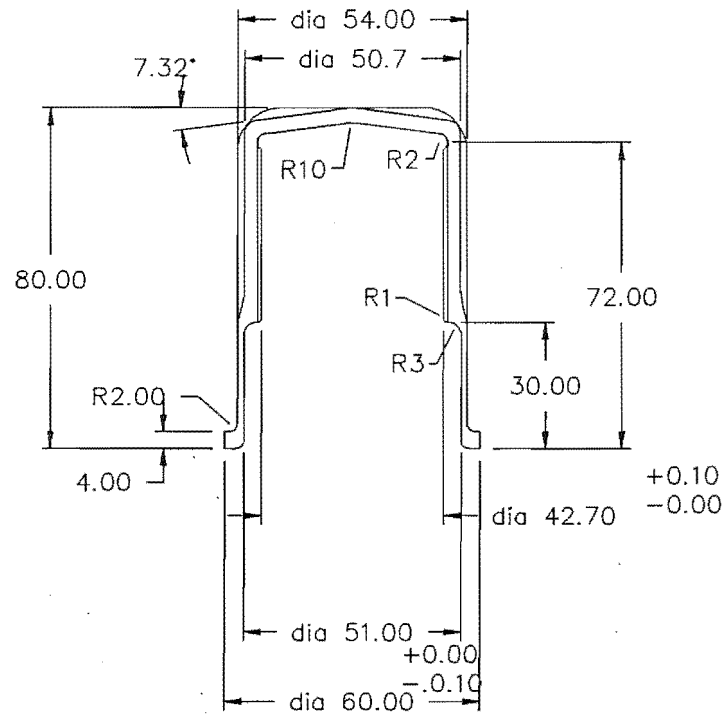


Do Not Scale.	Material. 0.9 Copper	Base Tolerance.	Scale.
Title. COLD HX	Stirling Engine Research		Dwg. No. DMC 5-21

DMC 5-21

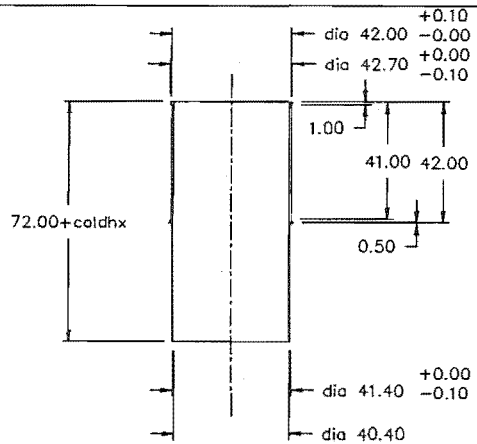


Do Not Scale.	Material. 1.2 Copper	Base Tolerance.	Scale.
Title. HX Base Plate	Stirling Engine Research		Dwg. No. DMC 5-22

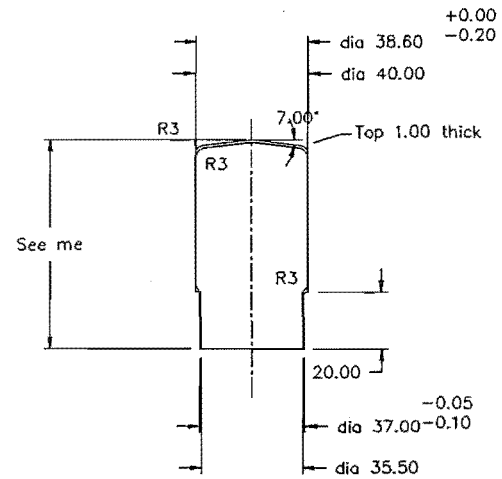


Do Not Scale.	Material. 253 MA	Base Tolerance.	Scale.
Title. Hot End HX	Stirling Engine Research		Dwg. No. DMC 5-23

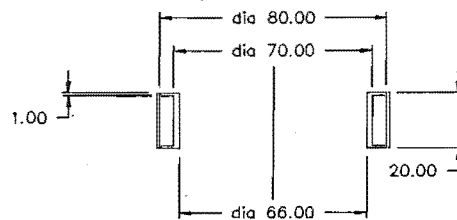
DMC 5-23



Sleeve Material 316 S/Steel

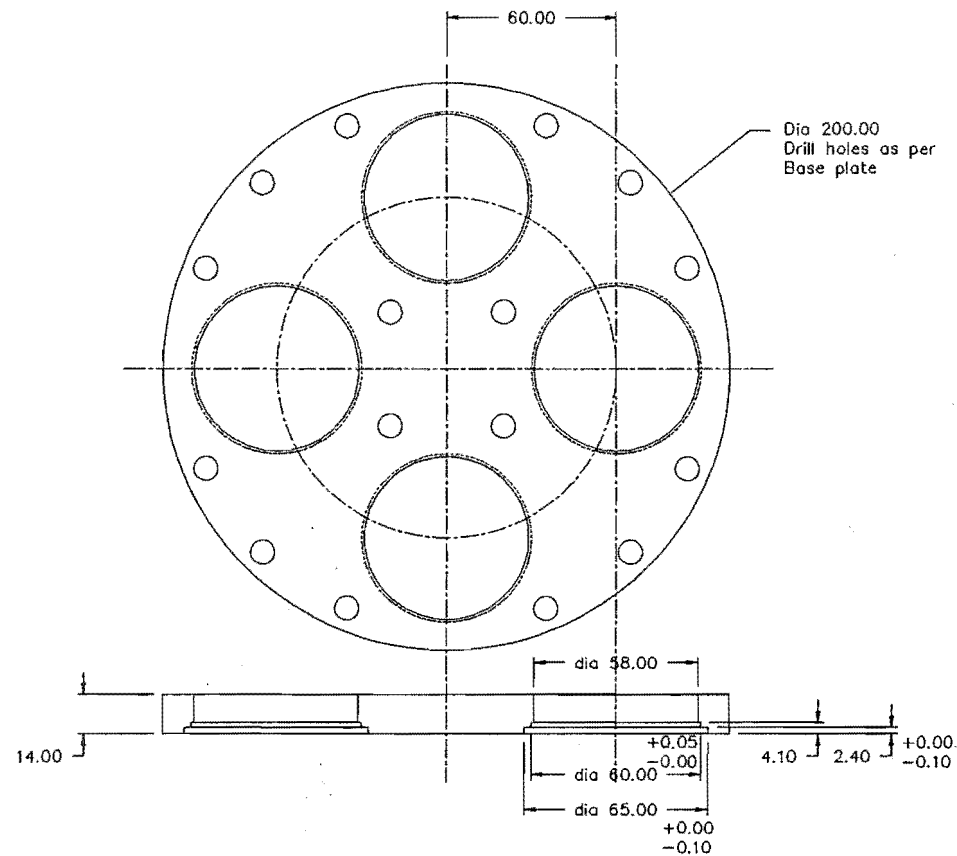


Piston Top Cap
Material 316 S/Steel



Burner
Material Mild Steel

Do Not Scale.	Material.	Base Tolerance.	Scale.
Title. Flow Guide Piston Top Cap	Stirling Engine Research		Dwg. No. DMC 5-24



Do Not Scale.	Material.	Base Tolerance.	Scale.
Title. Top Plate	Stirling Engine Research		Dwg. No. DMC 5-25

DMC 5-25

Drawing DMC 5-26 Circuit diagram for DMC 5. LCD display not shown.

